AN INVESTIGATION OF THE ANTIMICROBIAL AND ANTIFOULING PROPERTIES OF MARINE ALGAL METABOLITES

A Thesis Submitted in Fulfillment of the Requirements for the Degree of

MASTER OF SCIENCE (PHARMACY)

Of

RHODES UNIVERSITY

By

MARYSSA GUDRUN AILSA MANN

JANUARY 2008

Acknowledgements

Sincere thanks go to my supervisor, Dr. Denzil R. Beukes; a true friend, a wise advisor and a compassionate mentor who has had a significant and positive effect on my life.

To my mother and father, for your love and support. For your patience, for encouragement and for laughter. For passion, an interest in all things weird and wonderful and for being great examples of perseverance in adversity.

To Craig, a truly wonderful companion and now my husband, thank you for your undying love, support and wonderful sense of humor.

To Yoland and Barry Irwin, valued friends who have unfalteringly been there to support me, feed me and put a roof over my head in some of the most stressful days of my life; to whom I owe much of my sanity.

To Dr. Edith Antunes for friendship, motivation and positive attitude, for assistance with the mass spectrometry and gas chromatography and the all important shoulder to cry on.

To Koos Fernhout for the beautiful opening photograph and many interesting conversations over the years.

Thanks go to the following members of the Rhodes community, my friends and colleagues:

- Mr. and Mrs. Morley for their friendship and guidance as well as immense technical assistance
- Mr. Aubrey Sonemann for his assistance with mass spectrometry
- Professor John Bolton (University of Cape Town) for the collection and identification of marine algae
- The Faculty of Pharmacy for providing me with a family away from home
- My fellow laboratory researchers Yolisa, Anthonia, Renata, Kudzai, Monique, Paul and Nash for their companionship
- Members of the Department of Chemistry, Rhodes University for their technical assistance

Abstract

Prevention of the accumulation of undesirable biological material i.e. biofouling upon a solid surface requires the use of antifouling systems. The solid surface may be a contact lens, an off shore oil rig or a living organism. When chemicals are employed as a mechanism of defense against biofouling, the agents involved are known as antifouling agents.

Marine algae must protect themselves from fouling organisms and it is thought that one of the mechanisms used by these organisms is the production of secondary metabolites with an array of biological activities. *In vitro* studies have shown numerous compounds isolated from marine algae to possess antibacterial, antifungal and antimacrofouling activity.

The aim of this study was to evaluate the secondary metabolite extracts of selected Southern African marine macro-algae as a potential source of compounds that inhibit biofilm formation and that could be used as antifouling agents.

In this project, marine macro-algae were collected from various sites along the South African coastline. Their extracts were screened for antimicrobial activity against four ubiquitous micro-organisms, *Staphylococcus aureus*, *Klebsiella pneumoniae*, *Mycobacterium aurm* and *Candida albicans*. Results of screening assays guided the fractionation of two Rhodophyta, *Plocamium corallorhiza* and *Laurencia flexuosa*. The algae were fractionated using silica gel column chromatography and compounds were isolated by semi-preparative normal phase HPLC. Compound characterization was performed using UV, IR and advanced one- and two-dimensional NMR (^{1}H, ^{13}C NMR, COSY, HSQC, HMBC and NOESY) spectroscopy and mass spectrometry.

Ten halogenated monoterpenes including four members of the small class of halogenated monoterpene aldehydes were isolated from extracts of *P. corallorhiza*. The compounds isolated included the known compounds **3,4,6,7-tetrachloro-3,7-dimethyl-1-octene**; **4,6-dibromo-1,1-dichloro-3,7-dimethyl-2*E*,7octadiene**; **4,8-dibromo-1,1,7-trichloro-3,7-dimethyl-2,5*E*-octadiene**; **1,4,8-tribromo-3,7-dichloro-3,7-dimethyl-1*E*,5*E*-octadiene**; **8-bromo-6,7-dichloro-3,7-dimethyl-octa-2*E*,4*E*-dienal**; **4-Bromo-8-chloro-3,7-dimethyl-octa-2*E*,6*E* -dienal**; **4,6-Dibromo-3,7-dimethyl-octa-2*E*,7-dienal**; **2,4-dichloro-1-(2-chlorovinyl)-1-methyl-5-methylidene-cyclohexane** and two new metabolites **4,8-chloro-3,7-dimethyl-2*Z*,4,6*Z*-octatrien-1-al** and Compound **3.47**. Methodology was developed for the chemical derivatization and mass spectrometric analysis of the aldehydic compounds. The aldehyde trapping reagent *O*-(2,3,4,5,6-pentafluorobenzyl)hydroxylamine hydrochloride was used to derivatize the molecules, stabilizing them and allowing for their complete characterization.

From *Laurencia flexuosa* a new cuparene sesquiterpene **4-bromo-2-(5-hydroxy-1,2,2-trimethylcyclopent-3-enyl)-5-methylphenol** was isolated along with two geometric isomers of the vinyl acetylene **bromofucin**. An halogenated monoterpene **3*S**,4*R**-1-bromo-3,4,8-trichloro-9-**

dichloromethyl-1-*E*,5-*E*,7-*Z*-octatriene was also isolated but was suspected to be a contaminant and an investigation into its biological source revealed that it originated from *Plocamium suhrii*.

A third alga, *Martensia elegans* was extracted based on published reports of antimicrobial compounds in related species. A new a-alkyl malate derivative was isolated and characterized.

Selected compounds isolated during the course of the study were employed in preliminary assays that tested their ability to inhibit biofilm formation by *Pseudomonas aeruginosa*. The halogenated monoterpenes isolated from the *Plocamium* species were the only active compounds. **3*S***,4*R***-1-bromo-3,4,8-trichloro-9-dichloromethyl-1-*E*,5-*E*,7-octatriene** from *P. suhrii* inhibited biofilm formation through antibacterial activity on planktonic cells but could not prevent biofilm formation when employed as a film on the surface of microtitre plate wells. **1,4,8-tribromo-3,7-dichloro-3,7-dimethyl-1*E*,5*E*-octadiene** and **4,6-dibromo-1,1-dichloro-3,7-dimethyl-2*E*,7-octadiene** inhibited biofilm formation when applied as a film to the microtitre plate wells but had no significant antibacterial activity.

No potential antifouling agents were identified in this project but the antimicrobial activity exhibited by the crude algal extracts was highly encouraging and a number of new research areas have been identified.

TABLE OF CONTENTS

Chapter Three: Halogenated Monoterpenes from *Plocamium corallorhiza*

LIST OF FIGURES

LIST OF TABLES

LIST OF SCHEMES

LIST OF ABBREVIATIONS

APCI-MS	Atmospheric Pressure Chemical Ionization Mass Spectrometry
APPI-MS	Atmospheric Pressure Photoionization-Mass Spectrometry
°C	Degrees Celsius
CI-MS	Chemical Ionization-Mass Spectrometry
CET	Carboxyethylethylidine
COSY	^{1}H-^{1}H Homonuclear Correlation Spectroscopy
d	Doublet
dd	Doublet of doublets
eV	Electron Volt
DEPT	Distortionless Enhancement by Polarisation Transfer
DMSO	Dimethyl Sulphoxide
EI-MS	Electron Impact Mass Spectrometry
ESI-MS	Electrospray Ionization-Mass Spectrometry
EtOAc	Ethyl Acetate
FAB-MS	Fast Atom Bombardment Mass Spectrometry
Fctn	Fraction
GC	Gas Chromatograpy
GC-MS	Gas Cromatography – Mass Spectrometry
H/E	Hexane / ethyl acetate
HMBC	Heteronuclear Multiple Bond Correlation
HSQC	Heteronuclear Single Quantum Coherence
HPLC	High Performance Liquid Chromatography
HREI-MS	High Resolution Electron Impact Mass Spectrometry
Hz	Hertz
IC_{50}	Inhibitory Concentration 50 %
IR	Infrared
J	Spin-Spin coupling constant (Hz)
LR-MS	Low Resolution Mass Spectrometry
MeOH	Methanol

m	Multiplet
m/z	Mass to charge ratio
multi	Multiplicity
MW	Molecular weight
NMR	Nuclear Magnetic Resonance Specroscopy
NOESY	Nuclear Overhauser enhancement spectroscopy
ppm	Parts per million
PFBHA	*O*-(2,3,4,5,6-pentafluorobenzyl)hydroxylamine
q	Quartet
s	Singlet
t	Triplet
Prtn	Partition
TLC	Thin Layer Chromatography
UV	Ultra Violet

Chapter One
General Introduction and Review of Literature

1.1 Introduction

Biofouling, once thought of as a maritime phenomenon, is recognized today in many distinct areas. Biofouling, simply put, means the accumulation of unwanted biological material upon a surface. That surface may be an intravenous catheter delivering lifesaving medicines to a patient in hospital, it may be the membrane that filters the water we drink each day; biofouling ranges from the mould on the shower tiles to the complex layer made up of a variety of organisms coating the hull of a slow moving ship.

The unfavorable effects resulting from biofouling, i.e. chronic human microbial infections, increased drag on ships, corrosion and dilapidation of underwater infrastructure, or simply the hours of scrubbing those mouldy tiles, has naturally instilled in us a strong desire to prevent it.

In likeness to humans, marine algae experience negative effects relating to biofouling. They have, over evolutionary time, adapted a number of useful defense mechanisms aimed at preventing the accumulation of biological material upon their thalli. The production of biogenic compounds that exhibit antibacterial, antifungal, antialgal and antimacrofouling activity is one manner in which algae prevent this phenomenon.

It has been suggested that an intrinsic link exists between the colonization of a surface by bacteria and the onset of macrofouling. The aim of this project was to investigate the antimicrobial potential of selected Southern African marine algae with the hope of isolating compounds that may posses the ability to inhibit bacterial biofilm formation. Marine natural products have, and may still provide useful leads for the discovery of antifouling agents, which may find use as antibiotics for use in humans and animals, or the use of antimacrofouling compounds for use in marine antifouling systems.

1.2 Drug Discovery and Marine Natural Products Chemistry

Marine ecosystems are highly complex environments in which macro- and micro-organisms constantly compete for space and nutrients. Those organisms living in this environment must continuously defend themselves against other pathogenic, parasitic, saprophytic and fouling organisms (Kubanek *et al.*, 2003).

With global climate changes, the introduction of pathogens to new areas (Harvell *et al.*, 1999; Drake *et al.*, 2005) and the increased stress on marine hosts caused by human activity, the frequency of disease among marine macro-organisms is increasing (Harvell *et al.*, 1999). Nevertheless, it has been demonstrated that most epidemics caused by pathogens in the marine environment are host specific and although devastating, are apparently infrequent with the elimination of susceptible organisms resulting in the selection of disease resistance traits over evolutionary time (Kubanek *et al.*, 2003).

Competition for space, fouling of the surface, predation, the need for successful reproduction and the need for defense against pathogens, has led to the evolution of unique secondary metabolites (Donia and Hamann, 2003; Bhadury and Wright, 2004).

Natural products obtained via marine bioprospecting include a substantial number of biologically active compounds that may be useful in the treatment of human ailments (Donia and Hamann, 2003; Haefner, 2003). Unfortunately it regularly occurs that compounds heralded for their potency *in vitro* exhibit less than ideal activity *in vivo* with regard to bioavailability and unwanted side effects (Haefner, 2003). Tulp and Bohlin (2002) suggest that the natural environment of humankind is the more likely source of compounds with relevant mechanisms of action. Indeed, approved and registered drugs of terrestrial origin far outnumber those from the marine biota. Even so the comparative periods of investigation differ so drastically that one cannot hope to draw reasonable conclusions as to the superior source. It must also be remembered that the molecular physiology of eukaryotic cells evolved in early marine ancestors whose molecular mechanisms are highly conserved, and it is these mechanisms that are targeted by many novel drug candidates (Haefner, 2003).

The escalation in resistance of pathogenic microbes to contemporary therapeutic agents has lead to increased pressure to find compounds with novel scaffolds and mechanisms of action (Clardy *et al.*, 2006). Although research and development of natural products by larger pharmaceutical companies has waned in recent years, advances in technology have eliminated many hurdles that hindered progress in the past, allowing smaller initiatives to persevere in the field (Marris, 2006).

1.2.1 Anti-infective Natural Products

1.2.1.1 Antifungals

While increasing microbial resistance is alarming, another motivating force behind the search for potent anti-infectives is the rapidly rising number of immunocompromised patients. As a result of immune debilitation, previously innocuous microbial contagions are able to overwhelm host defenses and establish chronic infection, subsequently increasing morbidity and mortality of the host. Infection of a healthy human being by the fungus *Cryptococcus neoformans* rarely causes harm; however, the inability of HIV/AIDs, chemotherapy and transplant patients to combat this yeast (Mitchell and Perfect, 1995) often has fatal consequences.

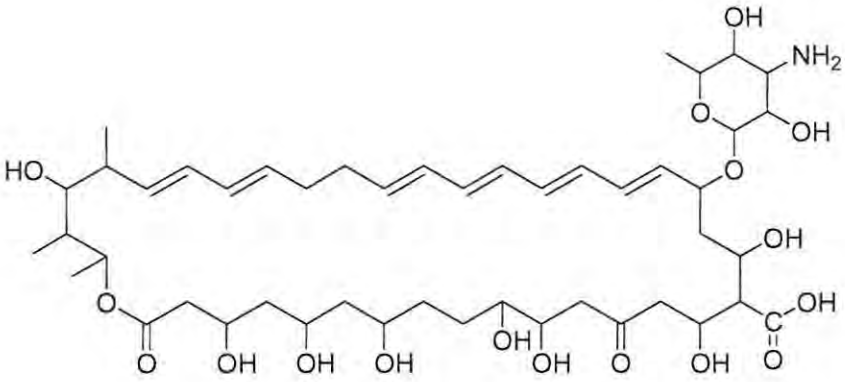

Amphoteracin B **1.1**

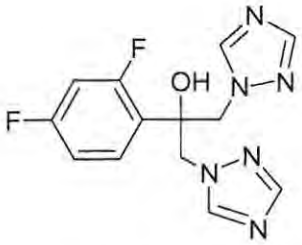

Fluconazole **1.2**

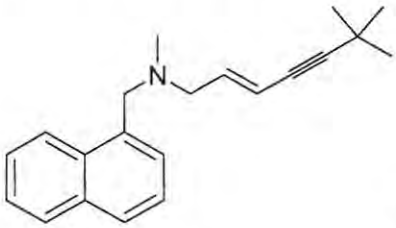

Terbinafine **1.3**

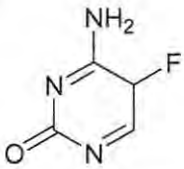

5-fluorocytosine **1.4**

Figure 1.1 Contemporary antifungal agents used for the treatment of human mycoses

Most antimycotics in use today have been in existence for decades and have undesirable side effects. Amphotericin B (**1.1**), a polyene macrolide binds nonspecifically to sterols, causing membrane permeability and inhibition of cytochrome P-450 and the electron transport chain. Unfortunately this mechanism is not selective for the fungal cell as are the mechanisms employed by many other agents of today. Like mammalian cells, fungi are eukaryotes; for that reason agents that inhibit protein, RNA or DNA biosynthesis in fungi also have potential for host toxicity (Georgopapadakou and Walsh, 1994).

Antifungal compounds from marine sources include macrolides, polyketides, alkaloids and fatty acid esters (Donia and Hamann, 2003).

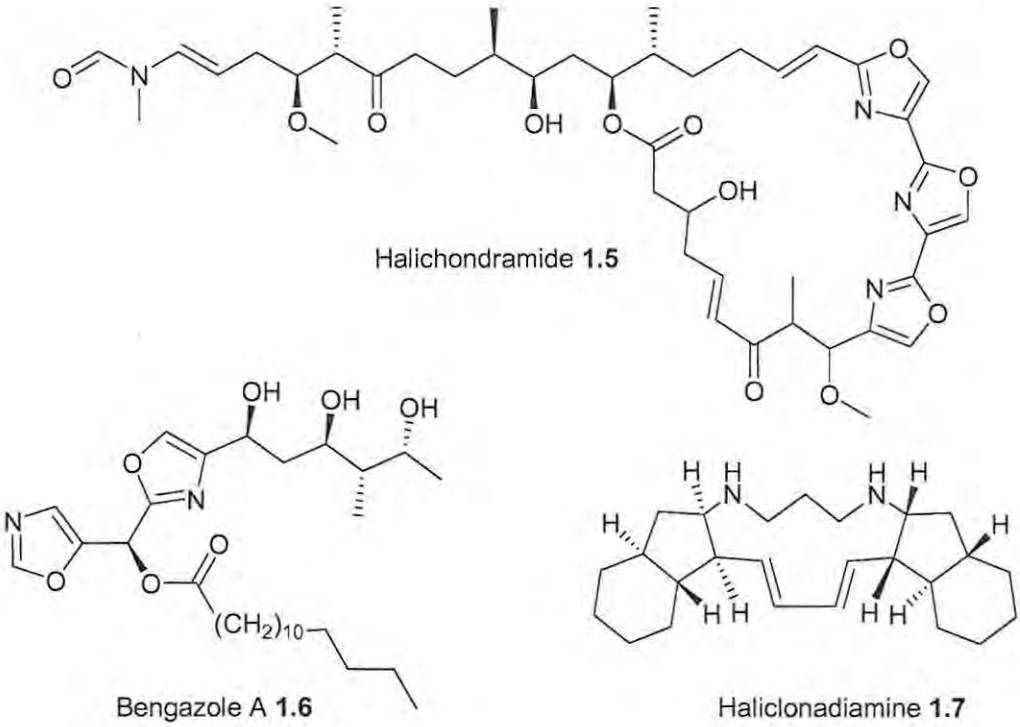

Halichondramide **1.5**

Bengazole A **1.6**

Haliclonadiamine **1.7**

Figure 1.2 Antifungal compounds of marine origin

Halichondramide (**1.5**), is a macrolide isolated from the sponge genus *Halichondria*. Like Amphotericin B, it has been found to be generally cytotoxic. Halichondramide exhibits activity against *Candida albicans* at a concentration of 0.2 µg/ml and is highly toxic to mice at 1.4 mg/kg (Kernan *et al.*, 1988). Unfortunately, until now, the cytotoxicity of such compounds has outweighed the benefits of their antifungal activity. The cytotoxicity of other examples such as Bengazole A (**1.6**) and Haliclonadiamine (**1.7**) has not been measured and as yet few reasonable candidates for clinical use have emerged (Donia and Hamann, 2003).

1.2.1.2 Antimycobacterials

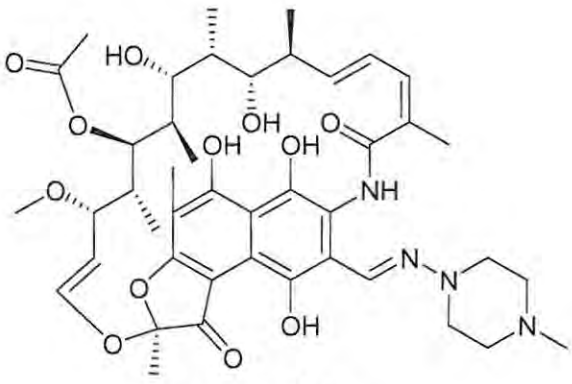

Rifampicin **1.8**

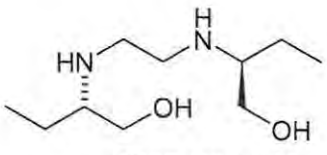

Ethambutol **1.9**

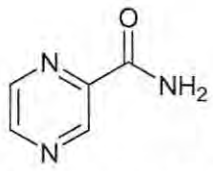

Pyrazinamide **1.10**

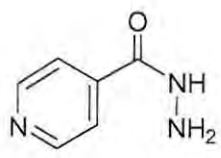

Isoniazid **1.11**

Figure 1.3 Antimycobacterial compounds used to treat tuberculosis in humans

The resurgence of tuberculosis (TB) globally has prompted renewed interest in the development of antituberculosis drugs. After having been almost completely eliminated in some countries by the widespread use of the BCG vaccine and successful treatment of those infected, the HIV/AIDs pandemic has once again allowed the mycobacterium to regain a foothold in the lethal and serious disease category (Zhang, 2005). Tuberculosis is found predominantly in developing countries whose populations cannot afford to pay high prices for treatment. Low return on investment by pharmaceutical companies meant that little research was done into new anti-TB drugs, because of this no novel agents have emerged in the last few decades (Zhang, 2005[1]). In South Africa, the proposed treatment for extremely drug resistant tuberculosis (XDR TB) consists of the archaic TB drugs capreomycin (**1.12**) and para-amino salicylic acid (**1.13**)[1]; these were initially replaced by the more effective and less toxic multi-drug regimen of rifampicin (**1.8**), ethambutol (**1.9**), pyrazinamide (**1.10**) and izoniazid (**1.11**) (Jindani *et al.*, 2004).

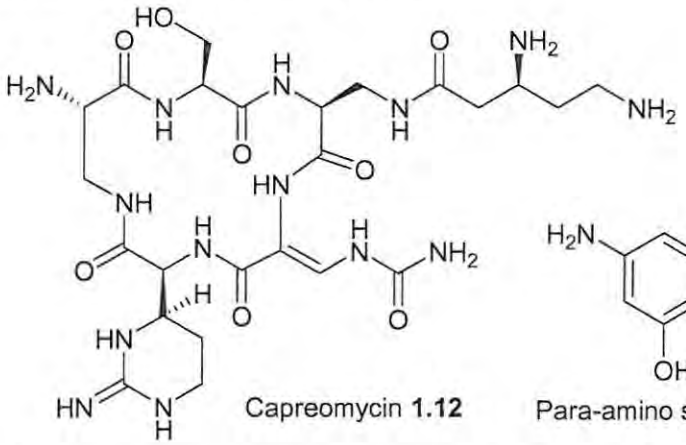

Capreomycin **1.12** Para-amino salicylic acid **1.13**

Figure 1.4 Antimycobacterial compounds proposed to treat XDR TB

Relatively little marine natural products research has been done in this area; despite this, a number of compounds isolated from sponges, soft corals and other marine invertebrates display sufficient mycobacterial inhibitory activity to warrant further clinical investigation (Donia and Hamann, 2003).

A noteworthy example is the alkaloid Ircinol A (**1.14**), thought to be the likely biogenetic precursor to (+)-8-hydroxymanzamine (**1.15**) isolated from a sponge of the *Pachypellina* sp. (Donia and Hamann, 2003) as well as from an unidentified *Petrosiidae* genus (Yousaf *et al.*, 2002). This manzamine-type alkaloid displays a minimum inhibitory concentration (MIC) of 0.91 µg/ml, in comparison with Ircinol A (**1.14**) with an MIC of 1.93 µg/ml. Although not as potent, Ircinol A (**1.14**) displays low cytotoxicity making it a more likely drug candidate (Yousaf *et al.*, 2002).

[1] SA Government report

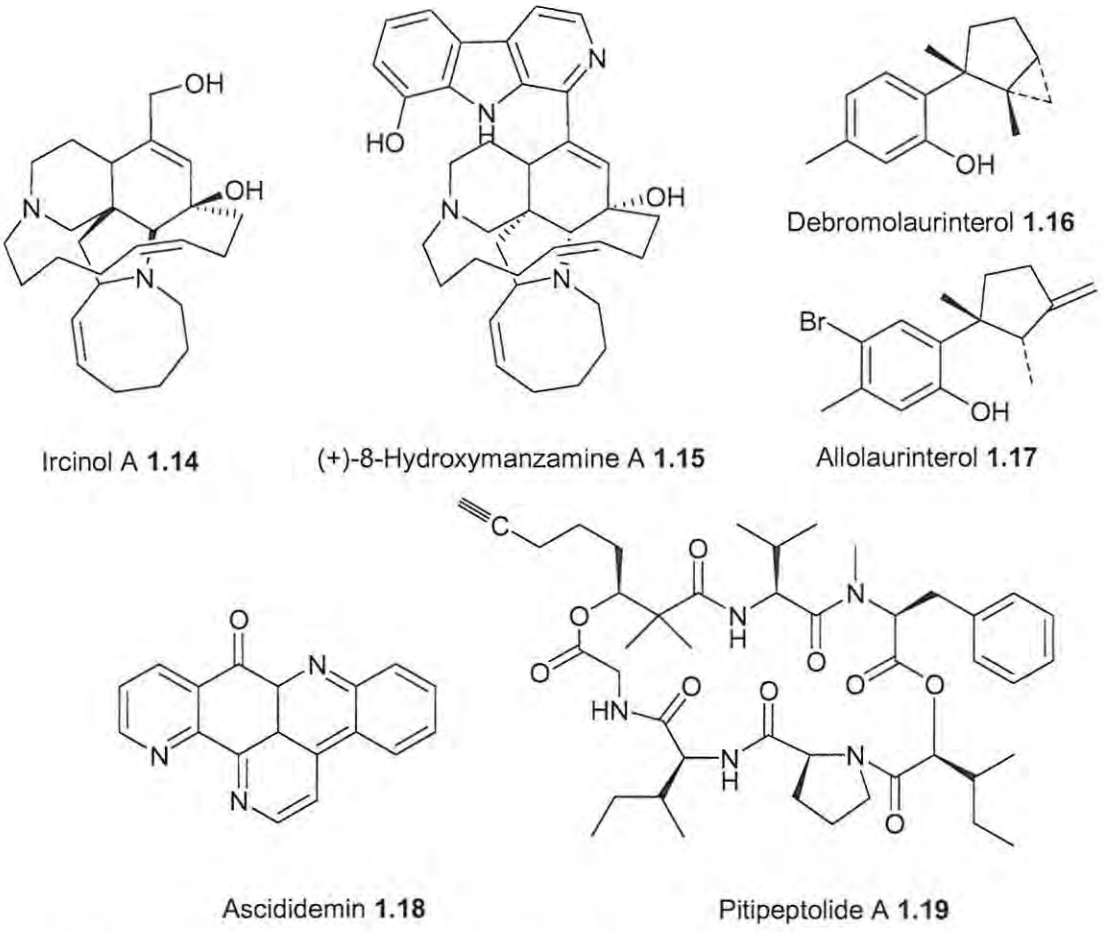

Figure 1.5 Compounds with antimycobacterial activity of marine origin

1.2.1.3 Antivirals

The isolation of arabinosyl nucleosides from the sponge *Cryptotethia crypta* provided an important therapeutic lead in the anti-viral arena. Modification of the molecule's sugar moiety lead to the development of ara-A (**1.20**), a semisynthetic compound that is known by the trade name vidarabine. Further alteration of the nucleoside afforded azidothymidine (**1.22**) (zidovudine), ara-C (**1.21**) (cytarabine) and acyclovir (Georgewill and Ikimalo, 2004; Donia and Hamann, 2003). Azidothymidine (**1.22**) is an antiretroviral drug used to control the viral load in HIV infected persons (De Clercq, 2004).

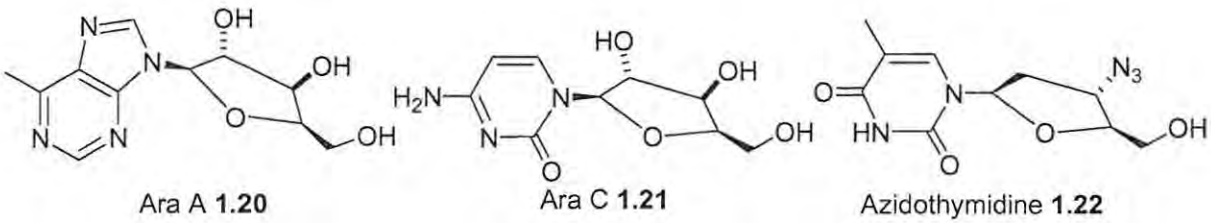

Figure 1.6 Antiviral compounds of marine origin

1.2.1.4 Antibacterials

Bacterial infection still presents a serious danger to humankind and the discovery of new antibiotics is of high priority. Clinically useful antibiotics have mainly been produced by actinomycetes and fungi (Table 1.1).

Table 1.1 Clinically useful antibiotics produced by microbes

Antibiotic	Producer organism	Activity	Site or mode of action
Penicillin	*Penicillium chrysogenum*	Gram-positive bacteria	Wall synthesis
Cephalosporin	*Cephalosporium acremonium*	Broad spectrum	Wall synthesis
Griseofulvin	*Penicillium griseofulvum*	Dermatophytic fungi	Microtubules
Bacitracin	*Bacillus subtilis*	Gram-positive bacteria	Wall synthesis
Polymyxin B	*Bacillus polymyxa*	Gram-negative bacteria	Cell membrane
Amphotericin B	*Streptomyces nodosus*	Fungi	Cell membrane
Erythromycin	*Streptomyces erythreus*	Gram-positive bacteria	Protein synthesis
Neomycin	*Streptomyces fradiae*	Broad spectrum	Protein synthesis
Streptomycin	*Streptomyces griseus*	Gram-negative bacteria	Protein synthesis
Tetracycline	*Streptomyces rimosus*	Broad spectrum	Protein synthesis
Vancomycin	*Streptomyces orientalis*	Gram-positive bacteria	Protein synthesis
Gentamicin	*Micromonospora purpurea*	Broad spectrum	Protein synthesis
Rifamycin	*Streptomyces mediterranei*	Tuberculosis	Protein synthesis

Table reproduced from http://helios.bto.ed.ac.uk/bto/microbes/penicill.htm

Cephalosporins were the first antibiotics isolated from a marine source and although few other agents from marine biota have been registered, many extracts and compounds isolated from marine organisms show potent antibacterial activity (Donia and Hamann, 2003; Haefner, 2003; Clardy *et al.*, 2006). Unfortunately, despite their activity, few compounds are studied further in this regard. Squalamine (**1.23**) is an example of a marine natural product that displayed potent antibacterial activity, however is undergoing clinical trials for the treatment of cancer (Moore *et al.*, 1993).

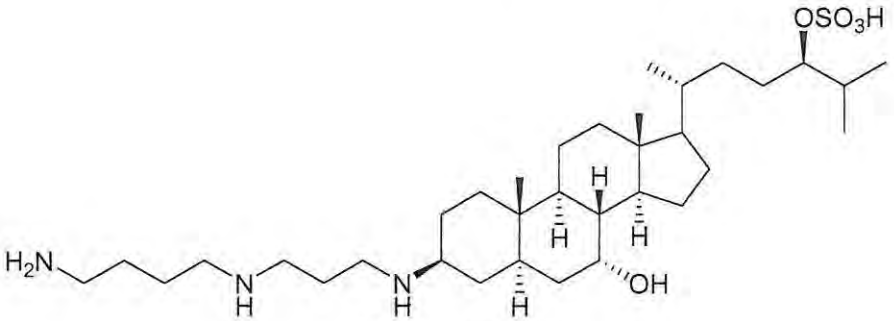

Squalamine **1.23**

Halogenated furanones (e.g. **1.24** and **1.25**) from the red alga *Delisea pulchra* are unique agents that may offer leads for the treatment of chronic human infections. Without injuring the bacteria, they interfere with vital chemical signaling required to initiate the infection process and express virulence traits in certain bacteria such as *Pseudomonas aeruginosa* (Hentzer *et al.*, 2002; Hentzer and Givskov, 2003).

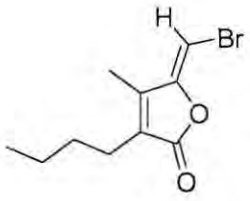

1.24

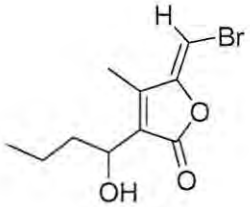

1.25

1.2.2 General Medicinal Applications of Natural Products

Natural products isolated from marine organisms are regularly screened for activity against non-infectious disease states. The isolation of therapeutic leads with antineoplastic properties has encouraging implications in the search for novel antitumour drugs.

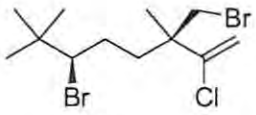

Halomon **1.26**

Halomon (**1.26**), a halogenated monoterpene from the red alga *Portieiria hornemannii* (Fuller *et al.*, 1994) and palmerolide A (**1.27**), a macrolide from the Antarctic tunicate *Synoicum adareanum* (Diyabalanage *et al.*, 2006) are examples of compounds with potent anticancer activity. Trabectidin (**1.28**) also known as ecteinascidin 743 and Yondelis™ from the Mediterranean and Caribbean sea squirt *Ecteinascidia turbinata* and Aplidin™ from the sea squirt *Aplidium albicans* are two antitumour agents currently on the market (Marris, 2006; Erba *et al.*, 2001; Jimeno *et al.*, 2004).

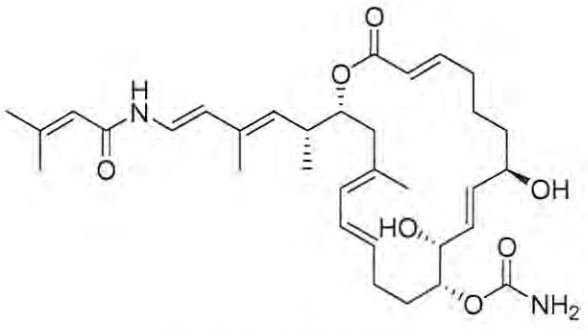

Palmerolide A **1.27**

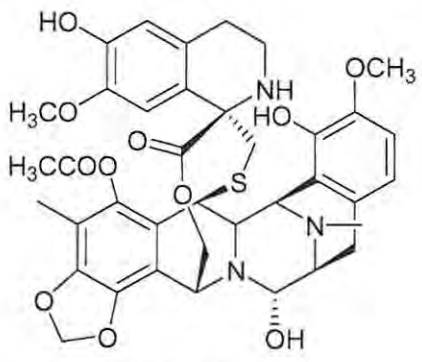

Trabectedin **1.28**

The management of chronic pain has been revolutionized by the FDA approval of Ziconotide, a non-narcotic analgesic isolated from cone snail venom of *Conus magus* (Mathur, 2000; Haefner, 2003; Marris, 2006).

Although a great deal of research has been done into the chemical and biological diversity of the marine environment, it is suspected that we have merely glimpsed the tip of the iceberg. Unfortunately, despite hundreds of new compounds being reported annually, only a fraction of these reach pre-clinical or clinical trials, and even fewer are registered as medicines for humans use (Rouhi, 2003).

Nevertheless, despite many secondary metabolites not being ideal drug candidates, there are other ways in which they may be useful to mankind. One of the possibilities, especially for compounds with antimicrobial properties, is the potential for use as industrial or maritime antifouling agents.

1.3 Antifouling and Marine Natural Products Chemistry

1.3.1 Marine Biofouling and Antifouling

Marine biofouling is the progressive colonization of both living and inanimate undefended surfaces mainly by micro-organisms, barnacles, tunicates, bryozoans and macro-algae (Wahl, 1989; Bhadury, 2004; Krug, 2006). The process is sequential and commences seconds after immersion of a solid surface in seawater. The initial stage is known as the conditioning phase and involves the adsorption of organic (mainly macromolecules) and inorganic molecules to the surface, whereby it becomes coated in a nutritional layer suitable for colonization by bacteria. Initially, like macromolecules before them, bacterial cells are adsorbed onto the surface, after which they may or may not become detached. Those cells whose glycocalix form covalent bonds with the macromolecular film, secrete a polysaccharide slime which initiates adhesion and is irreversible. A primary biofilm begins to form. The third stage involves colonization of the surface by yeasts, protozoans and diatoms, usually occurring a number of days post immersion. From one week after immersion onwards, the fourth stage then begins, which entails the attachment of barnacle larvae and algal spores (Wahl, 1989). A dynamic, vital and complex layer forms which often exerts deleterious effects on a living host as well as man-made underwater infrastructure and maritime vessels (Clare, 1995; Watermann, 1999; Lopez *et al.*, 2006).

For benthic marine organisms, fouling by calcareous epibionts increases weight and decreases buoyancy. Especially crustose epibionts can reduce elasticity of the host organism and enhance breakage in turbulence. The increase in friction and drag can even result in the host being torn from the substrata (Wahl, 1989).

Fouling of ships' hulls, underwater pipelines, off shore oil platforms and other forms of maritime infrastructure causes corrosion, drag and dilapidation which decreases efficiency and increases maintenance costs. The cost of keeping fouling organisms from settling on these structures comes to billions of Dollars each year (Clare, 1995).

Ocean going vessels have long since been struggling to keep their hulls free of fouling organisms; to this end a number of noxious chemical such as arsenic, sulphur and gunpowder have been used (Clare, 1995; Chambers *et al.*, 2006). In the 1960's tributyltin (TBT, **1.29**) containing products were introduced as effective, inexpensive and long lasting antifouling paints for the use on ships' hulls and underwater infrastructure (Clare, 1995; Bray, 2007).

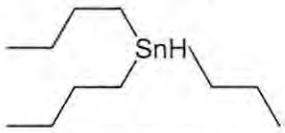

Tributyltin **1.29**

In the 1980's serious concerns were raised about the toxicity of TBT (**1.29**) and other organotins which were found to be responsible for the development of imposex (masculinisation of females) in gastropods (*Nucella lapillus*) and non-coastal snails. Toxic effects were first noted in oyster crops (*Crassostrea gigas)* where TBT (**1.29**) caused unnatural shell thickening and ultimate crop failure. The organotin's presence has also been detected in oceanic species of cetaceans and pelagic fish such as skipjack tuna (*Katsuwonus pelanus)* (Bray, 2007).

Over time the toxicity became apparent and in 1990 the International Maritime Organization (IMO) - the United Nations Agency concerned with the safety of shipping - adopted a resolution recommending that governments assume measures to eliminate antifouling paints containing TBT (**1.29**). In 2001 the IMO adopted the International Convention on the Control of Harmful Antifouling Systems on Ships (AFS) citing substantial risk of toxicity and other chronic impacts of TBT (**1.29**) to ecologically and economically important marine organisms. A global ban on TBT (**1.29**) and organotin containing antifouling systems was to have come into effect of the 1st January 2008, but as of July 2007, only 24 of the required 25 nations required to ratify the convention, had signed.[2]

In the 1990's impending legislation restricting the application and use of organotin containing antifouling paints prompted the development of tin free coatings. Many of the early replacements exhibited a short life-span and their potential for ecotoxicity was largely unknown (Watermann, 1999). In the past decade, a number of alternative approaches to antifouling have emerged (Table 1.2) of which two main directions have been pursued.

Table 1.2 Antifouling systems developed to replace TBT containing products. (Watermann, 1999)

Antifouling approach	Brief Description
Copper containing paints	Initially replaced TBT containing paints; Persistent, thus risk of bioaccumulation; ecotoxic.
Natural products	Utilizing natural products with antifouling activity; natural degradation pathways; repellant rather than toxic; acquiring large quantities problematic.
Hydrogels and viscous layers	Mucopolysaccharide surface reduces friction, prevents attachment; utilized by fish; may offer a vehicle for incorporation of antifouling compounds.
Non-stick coatings	Silicones and fluoropolymers, merely lower surface attachment. Also include the self cleansing coatings, the fouling peels away. High price, difficult application, mechanical frailty
Electrical currents	Electrical currents are conducted through the hull; highly effective; can be switched on when ship is stationary or traveling slowly

[2] Seas at Risk Electronic Web Page

The first was to develop foul release coatings that prevented the normal adhesion of hard fouling organisms such as barnacles to surfaces. The second avenue involved the investigation of biogenic compounds with antifouling activity from marine organisms (Clare, 1998; Fusetani, 2004). Ideally approaches to contemporary antifouling systems should concentrate on systems possessing a favorable profile with respect to acute and chronic toxicity. If an antifouling agent is employed, it should not result in developmental and reproductive toxicity or disrupt endocrine function in non-target organisms. The agent should not bio-accumulate or become accumulated in marine sediments. It should not affect the food web or have any population effects. The agent should not have adverse effects in the field, in fish populations, result in strandings by pelagic creatures or be found in seafood (AFS, 2001).

1.3.2 Antifouling Natural Products

There are a number of advantages in employing a natural product found in the marine environment as an antifouling agent. Pathways for the compound's degradation are very likely to exist already, limiting the risk of bioaccumulation (Sjögren *et al.*, 2004). In addition, marine natural products exhibiting antifouling activity have been found to act as repellants rather than relying on toxicity (Fusetani, 2004).

Biofouling is a non-discriminate process that occurs as rapidly upon undefended living surfaces as upon inanimate objects (Steinberg *et al.*, 2002). In order to survive in the highly competitive marine environment, soft bodied, sessile marine organisms have developed chemical defense mechanisms that enable them to resist fouling (Bhadury and Wright, 2004).

Fractionation of extracts obtained from marine species has lead to the isolation of a variety of compounds from sponges, corals, macro-algae, sea grasses, bryozoans and sea-squirts (Clare, 1995; Fusetani, 2004; Bhadury and Wright, 2004). The investigation of the biogenic compounds from such organisms reveals that the prevention of biofouling may occur at multiple levels.

It is suspected that one mechanism of defense against fouling is to prevent the fundamental stage of bacterial colonization (Hellio *et al.*, 2001; Krug, 2006). By maintaining a relatively bacteria free surface, fungal and diatom attachment is reduced and the chemical cues required by copepod larvae for the induction of settlement are removed or limited, thus preventing the attachment of these macro-organisms (Krug, 2006).

Similarly by inhibiting fungal growth with compounds such as Lobophorolide (**1.30**), marine organisms like macro-algae may be more able to resist fouling by other organisms (Kubanek *et al.*, 2004).

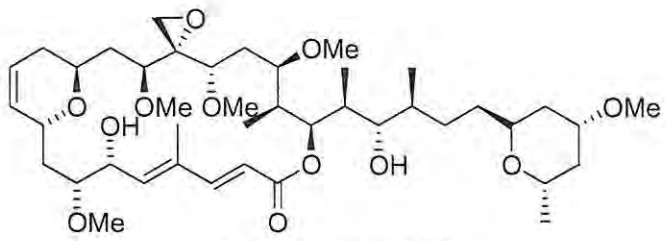

Lobophorolide **1.30**

Selected compounds act directly on the planktonic larvae, preventing settlement without adverse effects to the juvenile organism. Compound **1.31** was isolated from extracts of the sponge *Geodia barretti*, the metabolite completely inhibited *Balanus improvisus* larvae settlement at concentrations of 1.9 µg/ml. The same larvae were washed and transferred to fresh seawater in which they metamorphosed to a similar extent as those used in the control (Sjögren *et al.*, 2004).

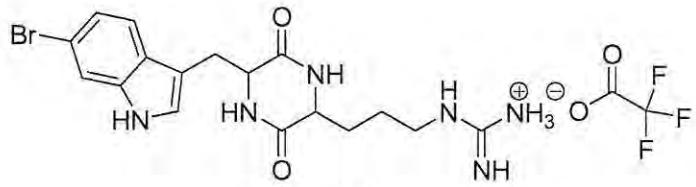

1.31

Natural product antifoulants are highly variable in their structure; nevertheless, there does appear to be a tendency for compounds with antifouling activity to possess furan and or lactone rings (Clare, 1998).

1.32

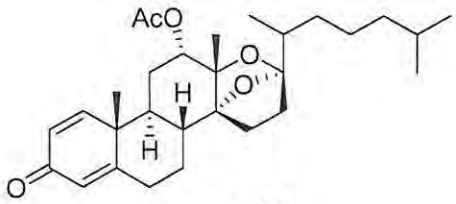

1.33

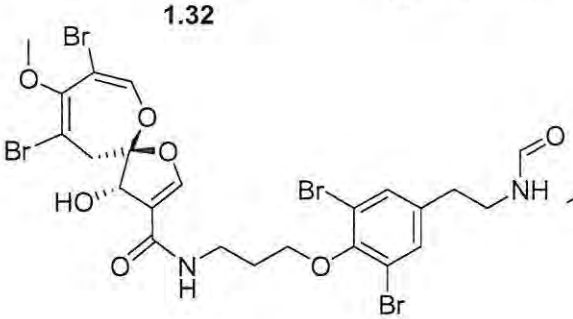

1.34

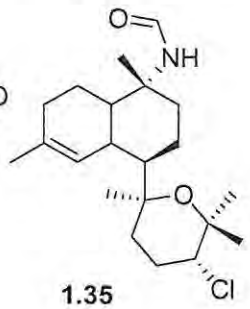

1.35

Figure 1.7 Marine natural products with antifouling activity

The brominated furanones (e.g. **1.32**) isolated from *D. pulchra* are the most potent agents yet to be isolated. These compounds and many of their analogues also prevent the settlement of algal spores and inhibit bacterial growth (Manefield *et al.*, 2000; de Nys and Steinberg 2002; Fusetani, 2004). Bromotyrosine derivatives such as Ceratinamide A (**1.34**) from the marine sponge

Pseudoceratina purpurea have also been found to inhibit barnacle larval settlement with an EC_{50} of 0.10 µg/ml (Tsukamoto *et al.*, 1996). **1.33** and **1.35** are further examples of secondary metabolites that are recognised as potential antifoulants (Fusetani, 2004).

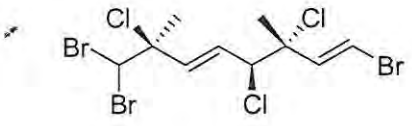

1.36

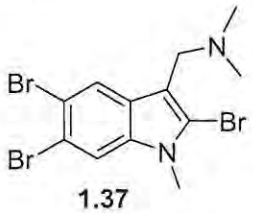

1.37

Albeit common, not all compounds exhibiting antifouling activity possess furan and lactone rings, as evidenced by the antifouling activity displayed by the halogenated monoterpene (**1.36**) isolated from the red marine alga *Plocamium costatum* (König *et al.*, 1999a) and the highly potent heterocyclic compound 2,5,6-tribromo-1-methylgramine (**1.37**) from the bryozoan *Zoobotryon verticillatum*. Compound **1.37** is reported to be ten times more potent than TBT (**1.29**) yet exhibits very low toxicity (Sato and Fenical, 1983).

Particularly pertinent to this study are the examples of marine macro-algae that have shown antifouling and antimicrobial activity (Table 1.3). The chemical defense systems employed by macro-algae have long since been investigated, however the focus of such investigations was largely on their ability to deter herbivorous predators (Paul and Puglisi, 2004). Because macro-algae are restricted to growing in zones that are optimal for growth, they are particularly vulnerable to fouling (Wahl, 1989). It is plausible that over time these organisms have adapted to resist fouling by a number of means. The biological activity of many compounds isolated from extracts of marine algae, ranging from antimicrobial to antimacrofouling, provides evidence that supports the theory of a multi-pronged defense.

Table 1.3 Antifouling and antimicrobial activity of selected macro-algae (Adapted from Bhadury and Wright, 2004)

Source	Biogenic compounds	Activity	References
Rhodophyceae			
Laurencia majuscula	Elatol, iso-obtusol	Antibacterial	Vairappan, 2003
Laurencia nifidica	Halogenated metabolites	Antibacterial	Vairappan *et al.*, 2001
Laurencia yonaguniensis	Brominated diterpene	Antibacterial	Takahashi *et al.*, 2002
Laurencia mariannesis	Halogenated metabolites	Antibacterial	Vairappan *et al.*, 2001
Rhodomela confervoides	Bromophenols	Antibacterial	Xu *et al.*, 2003
Polysiphonia lanosa	Dichloromethane fraction	Antibacterial	Hellio *et al.*, 2001
Chondrus crispus	Ethanolic fraction	Antibacterial	Hellio *et al.*, 2001
Plocamium costatum	Halogenated monoterpenes	Antifouling (*Balanus amphirite*)	König *et al.*, 1999a
Plocamium hamatum	Halogenated monoterpenes	Antialgal	König *et al.*, 1999b
Delisea pulchra	Halogenated furanones	Antifouling	Rasmussen *et al.*, 2000
Phaeophyceae			
Sargassum muticum	Ethanolic extract	Antialgal	Hellio *et al.*, 2002
Dictyota menstrualis	Diterpene alcohols e.g. dictyol E, pachydictyol A	Antimacrofouling (*Bugula neretina*)	Schmitt *et al.*, 1995

Thus far several natural product antifouling agents tested in the field have shown promising results. Secondary metabolites from marine organisms have also provided useful leads for the development of synthetic analogues which show both potent antifouling activity and low ecotoxicty. Highly encouraging is the fact that many of these synthetic analogues have been successfully incorporated into paints and coatings and are being tested in field studies (Fusetani, 2004).

1.4 Project Objectives

The main aim of this research was to investigate the potential of South African marine algae as a source of antimicrobial agents with a focus on antifouling compounds.

The objectives of this project were:

1. To extract secondary metabolites from Southern African marine macro-algae.
2. To screen the crude solvent extracts for antimicrobial activity against four clinically relevant pathogens.
3. To fractionate the crude extracts and isolate secondary metabolites contained therein.
4. To characterize the compounds isolated and to solve specific problems with regard to structure determination of certain metabolites.
5. To employ the secondary metabolites in assays to asses their ability to inhibit bacterial biofilm formation by *Pseudomonas aeruginosa*.

1.5 References

Bhadury, P.; Wright, P. C. Exploitation of marine algae: Biogenic compounds for potential antifouling applications. *Planta* **2004**, *219*, 561-578.

Bray, S. Tributyltin pollution on a global scale. An overview of relevant and recent research: impacts and issues. In *Evidence of the Global Impact of Organotin Highlighting the Need to Urgently Ratify the AFS Convention*. IMO document submitted by the WWF, FOEI, IUCN, INTERTANKO and Bulgaria to the Marine Environment Protection Committee. 7 July **2006**.

Chambers, L. D.; Stokes, K. R.; Walsh, F. C.; Wood, R. J. K. Modern approaches to marine antifouling coatings. *Surface & Coatings Technology* **2006**, *201*, 3642-3652.

Clardy, J.; Fischbach, M. A.; Walsh, C. T. New antibiotics from bacterial natural products. *Nature Biotechnology* **2006**, *24*, (12), 1541-1550.

Clare, A. S. Towards nontoxic antifouling. *Journal of Marine Biotechnology* **1998**, *6*, 3-6.

Clare, A. S. Natural ways to banish barnacles. *New Scientist* **1995**. http://www.newscientist.com/article/mg14519654.300-natural-ways-to-banish-barnacles.html date accessed January 14 2008.

De Clercq, E. Antiviral drugs in current clinical use. *Journal of Clinical Virology* **2004**, *30*, 115-133.

de Nys, R.; Steinberg, P.D. Linking marine biology and biotechnology. *Current Opinion in Biotechnology* **2002**, *13*, 244-248.

Diyabalanage, T.; Amsler, C.; McClintock, J. B.; Baker, B. J. Palmerolide A, a cytotoxic macrolide from the Antarctic tunicate *Synoicum adareanum*. *Journal of the American Chemical Society* **2006**, *128*, 5630-5631.

Donia, M.; Hamann, M. Marine natural products and their potential applications as anti-infective agents. *The Lancet* **2003**, *3*, 338-348.

Drake, L. A.; Meyer, A. E.; Forsberg, R. L.; Baier, R. E.; Doblin, M. A.; Heinemann, S.; Johnson, W. P.; Koch, M.; Rublee, P. A.; Dobbs, F. C. Potential invasion of microorganisms and pathogens via 'interior hull fouling': Biofilms inside ballast water tanks. *Biological invasions* **2005**, *7*, 969-982.

Erba, E.; Bergamaschi, D.; Bassano, L.; Damia, G.; Ronzoni, S.; Faircloth, G. T.; D'Incalci, M. Ecteinascidin-743 (ET-743), a natural marine compound, with a unique mechanism of action. *European Journal of Cancer* **2001**, *37*, 97-105.

Eguia López, E.; Trueba Ruiz, A.; Rio Calonge, B. R.; Girón Portilla, Bielva Tejera, C. Recent studies on antifouling systems to artificial structures in marine ecosystems. *Journal of Maritime Research* **2006** *3*, (1), 73-89.

Fusetani, N. Biofouling and antifouling. *Natural Product Reports* **2004**, *21*, 94-104.

Fuller, R. W.; Cardellina II, J. H.; Jurek, J.; Scheuer, P. J.; Alvarado-Lindner, B.; McGuire, M.; Gray, G. N.; Steiner, J. R.; Clardy, J.; Menez, E.; Shoemaker, R. H.; Newman, D. J.; Snader, K. M.; Boyd, M. R. Isolation and structure/activity features of halomon-related antitumour monoterpenes from the red alga *Portieria hornemannii*. *Journal of Medicinal Chemistry* **1994**, *37*, 4407-4411.

Georgopapadakou, N. H.; Walsh, T. J. Human mycoses: Drugs and targets for emerging pathogens. *Science* **1994**, *264*, 371-373.

Georgewill, O. A.; Ikimalo, J. Effect of Azidothymidine on CD4 positive T cells in HIV positive patients. *Journal of Applied Sciences and Environmental Management* **2004**, *8*, (2), 35-37.

International maritime organization (IMO) International convention on the control of harmful antifouling systems on ships (AFS) **2001**.

Haefner, B. Drugs from the deep: marine natural products as drug candidates. *Drug Discovery Today* **2003**, *8*, (12), 536-544.

Harvell, C. D.; Kim, K.; Burkholder, J. M.; Colwell, R. R.; Epstein, P. R.; Grimes, D. J.; Hofmann, E. E.; Lipp, E. K.; Osterhaus, A. D. M. E.; Overstreet, R. M.; Porter, J. W.; Smith, G. W.; Vasta, G. R. Emerging marine diseases – Climate links and anthropogenic factors. *Science* **1999**, *285*,1505-1510.

Hellio, C.; De La Broise, D.; Dufossé, L.; Le Gal, Y.; Bourgougnon, N. Inhibition of marine bacteria by extracts of macroalgae: potential use for environmentally friendly antifouling paints. *Marine Environmental Research* **2001**, *52*, 231–247.

Hentzer, M.; Givskov, M. Pharmacological inhibition of quorum sensing for the treatment of chronic bacterial infections. *The Journal of Clinical Investigation* **2003**, *112*, (9), 1300-1307.

Hentzer, M.; Riedel, K.; Rasmussen, T. B.; Heydorn, A.; Andersen, J. B.; Parsek, M. R.; Rice, S. A.; Eberl, L.; Molin, S.; Høiby, N.; Kjelleberg, S.; Givskov, M. Inhibition of quorum sensing in *Pseudomonas aeruginosa* biofilm bacteria by a halogenated furanone compound. *Microbiology* **2002**, *148*, 87-102.

Jimeno, J.; Faircloth, G.; Fernández Sousa-Faro, J. M.; Scheuer, P.; Rinehart, K. New marine derived anticancer therapeutics – A journey from the sea to clinical trials. *Marine Drugs* **2004**, *2*, 14-29.

Jindani, A.; Nunn, A. J.; Enarson, D. A. Two 8-month regimens of chemotherapy for treatment of newly diagnosed pulmonary tuberculosis: International multicentre randomized trial. *The Lancet* **2004**, *364*, 1244-1251.

Kernan, M. R.; Molinski, T. F.; Faulkner, D. J. Macrocyclic antifungal metabolites from the Spanish Dancer nudibranch *Hexabranchus sanguineus* and sponges of the genus *Halichondria*. *Journal of Organic Chemistry* **1988**, *53*, 5014-5020.

König, G. M.; Wright, A. D.; de Nys, R. Halogenated monoterpenes from *Plocamium costatum* and their biological activity. *Journal of Natural Products* **1999a**, 62, 383–385.

König, G. M.; Wright, A. D.; Linden, A. *Plocamium hamatum* and its monoterpenes: Chemical and biological investigations of the tropical marine red alga. *Phtyochemistry* **1999b**, *52*, 1047–1053.

Krug, P. J.; Defense of benthic invertebrates against surface colonization by larvae: A chemical arms race. *Progress in Molecular and Subcellular Biology, Subseries Marine Molecular Biology, Antifouling compounds*; Fusetani, N.; Clare, A. S. (Eds); Springer-Verlag: Berlin Heidelberg **2006**.

Kubanek. J.; Jensen, P. R.; Keifer, P. A.; Sullards, M. C.; Collins, D. O.; Fenical, W. Seaweed resistance to microbial attack: A targeted chemical defense against marine fungi. *Proceedings of the National Academy of Sciences of the United States of America* **2003**, *100*, (12), 6916-6921.

Manefield, M.; Harris, L.; Rice, S. A.; de Nys, R.; Kjelleberg, S. Inhibition of luminescence and virulence in the Black Tiger Prawn (*Penaeus monodon*) pathogen *Vibrio harveyi* by intercellular signal antagonists. *Applied and Environmental Microbiology* **2000**, *66*, (5), 2079-2084.

Marris, E. Drugs from the Deep. *Nature* **2006**, *443*, 904-905.

Mathur, V. S. Ziconotide: A new pharmacological class of drug for the management of pain. *Seminars in Anesthesia, Perioperative Medicine and Pain* **2000**, *19*, 67-75.

Mitchell, T. G.; Perfect, J. R. Cryptococcosis in the era of AIDS – 100 years after the discovery of *Cryptococcus neoformans*. *Clinical Microbiology Reviews* **1995**, *8*, (4), 515-548.

Moore, K. S.; Wehrli, S.; Roder, H.; Rogers, M.; Forrest, J. N. Jr.; McCrimmon, D.; Zasloff, M. Squalamine: An aminosterol antibiotic from the shark. *Proceedings of the National Academy of Sciences of the United States of America* **1993**, *90*, 1354-1358.

Paul, V. J.; Puglisi, M. P. Chemical mediation of interactions among marine organisms. *Natural Product Reports* **2004**, *21*, 189-209.

Rasmussen, T. B.; Manefield, M.; Andersen, J. B.; Eberl, L.; Anthoni, U.; Christophersen, C.; Steinberg, P.; Kjelleberg, S.; Givskov, M. How *Delisea pulchra* furanones affect quorum sensing and swarming motility in *Serratia liquefaciens* MG1. *Microbiology* **2000**, *12*, 3237–3244.

Report on TB, Including XDR-TB in South Africa. http//www.doh.gov.za/docs/reports/2006/xdr-tb/index.html date accessed March 28, **2007.**

Rouhi, A. M. Betting on natural products for cures. *Chemical and Engineering News* **2003**, *81*, (41), 93-94, 96-98, 100-103.

Sato, A.; Fenical, W. Gramine-derived bromo-alkaloids from the marine bryozoan *Zoobotryon verticillatum*. *Tetrahedron Letters* **1983**, *24*, (5), 481-484.

Schmitt, T. M.; Hay, M. E.; Lindquist, N. Constraints on chemically mediated coevolution: multiple functions for seaweed secondary metabolites. *Ecology* **1995**, *76*, 107–123.

Seas At Risk Issues Count Down to TBT Ban. http://www.seas-at-risk.org/n3.php?page=81 date accessed January 23, **2008**.

Sjögren, M.; Göransson, U.; Johnson, A. L.; Dahlström, M.; Andersson, R.; Bergman, J.; Jonsson, P. R.; Bohlin, L. Antifouling activity of Brominated cyclopeptides from the Marine Sponge *Geodia barretti*. *Journal of Natural Products* **2004**, *67*, 368-372.

Takahashi, Y.; Daitoh, M.; Suzuki, M.; Abe, T.; Masuda, M. Halogenated metabolites from the new Okinawan red alga *Laurencia yonaguniensis*. *Journal of Natural Products* **2002**, *65*, 395–398.

The Microbial World. http://helios.bto.ed.ac.uk/bto/microbes/penicill.htm date accessed April 20, **2007**.

Tsukamoto, S.; Kato, H.; Hirota, H.; Fusetani, N. Ceratinamides A and B: New antifouling dibromotyrosine derivatives from the marine sponge *Pseudoceratina purpurea*. *Tetrahedron* **1996**, *52*, (24), 8181-8186.

Tulp, M.; Bohlin, L. Chemical diversity: Independent of functional diversity. *Trends in Pharmacological Sciences* **2002**, *23*, 405.

Vairappan, C. S. Potent antibacterial activity of halogenated metabolites from Malaysian red algae, *Laurencia majuscule* (*Rhodomelaceae, Ceramiales*). *Biomolecular Engineering* **2003**, 20, 255-259.

Vairappan, C. S.; Suzuki, M.; Abe, T.; Masua, M. Halogenated metabolites with antibacterial activity from the Okinawan *Laurencia* species. *Phytochemistry* **2001**, *58*, 517–523.

Vecchiarelli, A.; Retini, C.; Monari, C.; Casadevall, A. Specific antibody to *Cryptococcus neoformans* alters human leukocyte cytokine synthesis and promotes T-cell proliferation. *Infection and Immunity* **1998**, *66*, (3), 1244-1247.

Wahl, M.; Marine epibiosis. I. Fouling and antifouling: some basic aspects. *Marine Ecology Progress Series* **1989**, *58*, 175-189.

Watermann, B. Alternative antifouling techniques, present and future. LimnoMar **1999**, 1-6.

Xu, N.; Fan, X.; Yan, X.; Li, X.; Niu, R.; Tseng, C. K. Antibacterial bromophenols from the marine red alga *Rhodomela confervoides*. *Phytochemistry* **2003**, *62*, 1221–1224.

Yousaf, M.; El Sayed, K. A.; Rao, K. V.; Lim, C. W.; Hu, J.; Kelly, M.; Franzblau, S. G.; Zhang, F.; Peraud, O.; Hill, R. T.; Hamann, M. 12,34-Oxamanzamines, novel biocatalytic and natural products from manzamine producing Indo-Pacific sponges. *Tetrahedron* **2002**, *58*, (37), 7397-7402.

Zhang, Y. The magic bullets and Tuberculosis drug targets. *Annual Review Pharmacology and Toxicology* **2005**, *45*, 529–564.

Chapter Two
Antimicrobial Screening of Southern African Marine Algae

2.1 Introduction

The screening of extracts from marine macro-algae has been well documented (Vlachos and Critchley, 1997; Tüney *et al.*, 2006; Taskin *et al.*, 2007; Mtolera and Semesi, 1996; Lima-Filho *et al.*, 2002; Hellio *et al.*, 2001; González del Val *et al.*, 2001) although studies on Southern African marine algae are limited. Vlachos and Critchley (1997) investigated the antimicrobial activity of 56 Southern African marine algae against a number of bacteria, moulds and yeasts. The findings presented showed that the majority of extracts were selective for Gram-positive bacteria, with few exhibiting activity against Gram-negative bacteria, yeasts or moulds. These data are consistent with results obtained from studies conducted globally (González del Val *et al.*, 2001; Hellio *et al.*, 2001; Mtolera and Semesi, 1996). Interestingly it was reported that extracts from algae of the division Phaeophyta were the most active in the assays, while extracts from members of the division Rhodophyta displayed moderate activity. Extracts from algae of the division Chlorophyta were least active against the test organisms. This was in contrast to findings obtained by González del Val *et al.* (2001) who reported members of Chlorophyta to be the most active, when compared to those from Rhodophyta and Phaeophyta.

It has been established that variation in growth conditions of the algae (González del Val *et al.*, 2001), extraction procedures (Cronin *et al.*, 1995; Lima-Filho *et al.*, 2002; Tüney *et al.*, 2006) and the type of antimicrobial assay employed (Valgas *et al.*, 2007) can significantly affect the antimicrobial activity of the extracts. Tüney *et al.* (2006) demonstrated the negative effect drying of the algae has on antimicrobial activity, while Cronin *et al.* (1995) provided evidence to suggest that employing polar solvents such as methanol (MeOH) may lead to the creation of artefacts within the extracts. The use of MeOH alone, also has decreased extraction efficacy as compared to extraction with a combination of solvents such as CH_2Cl_2-MeOH (2:1) (Cronin *et al.*, 1995). Both Lima-Filho *et al.* (2002) and Tüney *et al.* (2006) showed that non-polar extracts possess greater antimicrobial activity than their polar counterparts. This is not highly surprising as chemical cues for inhibition of settlement and colonization of marine organisms have been found to be lipophilic; required on the surface of the organisms rather than being widely dispersed in the water column (Steinberg *et al.*, 2002). Heating of the solvent and algal material for prolonged periods of time may also lead to decreased activity, with the loss of volatile metabolites and degradation of thermolabile compounds.

Screening methods most commonly used when testing crude algal extracts include the disc and well agar diffusion methods; and the bioautographic methods (direct, using a TLC chromatogram and indirect, agar overlay of TLC chromatogram). Studies conducted to compare techniques showed that the well agar diffusion method displayed greater sensitivity than the disc variant and

that, although there was no significant difference between agar diffusion and bioautographic methods, the latter provided better conditions for microbial growth (Valgas *et al.*, 2007). For each of these methods, antimicrobial activity is measured in millimetres of growth inhibition. Alternative approaches such as colorimetric, quantitative dilution methods afford minimum inhibitory concentrations (MIC's) for extracts (Hunfeld *et al.*, 2000). The MIC is the lowest concentration of extract at which no microbial growth is detected and is considered the "gold standard" for determining the susceptibility of a micro-organism to antimicrobials (Andrews, 2001). Colorimetric antimicrobial assays often employ tetrazolium salts which are reduced by metabolically active micro-organisms to an easily quantified coloured substance (Tunney *et al.*, 2004).

Although extraction techniques and screening methods vary, the very fact that a great number of algal extracts in a wide variety of studies exhibit remarkable antimicrobial activity is both encouraging and exciting to the natural products chemist.

Throughout the history of marine natural products chemistry, there has been much debate about the ecological role of biogenic compounds (Fenical, 1975; Hay and Fenical, 1988; Bhadury and Wright, 2004; Paul and Puglisi, 2004; Krug, 2006). However, in the search for natural product antifoulants for industrial application, or new antibiotics, the ecological function in the alga has little bearing; the compound simply needs to work in a way that is effective yet harmless to non-target organisms.

On the other hand an understanding of the ecological interactions between algae and their microbial populations is by no means insignificant. There is much to learn from the natural world, and it would be to our detriment to discount the possibility of learning alternative ways to prevent and control the growth of micro-organisms. The most efficient prevention of fouling in algae may be more deterrent than toxic (Fusetani, 2004), more gentle persuasion, than outright biocidal; thus relying solely on antimicrobial assays in the search for antifouling compounds has its limitations.

With this knowledge in mind, results of antimicrobial screening assays were not accepted *verbatim*, but were used as a guide for possible sources of antifouling compounds. Extraction of numerous algae also has as its aim, a broadening of knowledge of the biological activity and natural products chemistry of Southern African marine flora.

2.1.1 Chapter aims

As part of a programme to explore the biomedical potential of South African marine algae, 26 algal extracts were screened for antimicrobial activity against four human pathogens. Preliminary biological activity data for the extracts was required in the selection of algae that were to be investigated for their potential to produce secondary metabolites with antifouling activity.

Figure 2.1 Low tide at one of the Eastern Cape collection sites near Kenton-On-Sea

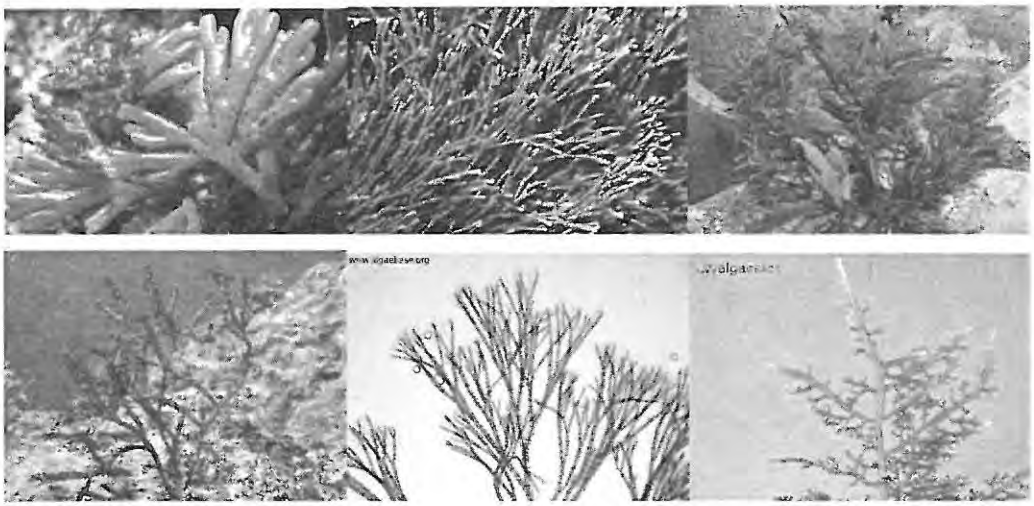

Figure 2.2 Selected South African marine algae extracted for antimicrobial screening (Guiry and Guiry, 2008). Top row from left to right: *Laurencia flexuosa*, *Amphiroa ephedraea*, *Sargassum elegans.* Bottom row from left to right: *Gracilaria aculeata*, *Polysiphonia incompta*, *Gelidium capense.*

2.2 Results and Discussion

2.2.1 Collection of algae

Several collections were made from various sites along the Southern African coastline, including Kenton-on-Sea and Noordhoek in the Eastern Cape and Kalk Bay in the Western Cape. Voucher specimens were identified by Professor John J. Bolton of the Department of Botany, University of Cape Town. Subsequent to collection, the samples were transported to the laboratory on ice where they were carefully sorted and stored at -4 °C.

2.2.2 Extraction and prefractionation of algae

The algae were all extracted following a standard protocol which involved sequential extraction with methanol, and dichloromethane-methanol (CH_2Cl_2-MeOH, 2:1). The solvent extracts were further partitioned between MeOH-H_2O-*n*-hexane (9:1:10), MeOH-H_2O-CH_2Cl_2 (7:3:10) and H_2O-EtOAc (1:1) to give a *n*-hexane (fr A), a CH_2Cl_2 (fr B) and EtOAc (fr C) crude fractions. Organic material was recovered from the aqueous partition using an HP-20 column which was subsequently washed with MeOH, CH_2Cl_2 and *n*-hexane to afford an HP-20 fraction (fr D). Extracts with a mass greater than 300 mg were then screened for antimicrobial activity against four ubiquitous micro-organisms.

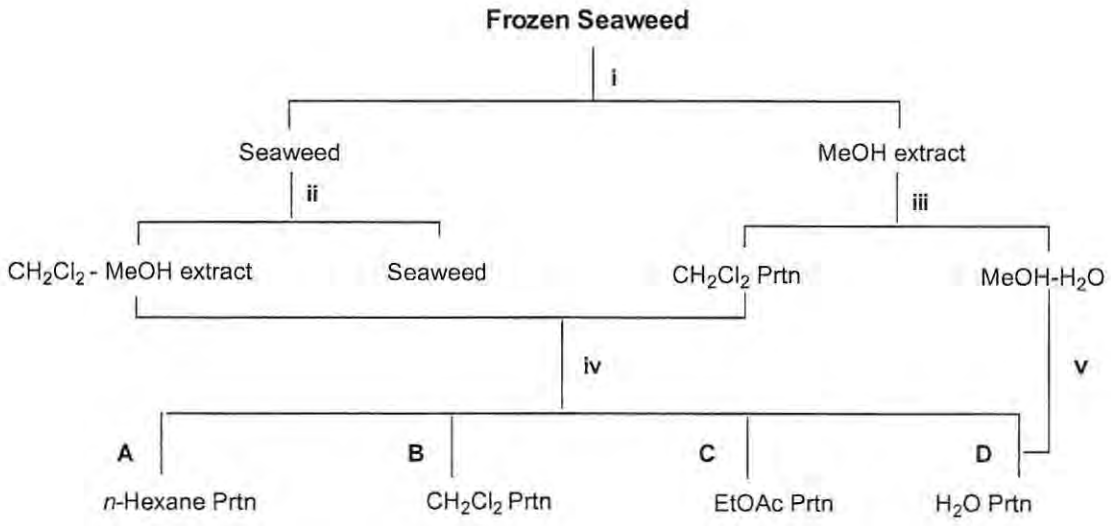

Scheme 2.1 General scheme for the extraction and prefractionation of Southern African marine macro-algae.

Conditions: i) MeOH, 1 hour, 4 °C ii) CH_2Cl_2-MeOH (2:1) 30 minutes 30 °C iii) Liquid-liquid extraction of MeOH with CH_2Cl_2 iv) Solvent partitioning v) Evaporation of MeOH *in vacuo*

Table 2.1 Algae collected and extracted for this study

Class	Order	Family	Species	Collection code	Site of Collection	Dry weight*
Rhodophyta						
Florideophyceae	Ceramiales	Rhodomelaceae	*Laurencia flexuosa*	KOS06-6	Kenton-On-Sea	15.0 g
	Ceramiales	Rhodomelaceae	*Laurencia flexuosa*	NDK06-6	Noordhoek	33.3 g
	Ceramiales	Rhodomelaceae	*Pterosiphonia cloiophyla*	KB06-9	Kalk Bay	8.8 g
	Ceramiales	Rhodomelaceae	*Polysiphonia incompta*	KOS06-15	Kenton-On-Sea	35.05 g
	Ceramiales	Rhodomelaceae	*Polysiphonia incompta*	NDK06-19	Noordhoek	28.9 g
	Corallinales	Corallinaceae	*Amphiroa ephedraea*	KOS06-23	Kenton-On-Sea	101.3 g
	Gelidiales	Gelidiaceae	*Gelidium abbottiorum*	KOS06-2	Kenton-On-Sea	106.5 g
	Gelidiales	Gelidiaceae	*Gelidium capense*	NDK06-10	Noordhoek	55.3 g
	Gelidiales	Gelidiaceae	*Gelidium pteridifolium*	KOS06-3	Kenton-On-Sea	26.0 g
	Plocamiales	Plocamiaceae	*Plocamium corallorhiza*	NDK06-1	Noordhoek	33.8 g
Rhodophyceae	Gigartinales	Gracilariaceae	*Gracilaria aculeata*	KOS06-1	Kenton-On-Sea	21.5 g
Phaeophyta						
Phaeophyceae	Fucales	Sargassaceae	*Bifurcaria brassicaeformis*	KB06-5	Kalk Bay	14.3 g
	Fucales	Sargassaceae	*Sargassum elegans*	KOS06-17	Kenton-On-Sea	15.1 g
	Fucales	Sargassaceae	*Sargassum heterophyllum*	NDK06-5	Noordhoek	52.6 g

*After extraction

2.2.3 Antimicrobial screening

Antimicrobial testing was done at the Division of Pharmacology, University of Cape Town. Crude algal samples were tested against a Gram-negative bacterium (*Klebsiella pneumoniae* ATCC 13883), a Gram-positive bacterium (*Staphylococcus aureus* ATCC 12600), a fungus (*Candida albicans* ATCC 90028) and a mycobacterium (*Mycobacterium aurum* A+) in duplicate in each of two separate colorimetric assays. The assays are based on visualization of red formation in INT

(*p*-iodonitrotetrazolium violet) in the presence of organism growth and results are expressed as minimum inhibitory concentrations (MIC). The concentrations ranged from 31.25 µg/ml to 4 mg/ml.

Table 2.2 Algal extracts and results of antimicrobial screening.

Collection code	Partition	Mass (mg)	MIC SA	MIC KP	MIC MA	MIC CA
NDK06-6	Hexane	300.0	>4	>4	2-4	1
	CH_2Cl_2	550.0	NT	NT	NT	NT
	EtOAc	15.0	NT	NT	NT	NT
	MeOH/H_2O	50.0	NT	NT	NT	NT
KOS06-6	Hexane	241.7	>4	>4	4	4
	CH_2Cl_2	228.8	>4	>4	>4	>4
	EtOAc	27.6	NT	NT	NT	NT
	MeOH/H_2O	123.0	NT	NT	NT	NT
KB06-9	Hexane	90.0	0.25	0.25	>4	1-2
	CH_2Cl_2	320.0	NT	NT	NT	NT
	EtOAc	32.0	NT	NT	NT	NT
	MeOH/H_2O	262.0	NT	NT	NT	NT
KOS06-15	Hexane	151.3	1	2	>4	1
	CH_2Cl_2	407.5	NT	NT	NT	NT
	EtOAc	144.9	NT	NT	NT	NT
	MeOH/H_2O	61.1	NT	NT	NT	NT
NDK06-19	Hexane	125.0	1	>4	1	2-4
	CH_2Cl_2	340.0	0.125	2	1	0.5
	EtOAc	36.0	NT	NT	NT	NT
	MeOH/H_2O	390.0	NT	NT	NT	NT
KOS06-23	Hexane	301.7	=4	>4	2	4
	CH_2Cl_2	223.7	NT	NT	NT	NT
	EtOAc	55.4	NT	NT	NT	NT
	MeOH/H_2O	169.1	NT	NT	NT	NT
KOS06-2	Hexane	1000.0	2	>4	1	>4
	CH_2Cl_2	250.0	NT	NT	NT	NT
	EtOAc	50.0	NT	NT	NT	NT
	MeOH/H_2O	300.0	NT	NT	NT	NT
NDK06-10	Hexane	315.0	>4	>4	>4	1
	CH_2Cl_2	525.0	NT	NT	NT	NT
	EtOAc	30.0	NT	NT	NT	NT
	MeOH/H_2O	126.0	NT	NT	NT	NT
KOS06-2	Hexane	394.0	=4	4	2-4	>4
	CH_2Cl_2	147.6	2	4	1	4
	EtOAc	73.0	NT	NT	NT	NT
	MeOH/H_2O	385.0	NT	NT	NT	NT

Table 2.2 continued.

Collection code	Partition	Mass (mg)	MIC SA	MIC KP	MIC MA	MIC CA
NDK06-1	Hexane	795.0	2-4	4	2	0.5
	CH_2Cl_2	745.0	1	4	2	0.25
	EtOAc	35.0	NT	NT	NT	NT
	$MeOH/H_2O$	67.0	NT	NT	NT	NT
KOS06-1	Hexane	356.4	>4	>4	>4	4
	CH_2Cl_2	346.8	>4	4	4	2-4
	EtOAc	64.8	NT	NT	NT	NT
	$MeOH/H_2O$	1400.0	NT	NT	NT	NT
KB06-5	Hexane	327.0	>4	4	>4	>4
	CH_2Cl_2	650.0	>4	4	2-4	2
	EtOAc	2.0	NT	NT	NT	NT
	$MeOH/H_2O$	65.0	NT	NT	NT	NT
KOS06-17	Hexane	405.4	>4	>4	>4	2-4
	CH_2Cl_2	234.0	>4	>4	4	4
	EtOAc	717.8	NT	NT	NT	NT
	$MeOH/H_2O$	35.9	NT	NT	NT	NT
NDK06-5	Hexane	2000.0	>4	>4	2-4	>4
	CH_2Cl_2	2000.0	>4	>4	0.5	>4
	EtOAc	105.0	2	2	2	4
	$MeOH/H_2O$	970.0	NT	NT	NT	NT
Nystatin			n/a	n/a	n/a	0.008-0.016
Ciprofloxacin			0.0004	0.0004	0.0008	n/a
DMSO			>2.5%	>2.5%	>2.5%	>2.5%

SA *Staphylococcus aureus*, KP *Klebsiella pneumoniae*, MA *Mycobacterium aurum*, CA *Candida albicans*
MIC expressed in mg/ml

A minimum inhibitory concentration of >4 mg/ml indicated that growth was present at the highest concentration of extract tested. Where a range of concentrations is reported, it indicates that for the duplicates in each of the two experiments (four tests per sample per organism) there was variation in MIC's. This was thought to be a result of incomplete solubility of the sample in 10 % DMSO that led to differences in the amount of extract added to each well. Where variations were more than one doubling concentration, a half-dilution was prepared of the extract in 50 % methanol and the experiment was repeated. MIC's of less than or equal to 2 mg/ml against any of the four pathogens were considered significant.

K. pneumoniae is a pathogenic encapsulated Gram-negative *Bacillus* whose prevalence and multiple drug resistance is escalating rapidly (Fang *et al.*, 2000; Keynan and Rubinstein, 2007). *S. aureus* is considered a dangerous pathogen in humans and resistant strains such as Methiciliin-resistant *S. aureus* are widespread globally (Menichetti, 2005). Non-pathogenic *M. aureus* was

used as a safe alternative to the slow growing and the highly infectious *M. tuberculosis*. The inhibition of *M. aurum* A+ growth is reported to be highly predictive of activity against *M. tuberculosis* (Eldeen and Van Staden, 2007). *C. albicans* is an opportunistic fungal pathogen (Molero *et al.*, 1998) that is recognised as the most common oral infection in HIV disease (Fidel, 2006). These micro-organisms are relevant for testing of antimicrobial agents towards the discovery of new antibiotics. With a view to marine antifoulants it would have been preferable to employ marine micro-organisms in the assay. Nevertheless, any product employed in the marine environment would be required to have an especially broad spectrum of activity to prevent the colonization of a submerged surface, thus activity observed in this assay may yet serve to indicate possible sources of marine natural product antifoulants.

Of the extracts screened for antimicrobial activity, 26% were active against the Gram-positive bacterium *S. aureus* and 15% were active against the Gram-negative bacteriaum *K. pneumoniae*. A surprising 46% of extracts displayed activity against *M. aurum*, while 42% were active against *C. albicans*. The results for the bacterial strains are comparable with the trends reported in the literature, however the high percentage of extracts that were active against the mycobacterium and the fungus far exceeded those of published studies. In this particular study, no alga of the division Chlorophyta and only three algae of the division Phaeophyta were tested, the bulk being made up by members of the division Rhodophyta. Of the Phaeophyta tested, none showed any greater activity than the Rhodophyta, although there are limited numbers for comparison. The extracts tested consisted mainly of *n*-hexane and CH_2Cl_2 fractions of which the latter were marginally more active in general. Although only extracts from *Polysiphonia incompta* exhibited activity against all of the test organisms, the broad spectrum of activity of extracts from *P. cloiophyla* and *P. corallorhiza* suggests that South African marine macro-algae are a promising source of antimicrobial compounds. After analysing the antimicrobial results, *Pterosiphonia cloiophyla*, *Plocamium corallorhiza*, *Amphiroa ephedraea*, *Polysiphonia incompta*, *Laurencia flexuosa* and *Sargassum heterophyllum* were considered worth exploring further.

2.3 Conclusion

This project involves an investigation into the ability of marine natural products to prevent a fundamental stage of biofouling i.e. bacterial colonization. Although subsequent studies of the toxicity of the extracts and their ability to inhibit biofilm formation and macro-fouling would undoubtedly have added further value to the results, data obtained was useful in the selection of algae for further investigation. The following chapters will focus on the investigation of the natural product chemistry of *P. corallorhiza* and *L. flexuosa*.

2.4 Experimental

2.4.1 Solvents

All solvents were distilled before use or were of HPLC grade (HiPerSolv^{TM}, Merck and Saarchem).

2.4.2 Collection of algae

Collections were made at various locations including Kalk Bay, Noordhoek and Kenton-On-Sea in 2006. The algae were transported to the laboratory where they were sorted and stored at -4 °C until extraction. The algae were identified by Prof John J. Bolton of the Department of Botany, University of Cape Town. Voucher specimens are retained in our repository at the Faculty of Pharmacy Rhodes University, Grahamstown, South Africa. The algae extracted were: *Laurencia flexuosa* Kützing; *Pterosiphonia cloiophyla* Falkenberg; *Polysiphonia incompta* Harvey; *Amphiroa ephedraea* Lamarck, Decaisne; *Gelidium abbottiorum* R. E. Norris; *Gelidium capense* Gmelin, Silva; *Gelidium pteridifolium* R. E. Norris, Hommers and Fredricq; *Plocamium corallorhiza* Turner, J. Hooker & Harvey; *Bifurcaria brassicaeformis* Stackhouse; *Sargassum elegans* Suhr; *Sargassum heterophyllum* Turner, C. Agardh; *Gracilaria aculeate* Hering, Papenfuss.

2.4.3 General procedure for the extraction and prefractionation of algae

The frozen alga was steeped in MeOH for 1 hour at 4 °C after which the solvent was decanted and extracted with CH_2Cl_2. The alga was then steeped in CH_2Cl_2-MeOH (2:1) and heated at 30 °C for 30 minutes (x 3). The CH_2Cl_2-MeOH extract was drained and separated by the addition of distilled water after which the CH_2Cl_2 layer was run off. The aqueous MeOH partition was extracted with CH_2Cl_2 (3 x 50 ml). The CH_2Cl_2 extracts were combined, dried over $MgSO_4$, filtered and evaporated to dryness *in vacuo* at 30 °C. The solvent extracts were sequentially partitioned between MeOH-H_2O-*n*-hexane (9:1:10), MeOH-H_2O-CH_2Cl_2 (7:3:10) and H_2O-EtOAc (1:1). Organic material was recovered from the aqueous partition using an HP-20 column which was subsequently washed with MeOH, CH_2Cl_2 and *n*-hexane. For masses of individual extracts see **Table 2.2**. Extracts were stored under *n*-hexane at -4 °C.

2.4.4 Antimicrobial Assay

Experiments were performed by Tracy Seaman at the Division of Pharmacology, University of Cape Town. Crude algal samples were prepared to a concentration of 16 mg/ml in 10% DMSO (DMSO was first added and the samples were thoroughly vortexed, after which sterile water was added). Each sample was tested in duplicate in each of two separate assays.

2.5 References

Andrews, J. M. Determination of minimum inhibitory concentrations. *Journal of Antimicrobial Chemotherapy* **2001**, *48*, (S1), 5-16.

Bhadury, P.; Wright, P. C. Exploitation of marine algae: Biogenic compounds for potential antifouling applications. *Planta* **2004**, *219*, 561-578.

Fenical, W. Halogenation in the Rhodophyta: A review. *Journal of Phycology* **1975**, 11, 245-249.

Chambers, H. F. The changing epidemiology of *Staphylococcus aureus*. *Emerging infectious diseases* **2001**, 7, (2), 178-182.

Cronin, G.; Lindquist, N.; Hay, M. E.; Fenical, W. Effects of storage and extraction procedures on yields of lipophilic metabolites from the brown seaweeds *Dictyota ciliolata* and *D. menstrualis*. *Marine Ecology Progress Series* **1995**, *119*, 265-273.

Eldeen, I. M. S.; Van Staden, J. Antimycobacterial activity of some trees used in South African traditional medicine. *South African Journal of Botany* **2007**, *73*, 248-251.

Fang, C. T.; Chen, Y. C.; Chang, S. C.; Sau, W. Y.; Luh, K. T. *Klebsiella pneumoniae* meningitis: Timing of antimicrobial therapy and prognosis. *Quarterly Journal of Medicine* **2000**, *93*, 45-53.

Fenical, W. Halogenation in the Rhodophyta A Review. *Journal of Phycology* **1975**, *11*, 245-259.

Fidel. P. L. Jr. *Candida*-host interactions in HIV Disease: Relationships in oropharyngeal candidiasis. *Advances in Dental Research* **2006**, *19*, 80-84.

Fusetani, N. Biofouling and antifouling. *Natural Product Reports* **2004**, *21*, 94-104.

González del Val, A.; Platas, G.; Basilio, A.; Cabello, A.; Gorrochategui, J.; Suay, I.; Vicente, F.; Portillo, E.; Jimenez del Rio, M.; Garcia Reina, G.; Pelaez, F.; Screening of Antimicrobial activities in red, green and brown macroalgae from Gran Canaria (Canary Islands, Spain), *International Microbiology* **2001**, *4*, 35-40.

Guiry, M. D.; Guiry, G. M. **2008**. AlgaeBase version 4.2. World-wide electronic publication, National University of Ireland, Galway. http://www.algaebase.org; date accessed January 20, 2008.

Haefner, B. Drugs from the deep: marine natural products as drug candidates. *Drug Discovery Today* **2003**, *8*, (12), 536-544.

Hay, M. E.; Fenical, W. Marine plant-herbivore interactions: The ecology of chemical defense. *Annual Review of Ecology and Systematics* **1988**, *19*, 111-145.

Hellio, C.; De La Broise, D.; Dufosse´, L.; Le Gal, Y.; Bourgougnon, N. Inhibition of marine bacteria by extracts of macroalgae: potential use for environmentally friendly antifouling paints. *Marine Environmental Research* **2001**, *52*, 231–247.

Hunfeld, K. P.; Kraiczy, P.; Wichelhaus, T. A.; Schäfer, V.; Brade, V. Colorimetric *in vitro* susceptibility testing of penicillins, cephalosporins, macrolides, streptogramins, tetracyclines, and aminoglycosides against *Borrelia burgdorferi* isolates. *International Journal of Antimicrobial Agents* **2000**, *15*, 11-17.

Keynan, Y.; Rubinstein, E. The changing face of *Klebsiella pneumoniae* infections in the community. *International Journal of Antimicrobial Agents* **2007**, *30*, 385-389.

Krug, P. J. Defense of benthic invertebrates against surface colonization by larvae: A checmical arms race, *Progress in Molecular and Subcellular Biology, Subseries Marine Molecular Biology, Antifouling compounds*; Fusetani, N.; Clare, A. S. (Eds); Springer-Verlag: Berlin Heidelberg **2006.**

Lima-Filho, J. V. M.; Carvalho, A. F. F. U.; Freitas, S. M.; Melo, V. M. M. Antibacterial activity of extracts of six macroalgae from the Northeastern Brazilian coast. *Brazilian Journal of Microbiology* **2002**, *33*, 311-313.

Menichetti, F. Current and emerging serious Gram-positive infections. *Clinical Microbiology and Infection* **2005**, *11*, (3), 22-28.

Molero, G.; Diez-Orejas, R.; Navarro-Garcia, F.; Monteoliva, L.; Pla, J.; Gil, C.; Sánchez-Pérez, M.; Nombela, C. *Candida albicans*: Genetics, dimorphism and pathogenicity. *International Microbiology* **1998**, *1*, 95-106.

Mtolera, M. S. P.; Semesi, A. K. Antimicrobial activity of extracts from six green algae from Tanzania. *Current Trends in Marine Botanical Research in East African Region* **1996**, 211-217.

Paul, V. J.; Puglisi, M. P. Chemical mediation of interactions among marine organisms. *Natural Product Reports* **2004**, *21*, 189-209.

Steinberg, P. D.; de Nys, R.; Kjelleberg, S. Chemical cues for surface colonization. *Journal of Chemical Ecology* **2002**, *28*, (10), 1935-1951.

Taskin, E.; Ozturk, M.; Taskin, E.; Kurt, O. Antibacterial activities of some marine algae from the Aegean Sea (Turkey). *African Journal of Biotechnology* **2007**, *6*, (24), 2746-2751.

Tüney, I.; Cadirci, B. H.; Unal, D.; Sukatar, A. Antimicrobial activities of the extracts of marine algae from the coast of Urla (Izmir, Turkey). *Turkish Journal of Biology* **2006**, *30*, 171-175.

Tunney, M. M.; Ramage, G.; Field, T. R.; Moriarty, T. F.; Storey, D. G. Rapid colorimetric assay for antimicrobial susceptibility testing of *Pseudomonas aeruginosa*. *Antimicrobial Agents and Chemotherapy* **2004**, *48*, (5), 1879-1881.

Valgas, C.; Machado de Souza, S.; Smania, E. F. A.; Smania Jr. A.; Screening methods to determine antibacterial activity of natural products. *Brazillian Journal of Microbiology* **2007**, *38*, 369-380.

Vlachos, V.; Critchley, A. T. Antimicrobial activity of extracts from selected South African marine macroalgae. *South African Journal of Science* **1997**, *93*, (7), 328-338.

Chapter Three
Halogenated Monoterpenes from *Plocamium corallorhiza*

3.1 Introduction

Monoterpenes are produced by terrestrial and marine plants; significantly, the presence of halogen atoms in marine monoterpenes sets them apart from those of terrestrial origin. In terrestrial plants monoterpenes are responsible for the flavour and aroma of essential oils and are involved in selected ecological interactions; examples of their use are as insect deterrents or attractants (Renault-Roger, 1997; Alipieva *et al.*, 2003). Humans have also found therapeutic uses for these aromatic oils which display an array of biological activities such as being antioxidant (Misharina and Polshkov, 2005) and antimicrobial (Chang *et al.*, 2001; Prabuseenivasan *et al.*, 2006), they may also be used to enhance transdermal drug delivery (Fang *et al.*, 2004). The role that halogenated monoterpenes play in marine algae has not been fully established, although *in vitro* studies have shown them to have feeding deterrent (Paul *et al.*, 1980), antifouling (König *et al.*, 1999a) and antialgal (König *et al.*, 1999b) activity.

3.1.1 Halogenated monoterpenes: Structural classes

Marine monoterpenes can be divided into a number of classes; the first distinction can be made between the acyclic monoterpenes, which can be divided into myrcene (**3.1**) derivatives and ocimene (**3.2**) derivatives. Myrcene derivatives have been isolated only from algae of the family Rhizophyllidaceae, while ocimene derivatives are only found in the family Plocamiaceae (Naylor *et al.*, 1983). The cyclic monoterpenes originate from these two classes.

3.1

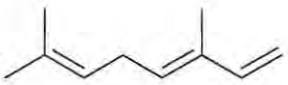

3.2

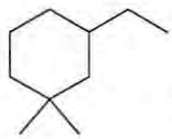

3.3

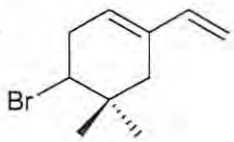

3.4

The ochtodanes or 1-ethyl-3,3-dimethylcyclohexanes (**3.3**) form by cyclization of myrcene derivatives. An example of an ochtodane is 4-bromo-5,5-dimethyl-1-vinylcyclohexane (**3.4**) isolated from *Chondrococcus hornemannii* (Naylor *et al.*, 1983).

Ocimene derivatives afford two classes of cyclic monoterpenes, 1-ethyl-1,3-dimethylcyclohexanes (**3.5**) and upon ethyl migration, the 1-ethyl-2,4-dimethylcyclohexanes (**3.6**). Examples of both cyclic classes (**3.7** and **3.8**) can be found in red algae such as *Plocamium cartilagineum* (König *et al.*, 1990).

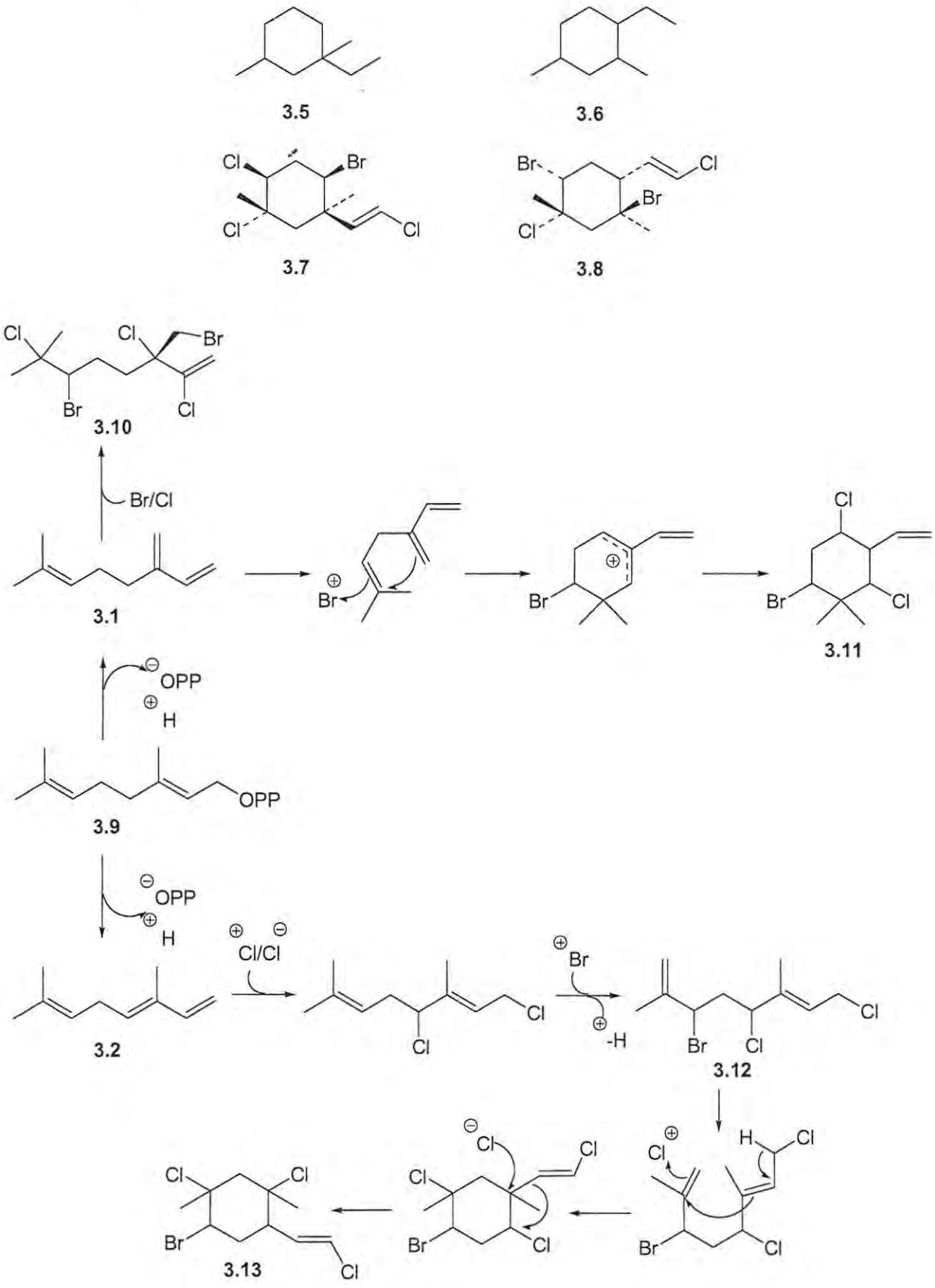

Scheme 3.1 Acyclic and Cyclic halogenated monoterpenes originate from myrcene (**3.1**) and ocimene (**3.2**). (Scheme reproduced from Wise *et al.*, 2002)

3.1.2 Previous studies on *Plocamium corallorhiza*

3.1.2.1 Compounds isolated

Red algae of the *Plocamium* genus are known to be prolific producers of halogenated monoterpenes (Crews *et al.*, 1984; Kladi *et al.*, 2004; Blunt *et al.*, 2007) and *P. corallorhiza*, a red alga of the family Plocamiaceae has been found by our research group to contain a number of acyclic and cyclic ocimene derivatives (Table 3.1) (Knott, 2003; Mkwananzi, 2005). Halogenated monoterpenes from *P. corallorhiza* have exhibited both moderate antimicrobial acitivity against Gram positive bacteria *Staphylococcus aureus* and *Bacillus subtilis*, and anticancer activity in oesophageal cancer cell line assays. Crude extracts as well as pure compounds from *P. corallorhiza* were found to be toxic to *Artemia salina* (Mkwananzi, 2005).

Table 3.1 Halogenated monoterpenes isolated from *Plocamium corallorhiza*

No.	Structure	Structural subclass	No.	Structure	Structural subclass
3.13	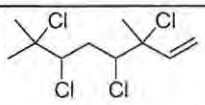	3,7-dimethyl-octene	**3.21**	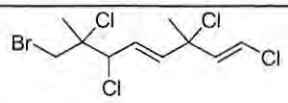	3,7-dimethyl-octadiene
3.14	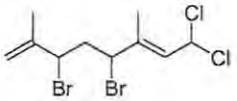	3,7-dimethyl-octadiene	**3.22**	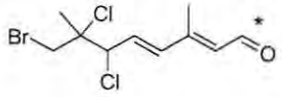	3,7-dimethyl-octadienal
3.15	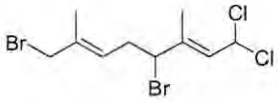	3,7-dimethyl-octadiene	**3.23**		3,7-dimethyl-octadienal
3.16	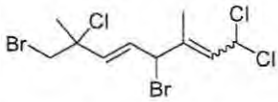	3,7-dimethyl-octadiene	**3.24**	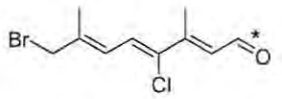	3,7-dimethyl-octatrienal
3.17	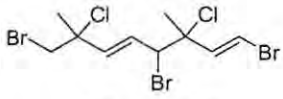	3,7-dimethyl-octadiene	**3.25**	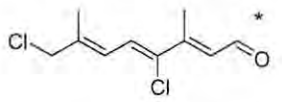	3,7-dimethyl-octatrienal
3.18	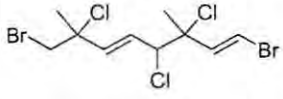	3,7-dimethyl-octadiene	**3.26**	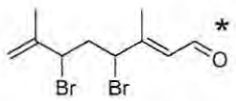	3,7-dimethyl-octadienal
3.19	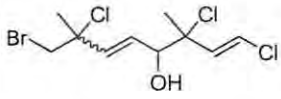	3,7-dimethyl-octadiene	**3.27**	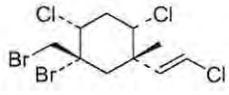	1-Ethyl-1,3-dimethyl-cyclohexanes
3.20	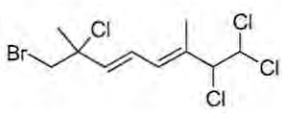	3,7-dimethyl-octadiene	**3.28**	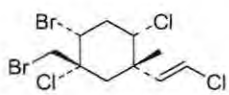	1-Ethyl-1,3-dimethylcyclo hexanes

Knott, 2003, Mkwananzi, 2005 * No mass spectral data was obtained in support of these structures

Extraction of the alga also yielded some novel halogenated monoterpene aldehydes (plocoraldehydes) that were similar in structure to many of the plocoralides, halogenated

monoterpenes possessing a geminal dihalide at position 1. It was thought that these compounds may have been produced by the nucleophilic substitution of halogens during the extraction process.

3.1.2.2 Spectroscopic characterization of halogenated monoterpenes

Halogenated monoterpenes are deceptively simple molecules whose planar structures are relatively straightforward to assemble from 2D NMR data. Challenges are presented when assigning the position and identity of halogen atoms and when assigning stereochemistry. Ambiguous spectroscopic data may lead to erroneous stereochemical assignments and a number of metabolites have later been structurally re-assigned (Van Engen *et al.*, 1978; Sardina *et al.*, 1985; Woolard *et al.*, 1978).

^{13}C NMR data is a useful indicator of halogen regiochemistry and substituent stereochemistry (Crews *et al.*, 1984) while ^{1}H NMR coupling constants may offer insight into the planar structure of a rigid diene chromophore (Crews and Kho, 1974). Both ^{13}C and ^{1}H NMR chemical shifts of the methyl group at position 3 may be used to assign relative stereochemistry to C-3 and C-4 (Naylor *et al.*, 1983).

X-ray crystallography is an unambiguous method for the determination of molecular structure, however its use is limited to crystalline substances. Many halogenated monoterpenes are isolated as oils and thus cannot be analysed in this manner.

High resolution mass spectrometry is an invaluable tool in the determination of the molecular formula; unfortunately, many halogenated monoterpenes fail to exhibit molecular ion peaks (M^+). Upon fragmentation of the molecule, daughter ions are created. These daughter ions are often reproducible and may be characteristic of a certain fragment. These ions may be used to construct what is termed a "fragmentation map" of the molecule, which may afford reasonably reliable projections of M^+ (Naylor *et al.*, 1983).

A characteristic feature of halogen atoms is that they occur in nature with different isotopic abundances. The relative isotopic abundances of a particular halogen are constant and are observed in mass spectra as *m/z* ion peak clusters. These ion peak clusters are extremely useful when assigning the halogen atoms. When interpreted in conjunction with the fragment ion, these clusters allow one to determine the positions of the halogens in the molecule (Naylor *et al.*, 1983).

Unfortunately, projections and overinterpretation of mass fragmentation patterns may lead to errors in halogen regiochemistry and assignment. Ideally, a molecular ion (M^+) is required to afford an unambiguous molecular formula. It is for these reasons that the structure determination of such deceptively simple structures become interesting research problems.

3.1.3 Analysis of short chain aldehydes by derivatization and mass spectrometry

The plocoraldehydes are new members of a small class of marine halogenated monoterpene aldehydes of which cartilagineal (**3.29**) was the first to be reported (Crews and Kho, 1974). What distinguishes plocoraldehydes (e.g. **3.26**) from cartilagineal (**3.29**) and others in the group is the position of the aldehyde moiety (Figure 3.1).

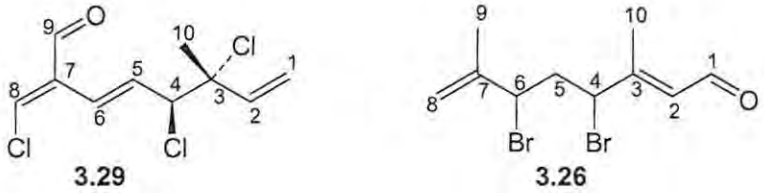

3.29 **3.26**

Figure 3.1 The relative positions of the aldehyde moiety in Cartilagineal (**3.29**) and Plocoraldehyde A (**3.26**)*

Although this is the first report of an aldehyde group at C-1 in marine halogenated monoterpenes, this functional group is also present in numerous terrestrial monoterpenes (e.g. geranial). Moreover, an aldehyde functionality attached to a terminal carbon atom is by no means unusual in marine natural products. The diatom *Thalassiosira rotula* is known to produce short chain conjugated aldehydes such as 2*E*,4*E*-decadienal (**3.30**), 2*E*,4*E*-octadienal (**3.31**) and 2*E*-decenal (**3.32**) (Figure 3.2) upon injury as part of a wound activated defensive reaction (Pohnert, 2002; Wichard *et al.*, 2005). These compounds have been shown to be highly toxic to copepod embryos, inducing arrest of cell division. They have also exhibited antibacterial, antifungal and weak algicidal activity (Adolph, *et al.*, 2004).

3.30

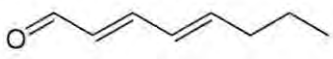

3.31

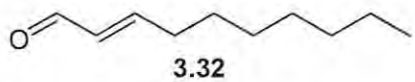

3.32

Figure 3.2 Short chain conjugated unsaturated aldehydes produced by marine diatoms

Another marine diatom *Skeletonema costatum* produces similar short chain aldehydes to *T. rotula* as part of its defensive arsenal (d'Ippolito *et al.*, 2002a).

Short chain aldehydes produced in biological environments are often produced in minuscule quantities; in addition, they are highly reactive and generally unstable molecules (Spiteller *et al.*, 1999). Compounds with aldehydic functionalities react in biological systems with components

* Compound numbering used for Halogenated Monoterpenes does not follow IUPAC rules, however is consistent with that found in the current literature.

containing basic amino groups to form Schiff bases (Gardener, 1979) and their non-selective reactivity towards nucleophilic biomolecules is thought to be the reason for their physiological toxicity (Adolph *et al.*, 2004).

The small quantities, reactivity and instability of short chain aldehydes have presented challenges in the characterization of these compounds. Derivatization of the aldehydic functionality was found to stabilize the compounds and allow for their detection and analysis.

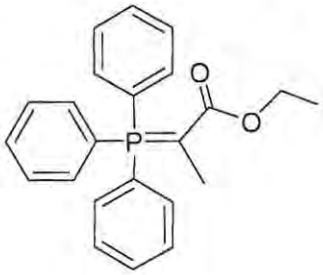

3.33

d' Ippolito *et al.* (2002b) developed methodology that allowed the analysis of short-chain aldehydes by GCMS and NMR after their transformation into the analogous carboxyethylethylidene (CET) (**3.33**) derivatives. Via a Wittig reaction, the aldehyde was converted to the CET derivative by treatment with (carbetoxyethylidene)-triphenylphosphorane (**3.33**) under very mild conditions. The method was found to be suitable for the detection of short and medium chain aldehydes as well as the analysis of raw biological samples.

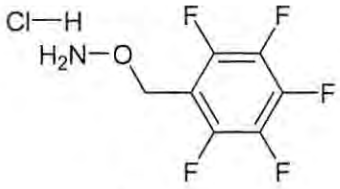

3.34

A second method utilized in the derivatization of aldehydes involves the reaction of the compounds with *O*-(2,3,4,5,6-pentafluorobenzyl)hydroxylamine hydrochloride (PFBHA·HCl, **3.34**) (Wichard *et al.*, 2005). PFBHA (**3.34**) derivatization is a popular method for the measurement of oxygenated organic compounds in environmental and biological samples (Spaulding and Charles, 2002). In a study conducted by Spaulding and Charles (2002) PFB oxime derivatives of aromatic and saturated aldehydes were found to be stable for = 66 days when stored under CH_2Cl_2 at 4 °C, while unsaturated aliphatic aldehydes were stable for approximately 38 days under the same conditions, this duration of stability would allow ample time for analysis.

The plocoraldehydes produced by *P. corallorhiza* were found to degrade rapidly during structure elucidation and attempts at obtaining mass spectrometry data proved futile. It was postulated that derivatization of the aldehyde moiety with an aldehyde trapping reagent may stabilize the compounds and enable their complete characterization.

3.1.4 Chapter Aims

Results of the antimicrobial screening of South African marine algal extracts (Chapter 2) indicated that *Plocamium corallorhiza* (NDK06-1) might contain antimicrobial compounds. The first objective of this study was therefore to isolate and characterize these antimicrobial substances.

In a previous study of this alga, a number of unstable halogenated monoterpene aldehydes were isolated and incompletely characterized. A second objective was therefore to reisolate these compounds and develop a method to derivatize them and complete their characterization.

Finally, *Plocamium corallorhiza* has been a productive source of biologically active halogenated monoterpenes and this study provided further opportunity to discover additional biologically active metabolites.

Figure 3.3 The deep pink, iridescent frond of *Plocamium corallorhiza*

3.2 Results and Discussion

3.2.1 Extraction and isolation of halogenated monoterpenes from *Plocamium corallorhiza*

Plocamium corallorhiza was collected from Noordhoek, near Port Elizabeth (collection number NDK06-22) and Kenton-On-Sea (collection number KOS06-14). Since a standard extraction and isolation protocol was followed for the isolation of metabolites, only the isolation of compounds from the Noordhoek collection (NDK06-22) will be discussed. The procedure is representative.

In September of 2006 at low tide, *P. corallorhiza* was collected from Noordhoek, near Port Elizabeth. The algae (176.3 g dry weight after extraction) was extracted with MeOH (4 °C, 1 hr) and CH_2Cl_2-MeOH (30 °C, 30 min, x3). The CH_2Cl_2-MeOH extract was decanted and separated into two partitions by the addition of distilled water. The CH_2Cl_2 was drained off and the aqueous MeOH was extracted with a further two portions of CH_2Cl_2. The CH_2Cl_2 extracts were combined and partitioned into *n*-hexane, dichloromethane and ethyl acetate affording extracts A (1.611 g, *n*-hexane), B (0.308 g, CH_2Cl_2) and C (0.063 g, EtOAc). Silica gel column chromatography employing an *n*-hexane-EtOAc step gradient yielded 9 fractions for extract A. Further silica gel column chromatography was used to create six further fractions (a-f Scheme 3.2), however A2a to A2c and A2d to A2f were later recombined. Exhaustive normal phase HPLC of these fractions yielded **3.13** (A2a-c3), **3.48** (A2a-c4), **3.14** (A2a-c5a), **3.47** (A2a-c5b), **3.16** (A2a-c6), **3.17** (A2a-c7), **3.44** (A2d-f5a) and **3.22** (A2d-f5b).

Table 3.2 Masses and percentage yields of compounds isolated from *P. corallorhiza* (NDK06-22)

Isolation code[‡]	Compound #	Mass (mg)	% yield
A2a-c3	**3.13**	2.0	0.001
A2a-c4	**3.48**	9.9	0.006
A2a-c5a	**3.14**	6.5	0.004
A2a-c5b	**3.47**	4.6	0.003
A2a-c6	**3.16**	2.1	0.001
A2a-c7	**3.17**	6.5	0.004
A2d-f5a	**3.44**	5.0	0.003
A2d-f5b	**3.22**	1.4	0.001

[‡]isolation code: Partition, silica column fr, silica column 2 fr, hplc fr e.g n-hexane pn, silica column fr 2, silica column 2 fr a-c, hplc fr 3. * Percentage yields calculated relative to dry weight after extraction

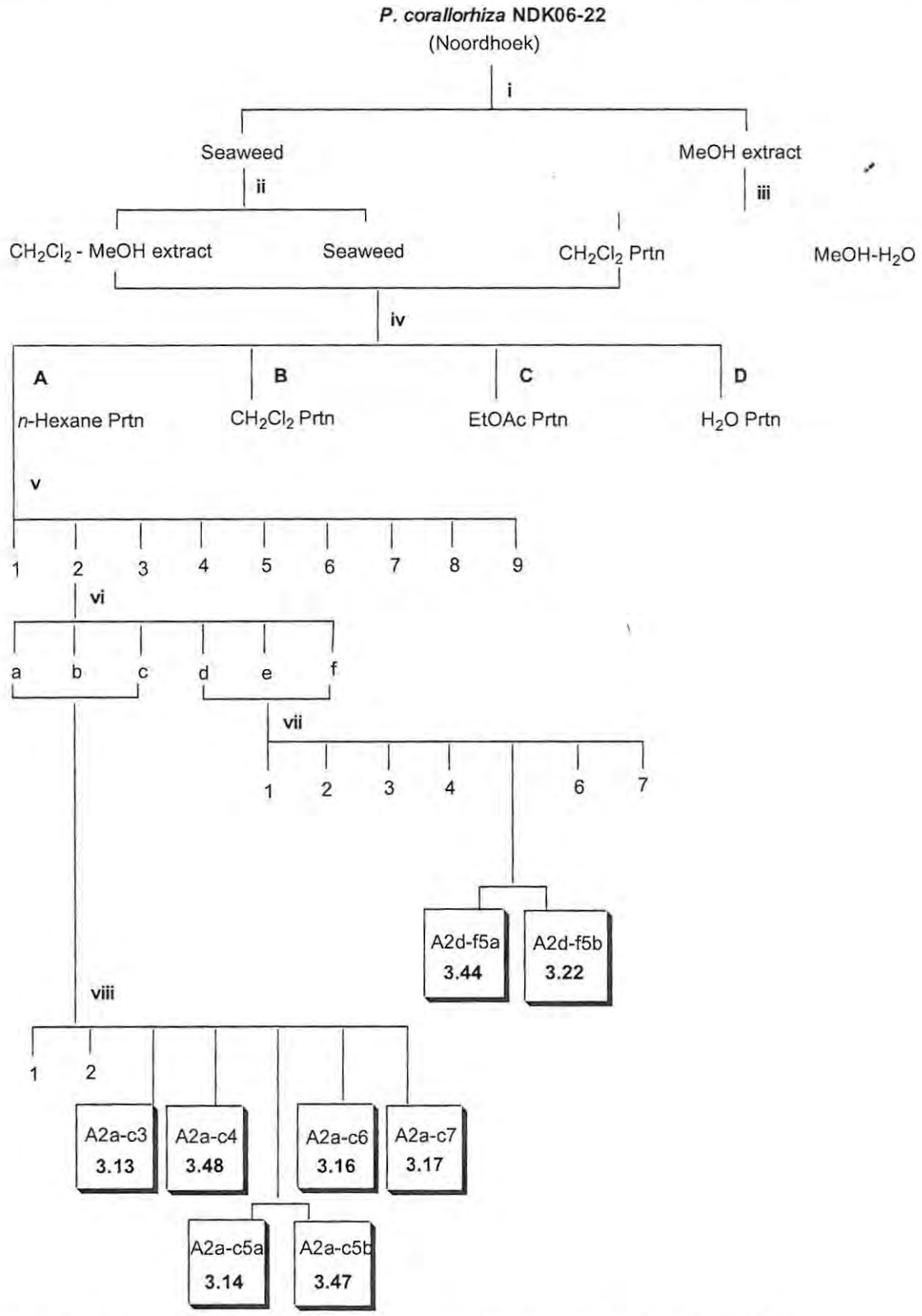

Scheme 3.2 Extraction and isolation of metabolites from *P. corallorhiza* (NDK06-22)

Conditions: i) MeOH extraction 4 °C 1 hour ii) CH_2Cl_2-MeOH (2:1) extract rt 24 hours x3 iii) CH_2Cl_2 liquid liquid extraction iv) Solvent partitioning v & vi) Silica gel column chromatography vii) normal phase HPLC *n*-hexane-EtOAc (9:1) viii) normal phase HPLC *n*-hexane

Table 3.3 Masses and percentage yields* of compounds isolated from *P. corallorhiza* (KOS06-14)

Isolation code[‡]	Compound #	Mass (mg)	% yield*
A2a	**3.14**	10 mg	0.032
A2c	**3.17**	9 mg	0.029
A2h	**3.26**	61 mg	0.194
A2i	**3.44**	39 mg	0.124
A3d	**3.23**	<1 mg	0.003
A3e	**3.22**	2mg	0.006

[‡]isolation code: Partition, silica column fr, hplc fr e.g n-hexane pn, silica column fr 2, hplc fr a. * Percentage yields calculated relative to dry weight after extraction.

Table 3.4 Monoterpenes isolated from *P. corallorhiza* collected from different locations

Compound No.	Noordhoek (NDK06-22)	Kenton-On-Sea KOS06-14	Kalk Bay Knott, 2003
3.13	*v*		*v*
3.48	*v*		
3.14	*v*	*v*	*v*
3.47	*v*		
3.16	*v*	*v*	*v*
3.17	*v*	*v*	*v*
3.44	*v*	*v*	
3.22	*v*	*v*	
3.26		*v*	
3.23		*v*	
3.25		*v*	
3.27			*v*
3.28			*v*
3.15			*v*

Table 3.4 illustrates the variation in the halogenated monoterpenes isolated from *P. corallorhiza* collected at different locations. Interestingly, a decidedly greater number of halogenated monoterpene aldehydes have been isolated from extracts of the Kenton-On-Sea collection than from extracts of the Noordhoek and Kalk Bay collections. It has yet to be established whether the variation is attributed to seasonal or geographical differences, the chronological age of the samples collected or their stage of reproduction. The analysis of these variables and others has been identified as an area for further study.

With the number of halogenated monoterpene aldehydes isolated from *P. corallorhiza* and their obvious similarity to the plocoralides, it was considered that these compounds could be artefacts of the isolation procedure in the presence of water. A simple experiment was conducted where the alga was lyophilized before extraction with CH_2Cl_2. The CH_2Cl_2 extract was decanted and following evaporation of the solvent *in vacuo*, the extract was reconstituted in $CDCl_3$ and a ^1H NMR spectrum was obtained.

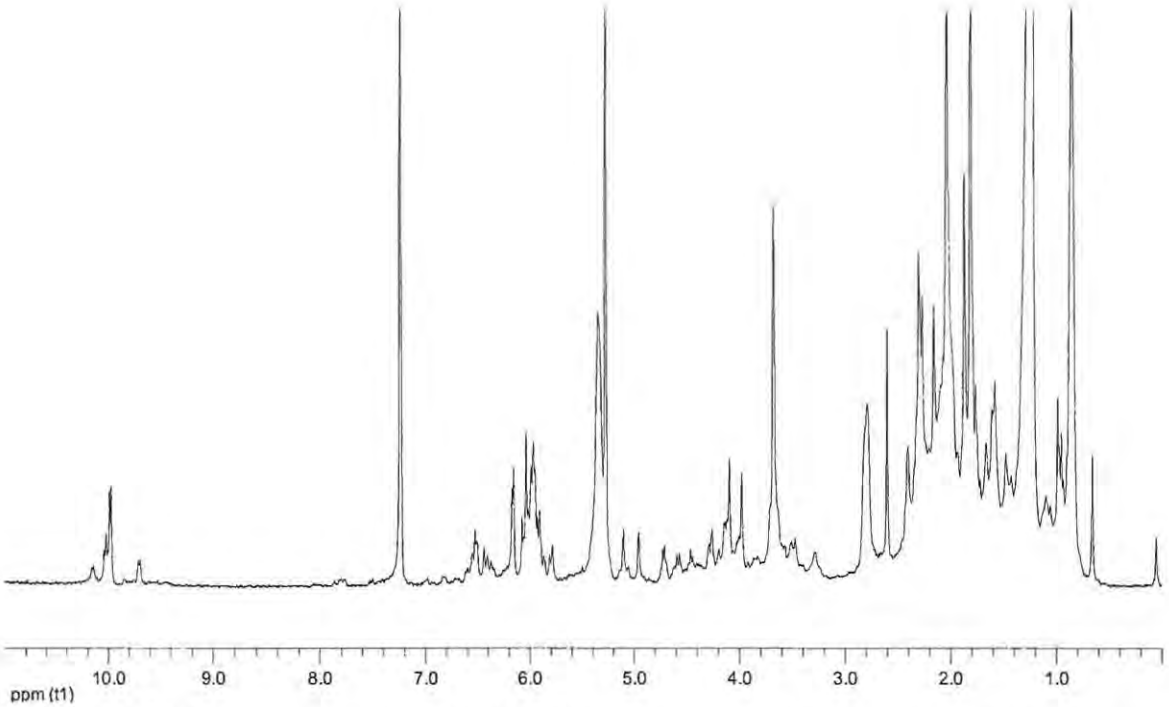

Figure 3.4 ^1H NMR spectrum ($CDCl_3$, 400 MHz) of the crude CH_2Cl_2 extract of *P. corallorhiza* following lyophilization

The ^1H NMR spectrum of the crude CH_2Cl_2 extract (Figure 3.4) contains signals typical of aldehyde functionalties (~ 10 ppm). The presence of the plocoraldehydes indicates that although the compounds may yet be degradation products, it is unlikely that they are formed by nucleophilic substitution of halogens at position 1 during the extraction process. There is also no precedent for this phenomenon in the literature.

3.2.2 Derivatization and mass spectrometric analysis of citral (3.35): A model study

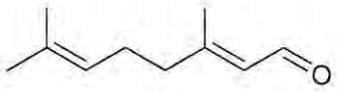

3.35

The instability of the plocoraldehydes presented challenges during structural characterization, especially in obtaining molecular mass by electron impact ionization mass spectrometry EIMS (70 eV). It is not uncommon for halogenated monoterpenes to have their molecular weights reported as [M – X] due to the loss of halogens (Naylor *et al.*, 1983), however the spectra afforded by the plocoraldehydes afforded no discernible fragmentation patterns which could be used in support of a proposed structure.

Aldehyde trapping reagents such as 2,4-dinitrophenylhydrazines have been used in compound characterization, most often in melting point determinations (Smith and Tatchell, 1965, Spiteller *et al.*, 1999). More recently similar reagents have been employed in the detection and quantification of low molecular weight aldehydic compounds by electron impact ionization-mass spectrometry (EIMS) (Spiteller *et al.*, 1999), chemical ionization-mass spectrometry (CIMS) (Zhong *et al.*, 2006), atmospheric pressure photoionization-mass spectrometry (APPI-MS) (van Leeuwen *et al.*, 2004) and electrospray ionization-mass spectrometry (ESI-MS) (Zwiener *et al.*, 2002).

The use of (carbetoxyethylidene (CET))-triphenylphosphorane (**3.33**) in the derivatization of short-chain aldehydes produced by marine organisms is reported to afford reliable GC-EIMS data (d'Ippolito *et al.*, 2002a). Another reagent used in aldehyde trapping reactions is *O*-(2,3,4,5,6-pentafluorobenzyl)hydroxylamine (PFBHA) (**3.34**); the reagent reacts with aldehydes at room temperature within relatively short periods of time (Spiteller *et al.*, 1999; Ferreira *et al.*, 2004). The resulting pentafluorobenzyl oxime derivatives are reported to be very volatile and well-suited to GC analysis and detection (Zhong *et al.*, 2006).

In an attempt to achieve greater stability and ultimately obtain reliable, reproducible mass spectra, we have explored the use of selected aldehyde trapping reagents. Due to limited sample all reactions were explored using citral (**3.35**) as model compound.

3.2.2.1 Derivatization of citral (3.35) using CET-triphenylphosphorane (3.33)

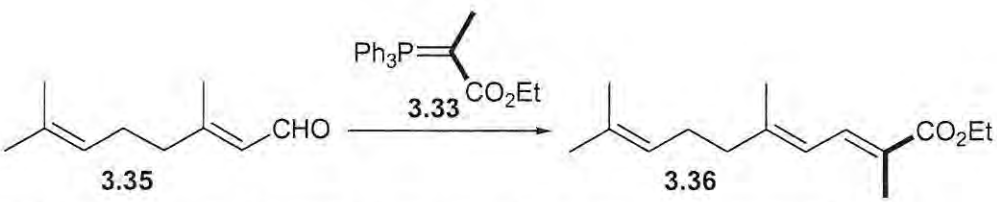

3.35 **3.36**

Scheme 3.3 Derivatization of citral (**3.35**) using CET-triphenylphosphorane (**3.33**)

Aldehydes were treated with the ylide CET-triphenylphosphorane (**3.33**) in dichloromethane and stirred at room temperature for a minimum of 24 hours. The mild conditions of this Wittig type reaction were considered favourable for use with halogenated monoterpenes. The highly polar triphenylphosphine oxide formed as a side product during the reaction was easily removed by passing the reaction mixture through a silica gel plug. The reaction proved low yielding and a molar ratio of 2:1 reagent-citral (**3.35**) with stirring for 48 hours produced inconclusive results. The reaction was nevertheless attempted on Plocoraldehyde A (**3.26**).

3.2.2.2 Derivatization of citral (3.35) using *O*-(2,3,4,5,6-pentafluorobenzyl)hydroxylamine (PFBHA) hydrochloride (3.34)

PFBHA (**3.34**) derivatization is often done in aqueous solution, (Spaulding and Charles, 2002) however this was deemed an inappropriate solvent system for use with halogenated monoterpenes due to the risk of substitution of halogens by nucleophilic substances[†]. On discovery that all compounds were soluble to some extent in acetonitrile (CH_3CN), this solvent was chosen as the reaction medium. Although CH_2Cl_2 is reported to be the most efficient solvent for the extraction of PFB oxime derivatives from aqueous media (Spaulding and Charles, 2002), the miscibility of CH_2Cl_2 with CH_3CN excluded its use. *n*-Hexane was thus used to partition the oxime derivatives from the reaction mixture.

The reaction on citral (**3.35**) was performed using sufficient quantities (= 50 mg) so as to monitor the reaction by ^1H NMR. It must be noted that our goal was to establish whether or not the derivatization of aldehyde monoterpene with PFBHA (**3.34**) and the detection and measurement of a molecular ion using mass spectrometry was possible. There are aspects, such as the formation of multiple geometric isomers and their relative ratios that will be discussed briefly but were not fully investigated.

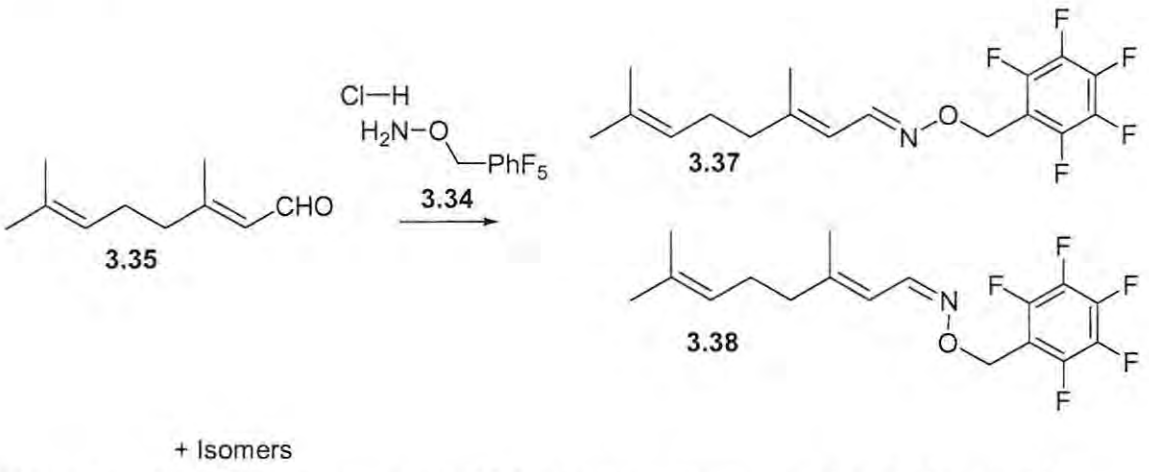

+ Isomers

Scheme 3.4 Citral (**3.35**) forms multiple PFB oxime geometric isomers (e.g. **3.37** and **3.38**)

[†] Knott (2003) has shown that the use of MeOH during extraction afforded a number of methoxylated derivatives

An equimolar ratio of citral (**3.35**) and PFBHA.HCl (**3.34**) were dissolved in acetonitrile and the reaction (monitored by normal phase TLC) occurred quantitatively at room temperature within 4 hours. On completion of the reaction the PFB oxime derivatives were extracted from the reaction mixture into *n*-hexane. Subsequent ^{1}H NMR experiments ($CDCl_3$, 400 MHz) were performed and the spectra showed distinct differences between that of citral (**3.35**) and of the product (**3.37** and **3.38**) (Figure 3.5).

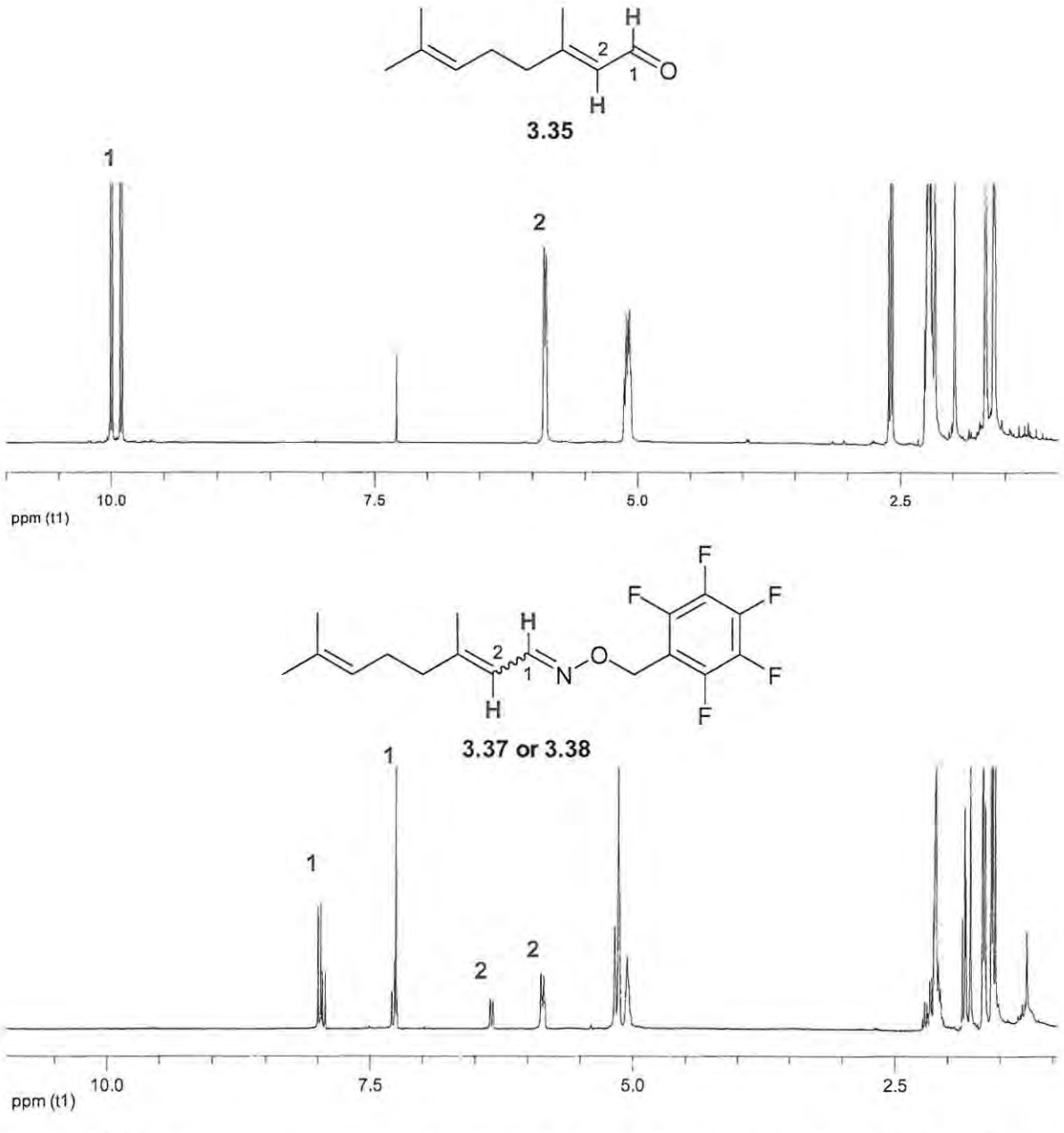

Figure 3.5 ^{1}H NMR spectra ($CDCl_3$, 400 MHz) of citral (**3.35**) and the PFB oxime derivatives of citral (**3.37** and **3.38**)

Most notably, the aldehydic doublets resonating at d 9.99 (J = 7.9) and 9.91 (J = 8.1) (Pihlasalo *et al.*, 2007) had shifted significantly up-field to approximately 8 ppm (d 7.98, d, J = 10.3 Hz and d 7.94 d, J = 10.6 Hz) and ~ d 7.3 (d 7.28, d, J = 10.0 Hz) and a new singlet resonated at ~ d 5.1.

Before derivatization, citral (**3.35**) exists as two geometric isomers, evidenced in the ^{1}H NMR spectrum by two doublets at approximately d 10 (Figure 3.5). In addition, derivatization with PFBHA (**3.34**) normally yields two geometric isomers (Hsu *et al.*, 1999). In this case, for each isomer of citral (**3.35**), two oximes were generated which led to the formation of four isomeric products observed as four peaks in the gas chromatography profile (Figure 3.6). The geometric isomers of pentafluorobenzyl (PFB) oximes are distinguishable by the relative intensities of certain fragments (Hsu *et al.*, 1999). In this study it was not established which peaks were attributed to which isomers.

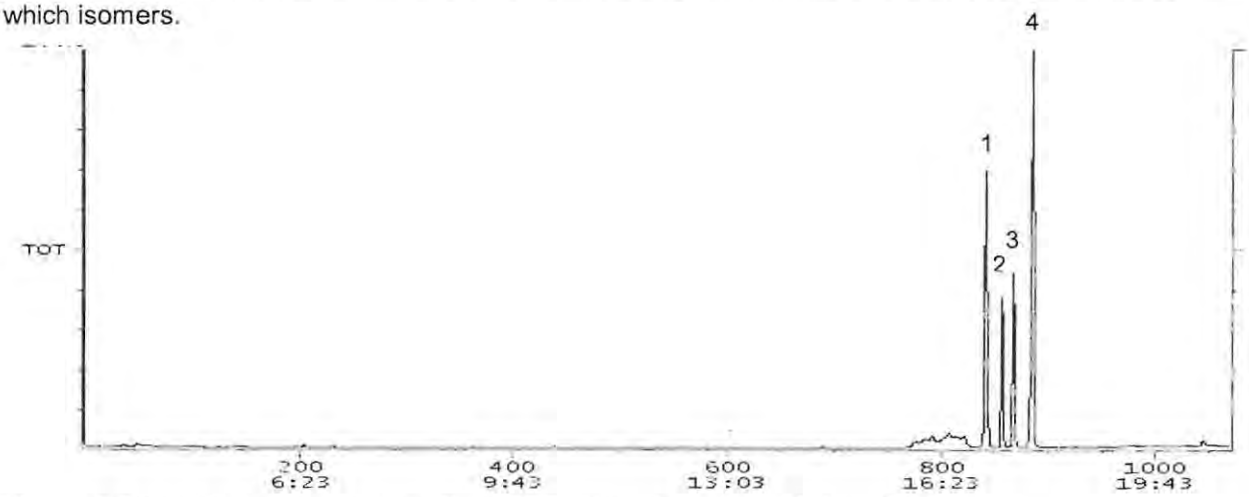

Figure 3.6 Gas chromatography profile of PFB oxime derivatives of citral (**3.35**)

Fragment ion intensities allow one to distinguish between syn and anti isomers of oxime derivatives (Hsu *et al.*, 1999)

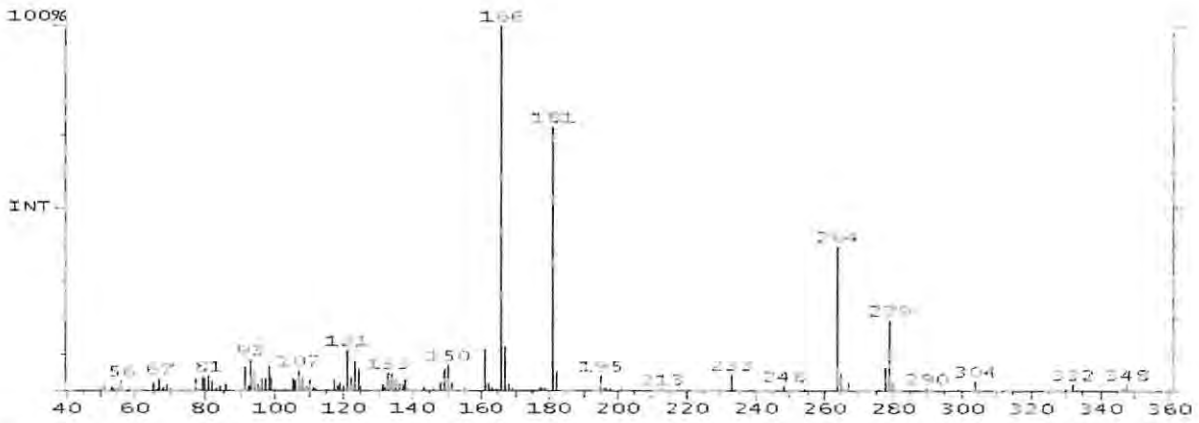

Figure 3.7 The EIMS (70 eV) spectrum for peak four (Figure 3.6) afforded by one of the isomers

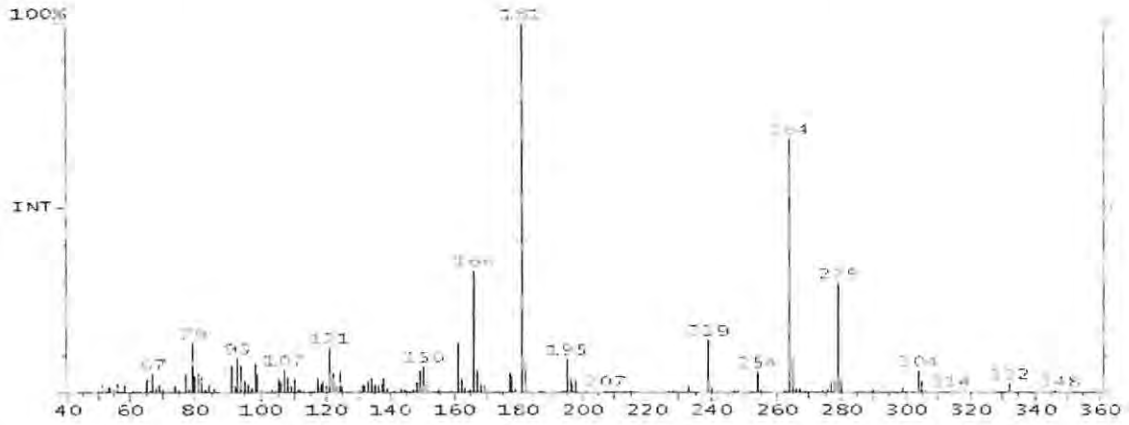

Figure 3.8 The EIMS (70 eV) spectrum produced by a second isomer (peak 3 Figure 3.6)

In the EIMS spectra of the citral PFB oxime derivatives (**3.37** and **3.38**) (Figure 3.7 and Figure 3.8), the fragment ion peak *m/z* 166 occurred with distinctly different relative abundances. Such differences in fragment ion abundances would allow the assignment of *syn* and *anti* geometries (Hsu *et al.*, 1999). Another characteristic feature of the mass spectra of PFB oxime derivatives is the base peak *m/z* 181 (seen in Figures 3.7 and 3.8) which can be attributed to the pentafluorobenzyl anion $C_6F_5CH_2^-$ (Zhong *et al.*, 2006; Spiteller *et al.*, 1999; Hsu *et al.*, 1999). Also typical of aliphatic aldehydes (C_n where n > 5) is the fragment ion of mass *m/z* 239 caused by McLafferty rearrangement (Spiteller *et al.*, 1999).

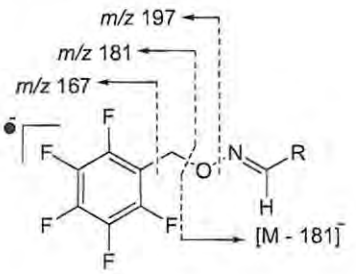

Figure 3.9 Fragment ions common to pentafluorobenzyl oxime derivatives.
Figure reproduced from Hsu *et al.* (1999) where electron capture mass spectrometry afforded anions.

The mild reaction conditions as well as the informative fragmentation pattern, together with gas chromatographic detection made *O*-(2,3,4,5,6-pentafluorobenzyl)hydroxylamine hydrochloride (**3.34**) the reagent of choice for derivatization of the halogenated monoterpene aldehydes from *P. corallorhiza*. Unfortunately, although GC-EIMS did produce the expected fragmentation pattern for citral (**3.35**), obtaining a reliable and reproducible molecular ion again proved difficult. This is reported to be a common problem associated with GC-EIMS of PFBHA oximes (Spiteller *et al.*, 1999). The solubility of the PFB oxime derivatives in CH_3CN opened up the possibility of employing more gentle ionization mass spectrometric techniques such as APCI-MS and ESI-MS. APCI and ESI are both classified as soft ionization methods that provide the molecular ion and produce less fragmentation.

Direct injection of a solution of the compound in CH_3CN into the APCI-MS produced the expected quasi molecular ion $[M+H]^+$. A molecular ion +1 is commonplace in soft ionization techniques and is produced by plasma proton transfer reactions within the ionization chamber. As expected very little fragmentation occurred on ionization (Figure 3.10) though fragments were created by increasing the collision energy from the APCI source and the base peak of *m/z* 181 characteristic of the PFB oxime (**3.7** and **3.8**) was again observed (Figure 3.11).

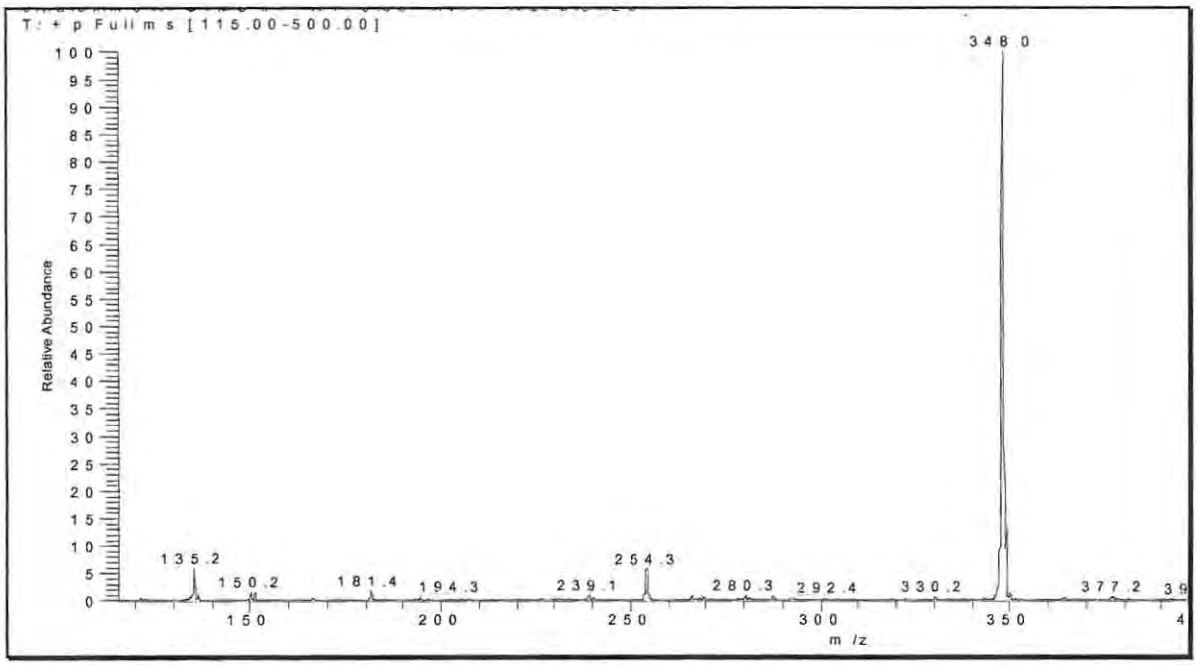

Figure 3.10 LR APCI mass spectrum of the PFB oxime derivative of citral (**3.37** and **3.38**)

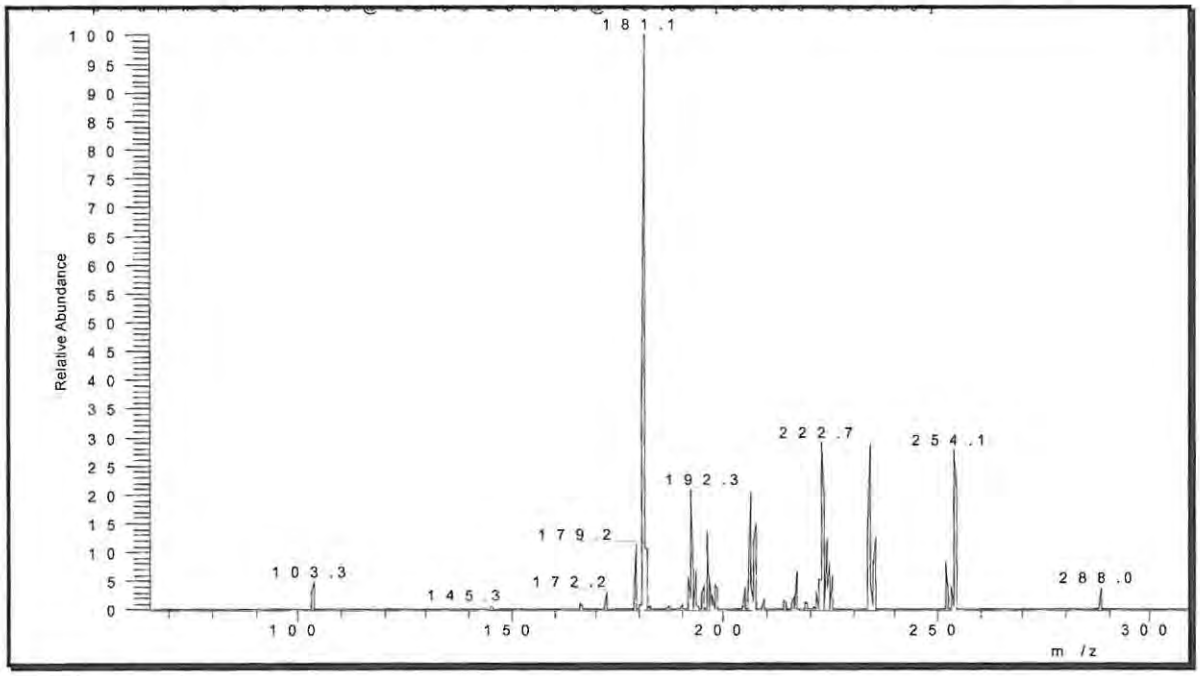

Figure 3.11 LR APCI-MS/MS daughter ion spectrum of PFB oxime derivative of citral (**3.37** and **3.38**)

3.2.3 Characterization of Plocoraldehyde A (3.26)

Plocoraldehyde A (**3.26**) was isolated as a green oil from the CH_2Cl_2-MeOH extract of *P. corallorhiza*. Immediately apparent in the ^1H NMR spectrum (Figure 3.17) of **3.26** were the doublets at 10.03 (1H, d, J = 7.4 Hz) and d 6.05 (1H, d, J = 7.5) which indicated an aldehydic moiety coupled to a vinylic proton. The spectrum also contained two triplets at d 4.74 (t, J = 7.5 Hz) and d 4.70 (t, J = 7.5 Hz) which are due to two methines existing in similar electronic and chemical environments. These two protons are coupled to the proton at d 2.42 (t, J = 7.0 Hz). Also very apparent was the terminal double bond observed as two singlets at d 5.11 and 4.96. Other signals in the proton spectrum included two methyl proton singlets at d 1.88 and 2.31. The data is consistent with 4,6-dibromo-3,7-dimethyl-octa-2,7-dienal (plocoraldehyde A) previously isolated by Mkwananzi (2005).

Compound **3.26** was present as the major aldehyde in the extract of the sample from Kenton-On-Sea (KOS06-14). It was not, however, isolated from the extract of the sample collected from Noordhoek (NDK06-22). Although the compound had been characterized almost fully by our research group, obtaining the mass spectrometry data by electron impact ionization proved futile. The successful derivatization of citral (**3.35**) with both CET triphenylphosphorane (**3.33**) and *O*-(2,3,4,5,6-pentafluorobenzyl)hydroxylamine (**3.34**) was encouraging and the reactions were attempted on the pure algal metabolite.

Derivatization of the aldehyde with CET triphenylphosphorane (**3.33**) was performed and although the reaction afforded extremely low yields, a molecular ion was observed in the low resolution APCI mass spectrum (Figure 3.12).

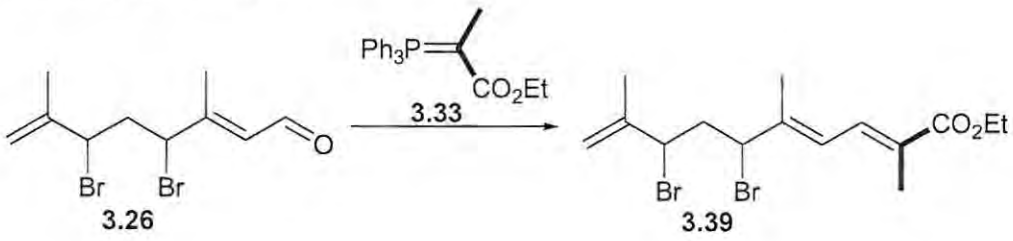

Scheme 3.5 Derivatization of Plocoraldehyde A (**3.26**) with CET triphenylphosphorane (**3.33**)

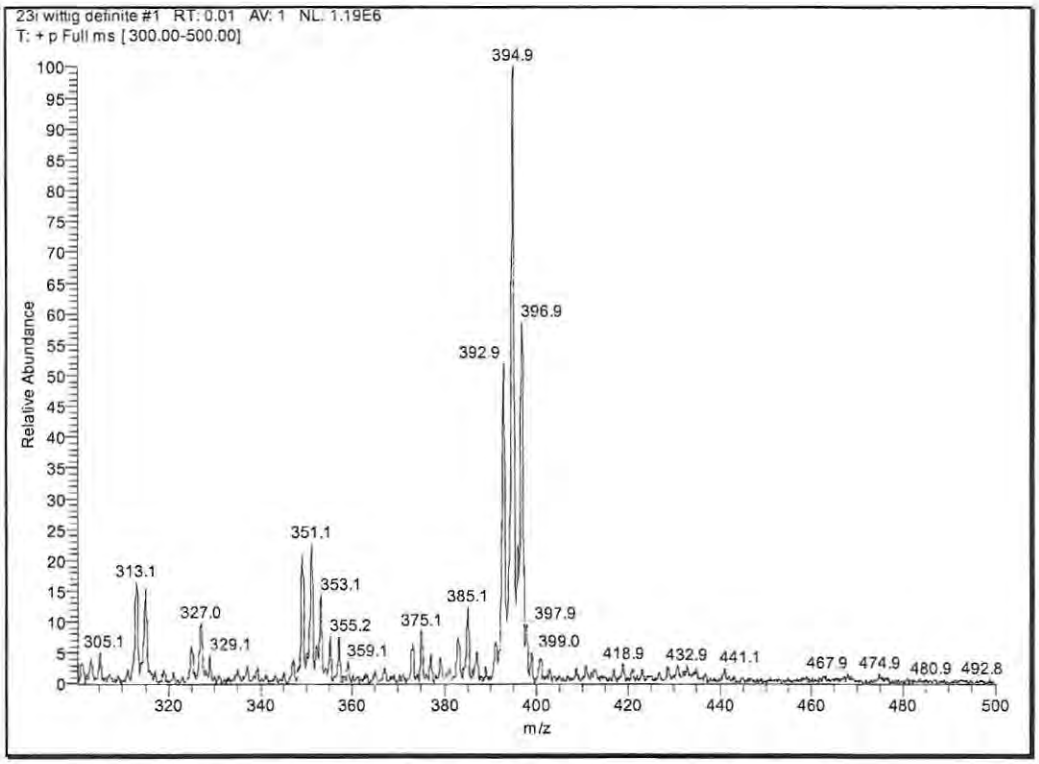

Figure 3.12 APCI mass spectrum of the CET derivative of **3.26** (**3.39**)

The molecular ion $[M+H]^+$ is observed as a multiple peak cluster due to the two naturally occurring isotopes of the bromine atom. The fragment *m/z* 313 occurs as two peaks after the loss of one bromine atom M^+ 393 – 80 = *m/z* 313, whereas the fragment *m/z* 351 still contains two bromine atoms and like the molecular ion, has three peaks. The isotopic abundances are extremely useful in the confirmation of the identity and position halogens in the molecule (Naylor *et al.*, 1983).

The reaction between PFBHA.HCl (**3.34**) and **3.26** occurred quantitatively at room temperature within four hours and afforded almost 100 % yield. Initially GC EIMS was attempted; upon injection into the gas chromatograph the derivative underwent a degree of fragmentation (Figure 3.13), however the molecular ion was observed in the EIMS spectrum (Figure 3.14). As was the case for the PFB oxime derivatives (**3.37** and **3.38**) of citral, M^+ was small and the isotope clusters were not as distinct as observed in the APCI-MS spectrum of the CET derivative (**3.39**).

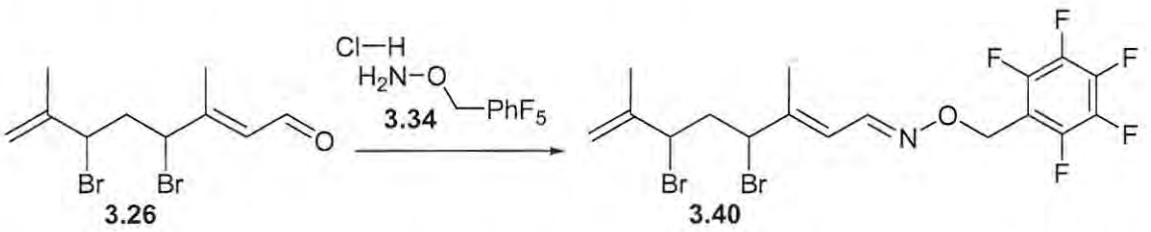

Scheme 3.6 Derivatization of Plocoraldehyde A (**3.26**) with *O*-(2,3,4,5,6-pentafluorobenzyl)-hydroxylamine (PFBHA) hydrochloride (**3.34**)

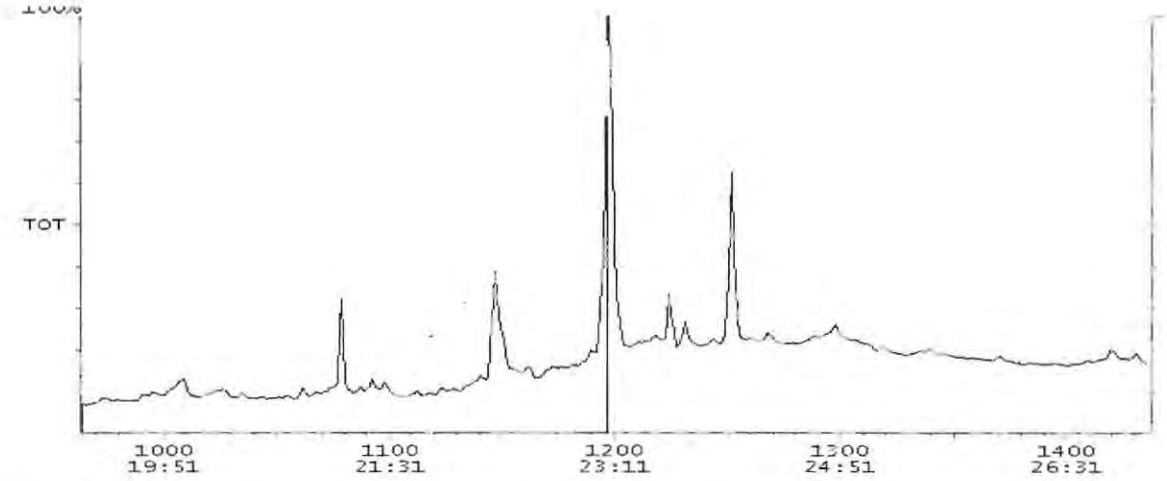

Figure 3.13 Gas chromatography profile of **3.40** shows peaks of low intensity

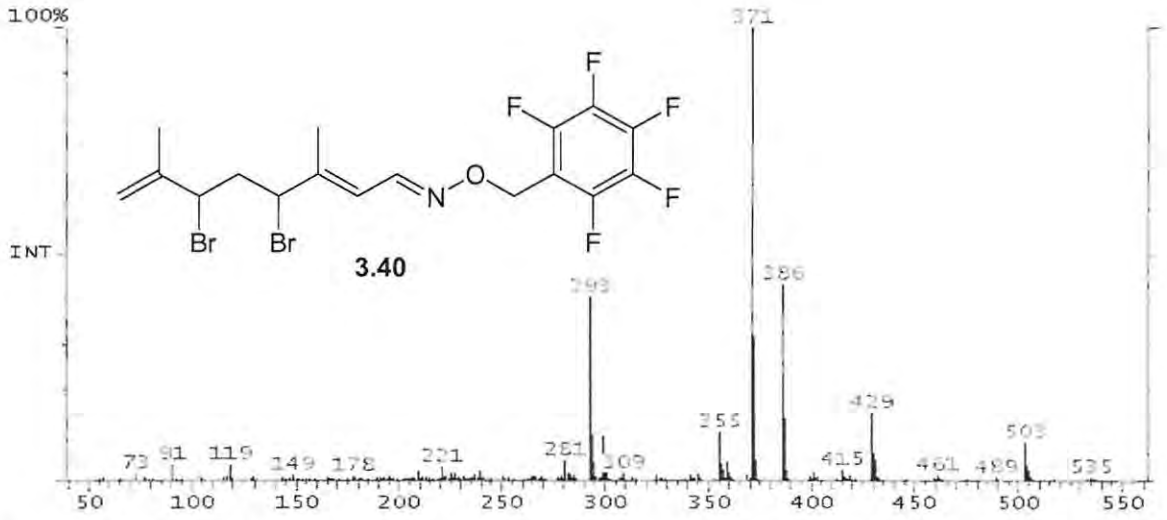

Figure 3.14 The LR EIMS spectrum containing the molecular ion *m/z* 503 for **3.40**

The compound's solubility in acetonitrile availed the use of soft ionization techniques and upon direct injection of a solution of **3.40** in CH_3CN into the APCI-MS; a strong and unambiguous molecular ion was observed (Figure 3.15).

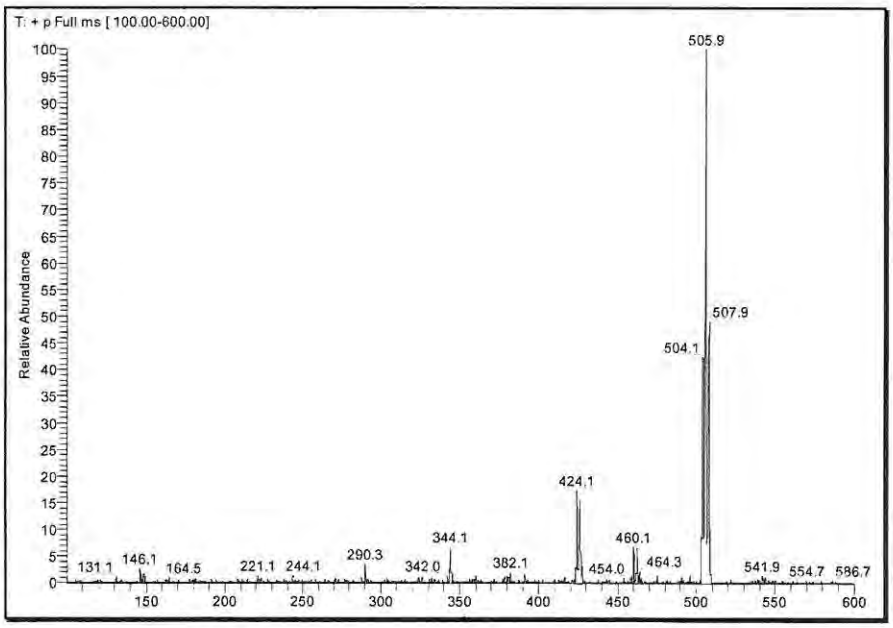

Figure 3.15 APCI-MS spectrum of the PFB oxime of **3.26** (**3.40**) clearly showing $[M+H]^+$

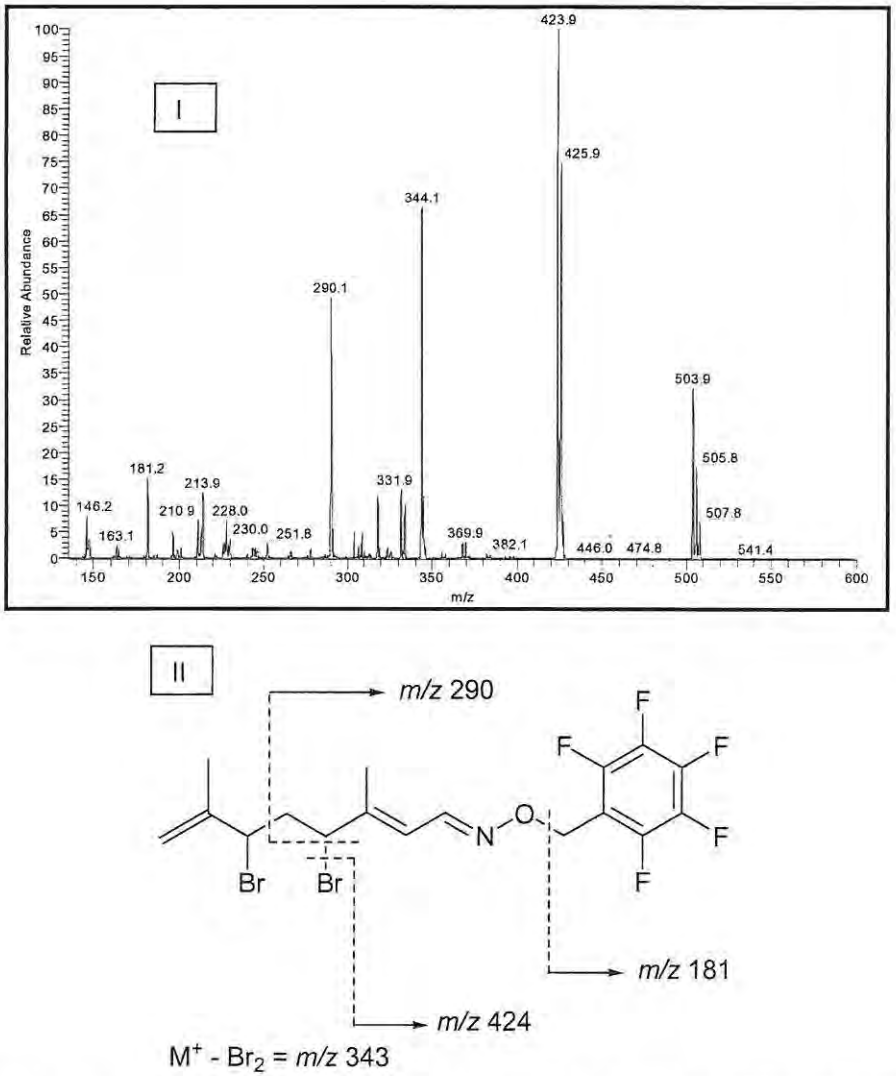

Figure 3.16 I) APCI-MS-MS spectrum showing fragment ions II) Possible fragment ions of **3.40**

In order to ascertain whether the correct derivative had formed, a series of one- and two-dimensional NMR experiments were performed.

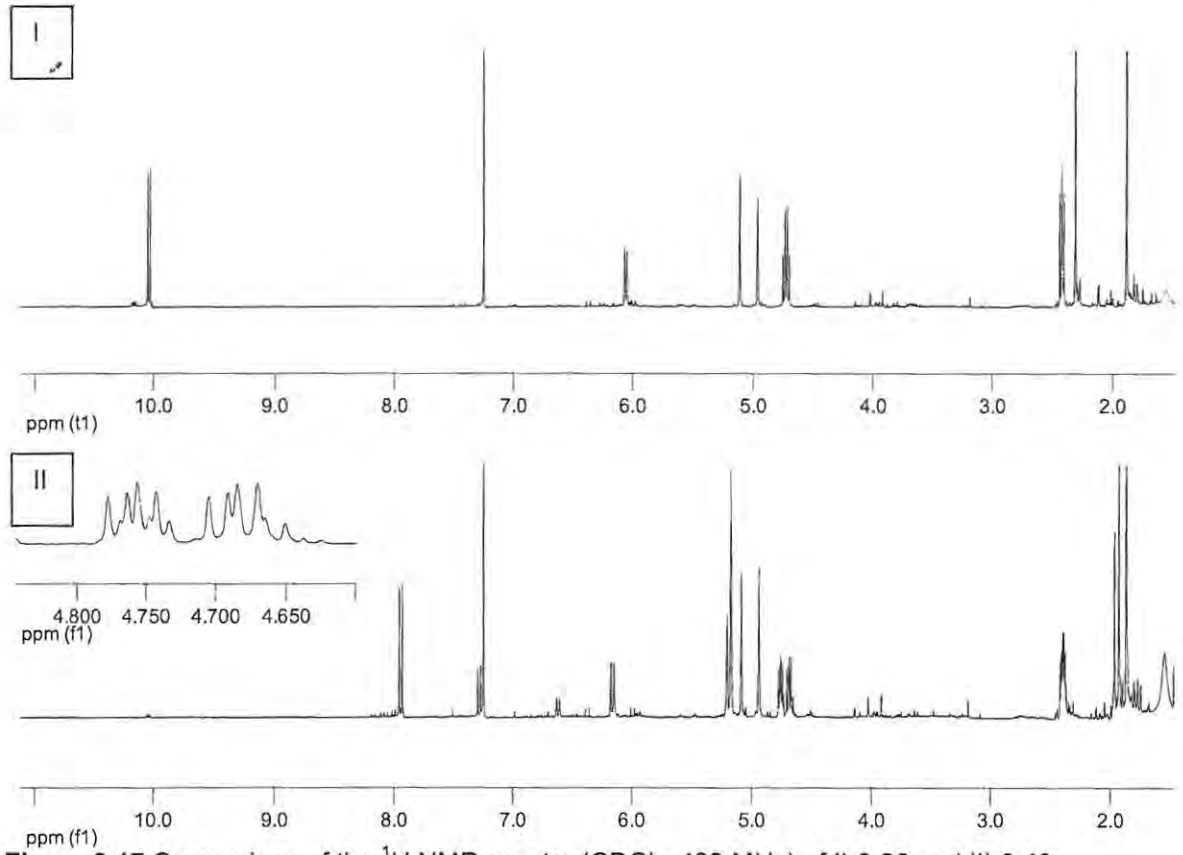

Figure 3.17 Comparison of the ^{1}H NMR spectra ($CDCl_3$, 400 MHz) of I) **3.26** and II) **3.40**

On evaluation of the ^{1}H NMR spectra (Figure 3.17), it was immediately apparent, as it was for citral (**3.35**), that the aldehydic doublet at d 10.03 had shifted noticeably up-field to ~ d 7.94 (The doublet of the less abundant isomer resonates at d 7.30), the nitrogen being less electronegative than the oxygen will cause less deshielding of protons. Substituting the aldehydic moiety for the bulky oxime substituent has an effect on the bromomethines placing them in different electronic environments; this causes the two-proton multiplet at d 4.72 to become two discrete multiplets resonating at d 4.76 and 4.68. The singlets attributed to the terminal olefin shifted slightly up-field due to decreased deshielding. A new absorption was observed at d 5.17.

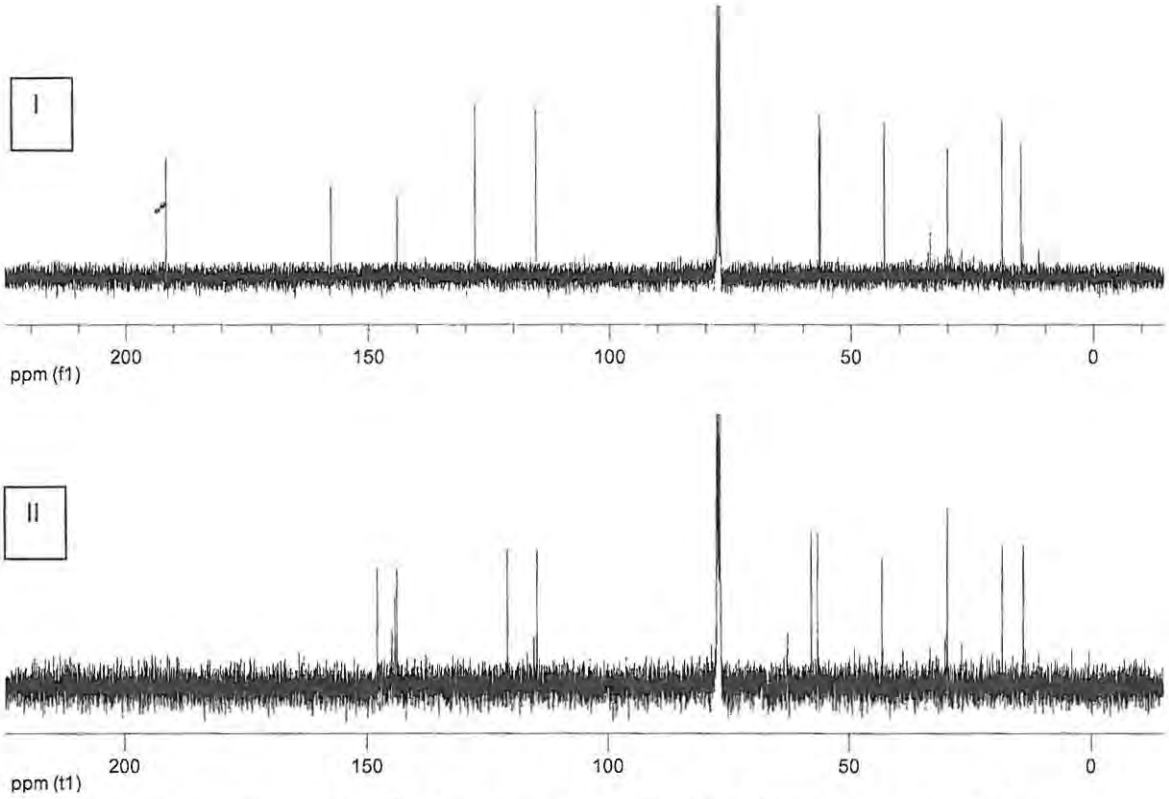

Figure 3.18 Comparison of the ^{13}C NMR spectra ($CDCl_3$, 100 MHz) of I) **3.26** and II) **3.40**

The carbonyl shift attributed to the aldehyde was absent in the ^{13}C NMR spectrum of the PBO oxime derivative (**3.40**) and a number of additional olefinic resonances were observed. Only one new absorbance appears below 100 ppm, a signal at d 62.7 which is due to the benzyl $-CH_2$ in the PFB oxime moiety of **3.40**.

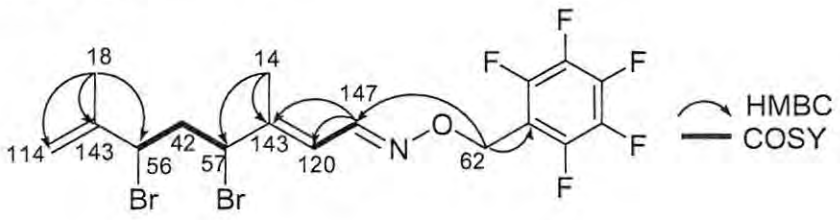

Figure 3.19 Key HMBC and ^1H-^1H COSY correlations used to determine the structure of **3.40**

The structure determined for the PFB oxime derivative of **3.26** by way of one-and two-dimensional NMR was identical to that of the aldehyde with exception of the carbonyl moiety which had been replaced with the pentafluorobenzyl oxime functionality. The reduced deshielding effect produced by the oxime allows visualization of the two bromomethine proton resonances previously superimposed upon one another.

Table 3.5 A comparison of the NMR data for **3.26** and **3.40** (^{1}H, 400 MHz; ^{13}C, 100 MHz; $CDCl_3$)

	3.26			**3.40**				
Carbon No.	d_C		d_H, multi, *J* (Hz)	d_C		d_H, multi, *J* (Hz)	HMBC	^{1}H-^{1}H COSY
1	191.2	C=O	10.03, d, 7.4	147.9	C=N	7.94, d, 10.2	C2, C3	H2
2	127.8	CH	6.05, d, 7.5	120.9	C=H	6.16, d, 9.7		H1, H10
3	157.3	C		143.8	C			
4	56.1*	CH	4.72, t, 7.5	57.9	CH	4.75, m	C6, C2	H5
5	42.7	CH_2	2.42, t, 7.0	43.2	CH_2	2.394 s	C4, C6, C7	H4, H6
6	56.0*	CH	4.72, t, 7.5	56.5	CH	4.68, m	C4	H5
7	143.7	C		143.7	C			
8	115.0	CH_2	5.10, s, 4.96, s	114.8	CH_2	5.09, s, 4.94, s	C6, C7, C9	H9
9	18.5	CH_3	1.88, s	18.4	CH_3	1.87, s	C8, C7, C6	H11
10	14.5	CH_3	2.31, s	14.0	CH_3	1.93, s	C2, C3, C4	
11				62.7	CH_2	5.17, s	C12, C^{AR}C1	
12				110.6	C			
13-16				144.2**				

* Carbon chemical shifts are interchangeable, ** Quaternary aromatic signals HMBC data ambiguous

The mass spectral data generated for the PFB oxime derivative of **3.26** provides evidence for the structure of the halogenated monoterpene aldehyde by confirming the number and identity of the halogens by way of isotopic clusters for both the molecular ion and daughter ions. Finally, the stability of the PFB oxime and its solubility in acetonitrile enables the use of soft ionization techniques which provide unambiguous molecular ions. The conclusion and of course ultimate goal of this part of the study was to obtain the molecular weight and formula by way of high resolution mass spectrometry. $[M+H]^+$ for **3.40** was found by ESI-MS to be 503.9608 consistent with the molecular formula $C_{17}H_{17}NOF_5Br_2$ (calcd for $C_{17}H_{17}NOF_5{}^{79}Br_2$, 503.9597).

3.2.4 Characterization of Plocoraldehyde C (3.22)

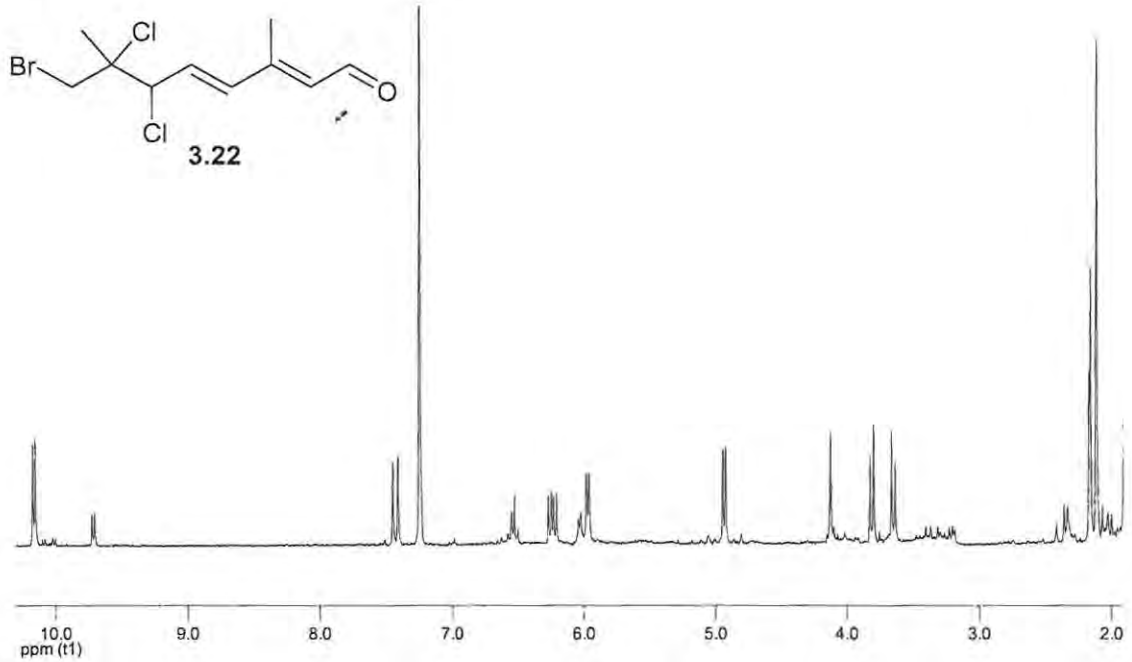

Figure 3.20 ^{1}H NMR spectrum ($CDCl_3$, 400 MHz) of **3.22**

The ^{1}H NMR spectrum of **Plocoraldehyde C** (**3.22**, Figure 3.20) showed a deshielded proton signal at d 10.15 (J = 7.8 Hz) coupled to the proton at d 6.00 (J = 7.8 Hz) which indicated the presence of an aldehyde adjacent a vinylic proton. Also observed, a vinyl methine signal at d 6.53 (d, J = 15.6 Hz) and 6.33 (dd, J = 8.8 and 15.6 Hz), the latter being coupled to a halomethine at d 4.91 (d, J = 8.8 Hz) indicative of a -CH=CH-CHX- moiety. The halomethylene signal was observed as a doublet of doublets d 3.84 and 3.64 (J = 10.9 Hz); the protons of this methylene group are diastereotopic as a result of the neighbouring stereogenic centre. This data is consistent with 8-bromo-6,7-dichloro-3,7-dimethyl-octa-2,4-dienal previously isolated by Mkwananzi (2005). Plocoraldehyde C was derivatised using PFBHA.HCl (**3.34**) in an identical manner to Plocoraldehyde A. By way of high resolution ESI-MS, the molecular weight of the PFB oxime derivative (**3.41**) was found to be *m/z* 493.9706 (calcd for $C_{17}H_{16}NOF_5{}^{35}Cl_2{}^{79}Br$, 493.9712).

3.2.5 Characterization of Plocoraldehyde B (3.25)

Successful derivatization of the pure Plocoraldehydes (**3.26** and **3.22**) prompted an attempt at derivatization of the aldehydic compounds prior to purification by semi-preparative HPLC. The reaction followed the same principles used for the pure compounds and no changes were made to the established procedure. The goal of this experiment was to obtain sufficient sample for mass spectrometry; the Plocoraldehydes themselves had already been almost fully characterized (Mkwananzi, 2005). It is because of this that a relatively small mass of crude extract was used in the reaction and hence the quantity of each oxime derivative was proportionately small.

The fozen alga was sequentially extracted with MeOH and CH_2Cl_2-MeOH. These extracts were fractionated by silica gel column chromatography. Silica gel column fractions A3, A4 and A5 were recombined after ^{1}H NMR data indicated the presence of aldehydic compounds in each fraction. The crude extracts were derivatized following the same procedure used for the pure compounds. Following derivatization, the compounds were extracted into *n*-hexane and isolated by way of normal phase HPLC (*n*-hexane) to give compounds **3.40**, **3.42** and **3.43**.

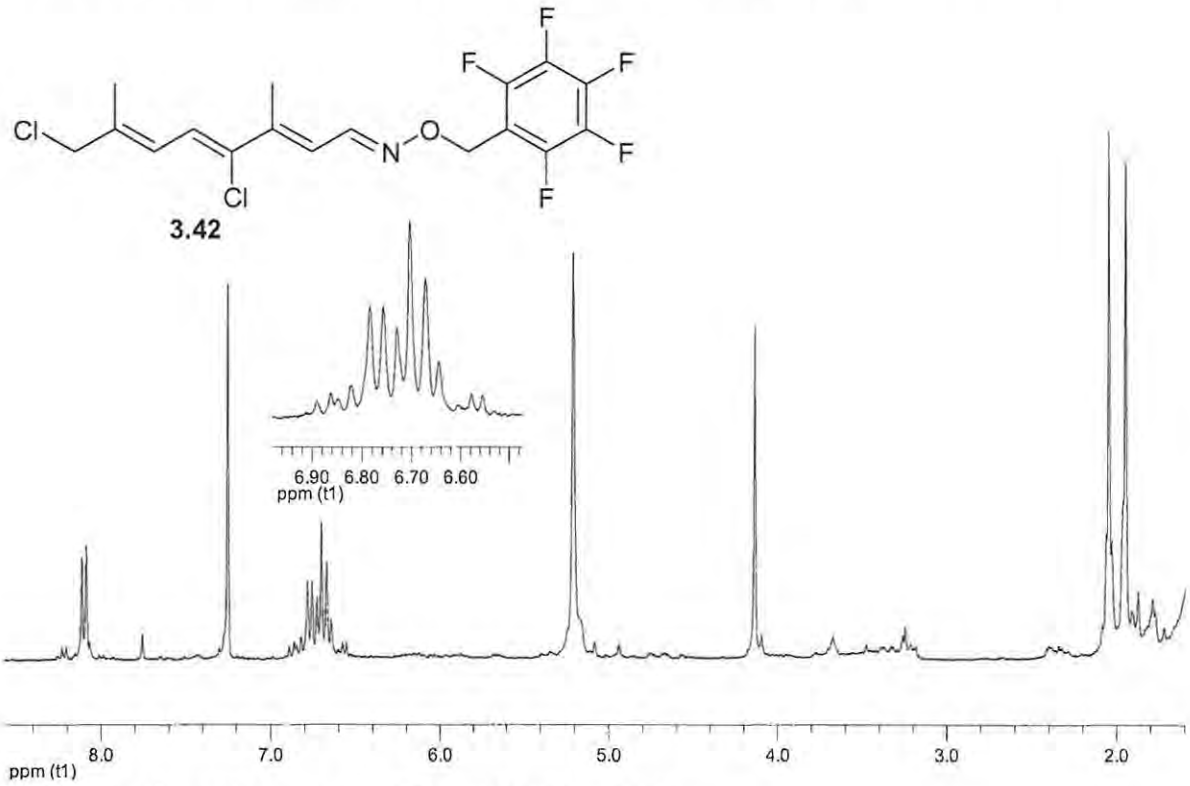

Figure 3.21 ^{1}H NMR spectrum ($CDCl_3$, 400 MHz) of **3.42**

Plocoraldehyde B (**3.25**) previously isolated by Mkwananzi (2005) was not isolated as the aldehyde; rather, the oxime derivative **3.42** was isolated from the crude extract following derivatization with PFBHA (**3.34**). The mass spectral data obtained for **3.42** (M^+ 414.0437) was in agreement with the molecular formula $C_{17}H_{15}NOF_5Cl_2$ (calcd for $C_{17}H_{15}NOF_5{}^{35}Cl_2$ 414.0451).

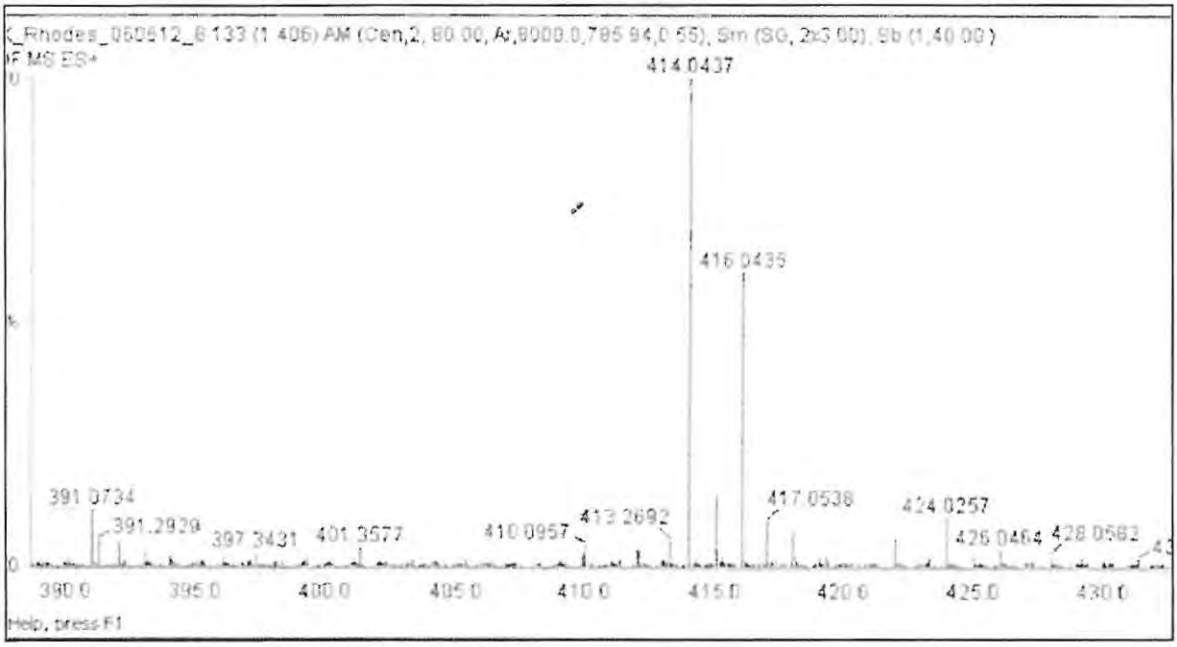

Figure 3.22 The high resolution ESI mass spectrum of **3.42**

3.2.6 Characterization of Plocoraldehyde D (3.23)

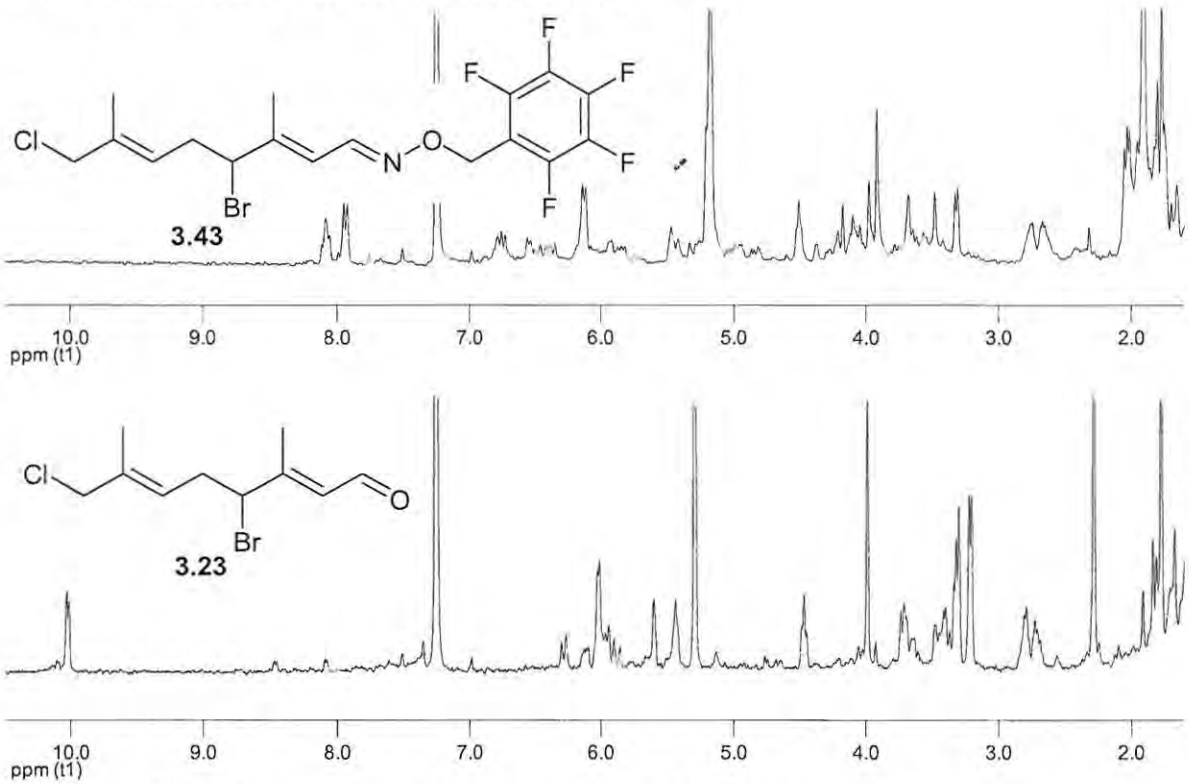

Figure 3.23 ^{1}H NMR spectrum ($CDCl_3$, 400 MHz) of **3.23** and **3.43**

Plocoraldehyde D (**3.23**) also described by Mkwananzi (2005) was isolated in very small quantities and the compound was not purified fully. The resonances were however, discernable in the ^{1}H NMR spectrum (Figure 3.23). The oxime derivative (**3.43**) provided the molecular ion (M^{+}) *m/z* 460.0148 which is consistent with the molecular formula $C_{17}H_{17}NOF_5BrCl$ (calcd $C_{17}H_{17}NOF_5{}^{79}Br^{35}Cl$ 460.0102). Unfortunately because of the small quantity of aldehyde and oxime, as well as the impure nature of the sample, there is a degree of doubt surrounding the validity of these results and it will be necessary to re-isolate the compounds in sufficient amounts so as to repeat the experiments and verify the data.

Table 3.6 ^{1}H NMR chemical shifts for **3.25** vs. **3.42** and **3.23** vs. **3.43** ($CDCl_3$, 400 MHz)

	3.25	**3.42**	**3.23**	**3.43**
Carbon No.	d_H, multi, *J* (Hz)	d_H, multi, *J* (Hz)	d_H, multi, *J* (Hz)	d_H, multi, *J* (Hz)
1	10.15, d, 7.66	8.10, d, 10.3	10.03, d, 7.3	7.94, d, 9.9
2	6.52, d, 7.66	6.72, d, 10.3	6.02, d, 7.3	6.13, d, 9.4
3				
4			4.47, t, 7.58	4.51, t
5	7.02, d, 10.61	6.77, d, 10.6	2.78, m	2.76, 2.72, m
6	6.71, d, 10.61	6.66, d, 10.6	5.43, t, 6.57	5.49, t
7				
8	4.15, s	4.14, s	3.98, s	3.91, s
9	2.00, s	1.95, s	1.81, s	1.71, s
10	2.41, s	2.05, s	2.25, s	1.90, s
11		5.21, s		5.17, s

3.2.7 Characterization of Plocoraldehyde E (3.44)

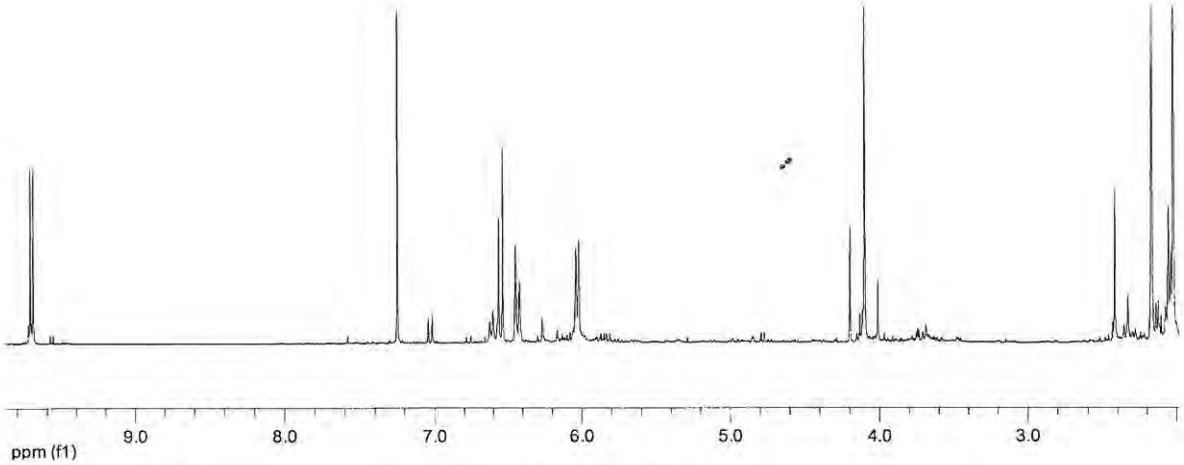

Figure 3.24 ^{1}H NMR spectrum ($CDCl_3$, 400 MHz) of **3.44**

Compound **3.44** was isolated as a yellow oil with UV chromophores absorbing at λ_{max} 226.4, 256.0, 291.2 and 312.0 nm. The oil was viscous and had a strong citrus odour. Immediately obvious in the ^{1}H NMR spectrum (Figure 3.24) was the aldehydic doublet resonating at d 9.70 (d, J = 7.7 Hz) coupled to an olefinic proton at d 6.03 (d, J = 7.7 Hz). The presence of an aldehyde was supported by the absorption band at 1670.1 cm^{-1} in the Infrared spectrum. Two coupled vinylic protons were observed at d 6.54 (d, J = 10.6 Hz) and 6.44 (d, J = 10.6 Hz) indicating a second double bond. The unsaturated nature of this oil was further evidenced by two vinylic methyl signals at d 2.01 (s) and 2.17 (s). Also in the spectrum a singlet due to two methylene protons was observed at d 4.10.

The ^{13}C NMR spectrum (Figure 3.25) confirmed that the compound was a monoterpene. Ten absorbances were observed including six sp^2 hybridized carbons resonating at d 157.2, 140.8. 131.3, 129.6, 126.6, 123.9, two methyl carbons d 22.7 and 22.9, a halomethylene carbon at d 42.8 and a carbonyl carbon at d 191.3. The number of olefinic carbon resonances supported by the deshielded vinylic proton shifts in the one-dimensional spectra point towards an acyclic highly unsaturated monoterpene.

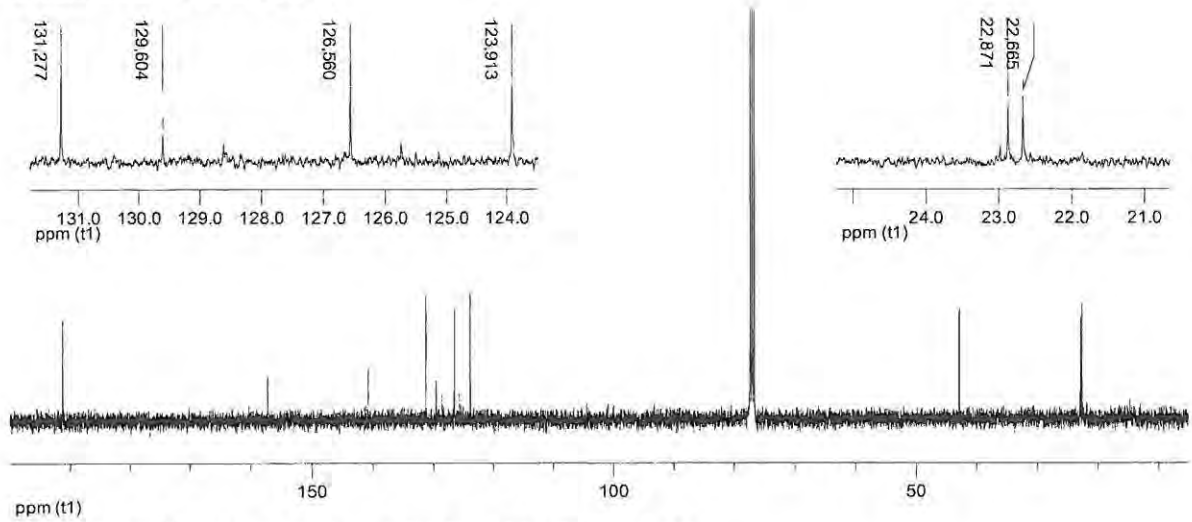

Figure 3.25 ^{13}C NMR spectrum ($CDCl_3$, 100 MHz) of **3.44**

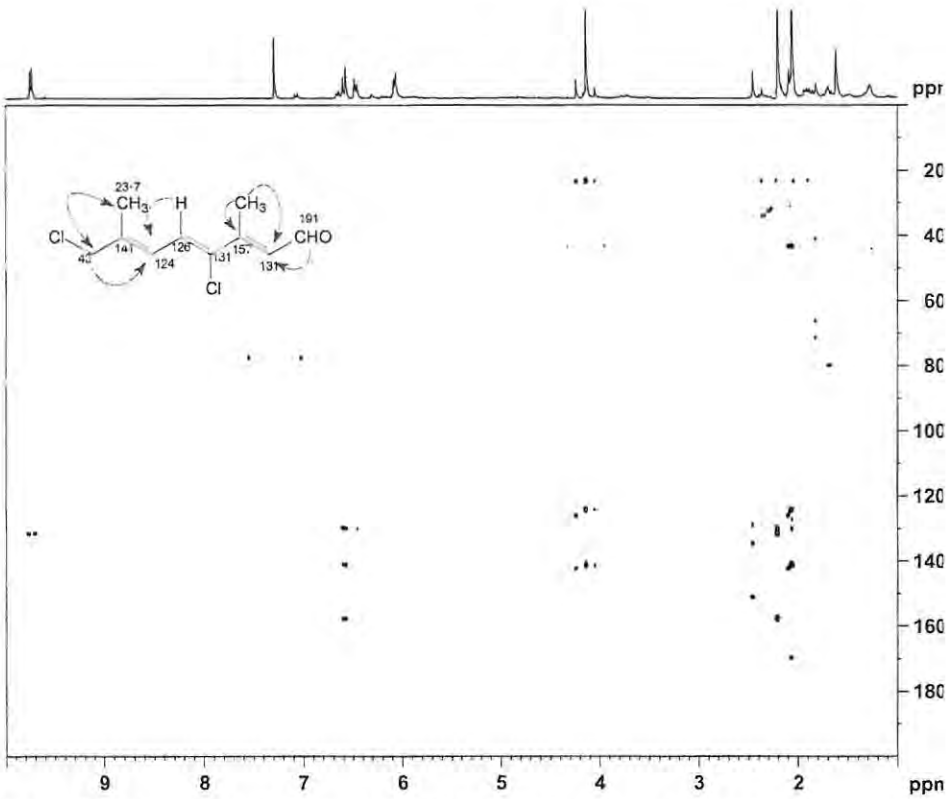

Figure 3.26 ^{1}H-^{13}C HMBC spectrum ($CDCl_3$, 400 MHz, 100 MHz) of **3.44**

Interpretation of two-dimensional HSQC and HMBC data (Table 3.7, Figure 3.27) provided important information necessary for the construction of two molecular fragments. HMBC correlations (Table 3.7, Figure 3.27) from the methyl protons at d 2.02 (C-9) to carbon atoms at d 42.8 (C-8), 140.8 (C-7), 123.9 (C-6), 126.6 (C-5) were observed. The methyl proton at d 2.17 displayed clear HMBC correlations to carbons at d 131.3 (C-2), 157.2 (C-3) and 129.6 (C-4). The proton coupled to the carbon at d 126.6 displays HMBC correlations to carbons at 157.2 (C-3).

Three and four bond ^{1}H-^{1}H COSY correlations were informative as to the relative positions of the methyl groups and the connectivity of the two fragments. The proton at d 6.54 (H-5) coupled to the carbon at d 126.6 displays ^{1}H-^{1}H COSY correlations to H-6. The proton at d 9.70 (H-1) showed strong ^{1}H-^{1}H COSY correlations to the proton at d 6.03 (H-2). Four bond ^{1}H-^{1}H COSY correlations were observed from the proton at d 6.03 (H-2) to the methyl protons at d 2.17 (H_3-10) and from the proton at d 6.71 (H-6) to the methyl protons at d 2.02, 129.6 (C-4) and 140.8 (C-7) (Figure 3.27).

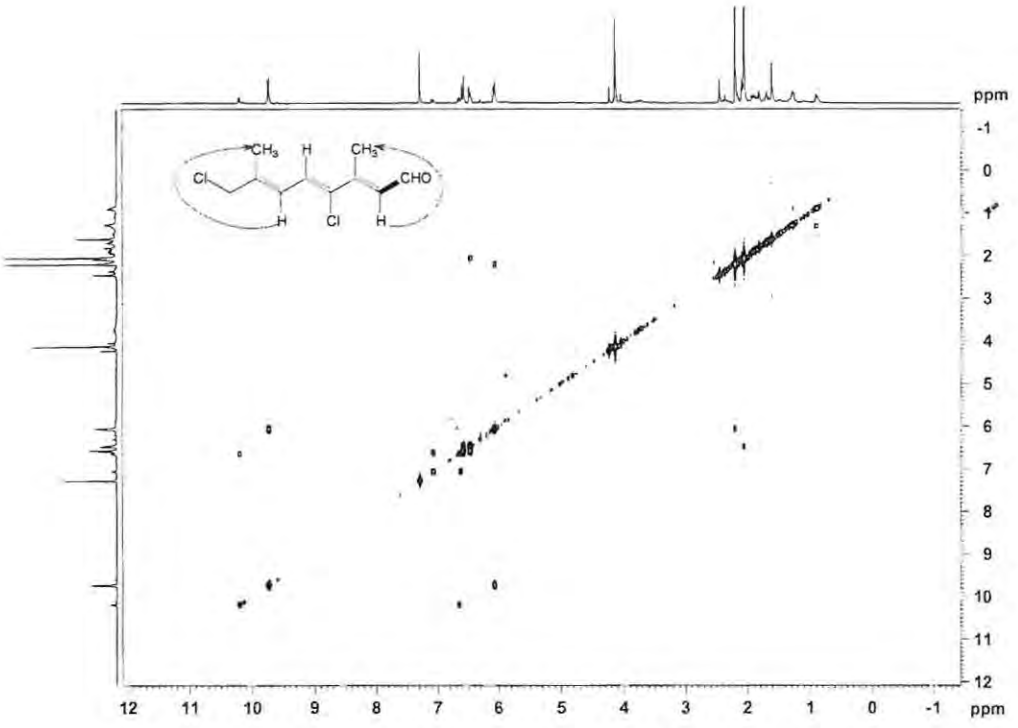

Figure 3.27 ^{1}H-^{1}H COSY spectrum ($CDCl_3$, 400 MHz) of **3.44**

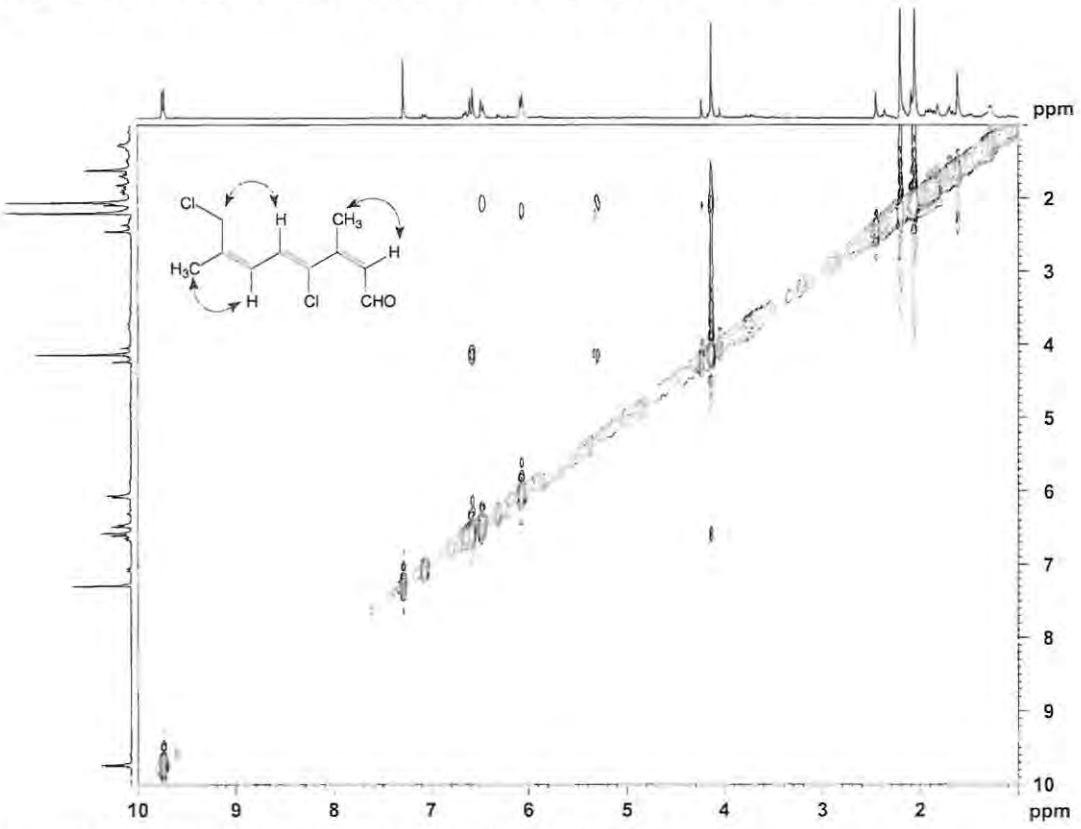

Figure 3.28 NOESY spectrum ($CDCl_3$, 400 MHz) of **3.44**

The double bond Δ^{1-2} was assigned the *Z* geometry from the ^{13}C NMR chemical shift value of the methyl group (C-10, d 22.9) and by NOE's between H-2 and H-10. *Z* geometry for the Δ^{2} double

bond has also been reported in related compounds such as Plocoralide C (**3.45**) (Knott *et al.*, 2005) where strong NOESY correlations were reported between H-2 and H-10.

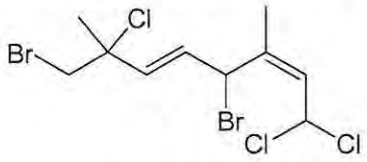

3.45

Further evidence in support of the proposed *Z* geometry is provided by the ^{13}C NMR chemical shifts of related monoterpene aldehydes. Citral (**3.35**) comprises of *Z* and *E* geometric isomers; the ^{13}C NMR chemical shift of the vinylic methyl (C-10) in *Z*-citral is reported to be d 24.93 while that of the *E*-isomer is d 17.41 (Pihlasalo *et al.*, 2007). A difference of 5-8 ppm in ^{13}C NMR shifts of vinylic methyl groups is a characteristic difference of *E* and *Z* geometry in halogenated monoterpenes (Crews and Kho-Wiseman, 1977). The methyl carbon (C-10) in Plocoraldehydes A (**3.26**), B (**3.25**) and C (**3.22**) all exhibit ^{13}C NMR chemical shifts of d ~ 14 ppm (Mann *et al.*, 2007); each of these plocoraldehydes have *E* geometry at the Δ^2 double bond. The double bond Δ^{6-7} was assigned *Z* geometry due to NOESY correlations between H-8 and H-5 as well as between H-9 and H-6. The geometry of the Δ^{4-5} double bond could not be determined due to a lack of clear NOESY correlations between H-6 and the two methyl groups.

Aside from the differences in double bond geometry, the data collected indicated a molecular structure similar to that of the previously described Plocoraldehyde B (**3.25**). The ^{1}H NMR data of Plocoraldehyde B (**3.25**) showed distinct differences in the chemical shifts of H-1, H-2, H-5, H-6, while the ^{13}C NMR shifts of Plocoraldehyde B (**3.25**) and E (**3.44**) of all but C-1 differed significantly (Table 3.7). The chemical shifts of C-4 (d 129.6) and C-8 (d 42.8) are suggestive of bromine atoms at these positions (Naylor *et al.*, 1983, Crews *et al.*, 1984), however mass spectrometry of the PFBHA oxime indicated that these atoms were infact chlorine atoms indicating that Plocoraldehyde E (**3.44**) is a geometric isomer of Plocoraldehyde B (**3.25**).

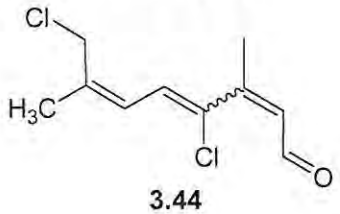

3.44

Table 3.7 A comparison of the NMR data for Plocoraldehyde B (**3.25**) and Plocoraldehyde E (**3.44**) in $CDCl_3$ (^1H NMR, 400 MHz; ^{13}C NMR, 100 MHz)

	3.25			**3.44**					
Carbon No.	d_C		d_H, multi, *J* (Hz)	d_C		d_H, multi, *J* (Hz)	^1H-^1H COSY	HMBC	NOE
1	191.2	CH	10.15, d, 7.7	191.3	CH	9.70, d, 7.7	H2	C2	H2
2	128.5	CH	6.62, d, 7.7	131.3	CH	6.03, d, 7.7	H1, H10	C10, C4	H10, H1
3	150.6	C		157.2	C				
4	135.0	C		129.6	C				
5	126.2	CH	7.02, d, 10.6	126.6	CH	6.54, d, 11.0	H6	C4, C7, C3	H8
6	125.1	CH	6.71, d, 10.6	123.9	CH	6.44, d, 11.0	H5	C10, C8, C4	H9
7	142.0	C		140.8	C				
8	51.2	CH_2	4.15, s	42.8	CH_2	4.10, s		C9, C6, C7, C4, C5	H5
9	15.9	CH_3	2.00, s	22.7	CH_3	2.02, s	H6	C8, C6, C5, C7	H6
10	14.7	CH_3	2.41, s	22.9	CH_3	2.17, s	H2	C1, C3, C2, C4	H1, H2

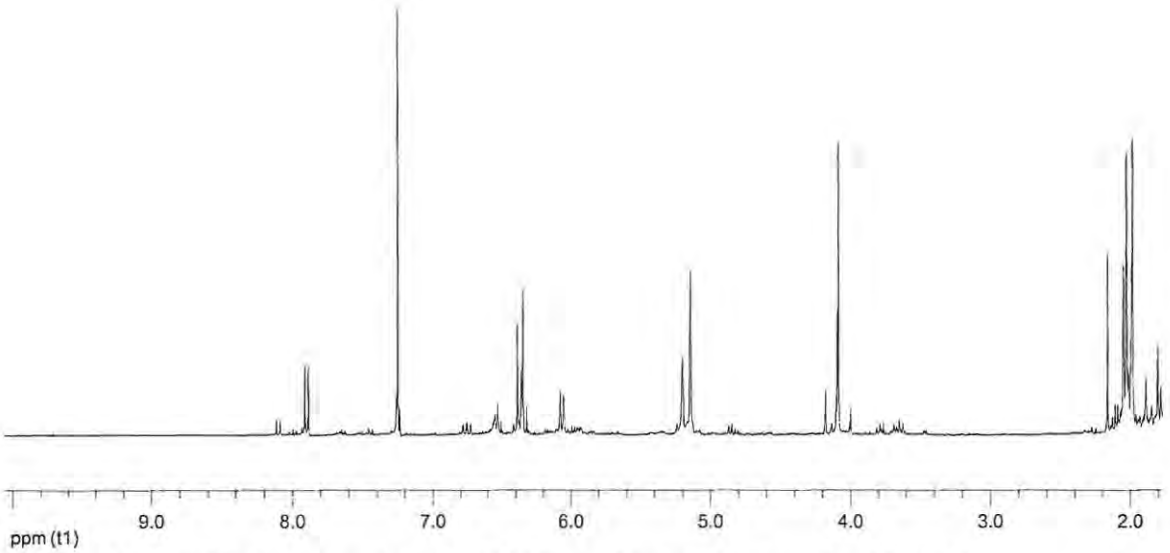

Figure 3.29 ^1H NMR spectrum ($CDCl_3$, 400 MHz) of the PFB oxime of **3.44** (**3.46**)

As with the aforementioned previously isolated Plocoraldehydes, attempts at obtaining the mass spectrometry data by EIMS were unsuccesful. The PFB oxime (**3.46**, ^1H NMR spectrum Figure 3.29) was formed following the procedure developed on citral (**3.35**). One- and two-dimensional NMR experiments were performed to establish whether the derivatization had modified the original structure other than substitution of the aldehyde with the pentafluorobenzyl oxime moiety. Unlike other PFB oxime derivatives of halogenated monoterpene aldehydes isolated from *Plocamium corallorhiza*, **3.46** degraded fairly rapidly, frustrating our efforts with regard to obtaining mass spectrometry data. A dark red precipitate formed in $CDCl_3$ over a period of 48 hours and the

strength of the NMR sample decreased proportionately. For this reason, NMR experiments were performed on slightly impure samples to avoid loss of product during the time taken in purification. Small amounts of impurities did not hinder the structural elucidation as the absorbances for **3.46** were discrete from those of the impurities. A molecular weight of 414.0452 was obtained by high resolution ESI-MS which is in agreement with the molecular formula of $C_{17}H_{15}NOF_5Cl_2$ (calcd for $C_{17}H_{15}NOF_5{}^{35}Cl_2$, 414.0451).

As for Plocoraldehyde A (**3.26**), one-and two-dimensional NMR experiments provided evidence (Table 3.8) that the structure had undergone no additional changes other than the substitution of the aldehyde group for an oxime moiety.

Table 3.8 One- and two-dimensional NMR chemical shifts and correlations for **3.44** and **3.46** ($CDCl_3$, ^1H NMR 400 MHz, ^{13}C NMR 100 MHz)

	3.44			**3.46**				
Carbon No.	d_C		d_H, multi, *J* (Hz)	d_C		d_H, multi, *J* (Hz)	^1H-^1H COSY	HMBC
1	191.3	CHO	9.70, d, 7.7	149.0	C=N	7.90, d, 10.2	H2	C2
2	131.3	CH	6.03, d, 7.7	122.7	CH	6.07, d, 10.2	H1, H10	C4, C10
3	157.2	C		144.2	C			
4	129.6	C		131.3	C			
5	126.6	CH	6.54, d, 11.0	124.4	CH	6.37, d, 16.7		
6	123.9	CH	6.44, d, 11.0	123.9	CH	6.34, d, 16.3	H9	C4, C8
7	140.8	C		138.6	C			
8	42.8	CH_2	4.10, s	43.1	CH_2	4.09, s		C6, C7, C9
9	22.7	CH_3	2.02, s	22.5	CH_3	1.98, s	H5, H6	C6, C7, C8
10	22.9	CH_3	2.17, s	22.7	CH_3	2.03, s	H2	C2, C3, C4
11				62.6	CH_2	5.13, s		C1, C12, C^{Ar}
12				111.2	C			
13-17^{Ar}				~140 *				

*Aromatic signals resonating around 140 ppm

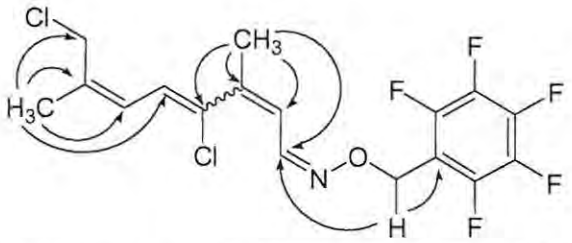

Figure 3.30 Important HMBC correlations in confirming the structure of the PFB oxime derivative of **3.46**

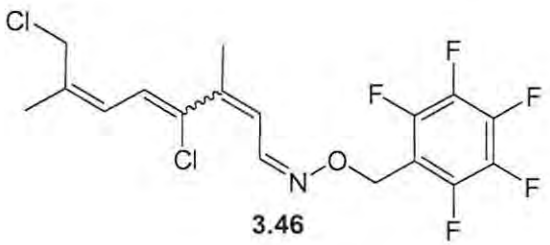

3.46

3.2.8 Characterization of 3.47

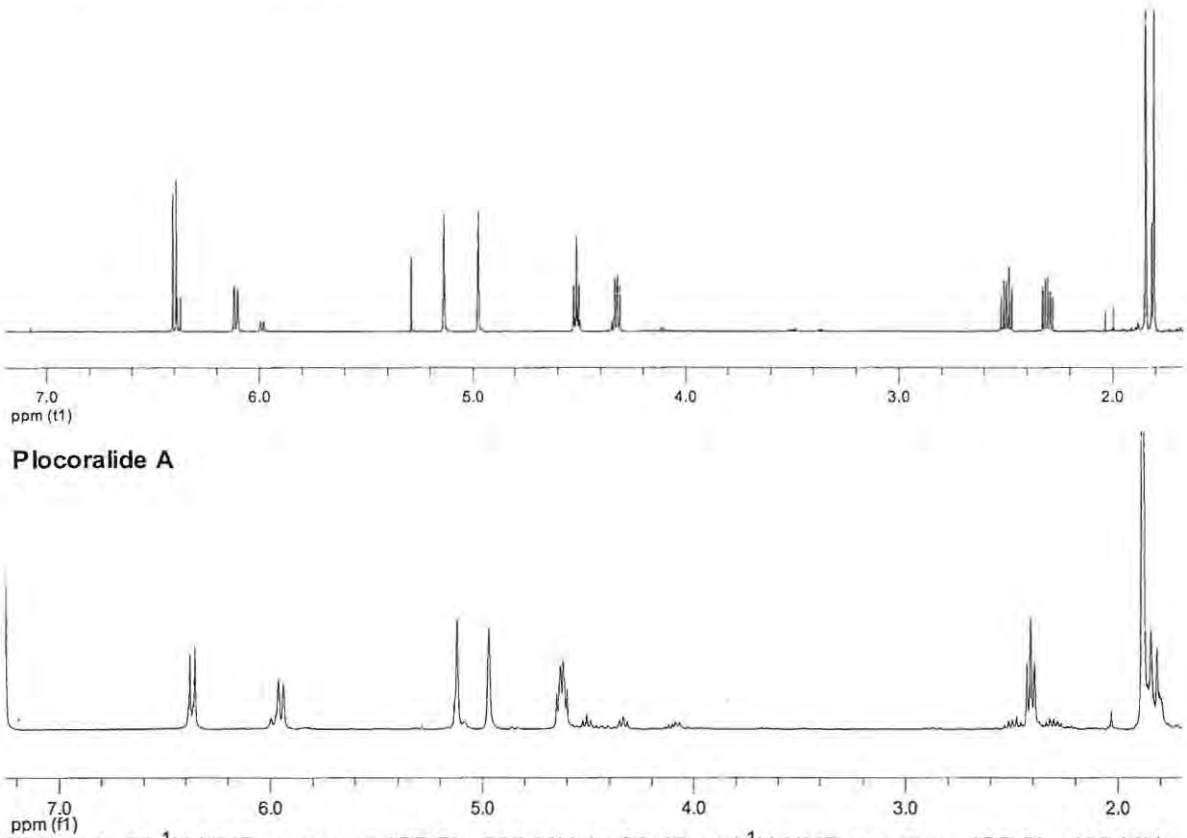

Figure 3. 31 ^{1}H NMR spectrum ($CDCl_3$, 600 MHz) of **3.47** and ^{1}H NMR spectrum ($CDCl_3$, 400 MHz of **3.14**

Compound **3.47** was isolated as clear oil from the *n*-hexane partition of the CH_2Cl_2-MeOH extract. The ^{1}H NMR spectrum (Figure 3.31) of this compound showed two mutually coupled doublets at d 6.39 (d, J = 9.8) and 6.12 (d, J = 9.8) consistent with an allylic dihalomethyl substituent (Knott, 2003). The other signals in the spectrum included two singlets at d 5.14 and 4.98 which indicate the presence of a terminal olefin as well as two methyl singlets at d 1.84 and 1.81. Multiplets at d 2.31 (m) and at d 2.50 (m) can be attributed to two diastereotopic protons that exist in slightly different electronic environments despite being coupled to the same carbon atom (C-5 at d 42.9 by HSQC). A triplet at 4.51 ppm is due to the presence of a halomethine, the ^{13}C chemical shift of which is consistent with a bromo substituent (C-6 at d 54.28); similarly the doublet of doublets seen at d 4.32 can be attributed to the presence of a second halomethine, however, in this case the ^{13}C chemical shift indicate a chloro substituent (C-4, d 63.4) (Naylor *et al.*, 1983). The ^{1}H NMR spectrum of **3.47** (Figure 3.31) is similar to that of Plocoralide A (**3.14**) (Figure 3.31) previously isolated by Knott (2003).

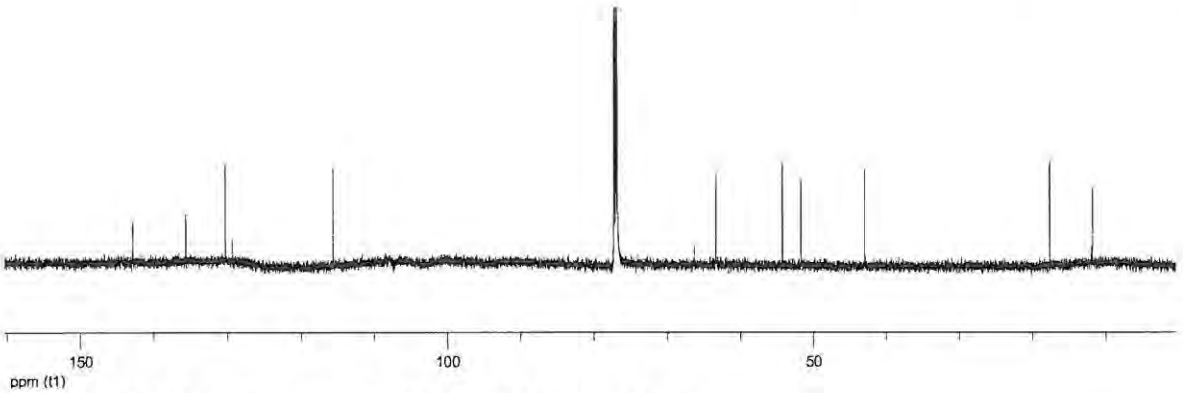

Figure 3.32 ^{13}C NMR spectrum ($CDCl_3$, 125 MHz) of **3.47**

The ^{13}C NMR spectrum (Figure 3.32) showed ten distinct signals. From the ^{13}C NMR and DEPT135 (Figure 3.33, Table 3.9) data, four vinylic carbons (two double bonds) were depicted at d 115.6 (C-8, CH_2), 142.8 (C-7, C), 135.6 (C-3, C) and 130.3 (C-2, CH); C-2 and C-7 being quaternary carbons. Two methyl signals resonated at d 17.6 and 11.8 while four methine (C-CH_2-C, C-CHX-C, C-CHX_2) signals could be seen at d 51.7 (C-1), 63.4 (C-4), 42.9 (C-5) and 54.18 (C-6). The chemical shift at d 115.6 in the DEPT135 spectrum confirms the presence of an olefinic CH_2.

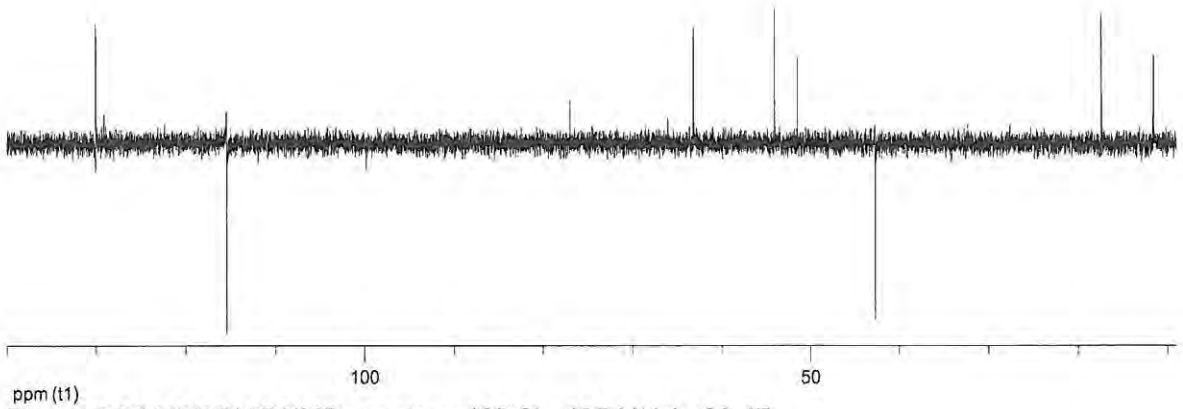

Figure 3.33 DEPT135 NMR spectrum ($CDCl_3$, 125 MHz) of **3.47**

The planar structure of this compound was confirmed mainly by interpretation of ^1H-^1H COSY (Table 3.9) and HMBC (Figure 3.35 and Table 3.9) data with the correlations of the methyl groups playing an important role in describing fragments (Figure 3.34).

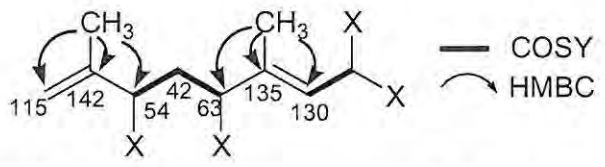

Figure 3.34 Important HMBC and ^1H-^1H COSY correlations in elucidating the structure of **3.47**

The methyl protons at d 1.84 showed HMBC correlations to carbons at d 54.3 (C-6), 115.6 (C-8) and 142.8 (C-7). The methyl proton at d 1.81 (H_3-10) showed HMBC correlations to carbons at d 63.4 (C-4), 130.3 (C-2) and 135.6 (C-3) with long range ^{1}H-^{1}H COSY correlations to H-2 (d 6.12). The two fragments were coupled by the HMBC correlations from the methylene protons at d 2.31 and 2.5 to carbons resonating at d 54.3 (C-6), 63.4 (C-4), 135.6 (C-3), and 142. 8 (C-7).

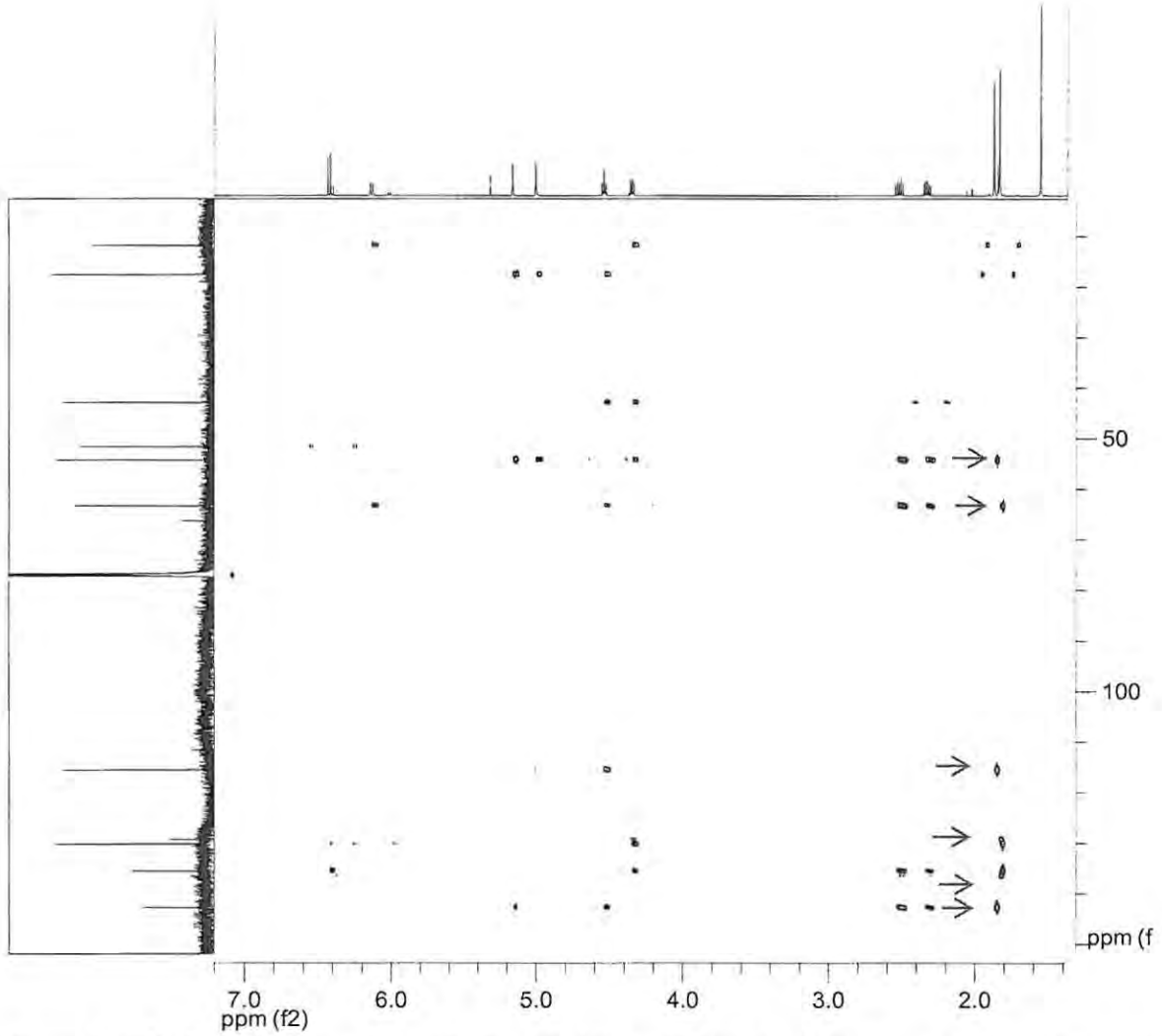

Figure 3.35 ^{1}H-^{13}C HMBC spectrum ($CDCl_3$, 600 MHz, 125 MHz) of **3.47**, arrows indicate important correlations from the protons of the methyl groups to nearby carbons

Table 3.9 ^{1}H NMR (600 MHz), ^{13}C NMR (125 MHz), ^{1}H-^{1}H COSY, HMBC correlations and NOE's for **3.47** in $CDCl_3$

Carbon No.	d_C		d_H, multi, *J* (Hz)	^{1}H-^{1}H COSY	HMBC	NOE
1	51.7	CH	6.39, d, 9.76	H2	C3, C2	
2	130.3	CH	6.12, d, 9.76	H10, H1	C10, C4	H4
3	135.6	C				
4	63.4	CH	4.32, dd, 6.5	H5	C10,C5,C6,C2,C3	H2
5a	42.9	CH_2	2.31, m	H4, H6	C6,C4,C3,C7	H4, H6
5b			2.50, m,			
6	54.3	CH	4.51,t , 7.5	H5, H8b	C9, C5, C4, C8,C7	
7	142.8	C				
8a	115.6	CH_2	4.98, s, 5,.14 s		C9, C6, C7, C8	H5, H4,
8b				H9		H6
9	17.8	CH_3	1.84, s	H8a	C6,C8,C7	H5
10	11.8	CH_3	1.81, s	H2	C4,C2,C3	

The position and identity of the halogen atoms was determined by a comparison of the monoterpene's ^{13}C NMR chemical shifts with known compounds reported in the literature. The halogen attached to C-6 effected a deshielded absorbance at d 54.3 indicating a bromine (Naylor *et al.*, 1983; Crews *et al.*, 1984) while a more electronegative halogen allowed for a lower frequency resonance of d 63.4 indicating that a chlorine atom was attached to C-4. The incidents of geminal dihalides at C-1 affords little for comparison, a chemical shift of d 51.7 occurs upfield of what one would expect for a geminal dichloride (normally, d_C ~ 65 ppm), yet downfield of what one would expect for a gem-dibromide (approximately d ~ 44 ppm when at position 1, but d ~ 37 ppm when at position 9). A bromine and chlorine would exhibit a ^{13}C NMR chemical shift at d ~ 69 ppm (Naylor *et al.*, 1983). The heterocyclic compound costatone contains a geminal dibromide that exhibits a ^{13}C NMR chemical shift of d 51.6 (Naylor *et al.*, 1983), however the structural differences between costatone and the acyclic halogenated monoterpene make it unsuitable for direct comparison. Unfortunately obtaining mass spectrometry data by EIMS, ESI-MS and FABMS for this compound proved futile and so the identity of the halogens at position 1 cannot be proposed with confidence as yet.

NOE's between H-2 and H-4 allowed the assignment of *E* geometry to the Δ^{2-3} double bond. No stereochemical assignments have been made. Based on the available spectroscopic data, the compound's structure is proposed to be that which is represented below.

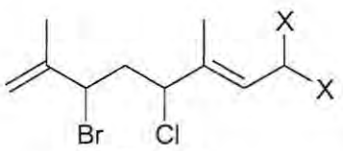

X = Cl or Br

3.47

3.2.9 Characterization of 3.13

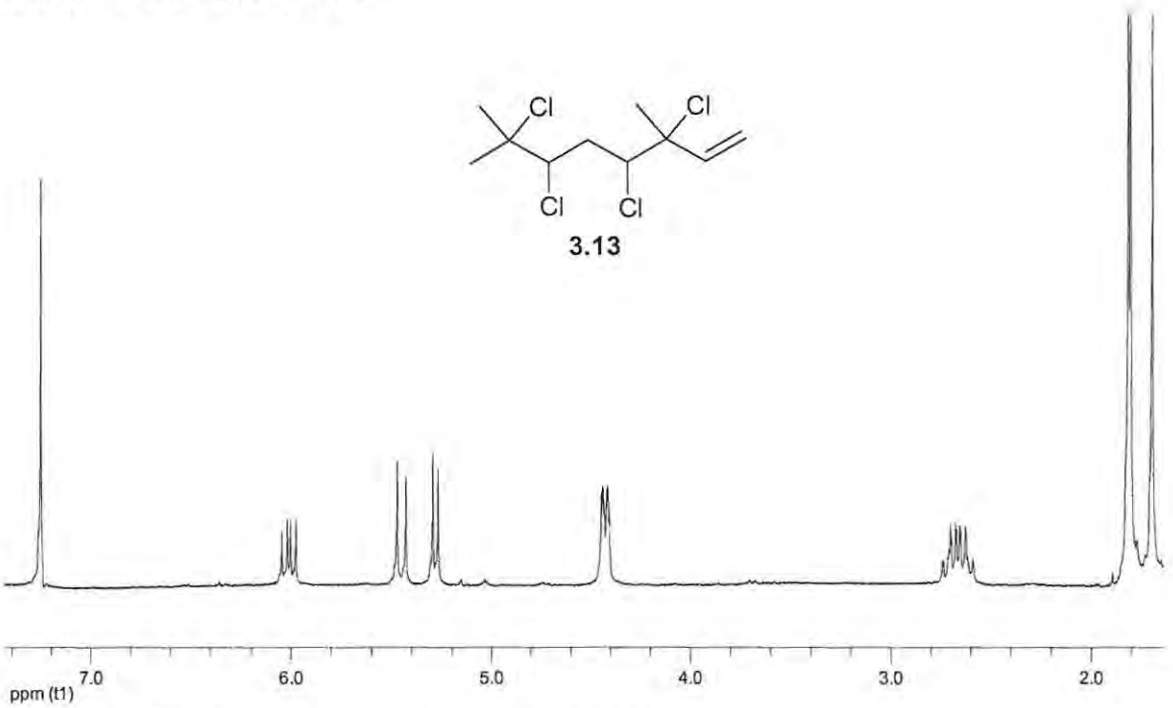

Figure 3.36 ^{1}H NMR spectrum ($CDCl_3$, 400 MHz) of **3.13**

The ^{1}H NMR spectrum (Figure 3.36, Table 3.10) of **3.13** showed deshielded absorbances at d 6.04 (dd, *J* = 10.6 Hz and 16.9 Hz), d 5.45 (d, *J* = 16.9 Hz) and at d 5.28 (d, J = 10.3 Hz) which are characteristic of a –CH=CH2 system. Two overlapping methines centered at d 4.43 together with a two proton multiplet, centered at d 2.64 were suggestive of a CHX-CH_2-CHX system. A further three methyl proton signals resonated at d 1.70, 1.80 and 1.82. The ^{13}C NMR chemical shifts at d 63.4 and 61.8 indicate chloro- substitution at both positions. These data are consistent with those of 3,4,6,7-tetrachloro-3,7-dimethyl-1-octene previously isolated by Knott (2003).

3.2.10 Characterization of 3.14

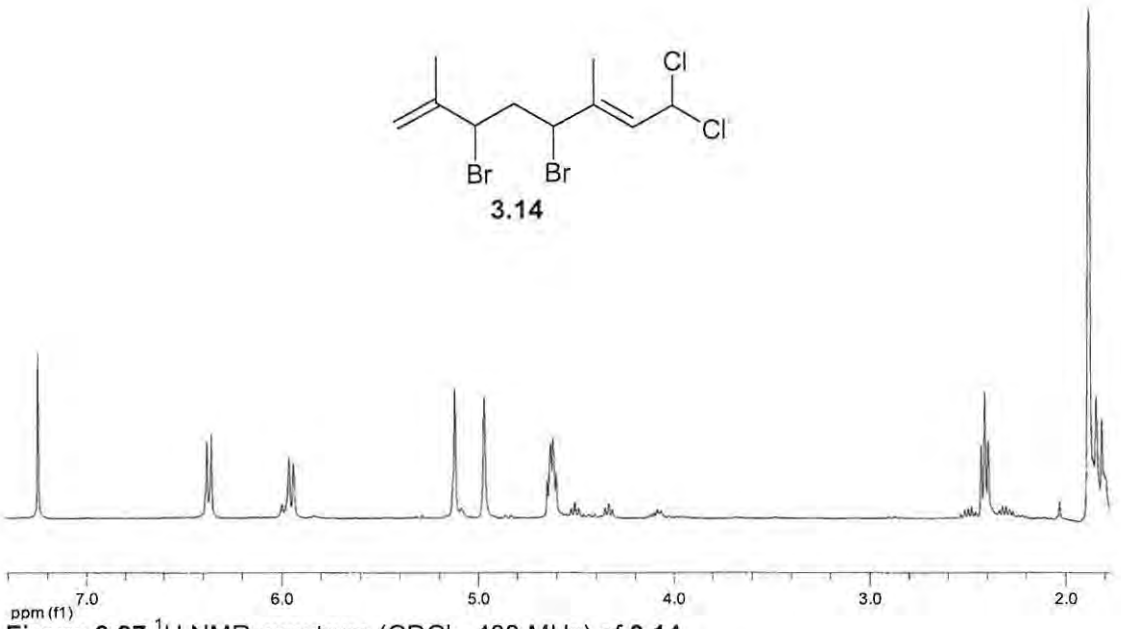

Figure 3.37 ^{1}H NMR spectrum ($CDCl_3$, 400 MHz) of **3.14**

The instantly recognizable singlets (at d 5.12 and 4.97) produced by a terminal double bond were apparent in the ^{1}H NMR spectrum (Figure 3.37, Table 3.10) of **3.14.** Like compound **3.13**, two overlapping methines at d 4.62 and a two proton triplet at d 2.41 (J = 7.1 Hz) is indicative of a CHX-CH_2-CHX system, however in this case the halogen substituents are both bromine atoms. The spectrum also showed two mutually coupled doublets at d 6.36 (d, J = 9.3 Hz) and 5.95 (d, J = 9.3 Hz) consistent with a dichloro substituent attached to a double bond. A singlet at d 1.89, when integrated consists of six protons, and is in fact due to two superimposed methyl signals. This data is consistent with 4,6-dibromo-1,1-dichloro-3,7-dimethyl-2,7octadiene previously isolated by Knott (2003).

3.2.11 Characterization of 3.16

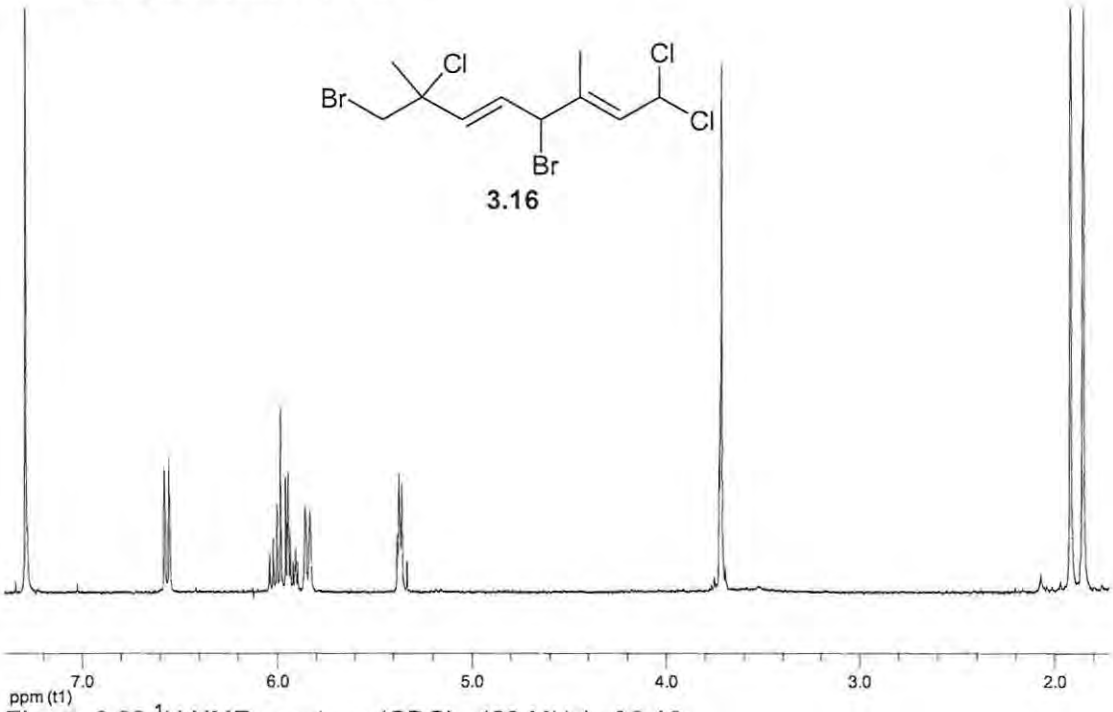

Figure 3.38 ^{1}H NMR spectrum ($CDCl_3$, 400 MHz) of **3.16**

The $-C(CH_3)=CH-CHX_2$ system was also apparent in the ^{1}H NMR spectrum of **3.16** (d 6.53 dd, J = 9.6 and 1.8 Hz and 5.81, dd, J = 9.6 and 1.3 Hz). A singlet observed at d 3.68 was consistent with a bromomethylene. Other signals included complex multiplets at d 5.98 and 5.33 as well as two methyl singlets at d 1.88 and 1.81. This data is consistent with 4,8-dibromo-1,1,7-trichloro-3,7-dimethyl-2,5-octadiene previously isolated by Knott (2003).

3.2.12 Characterization of 3.17

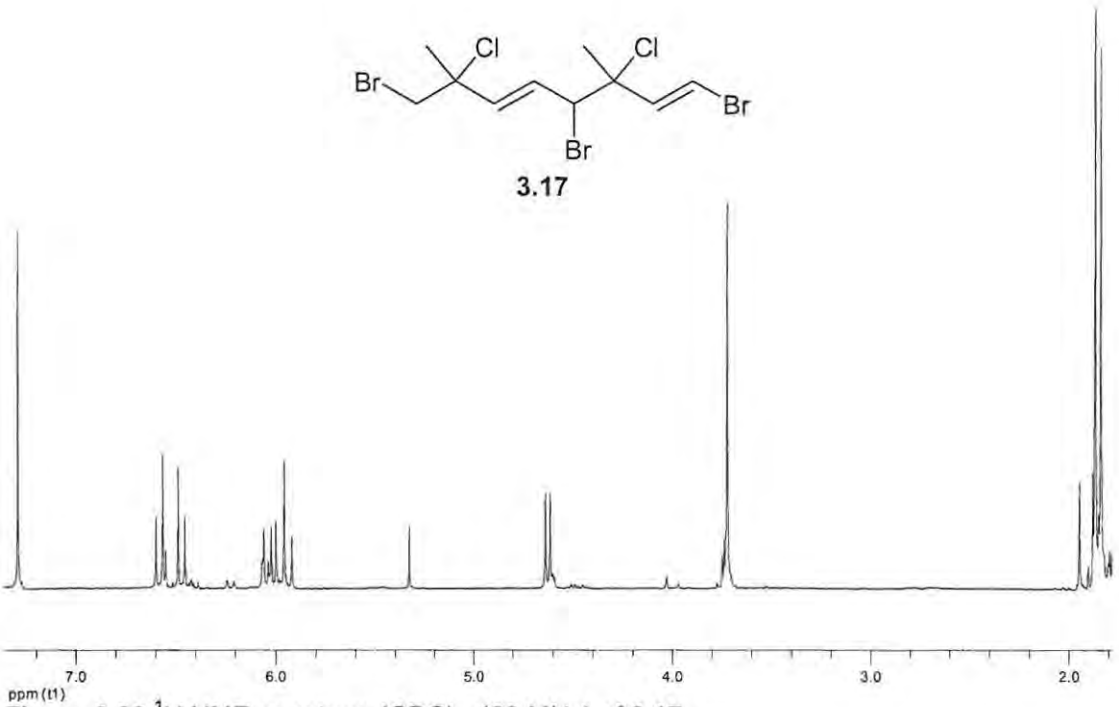

3.17

Figure 3.39 ^{1}H NMR spectrum ($CDCl_3$, 400 MHz) of **3.17**

The ^{1}H NMR spectrum of **3.17** showed two deshielded doublets at d 6.53 (d, *J* = 13.6) and 6.42 (d, *J* = 13.6) typical of a double bond with a halo substituent. The olefinic multiplet at d 5.97 and the doublet at d 4.57 (*J* = 9.6 Hz) indicated the presence of an allylic halomethine and the methylene singlet at d 3.67 indicated a bromomethylene group. The ^{1}H NMR spectrum also included the methyl signals at d 1.83 and 1.79. This data was consistent with 1,4,8-tribromo-3,7-dichloror-3,7-dimethyl-1,5-octadiene previously reported by Knott (2003) and Stierle and Sims (1979).

3.2.13 Characterization of 3.48

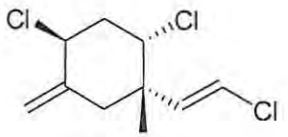

3.48

Figure 3.40 ^{1}H NMR spectrum ($CDCl_3$, 400 MHz) of **3.48**

The ^{1}H NMR spectrum (Figure 3.40, Table 3.10) of **3.48** showed two mutually coupled doublets at d 6.00 (J = 13.6 Hz) and 6.10 (J = 13.6 Hz) indicating a trans double bond. Two broad singlets at d 4.92 and 5.17 indicated a double bond, unsubstituted on the terminal carbon. The spectrum also included a broadened triplet at d 4.73 (J = 3.4 Hz) and a doublet of doublets at d 4.33 (J = 11.4 and 3.9 Hz) which were due to halomethine protons coupled to the methylene multiplet absorbing from d 2.23 to 2.43 ppm indicating a CH(X)-CH_2–CH(X) system. A second pair of methylene protons were indicated by signals at d 2.35 (d, J = 14.4 Hz) and 2.62 (d, J = 14.2 Hz) and a singlet observed at d 1.25 is due to a methyl group. The ^{13}C NMR spectrum contained four olefinic carbon resonances including a pair of signals at d 120.4 and 134.1 which indicated a disubstituted double bond. The second double bond was an exocyclic olefin and involved the carbons resonating at d 115.7 and 142.3. The ^{13}C NMR spectrum also included two methine carbon signals at d 63.3 and d 61.7, the chemical shifts indicated a chlorine atom was attached to each (Crews *et al.*, 1984; Naylor *et al.*, 1983). Two methylene carbons were evidenced by signals at d 41.5 and 41.1 ppm. A quaternary carbon singlet was observed at d 43.6 and the remaining carbon was a methyl which resonated at d 26.7. This data is consistent with 2,4-dichloro-1-(2-chlorovinyl)-1-methyl-5-methylidenecyclohexane reported by Sierle and Sims (1979).

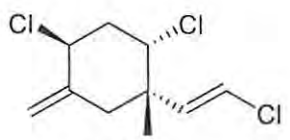

3.48

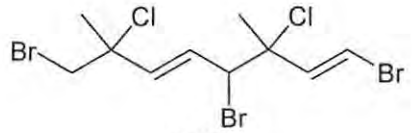

3.17

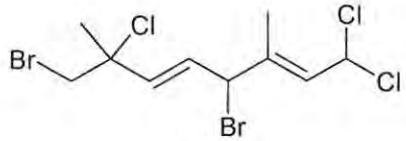

3.16

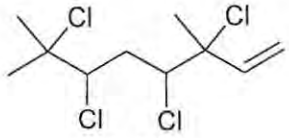

3.13

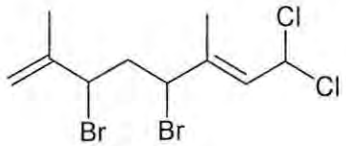

3.14

Table 3.10 ^{1}H and ^{13}C NMR chemical shifts for halogenated monoterpenes **3.13**, **3.14**, **3.16**, **3.17** and **3.48** isolated from *P. corallorhiza*.

	3.13			**3.14**			**3.16**	**3.17**			**3.48**		
Carbon No.	δ_C		δ_H, multi, *J* (Hz)	δ_C		δ_H, multi, *J* (Hz)	δ_H, multi, *J* (Hz)	δ_C		δ_H, multi, *J* (Hz)	δ_C		δ_H, multi, *J*(Hz)
1	116.2	CH_2	5.45, d, 16.9 5.28, d, 10.3	66.5	CH	6.36, d, 9.3	6.53, dd, 9.6, 1.8	110.0	CH	6.53, d, 13.6	43.6	C	
2	140.7	CH	6.04, dd, 10.6, 16.9	128.5	CH	5.95, d, 9.3	5.81, dd, 9.6, 1.3	138.8	CH	6.42, d, 13.6	63.3	CH	4.73, t, 3.4
3	71.9	C		137.4	C			71.1	C		41.5	CH_2	2.23-2.43, m
4	61.8	CH	4.42, dd, 2.0, 3.6	56.0*	CH	4.62, m	5.33, m	60.0	CH	4.57, d, 9.2	61.7	CH	4.33, dd, 11.4 and 3.9
5	39.2	CH_2	2.76-2.58, m	43.0	CH_2	2.41, t, 7.1	5.98, m	128.1	CH	5.97, m	142.3	C	
6	63.4	CH	4.45, dd, 2.0, 3.7	56.1*	CH	4.62, m	5.91, m	137.3	CH	5.92, m	41.1	CH_2	2.36, 2.64, dd, 14.5
7	68.9	C		143.4	C			66.9	C		134.1	CH	6.00, d, 13.6
8	28.3	CH_3	1.80, s	115.2	CH_2	5.12, s, 4.97, s	3.68, s	41.5	CH_2	3.69, s	120.4	CH	6.10, d, 13.6
9	32.8	CH_3	1.70, s	18.3	CH_3	1.89, s	1.88, s	27.3	CH_3	1.83, s	26.7	CH_3	1.25, s
10	26.4	CH_3	1.82, s	13.2	CH_3	1.89, s	1.81, s	26.3	CH_3	1.79, s	115.7	CH_2	4.92, s 5.17, s

* Carbon chemical shifts interchangeable. ($CDCl_3$; ^{1}H NMR, 400 MHz, ^{13}C NMR, 100 MHz)

3.2.14 Anticancer Activity

Numerous halogenated monoterpenes have been shown to exhibit activity against cancer cell lines (Fuller *et al.*, 1992; Mkwananzi, 2005). Compound **3.26** previously isolated by our research group showed greater toxicity than other metabolites isolated from *P. corallorhiza*, although at that time there was insufficient compound to obtain the IC_{50} value (Mkwananzi 2005). Upon re-isolation of **3.26**, the IC_{50} was determined in an oesophageal cancer cell line assay (WHC01) along with the IC_{50} for **3.44**.

Table 3.11 Anticancer activity of plocoraldehydes A and E

Compound No.	Isolation code	IC_{50} (µg/ml)
3.26	KOS06-14-A2i	2.324
3.44	KOS06-14-A2h	5.487

3.2.15 Antiplasmodial screening

Although extracts from *Plocamium* species have shown antiplasmodial activity (Afolayan, 2006), the selected compounds isolated from *P. corallorhiza* screened for activity against a chloroquine sensitive strain of *Plasmodium falciparum* were found to have only weak activity.

Table 3.12 Antiplasmodium activity of selected halogenated monoterpenes from *P. corallorhiza*

Compound No.	Isolation code	IC_{50} (µg/ml)
3.14	KOS06-14-A2a3	26.7
3.17	KOS06-14-A2c2	> 100
3.22	KOS06-14-A3n	43.9
3.26	KOS06-14-A2i	40.1
CQ	Chloroquine (ng/ml)	11.5

3.3 Experimental Section

3.3.1 General experimental

Chemicals and reagents

All solvents were distilled before use or of HPLC grade (HiPerSolv ™, Merck and Saarchem). Dry dichloromethane was distilled from calcium hydride under nitrogen and stored in a dark brown glass bottle over 3A molecular sieves. Reagents for synthesis were of analytical grade and used without further purification.

Chromatography

Gas chromatography was performed on a Hewlett Packard 6890 gas chromatograph and semi-preparative high performance liquid chromatographic separations were performed on a Spectra-Physics IsoChrom LC HPLC system which was equipped with a rheodyne injector, a Waters R401 differential refractometer, or a SpectraSERIES UV100 detector and a Rikadenki chart recorder. In all cases, normal phase HPLC was performed using a Whatman Magnum 10 Partisil 9 column. Normal phase TLC was performed on DC Alufolie Kieselgel $60F_{254}$ and plates were viewed under UV light (254 nm). Flash column chromatography was performed using Kieselgel 60 (230-400 mesh) silica.

Compound Characterization

The following general procedures were followed unless otherwise stated. The ^{1}H (400 MHz), ^{13}C (100 MHz), DEPT-135, ^{1}H-^{1}H COSY, HSQC, HMBC and NOESY NMR spectra were recorded on a Bruker Avance 400 spectrometer using standard pulse sequences. Chemical shifts are reported in ppm and referenced to residual undeuterated solvent resonances ($CHCl_3$ δ_H 7.25, δ_C 77.0) and coupling constants are reported in Hz. Optical rotations were measured on a Perkin-Elmer 141 polarimeter. IR spectra were obtained as films on KBr disks using a Perkin-Elmer Spectrum 2000 FT-IR spectrometer. Gas chromatography-mass spectrometry (GCMS) was performed on a FinniganMAT GCQ™ equipped with a DB-1 Column. LR-APCI-MS spectra were recorded on a ThermoFinnigan MAT LCQ ion trap mass spectrometer with Xcalibur software. HR-ESI-MS spectra were acquired on a Waters API-TOF Ultima mass spectrometer using positive ion electrospray ionization at the Mass Spectrometry Unit at Stellenbosch University, Stellenbosch, South Africa.

Conditions for GC

- Citral (3.35): Initial temp 75 °C, ramp 7 °C/min, final temp 220 °C, total time 21 min
- Halogenated monoterpene PFB oxime derivatives: Initial temp 100 °C, ramp 20 °C/min, final temp 220 °C, hold 10 min, total time 21 min
- All injections were performed using the splitless mode with a carrier gas velocity of 40 $cm.s^{-1}$. The injection port was held at 250 °C and the interface at 270 °C. Helium was used as the carrier gas.

Conditions for EIMS (70 eV)

- Citral (3.35): Ionization mode EI; Multiplier 1500 volts; Fore pressure 10 mTorr; Source temp 200 °C, Transfer line 275 °C
- Halogenated monoterpene PFB oxime derivatives: Ionization mode EI; Multiplier 1600 volts; Fore pressure 10 mTorr; Source temp 200 °C, Transfer line 275 °C

Conditions for APCI-MS

- Solvent acetonitrile, Source APCI+; Capillary temp 200 °C; Capillary voltage 6.00 V; Discharge current 5.00 µA; Sheath gas flow rate 60 arb.

Conditions for ESI-MS

- Sample introduction 0.1 ml/min; total injection volume 10 µl; Source ESI+; Capillary voltage 3.5kV; Cone voltage 35; RF1 40; Source 100 °C; Desolvation temp 370 °C, Desolvation gas 400L/h; Cone gas 50 L/h

3.3.2 Plant material

P. corallorhiza is a deep pink rhodophyte that grows ubiquitously along almost the entire length of the South African coastline (Branch 2005). The fronds are flat and waxy with a serrated edge and appear blue-purple underwater. Collection of the alga at low tide was made easy due to the abundance of the plant and it's relatively loose attachment to the rocks.

The alga was collected near Kenton-On-Sea (KOS06-14) and from Noordhoek, Port Elizabeth (NDK06-22) on the southeast coast of South Africa; collections were kept frozen until extraction.

The alga was identified by Prof John J. Bolton of the Department of Botany, University of Cape Town. Voucher specimens are retained in our repository at the Faculty of Pharmacy, Rhodes University, Grahamstown, South Africa.

3.3.3 Extraction and Isolation

KOS06-14 (Kenton-On-Sea)

The frozen algae (31.5 g dry weight after extraction) was submerged in MeOH (500 ml) at 4 °C for 1 hour, the solvent decanted and the alga re-extracted with CH_2Cl_2-MeOH (2:1, 3 x 500 ml) at 30 °C for 30 minutes. The MeOH and CH_2Cl_2 extracts were separately extracted with CH_2Cl_2 (with the addition of sufficient water for phase separation) and the two organic extracts combined and concentrated. The CH_2Cl_2 extract was prefractionated by successive solvent partitioning between *n*-hexane-MeOH-H_2O (4:5:1), CH_2Cl_2-MeOH-H_2O (5:3:2) and EtOAc-H_2O (1:1) to give *n*-hexane (fr A, 1.444 g), CH_2Cl_2 (fr B, 0.379 g), EtOAc (fr C, 0.051 g) and an aqueous fraction. A portion (500 mg) of the *n*-hexane extract (A) was applied to a silica gel column (Kieselgel 0.04-0.063 nm, 10 g,

2.5 x 6 cm) and successively eluted with 50 ml portions of an *n*-hexane-EtOAc mixture in a ratio 1:0 (fr A1), 9:1 (fr A2), 8:2 (fr A3), 7:3 (fr A4), 6:4 (fr A5), 4:6 (fr A6), 2:8 (fr A7) 0:1 (fr A8) followed by a 1:1 EtOAc-MeOH mixture (fr A9). Normal phase HPLC (*n*-hexane-EtOAc 9:1) of the *n*-hexane-EtOAc (9:1) column fraction of the *n*-hexane partition yielded the known compounds **3.14**, **3.17**, **3.26** and a new compound **3.44**. While normal phase HPLC (*n*-hexane-EtOAc 8:2) of the *n*-hexane-EtOAc (8:2) column fr of the *n*-hexane partition yielded the new compound **3.44** and the known compounds **3.23, 3.22** and again **3.14**.

Confirmation of the presence of halogenated monoterpene aldehydes after freeze-drying KOS06-14b (Kenton-On-Sea)

P. corallorhiza was frozen overnight after which lyophilization was performed on a Virtis Freezemobile 6 freeze drier. The alga was then extracted with dichloromethane at ambient temperature for 24 hours. Following removal of the solvent, the extract was reconstituted in $CDCl_3$ and a ^1H NMR experiment was performed.

NDK06-22 (Noordhoek)

176.3 g (Dry mass) was immersed in methanol at 4 °C for 1 hour after which the solvent was decanted and extracted with CH_2Cl_2. The seaweed was then steeped in CH_2Cl_2-MeOH (2:1) and heated at 30 ° C for 30 minutes (x3). Solvent partitioning between *n*-hexane, dichloromethane and ethyl acetate was carried out as described for KOS06-14, and afforded extracts A (1.611 g), B (0.308 g) and C (0.063 g). Silica gel column chromatography employing a *n*-hexane-EtOAc step gradient (as described for KOS06-14) gave 9 fractions for A. Further silica gel column chromatography was used to create six further fractions (fr a- f). Exhaustive normal phase HPLC of these fractions yielded the new compounds **3.47** and **3.44**. The following known compounds were also isolated: **3.13**, **3.48**, **3.14, 3.16**, **3.17** and **3.22**.

3.3.4 General procedure for the preparation and analysis of Carboxyethylethylidene (CET) derivatives

To a solution of CET-triphenylphosphorane (**3.33**) (230 mg, 0.660 mmol) in dry CH_2Cl_2 (1 ml) was added citral (3.35) (50 mg, 0.330 mmol) under a nitrogen atmosphere at room temperature. The reaction mixture was stirred for 48 hours and the reaction monitored by normal phase TLC (95:5 Pet ether:diethyl ether). Triphenylphosphine oxide was removed by passing the reaction mixture through a silica plug. The CH_2Cl_2 was then evaporated *in vacuo* to afford the product. No further work up was required.

3.3.5 General procedure for the preparation and analysis of pentafluorobenzyl-oxime derivatives

Isolated compounds

To a solution of the aldehyde (1 mg) in CH_3CN (0.5 mL) was added PFBHA.HCl (**3.34**) (1 mg) dissolved in CH_3CN (0.5 mL). MgSO4 (5 mg, anhydrous) was added to the reaction mixture to sequester water molecules formed and the reaction was then stirred at room temperature. The course of the reaction was followed by normal-phase TLC analysis (*n*-hexane-EtOAc 9:1). When the reaction was complete (4 h), the crude oxime product was extracted with *n*-hexane and purified by HPLC (*n*-hexane-EtOAc 19:1).

Crude extract derivatization

PFBHA.HCl (**3.34**) (30 mg, 0.120 mmols) was dissolved in methanol (1 ml) and added to the dry crude extract. The solvent was removed *in vacuo* and the mixture reconstituted in acetonitrile (10 ml). The reaction mixture was stirred for four hours where after it was transferred to a separating funnel and extracted with *n*-hexane. The PFB oxime derivatives were purified by normal phase HPLC (*n*-hexane-EtOAc 19:1).

3.3.6 Halogenated monoterpenes

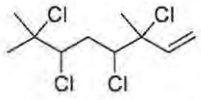

3.13 3,4,6,7-tetrachloro-3,7-dimethyl-1-octene ^{1}H NMR ($CDCl_3$, 400 MHz) and ^{13}C NMR ($CDCl_3$, 100 MHz) see **Table 3.10**.

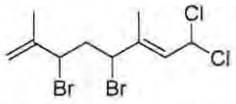

3.14 4,6-dibromo-1,1-dichloro-3,7-dimethyl-2*E*,7octadiene ^{1}H NMR ($CDCl_3$, 400 MHz) and ^{13}C NMR ($CDCl_3$, 100 MHz) see **Table 3.10**.

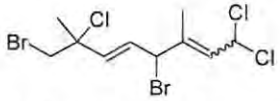

3.16 4,8-dibromo-1,1,7-trichloro-3,7-dimethyl-2,5*E*-octadiene ^{1}H NMR ($CDCl_3$, 400 MHz) see **Table 3.10**.

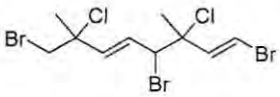

3.17 1,4,8-tribromo-3,7-dichloro-3,7-dimethyl-1*E*,5*E*-octadiene ^{1}H NMR ($CDCl_3$, 400 MHz) and ^{13}C NMR ($CDCl_3$, 100 MHz) see **Table 3.10**.

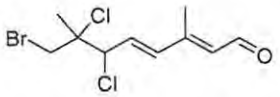

3.22 8-bromo-6,7-dichloro-3,7-dimethyl-octa-2*E*,4*E*-dienal yellow oil ^{1}H NMR ($CDCl_3$, 400 MHz) see **Table 3.10**.

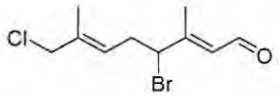

3.23 4-Bromo-8-chloro-3,7-dimethyl-octa-2*E*,6*E*-dienal; yellow oil; ^{1}H NMR ($CDCl_3$, 400MHz) see **Table 3.6**.

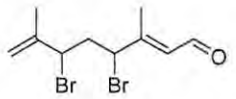

3.26 4,6-Dibromo-3,7-dimethyl-octa-2*E*,7-dienal: yellow-green oil ^{1}H NMR ($CDCl_3$, 400 MHz) and ^{13}C NMR ($CDCl_3$, 100 MHz) see **Table 3.5**. LR-APCI-MS *m/z* 309/311/313 $[M]^+$.

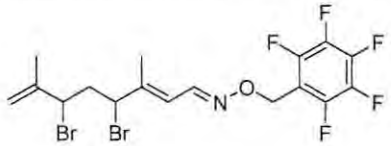

3.40 4,6-dibromo-3,7-dimethyl-*o*-(2,3,4,5,6-pentafluorobenzyl)-oxime-2*E*,7-octadienal ^{1}H NMR ($CDCl_3$, 400MHz) and ^{13}C NMR ($CDCl_3$, 100 MHz) see **Table 3.5;** LR-APCI-MS *m/z* 504/506/508 $[M+H]^+$; HR-ESI-MS *m/z* 503.9608 (calcd for $C_{17}H_{17}NOF_5{}^{79}Br_2$, 503.9597).

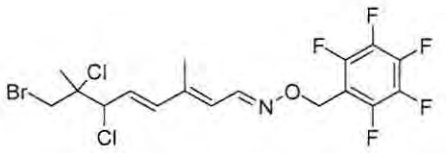

3.41 6,7-dichloro-8-bromo-3,7-dimethyl-*o*-(2,3,4,5,6-pentafluorobenzyl)-oxime-2*E*,4*E*-octadienal, ^{1}H NMR ($CDCl_3$, 400 MHz). δ_H, multi, *J* (Hz) 3.22 10.15, d, 7.8; 6.00, d, 7.8; 6.55, d, 15.6; 6.35, 6.31, dd, 8.8, 15.6; 4.91, d, 8.8; 3.80, d, 10.9; 3.64, d, 10.9; 1.82, s; 2.30, s. HR ESI-MS *m/z* 493.9706 (calcd for $C_{17}H_{16}NOF_5{}^{79}Br{}^{35}Cl_2$, 493.9712).

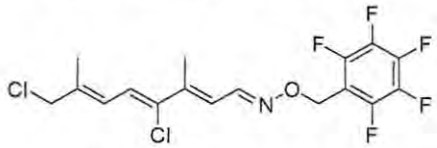

3.42 4,8-dichloro-3,7-dimethyl-*o*-(2,3,4,5,6-pentafluorobenzyl)-oxime-2*E*,4*E*,6*E*-octatrienal; green oil; ^{1}H NMR ($CDCl_3$, 400 MHz) see **Table 3.6;** HR-ESI-MS *m/z* 414.0437 (calcd for $C_{17}H_{15}NOF_5{}^{35}Cl_2$, 414.0451).

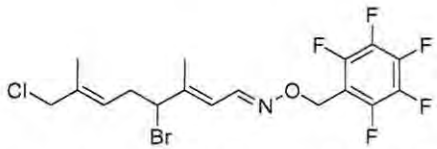

3.43 4-bromo-8-chloro-3,7-dimethyl-*o*-(2,3,4,5,6-pentafluorobenzyl)-oxime-2*E*,6*E*-octadienal; ^{1}H NMR ($CDCl_3$, 400MHz) see **Table 3.6**; *m/z* 460.0148 (calcd for $C_{17}H_{17}NOF_5{}^{79}Br{}^{35}Cl$, 460.0102).

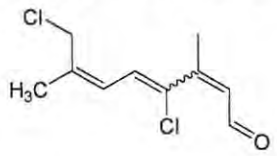

3.44 4,8-chloro-3,7-dimethyl-2*Z*,4,6*Z*-octatrien-1-al: yellow oil; UV (*n*-hexane) λ_{max} 226.4. 256.0, 291.2 and 312.0 (0.0001365 g/ml); IR (dry film, KBr) ν_{max} 3414.58, 2920.99, 2851.21, 1670.14, 1454.22, 1258.91, 1107.86, 910.01, 715.89, 507.38 cm $^{-1}$, ^{1}H NMR ($CDCl_3$, 400 MHz) and ^{13}C NMR ($CDCl_3$, 100 MHz) see **Table 3.7**; HMBC correlations, **H-1**/C-2, **H-2**/C-4, C-10; **H-5**/C-3, C-4, C-7; **H-6**/C-4,C-8, C-10; **H_2-8**/C-4, C-5,C-6, C-7, C-9; **H_3-9**/C-5, C-6, C-7, C-8; **H_3-10**/C-1, C-2, C-3, C-4; NOESY correlations, **H-1**/H-2,H-5; **H-2**/H-1, H-10; **H-5**/H-1, H-8, H-9; **H-6**/H-9; **H_2-8**/ H-5; **H_3-9**/H-5; **H_3-10**/H-1, H-2; IC50 = 5.487 µg/ml.

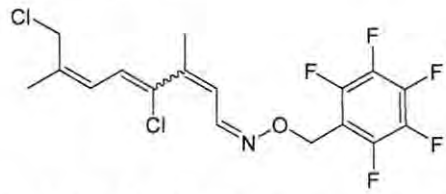

3.46 4,8-dichloro-3,7-dimethyl-*o*-(2,3,4,5,6-pentafluorobenzyl)-oxime-2*Z*,4,6*Z*-octatrienal ^{1}H NMR ($CDCl_3$, 400 MHz) and ^{13}C NMR ($CDCl_3$, 100 MHz) see **Table 3.8**; HMBC correlations, **H-1**/C-2, **H-2**/C-4, C-10; **H-6**/C-4,C-8; **H_2-8**/C-6, C-7, C-9; **H_3-9**/C-6, C-7, C-8; **H_3-10**/C-1, C-2, C-3, C-4; **H-11**/C-12, C^{Ar}; HR-ESI-MS *m/z* 414.0452 (calcd for $C_{17}H_{15}NOF_5{}^{35}Cl_2$, 414.0451).

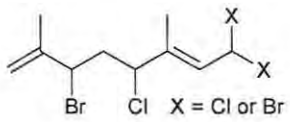

3.47 Colourless oil; $[\alpha]_D^{16}$ -38.7 ° ($CHCl_3$), UV (*n*-hexane) λ_{max} 210.4 nm (0.000776 g/ml); IR (dry film, KBr) ν_{max} 3445.36, 2963.57, 2917.25, 2852.39, 1718.32, 1658.30, 1621.35, 1515.15, 1381.24, 1261.18, 1201.16, 1085.72, 905.63, 817.90 cm^{-1}, ^1H NMR ($CDCl_3$, 600 MHz) and ^{13}C NMR ($CDCl_3$, 125 MHz) see **Table 3.9**; HMBC correlations, **H-1**/C-2, C3; **H-2**/C-4, C-10;**H-4**/C-2, C-3, C-5, C-6, C-10, **H_2-5**/C-3, C-4, C-6, C-7; **H-6**/C-4, C-5, C-7 C-8, C-9; **H_2-8**/C-6, C-7, C-8, C-9; **H_3-9**/C-6, C-7, C-8; **H_3-10**/C-2, C-3, C-4; NOESY correlations, **H-2**/H-4; **H-4**/H-2 **H_2-5**/H-4, H-6; **H_2-8**/H-4, H-5, H-6; **H_3-9**/H-1, H-5.

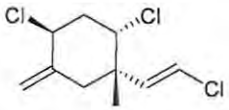

3.48 2,4-dichloro-1-(2-chlorovinyl)-1-methyl-5*E*-methylidenecyclohexane ^1H NMR ($CDCl_3$, 400 MHz) and ^{13}C NMR ($CDCl_3$, 100 MHz) See **Table 3.10**.

3.3.7 Anticancer Activity

Oesophageal cancer screening was performed by Catherine Arendse at the department of Medical Biochemistry, University of Cape Town, South Africa. WHC01 oesophageal cell lines were prepared and IC_{50} determinations were performed using the MTT kit from Roche (cat # 1465007) according to the manufacturer's instructions. 1500 cells (in 90 µl) were seeded per well in Cellstar 96-well plates. Cells were incubated for 24 hours then the halogenated monoterpenes were plated at various concentrations in 10 µl with a constant final concentration of 0.1% dmso. After 48 hours incubation, observations were made and 10 µl 3-(4,5-dimethylthiazol-2-yl)-2,5-diphenyltetrazilium bromide (MTT) solution was added to each of the wells. After four hours of incubation, 100 µl of solubilisation solution was added to each of the wells and the plates were incubated again overnight. The following morning, plates were read at 595 nm on an Anthos micro plate reader 2001.

3.3.8 Antiplasmodial screening

Antiplasmodial screening was performed by the Department of Medicine, Division of Pharmacology at the University of Cape Town. Continuous *in vitro* cultures of asexual erythrocyte stages of *Plasmodium falciparum* (D10) were maintained using a modified method of Trager and Jensen (1976). Samples were tested in duplicate on one occasion against a chloroquine sensitive strain of *P. falciparum*. Quantitative assessment of *in vitro* antiplasmodial activity was determined via the parasite lactate dehydrogenase assay using a modified method described by Makler *et al.* (1993). The test samples (halogenated monoterpenes) were prepared to a 2 mg/ml stock solution in 10% methanol or 10 % dmso and were tested as a suspension if not properly dissolved. Chloroquine was used as the positive control drug. The halogenated monoterpenes were stored at -20 °C until use. The monoterpenes were tested in a full dose-response assay with a starting concentration of 100 µg/ml, which was serially diluted 2-fold in complete medium to give 10 concentrations, the lowest being 0.195 µg/ml. Chloroquine was tested at a starting concentration of 100 µg/ml using the same dilution technique. The highest concentration of solvent to which the parasite was exposed had no measurable effect on the parasite. The IC_{50} values were obtained using a non-linear dose-response curve. Analysis was performed using GraphPad Prism 4.00 software

3.4 References

Adolph, S.; Bach, S.; Blondel, M.; Cueff, A.; Moreau, M.; Pohnert, G.; Poulet, S. A.; Wichard, T.; Zuccaro A. Cytotoxicity of diatom derived oxylipins in organisms belonging to different phyla. *Journal of Experimental Biology* **2004**, *207*, 2935-2946.

Afolayan, A. MSc Candidate, unpublished work, **2006**.

Alipieva, K.; Evstatieva, L.; Handjieva, N.; Popov, S. Comparative analysis of the composition of flower volatiles from *Lamium L.* species and *Lamiastrum galeobdolon* Heist. ex Fabr. *Verlag der Zeitschrift für Naturforschung* **2003**, *58c*, 779-782.

Blunt, J. W.; Copp, B. R.; Hu, W. P.; Munro, M. H. G.; Northcote, P. T.; Prinsep, M. R. Marine natural products. *Natural Product Reports* **2007**, *24*, 31-86.

Branch, G. M.; Griffiths C. L.; Branch, M. L.; Beckley, L. E. In *Two oceans: A guide to the marine life of Southern Africa* Second Edition **2005.** ISBN 0-86486-672-0, **1994** David Phillip Publishers, New Africa Books (Pty) Ltd. Cape Town, South Africa.

Chang, S.; Chen. P.; Chang, S. Antibacterial activity of leaf essential oils and their constituents from *Cinnamomum osmophloeum. Journal of Ethnopharmacology* **2001**, *77*, 123-127.

Crews, P.; Kho, E. Cartilagineal. An unusual monoterpene aldehyde from marine algae. *Journal of Organic Chemistry* **1974**, *39*, 3303-3304.

Crews, P.; Kho-Wiseman, E. Acyclic polyhalogenated monoterpenes from the red alga *Plocamium violaceum. Journal of Organic Chemistry* **1977**, *42*, (17), 2812-2815

Crews, P.; Naylor, S.; Hanke, F. J.; Hogue, E. R.; Kho, E.; Braslau, R. Halogen Regiochemistry and Substituent Stereochemistry Determination in Marine Monoterpenes by ^{13}C NMR. *Journal of Organic Chemistry* **1984**, *49*, 1371-1377.

d'Ippolito, G.; Romano, G.; Iadicicco, O.; Miralto, A.; Ianora, A.; Climino, G.; Fontana, A. New birth-control aldehydes from the marine diatom *Skeletonema costatum*: Characterization and biogenesis. *Tetrahedron Letters* **2002a**, *43*, 6133-6136.

d'Ippolito, G.; Iadicicco, O.; Romano, G.; Fontana, A. Detection of short-chain aldehydes in marine organisms: The diatom *Thalassiosira rotula. Tetrahedron Letters* **2002b**, *43*, 6137-6140.

Fang, J.; Leu, Y.; Hwang, T.; Cheng, H. Essential oils from Sweet Basil (*Ocimum basilicum*) as novel enhancers to accelerate transdermal drug delivery. *Biochemical and Pharmaceutical Bulletin* **2004**, *27*, (11), 1819-1825.

Ferreira, V.; Culleré, L.; López, R.; Cacho, J. Determination of important odor-active aldehydes of wine through gas chromatography–mass spectrometry of their O-(2,3,4,5,6-pentafluorobenzyl)oximes formed directly in the solid phase extraction cartridge used for selective isolation. *Journal of Chromatography A* **2004**, *1028*, 339-345.

Fuller, R. W.; Cardellina II, J. H.; Jurek, J.; Scheuer, P. J.; Alvarado-Lindner, B.; McGuire, M.; Gray, G. N.; Steiner, J. R.; Clardy, J.; Menez, E.; Shoemaker, R. H.; Newman, D. J.; Snader, K. M.; Boyd, M. R. Isolation and structure/activity features of halomon-related antitumour monoterpenes from the red alga *Portieria hornemannii*. *Journal of Medicinal Chemistry* **1994**, *37*, 4407-4411.

Gardener, H. W. Lipid hydroperoxide reactivity with proteins and amino acids: A review. *Journal of Agriculture and Food Chemistry* **1979**, *27*, (2), 220-229.

Guiry, M.D. & Guiry, G.M. 2007. AlgaeBase version 4.2. World-wide electronic publication, National University of Ireland, Galway. http://www.algaebase.org; searched on 14 November 2007.

Hsu, F. F.; Hazen, S. L.; Giblin, D.; Turk, J.; Heinecke, J. W.; Gross, M. L. Mass spectrometric analysis of pentafluorobenzyl oxime derivatives of reactive biological aldehydes. *International Journal of Mass Spectrometry* **1999**, *185/186/187*, 795-812.

Ianora, A.; Boersma, M.; Casotti, R.; Fontana, A.; Harder, J.; Hoffmann, F.; Pavia, H.; Potin, P.; Poulet, S. A.; Toth, G. The H. T. Odum synthesis essay, new trends in marine chemical ecology. *Estuaries and Coasts* **2006**, *29*, (4), 531–551.

Kladi, M.; Vagias, C.; Roussis. V. Volatile halogenated metabolites from marine red algae. *Phytochemistry Reviews* **2004**, *3*, 337–366.

Knott, M.; Mkwananzi, H.; Arendse, C.; Hendricks, D. T.; Bolton, J. J.; Beukes, D. R. Plocoralides A-C, polyhalogenated monoterpenes from the marine alga *Plocamium corallorhiza*, *Phytochemistry* **2005**, *66*, 1108-1112.

Knott, M. The Natural Product Chemistry of South African *Plocamium* species. MSc Thesis **2003**, Rhodes University, Grahamstown, South Africa.

König, G. M.; Wright, A. D.; Sticher, O. A new polyhalogenated monoterpene from the red alga *Plocamium cartilagineum*. *Journal of Natural Products* **1990**, *53*, (6), 1615-1618.

König, G. M.; Wright, A. D.; de Nys, R. Halogenated monoterpenes from *Plocamium costatum* and their biological activity. *Journal of Natural Products* **1999a**, *62*, 383-385.

König, G. M.; Wright, A. D.; Linden, A. *Plocamium hamatum* and its monoterpenes: Chemical and biological investigations of the tropical marine red alga. *Phytochemistry* **1999b**, *52*, 1047-1053.

Kubanek, J.; Jensen, P. R.; Keifer, P. A.; Sullards, M. C.; O. Collins, D.; Fenical, W. Seaweed resistance to microbial attack: A targeted chemical defense against marine fungi. *Proceedings of the National Academy of Sciences of the United States of America* **2003**, *100*, (12), 6916–6921.

Makler, M. T.; Ries, J. M.; Williams, J. A.; Bancroft, J. E.; Piper, R. C.; Gibbins, B. L.; Hinrichs, D. J. Parasite lactase dehydrogenase as an assay for *Plasmodium falciparum* sensitivity. *The American Society of Tropical Medicine and Hygiene* **1993**, *48*, 739-741.

Mann, M. G. A., Mkwananzi, H. B., Antunes, E. M., Whibley, C. E., Hendricks, D. T., Bolton, J. J., Beukes, D. R. Halogenated Monoterpene Aldehydes from the South African Marine Alga *Plocamium corallorhiza*. *Journal of Natural Products* **2007**, *70*, 596-599.

Misharina, T. A.; Polshkov, A. N. Antioxidant properties of essential oils: Autoxidation of essential oils from Laurel and Fennel and of their mixtures with essential oils from Coriander. *Applied Biochemistry and Microbiology* **2005**, *41*, (6), 610-618.

Mkwananzi, H. B. A study of *Plocamium corallorhiza* secondary metabolites and their biological activity. MSc Thesis **2005**, Rhodes University, Grahamstown, South Africa.

Naylor, S.; Hanke, F. J.; Manes, L. V.; Crews, P. Chemical and biological aspects of marine monoterpenes. *Progress in the Chemistry of Organic Natural Products* **1983**, *44*, 189-241 ISBN 3-211-81754-9 Springer-Verlag/Wien.

Paul, V. J.; McConnel, O. J.; Fenical, W. Cyclic monoterpenoid feeding deterrents from the red marine alga *Ochtodes crockery*. *Journal of Organic Chemistry* **1980**, *45*, 3401-3407.

Prabuseenivasan, S.; Jayakumar, M.; Ignacimuthu, S. *In vitro* antibacterial activity of some plant essential oils. *Complementary and Alternative Medicine* **2006**, *6*, 39.

Pihlasalo, J.; Klika, K. D.; Murzin, D. Y.; Nieminen, V. Conformational equilibria of citral. *Journal of Molecular Structure THEOCHEM* **2007**, *814*, 33-41.

Pohnert, G. Phospholipase A2 Activity Triggers the Wound-Activated Chemical Defense in the Diatom *Thalassiosira rotula*. *Plant Physiology* **2002**, *129*, 103-111.

Renault-Roger, C. The Potential of botanical essential oils for insect pest control. *Integrated Pest Management Reviews* **1997**, *2*, 25-34.

Sardina, F. J.; Quiñoã, E.; Castedo, L.; Riguera, R. Structural elucidation of marine halogenated monoterpenes by 2D-NMR and NOE difference spectroscopy. A stereochemical correction. *Chemistry Letters* **1985**, *697-700.*

Sierle D. B.; Sims J. J. Polyhalogenated cyclic monoterpenes from the red alga *Plocamium cartilagineum* of Antarctica. *Tetrahedron* **1979**, *35*, 1261-1265.

Smith, P. W. G.; Tatchell, A. R.; *Organic chemistry for general degree students.* Aliphatic aldehydes and ketones **1965** Chapter *9*, 159,Pergamon Press.

Spaulding, R. S.; Charles, M. J. Comparison of methods for extraction, storage and silylation of pentafluorobenzyl derivatives of carbonyl compounds and multifunctional carbonyl compounds. *Analytical and Bioanalytical Chemistry* **2002**, ***372***, 808-816.

Spiteller, G.; Kern, W.; Spiteller, P. Investigation of aldehydic lipid peroxidation products by gas chromatography-mass spectrometry. *Journal of Chromatography A* **1999**, *843*, 29-98.

Supelco Buletin 909A Guide to Derivatization Agents Sigma-Aldrich Co © **1997**.

Trager, W.; Jensen, J. B. Human malaria parasite in continuous culture. *Science* **1976**, *193*, (4254), 673-675.

Van Engen, D.; Clardy, J.; Kho-Wiseman, E.; Crews, P.; Higgs, M.; Faulkner, D. J. Violacene: A reassignment of structure. *Tetrahedron Letters* **1978**, *1*, 29-32.

van Leeuwen, S.; Hendriksen, L.; Karst, U. Determination of aldehydes and ketones using derivatization with 2,4-dinitrophenylhydrazine and liquid chromatography–atmospheric pressure photoionization-mass spectrometry. *Journal of Chromatography A* **2004**, *1058*, 107-112.

Vogel's Textbook of practical organic chemistry 5th Edition ISBN 0-582-46236-3 Longman Scientific & Technical, United States.

Wichard, T.; Poulet, S. A.; Pohnert, G. Determination and quantification of α,β,γ,δ-unsaturated aldehydes as pentafluorobenzyl-oxime derivatives in diatom cultures and natural phytoplankton populations: Applications in marine field studies. *Journal of Chromatography B* **2005**, *814*, 155-161.

Wise, M.; Rorrer, G. L.; Polzin, J. J.; Croteau, R. Biosynthesis of marine natural products: Isolation and characterization of a myrcene sythase from cultured tissues of the marine red alga *Ochtodes secundiramea*. *Archives of Biochemistry and Biophysics* **2002**, *400*, (1), 125-132.

Woolard, F. X.; Moore, R. E.; Van Engen, D.; Clardy, J. The structure and absolute configuration of Chondrocolactone, a halogenated monoterpene from the red alga *Chondrococcus hornemanni*, and a revised structure for Chondrocole A. *Tetrahedron Letters* **1978**, *27*, 2367-2370.

Zhong, L.; Jacobus, L. K.; Wuelfing, W. P.; Golden, M.; Martin, G. P.; Reed, R. A. Detection of low molecular weight aldehydes in pharmaceutical excipients by headspace gas chromatography. *Journal of Chromatography A* **2006**, *1104*, 1-10.

Zwiener, C.; Glauner, T.; Frimmel, F. H. Method optimization for the determination of carbonyl compounds in disinfected water by DNPH derivatization and LC-ESI-MS-MS. *Analytical and Bioanalytical Chemistry* **2002**, *372*, 615-621.

Chapter Four

Sesquiterpenes and Vinyl Acetylenes from *Laurencia flexuosa*

4.1 Introduction

The study of *Laurencia* species has been a focus of marine natural products chemistry since its inception (Coll and Wright, 1989). *Laurencia* species are taxonomically classified under the order of Ceramiales and the family of Rhodomelaceae (Fenical, 1975). Species of this genus grow ubiquitously in tropical to temperate and even Antarctic waters (Coll and Wright, 1989).

Table 4.1 Selected classes of carbon skeletons produced by *Laurencia* species

Structural Class	Example	No.	
Chamigrenes	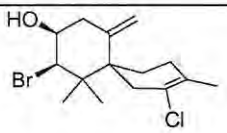	**4.1**	elatol
Bisabolene addition products	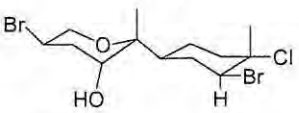	**4.2**	caespitol
Bromomonocyclofarnesyl derivatives	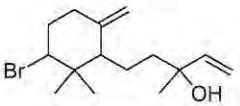	**4.3**	Snyderol
	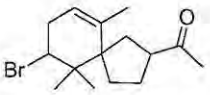	**4.4**	spirolaurenone
Cuparanes	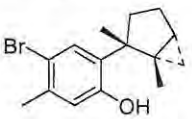	**4.5**	laurinterol
Diterpenes	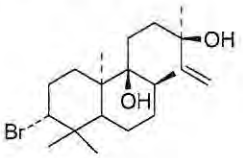	**4.6**	concinndiol
Polybromoindoles		**4.7**	
Non-terpenoids	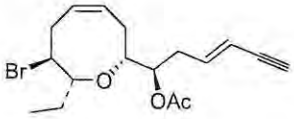	**4.8**	laurencin
	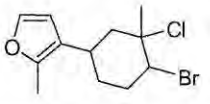	**4.9**	furocaespitane

(Fenical, 1975, Blunt *et al.*, 2007)

Laurencia species produce an assortment of halogenated secondary metabolites including terpenes and acetogenins of very complex types (Table 4.1) and there are many novel structural groups found only in this genus (Fenical, 1975; Hay and Fenical, 1988).

4.1.1 Cuparane Derived Sesquiterpenes

One large class of compounds produced by *Laurencia* is that of the cuparanes. Cuparane derived sesquiterpenes are not unique to marine algae and are produced by terrestrial plants such as the liverworts *Lejeunea aquatica* (Toyota *et al.*, 1997) and *Herbertus aduncus* (Asakawa *et al.*, 1982) and the flowering plant *Arabidopsis thaliana* (Tholl *et al.*, 2005). Many cuparanes have also been isolated from extracts of the specialised digestive gland of opisthobranch molluscs (genus *Aplysia*) (Yamamura and Hirata, 1963; Ichiba and Higa, 1986). Cuparanes from terrestrial sources are non-halogenated while those of marine origin often contain at least one halogen atom.

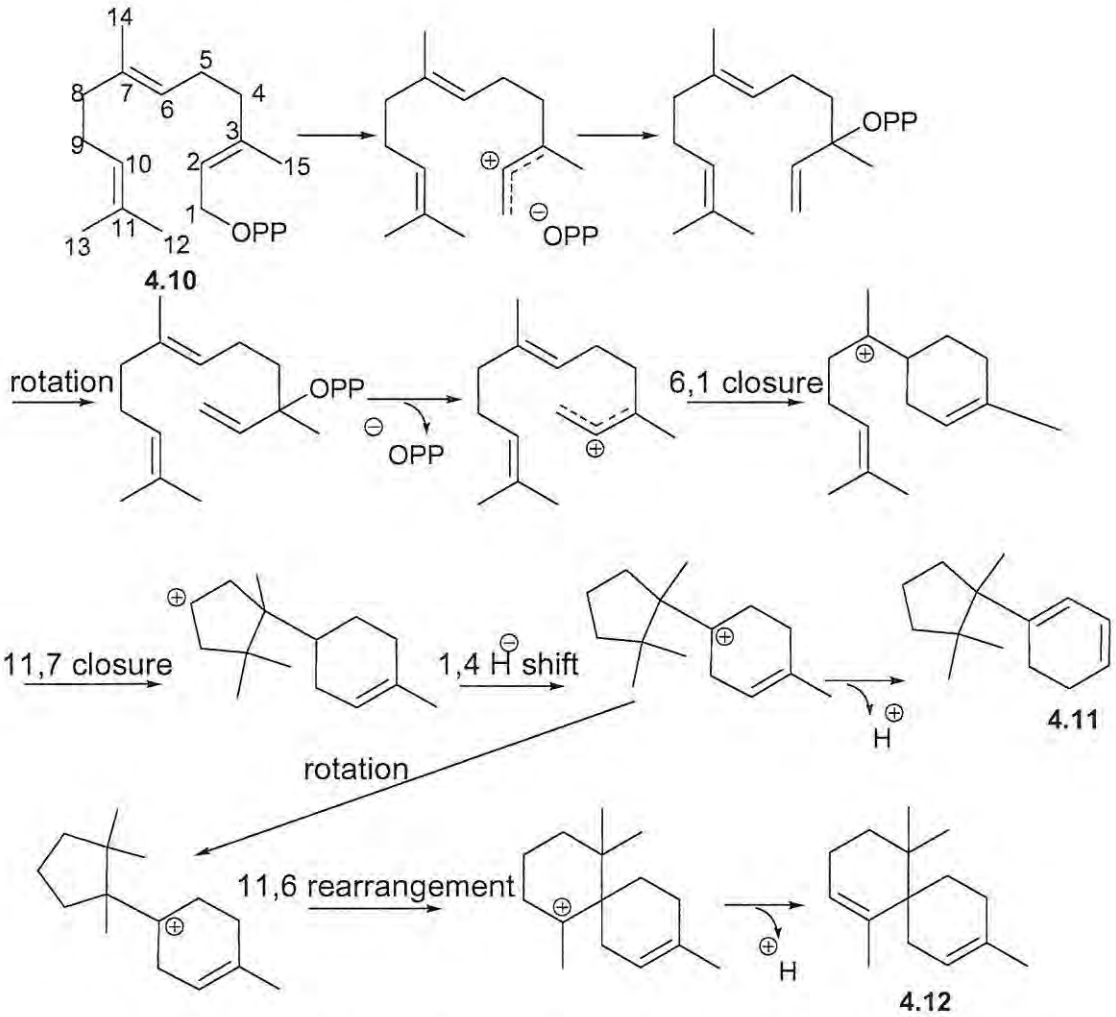

Scheme 4.1 The biosynthesis of a-cuprenene (**4.11**) and a-chamigrene (**4.12**) in *Arabidopsis thaliana*. (Adapted from Tholl *et al.*, 2005)

Sesquiterpenes such as the cuparanes and chamigrenes, both produced by *Laurencia* possess a common precursor, farnesyl diphosphate (**4.10**). Scheme 4.1 illustrates the proposed biosynthesis of a-cuprenene (**4.11**) and a-chamigrene (**4.12**) via a bisabolene cation intermediate in *Arabidopsis thaliana* (Tholl *et al.*, 2005).

4.1.2 Structural Rearrangements and Cyclization of Cuparane Derived Sesquiterpenes

Cuparane derived sesquiterpenes are known to undergo acid catalysed cyclization (Irie *et al.*, 1966). It is believed that selected sesquiterpenes isolated from opisthobranch molluscs originate from biogenic precursors that are present in the sea hare's algal diet (Laronze *et al.*, 1991; Rogers *et al.*, 2003). The original cuparane cation (**4.13**) is thought to undergo a series of methyl migrations, proton abstractions and cyclization as seen in scheme 4.2 (Goldsmith *et al.*, 1980; Laronze *et al.*, 1991).

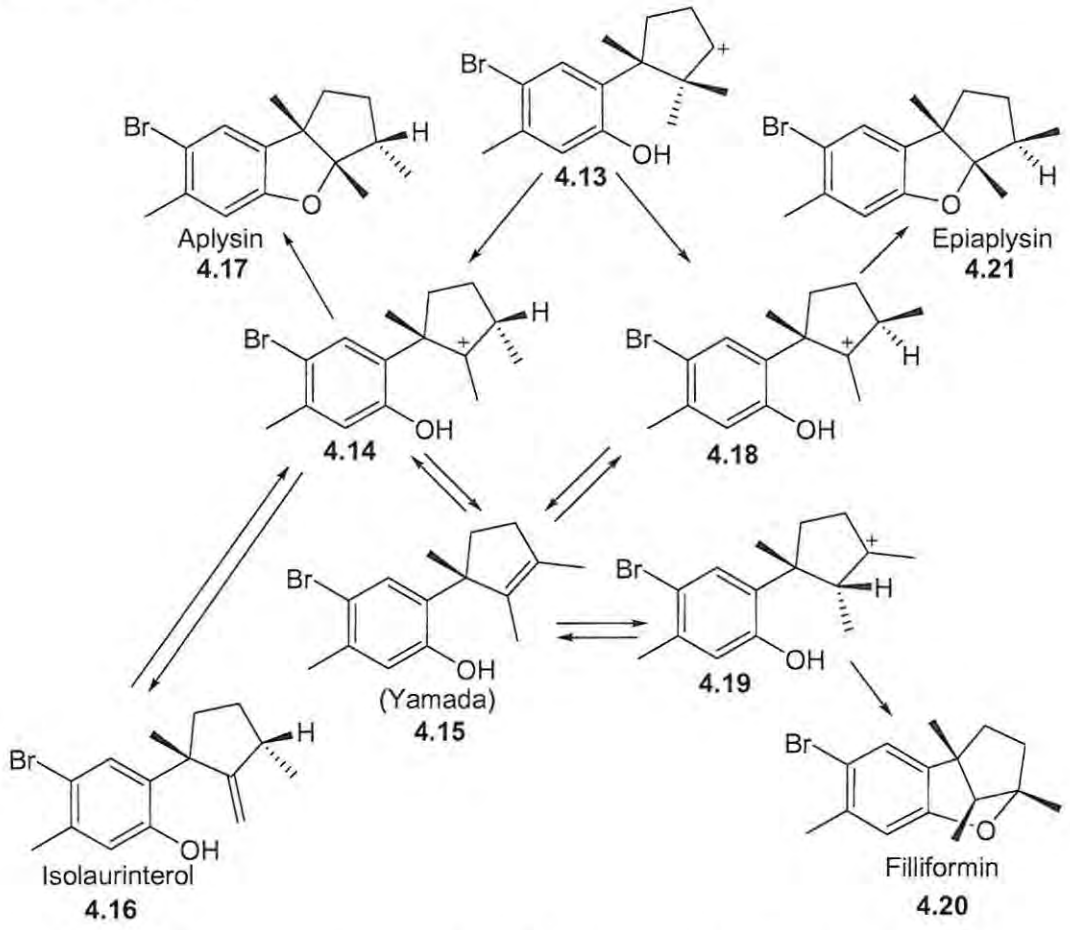

Scheme 4.2 The intramolecular rearrangements of cuparane derived sesquiterpenes (Reproduced from Laronze *et al.*, 1991)

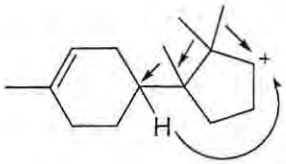

Figure 4.1 Methyl and proton migrations that occur in a cuparane cation (Goldsmith *et al.*, 1980)

Aplysin (**4.17**) from *Aplysia kurodai*, the first of this class of compounds to be isolated (Yamamura and Hirata, 1963), is thought to be the result of the rearrangement of isolaurinterol (**4.16**). Isolaurinterol (**4.16**) has been isolated from numerous species of *Laurencia* growing in warm to temperate waters (Hay and Fenical, 1988).

4.1.3 Biological Activity of Cuparane Derived Sesquiterpenes

Many cuparane type compounds have exhibited cytotoxic and antimicrobial activity and have been found to be more active against Gram-positive than Gram-negative bacteria. Laurinterol (**4.5**) first isolated from *L. intermedia* by Irie *et al.* (1966), is frequently isolated from a number of different *Laurencia* species and has been tested against numerous micro-organisms and several cancer cell lines. Table 4.2 and Table 4.3 briefly show some of the biological activity data of selected cuparanes from *Laurencia*. In terms of these few compounds, it is apparent that in the case of antimicrobial activity as well as antitumour activity, the brominated compounds are more potent than those lacking halogens.

Table 4.2 Antimicrobial activity of four cuparane sesquiterpenes isolated from *Laurencia* species

Micro-organism	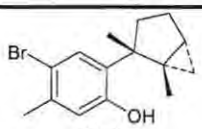 **4.5**	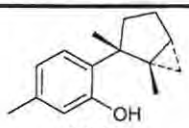 **4.21**	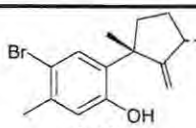 **4.16**	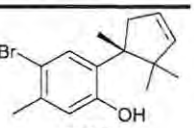 **4.22**
Salmonella choleraesuis[a]	>1000 µg/ml	>1000 µg/ml		
Mycobacterium smegmatis[a]	1-5 µg/ml	10-50 µg/ml		
Candida albicans CA-5[a]	10-30 µg/ml	10-30 µg/ml		
Escherichia coli[a]	>1000 µg/ml	>1000 µg/ml		
Staphylococcus aureus 209 PJC-1[b]	3.13 µg/ml		6.25 µg/ml	3.13 µg/ml
Staphylococcus epidemidis ATCC 14990[b]	3.13 µg/ml		6.25 µg/ml	6.25 µg/ml
Streptococcus pyogenes C-203[b]	1.56 µg/ml		3.13 µg/ml	1.56 µg/ml
Klebsiella pneumoniae[b]	>50 µg/ml		>50 µg/ml	>50 µg/ml
Escherichia coli NIHJ JC-2[b]	>50 µg/ml		>50 µg/ml	>50 µg/ml
Pseudomonas aeruginosa[b] ATCC 25619[b]	>50 µg/ml		>50 µg/ml	>50 µg/ml

[a] Minimum concentration for complete growth inhibition after 48 hours; Sims *et al.*, 1975, [b] Minimum inhibitory concentrations (MIC) Vairappan *et al.*, 2004

Cuparane sesquiterpenes are not the only compounds produced by *Laurencia* that exhibit antimicrobial activity (Blunt *et al.*, 2007), however, they have often been found to be the most potent (Sims *et al.*, 1975; Vairappan *et al.*, 2004). In addition, selected compounds (Figure 4.2) have exhibited antifouling activity *in vitro* (Fusetani, 2004; König and Wright, 1997).

Table 4.3 Antitumour activity (IC_{50} in μM) of selected cuparane sesquiterpenes isolated from *Laurencia* species

Tumour cell line	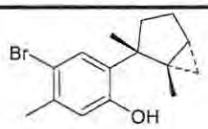 **4.5**	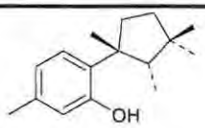 **4.23**	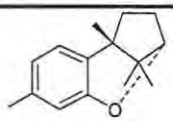 **4.24**	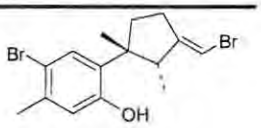 **4.25**
K562	128.3	>300	>200	112.7
MCF7	67.2	201.7	>200	78.3
PC3	76.6	182.3	>200	92.4
HeLa	83.9	121.3	>200	105.8
A431	74.6	176.4	>200	81.6
CHO	165.8	234.7	>200	>200

Kladi *et al.*, 2006

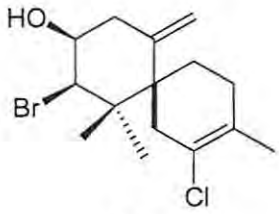

4.26

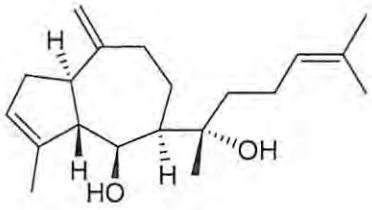

4.27

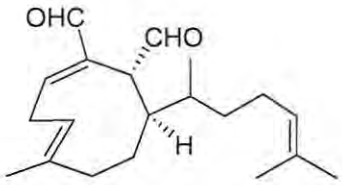

4.28

Figure 4.2 Secondary metabolites from *Laurencia* species that exhibit antifouling activity

The biological activity of compounds previously isolated from *Laurencia* species, coupled with the results of the antimicrobial screening assays (chapter 2), prompted the fractionation of extracts from the South African species *Laurencia flexuosa*. To date, only one prior study has been conducted on a Southern African *Laurencia* species. *Laurencia glomerata* was found to produce a number of halogenated chamigranes (Elsworth and Thomson, 1989).

4.1.4 Chapter aims

The key aims for this chapter were to isolate and characterize pure compounds that may have been responsible for the observed antimicrobial activity, with the hope of obtaining sufficient material for use in preliminary biofilm inhibition assays.

4.2 Results and Discussion

Laurencia flexuosa grows in the sheltered crevices that punctuate the rocky outcrops exposed at low tide. Often enmeshed with many other algae, it grows in small clumps and is difficult to detach from the rocks. Branch *et al.* (2005) describe *L. flexuosa* as having an uncomplicated appearance with symmetrically branched flattened fronds. The plant is deep red in colour lacking iridescence. The alga can be seen growing in close proximity with red algae of the *Plocamium* genus, often *P. corallorhiza* and *P. suhrii*. On inspection of the thalli, it was often apparent that some degree of fouling had occurred. Small shelled organisms were attached to the fronds of some plants while others had a dark rotting appearance.

4.2.1 Collection, extraction and isolation

Laurencia flexuosa was collected from Kenton-On-Sea (KOS06-6) and Noordhoek (NDK06-6) for purposes of screening as described in chapter 2. The extracts for each collection that were screened for antimicrobial activity degraded before further fractionation was carried out. In order to investigate the compounds responsible for the observed antimicrobial activity, re-extraction was necessary. A second extraction of the Noordhoek collection was made (NDK06-6&11) which yielded four compounds **4.29**, **4.32**, **4.33** and **4.34**. Compound **4.29** was present in very small amounts, while **4.34**, a halogenated monoterpene, was suspected to be from a different alga altogether. Since a standard protocol was followed for the extraction of *L. flexuosa*, only the procedure for NDK06-6&11 will be described here.

Figure 4.3 Kenton-On-Sea collection site, Eastern Cape coast South Africa

NDK06-6&11 (Noordhoek)

L. flexuosa was collected in April 2006 and was sequentially extracted with MeOH and CH_2Cl_2-MeOH (2:1). The MeOH extract was separately extracted with CH_2Cl_2 after which the remaining aqueous MeOH extract was reduced *in vacuo* to an aqueous mixture. The CH_2Cl_2-MeOH extract was combined with the CH_2Cl_2 partition of the MeOH extract and evaporated to dryness affording extract A. Residual organic material was recovered from the aqueous mixture by way of an HP-20 column to afford extract B. The extracts were fractionated by silica gel column chromatography (frs A1-9 and B1-9). Normal phase HPLC of the *n*-hexane-EtOAc (8:2) silica gel column fraction (A3) of the CH_2Cl_2-MeOH extract afforded compounds **4.32** (A3d Scheme 4.3), **4.33** (A3e Scheme 4.3) and **4.34** (A3b Scheme 4.3). Compound **4.29** (B4i Scheme 4.3) was isolated following column chromatography and normal phase HPLC of the extract B.

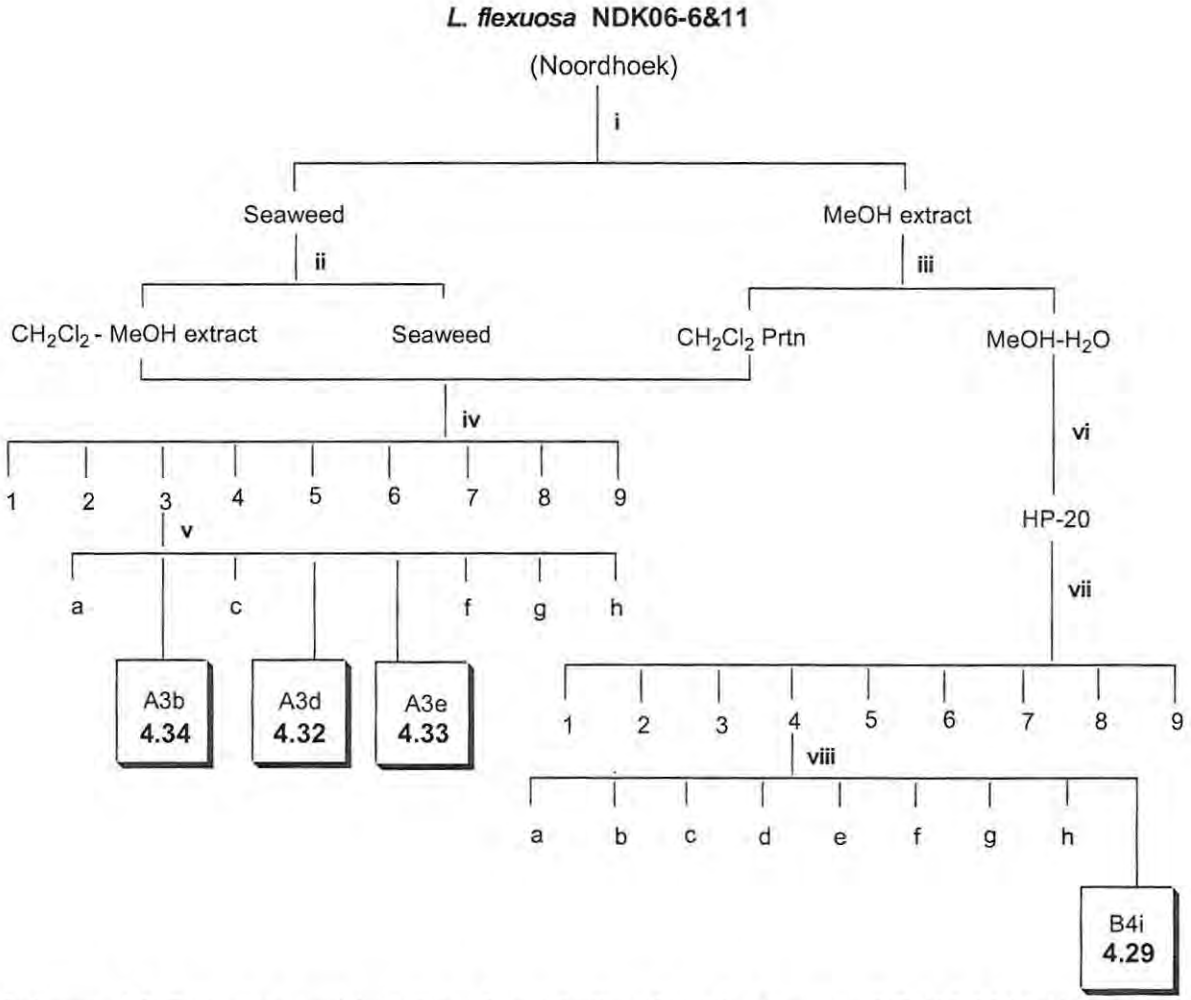

Scheme 4.3 Extraction and isolation of metabolites from *L. flexuosa* (NDK06-6&11 Noordhoek 2006)

Conditions: i) MeOH extraction ii) CH_2Cl_2-MeOH extraction iii) Partitioning into CH_2Cl_2 iv) Silica gel column chromatography of CH_2Cl_2-MeOH extract v) Normal phase HPLC *n*-hexane-EtOAc (19:1) vi) HP-20 Column vii) Silica column chromatography of HP-20 fr viii) Normal phase HPLC *n*-hexane-EtOAc (9:1)

Table 4.4 Masses and percentage yields* of compounds isolated from *L. flexuosa* (NDK06-6&11)

Isolation code‡	Compound #	Mass (mg)	% yield*
A3b	**4.34**	19.1	0.077
A3d	**4.32**	68.0	0.275
A3e	**4.33**	33.4	0.135
B4i	**4.29**	1.6	0.007

‡Isolation code: Partition, silica column fr, HPLC fr e.g CH_2CL_2-MeOH prtn, silica column fn 3, HPLC fr b. * Percentage yields calculated relative to dry weight after extraction

4.2.2 Characterization of compounds from *L. flexuosa*

4.2.2.1 Structure determination of 4.29

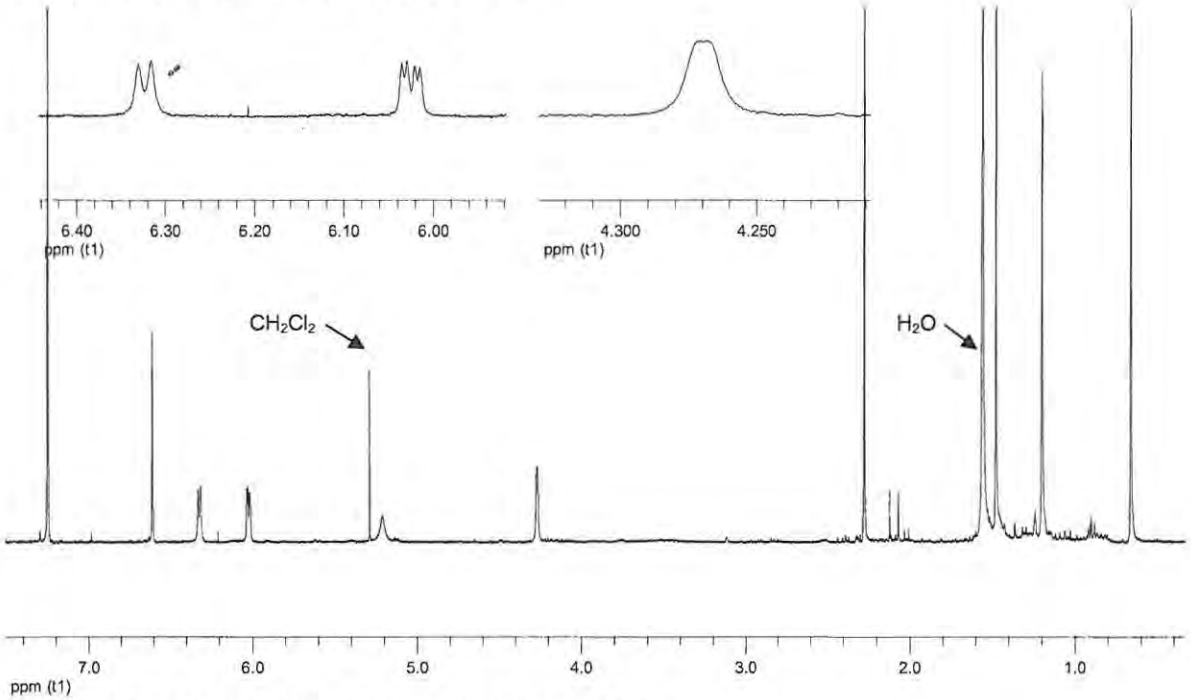

Figure 4.4 ^{1}H NMR spectrum ($CDCl_3$, 400 MHz) of **4.29**

Compound **4.29** was isolated as a transparent oil from the MeOH extract (B) of *L. flexuosa*. Low resolution EIMS data indicated a molecular ion at *m/z* 310/312. The molecular ion occurred as a cluster of two peaks indicating that one atom in the molecule had two naturally occurring isotopes, this was most likely to be the halogen bromine. High resolution FABMS confirmed the molecular weight to be 310.0567 amu which is consistent with a molecular formula of $C_{15}H_{19}BrO_2$ (calcd for $C_{15}H_{19}{}^{79}BrO_2$ 310.0568). The ^{1}H NMR spectrum (Figure 4.4) showed a deshielded doublet at d 6.32 (d, *J* = 5.8 Hz) coupled to a doublet of doublets at d 6.03 (dd, *J* = 5.7, 2.4 Hz). The latter was also coupled to a second doublet resonating at d 4.27 (d, *J* = 1.7 Hz). The proton responsible for the absorbance at d 4.27 is coupled to a carbon with a ^{13}C NMR chemical shift of d 85.5. This data is indicative of a -CH=CH-CHX- system where X is an hydroxyl substituent. Coupling constants of ~5.8 Hz indicate *cis* geometry about the double bond. A broad singlet at d 5.20 infers the presence of at least one hydroxyl group which was confirmed by an IR absorbance band at 3460 cm^{-1}. Four methyl singlets resonate at d 2.28, 1.48, 1.20 and 0.66 while two deshielded singlets were observed at d 6.61 and 7.25, the latter being obscured by the chloroform solvent peak.

Only twelve resonances were obvious in the ^{13}C NMR spectrum (Figure 4.5), however data from an HMBC experiment revealed the presence of 15 carbons and indicated a sesquiterpene skeleton. The compound contains four double bonds, three of which exist within a substituted aromatic ring. The carbons involved resonated at d 153.7 (C-1), 129.1 (C-2), 132.1 (C-3), 115.3 (C-4), 137.1 (C-5) and 119.0 (C-6).

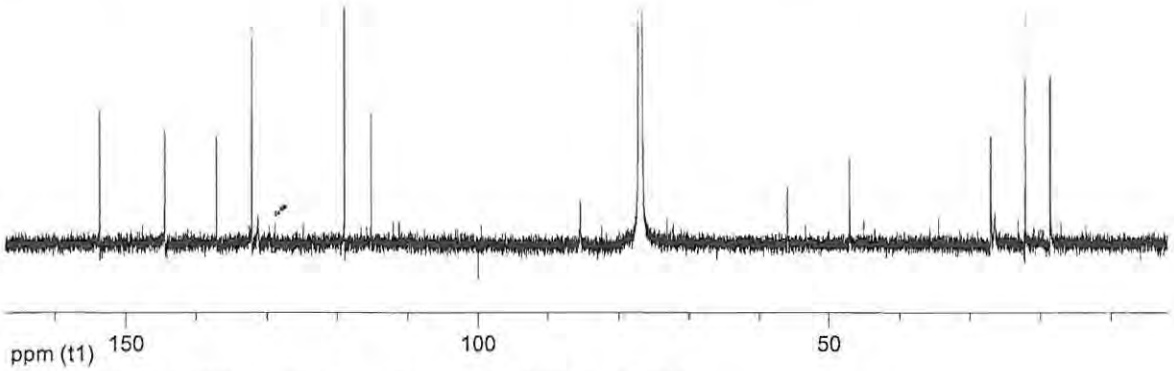

Figure 4.5 ^{13}C NMR spectrum ($CDCl_3$, 100 MHz) of **4.29**

The carbons of the fourth olefin resonated at d 144.5 (C-3') and 132.1 (C-4' by HMBC). Also observed in the ^{13}C NMR spectrum, a resonance at d 85.5 (C-5'), three methyl signals at d 27.0, 22.2 and 18.7 and two resonances at d 56.0 and 47.1 which are due to aliphatic quaternary carbons. The fourth methyl carbon resonated at d 27.1 (by HMBC).

A time delay of a couple of days occurred between performing the one- and two-dimensional NMR experiments. During this period, compound **4.29** was stored in $CDCl_3$ in the freezer at -4 °C. Prior to performing the 2D experiments, a second ^1H NMR experiment was run, it was then that an anomaly was observed. Compound **4.29** was undergoing structural changes observed as the disappearance of the original ^1H NMR resonances and the appearance of new ones.

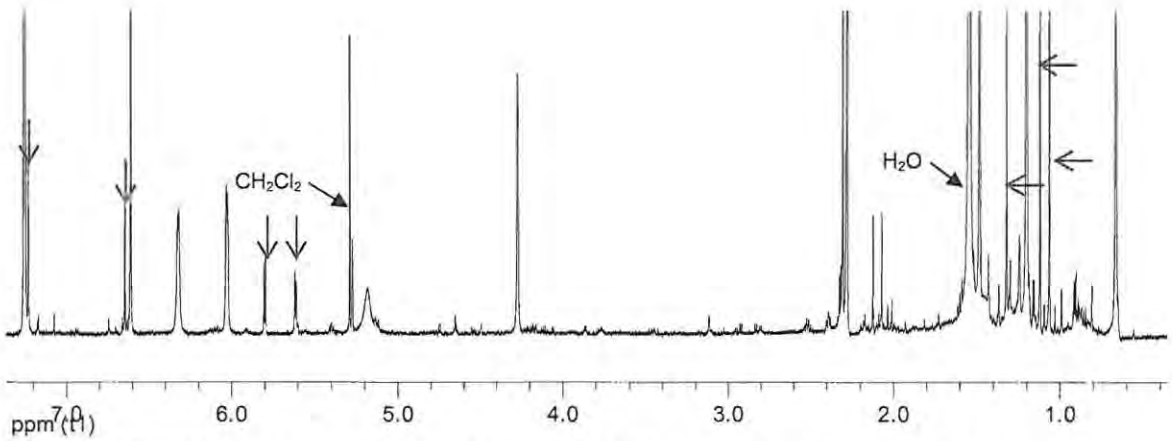

Figure 4.6 ^1H NMR spectrum ($CDCl_3$, 400 MHz) of **4.29** undergoing structural changes

^1H-^1H COSY, HSQC and HMBC experiments were performed on the mixture of the two compounds; fortunately the data obtained was distinct for each and allowed the elucidation of the original structure. HMBC data was used to determine the planar structure of the compound while the identity of the hetero-atoms was deduced by interpretation of ^{13}C NMR chemical shifts and mass spectrometry data.

The HMBC correlations from the methyl protons at d 2.28 to carbons in the aromatic ring (C-1 to C-6) as well as to d 56.0 (C-1') and 47.1 (C-2') (Table 4.5) played a significant role in the discernment

of fragment A (Figure 4.7). Fragment B (Figure 4.7) was determined predominantly by interpretation of the HMBC correlations between the proton resonating at d 6.03 and carbons at d 56.0 (C-1'), 47.1 (C-2'), 144.5 (C-3') and 85.5 (C-5').

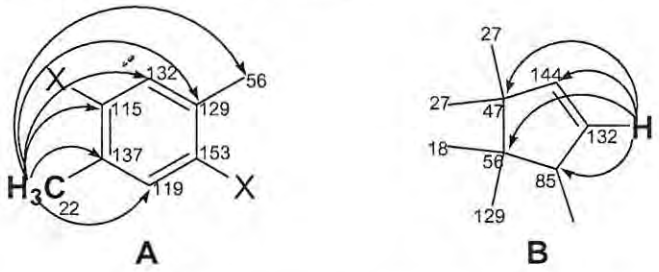

Figure 4.7 Key HMBC correlations in the structure determination of **4.29**

Further support for the structure of the two fragments was provided by HMBC correlations from the methyl protons at d 1.48, 1.20 and 0.66 to carbons in both fragments (Table 4.5).

Table 4.5 ^{1}H and ^{13}C NMR, ^{1}H-^{1}H COSY and HMBC data for **4.29** ($CDCl_3$, 400 MHz, 100 MHz)

Carbon No.	d_C	DEPT	d_H, multi, *J* (Hz)	^{1}H-^{1}H COSY	HMBC
1	153.7	C			
2*	129.1	C			
3*	132.1	CH	7.25, s	H7	C7, C1', C2', C4, C6, C5, C1
4	115.3	C			
5	137.1	C			
6	119.0	CH	6.61, s	H7	C7, C1', C4, C2, C1
7	22.2	CH_3	2.28, s	H3, H6	C4, C6, C2, C3, C5, C1', C2'
8	18.7	CH_3	1.20, s	H9	C10, C1', C2' C5'
9*	27.1	CH_3	0.66, s	H8	C8, C2', C1' C5'
10	27.0	CH_3	1.48, s		C8, C2', C1', C2, C3'
1'	56.0	C			
2'	47.1	C			
3'	144.5	CH	6.32, d, 5.8	H4'	C1', C2'
4'	132.1	CH	6.03, dd, 5.7, 2.4	H3', H5'	C1', C2' C5', C3'
5'	85.5	CH	4.27, d, 1.7	H4', H8, H10	C10, C1', C4', C3'

* ^{13}C NMR chemical shifts deduced from HMBC data

A ^{13}C NMR chemical shift of d 85.5 at position C-5' is indicative of an hydroxyl substituent, similarly d 153 at C-1 indicates an hydroxyl substituent but in this case on an aromatic ring.

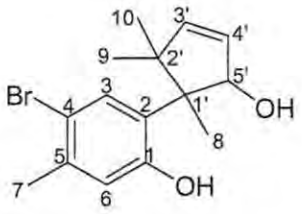

4.29

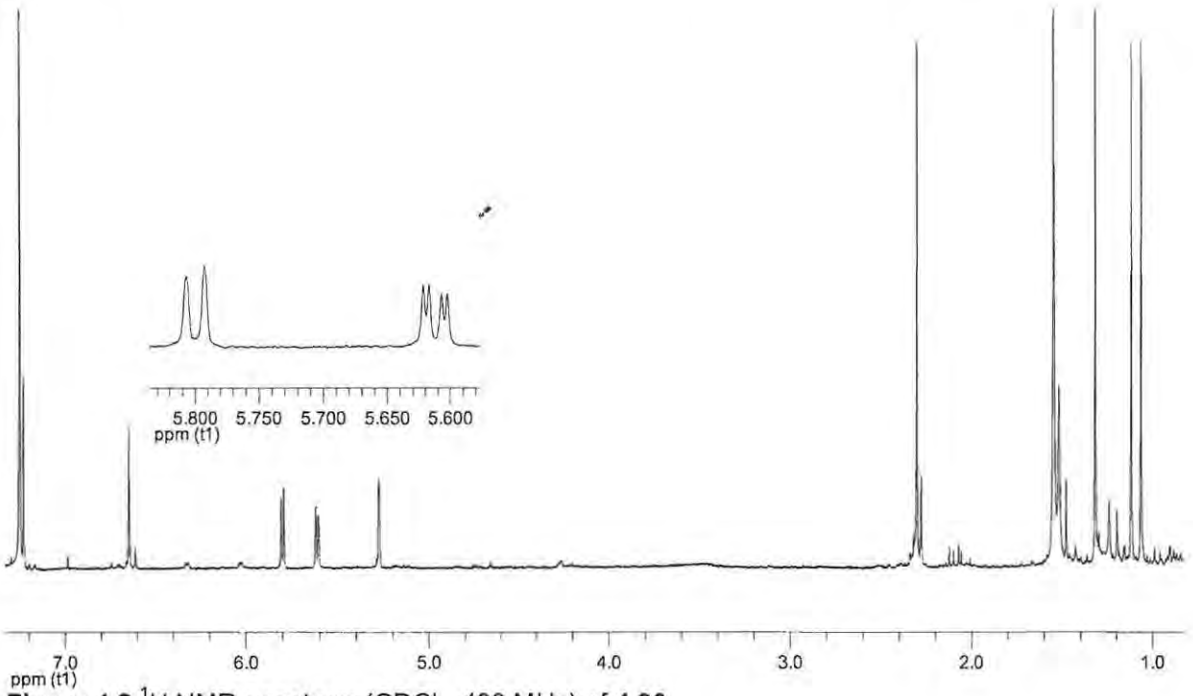

Figure 4.8 ^{1}H NMR spectrum ($CDCl_3$, 400 MHz) of **4.30**

After seven days, more than 90 % of the original compound had undergone alteration; it was also observed that the once transparent oil had become a white crystalline powder. Low resolution EIMS of **4.29b** revealed a new molecular mass of *m/z* 292/294 which points to the loss of H_2O (18 amu). A second NMR data set was obtained in order to elucidate the altered structure. Although some very apparent changes occurred in the ^{1}H NMR chemical shifts, upon building the fragments using HSQC, HMBC and COSY experimental data, it was discovered that the hydrocarbon skeleton was very much the same. However, the chemical shift of C-5' had changed from d 85.5 to 99.5 and the chemical shifts of C-3' and C-4' had changed from 144.5 and 132.1 to 147.6 and 124.8 respectively, inferring that whatever change had occurred was influencing the electronic environment of the pentene ring. Minor ^{13}C NMR chemical shift changes were also observed for carbons in the aromatic ring. In addition, the methine proton at d 5.27 which originally resonated at d 4.27 showed an HMBC correlation to the carbon at d 157.2 (C-1), indicating a new link between the two rings. Lack of evidence that the hydrocarbon skeleton had undergone change, the difference in molecular mass being that of one water molecule and the new HMBC correlation between the oxymethine at d 5.27 and C-1 implied that the observed changes were due to intra-molecular cyclization (Scheme 4.4.). **4.30** has a tricyclic ring system wherein the aromatic ring joins the pentene ring via a cyclic ether.

NOE's from the oxymethine (H-5') at d 5.27 to methyl protons at d 1.32 (H-8) and 1.12 (H10) are indicative of relative *S**, *S** stereochemistry for the chiral centres at C1' and C5'.

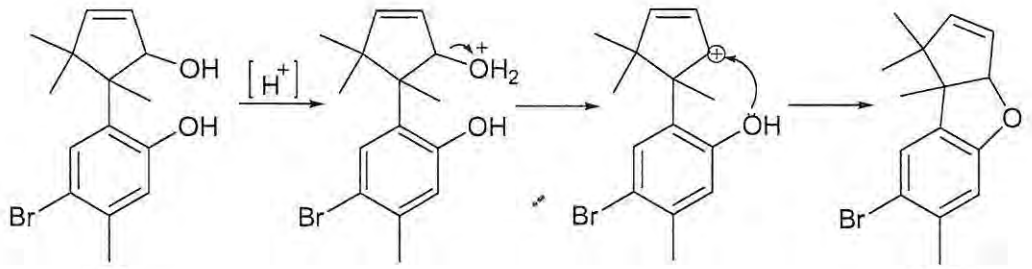

4.29 **4.30**

Scheme 4.4 The proposed cyclization of **4.29** via a dehydration mechanism

Table 4.6 ^{1}H (400 MHz) and ^{13}C (100 MHz) NMR, ^{1}H-^{1}H COSY and HMBC and NOESY data for **4.30** ($CDCl_3$)

Carbon No.	d_C	DEPT	d_H, multi, *J* (Hz)	^{1}H-^{1}H COSY	HMBC	NOESY
1	157.2	C				
2	134.9	C				
3	128.9	CH	7.23, s	H7	C1, C4, C5, C1'	H8, H9
4	114.1	C				
5	137.6	C				
6	112.1	CH	6.65, s		C1, C2, C4, C7	H7
7	22.3	CH_3	2.30, s	H3	C4, C5, C6	H6
8	22.2	CH_3	1.32, s		C1', C2', C5', C2	H3, H5'
9	26.9	CH_3	1.06, s		C1', C2', C3', C10	H8
10	27.0	CH_3	1.12, s		C1', C2', C3', C2, C8	H3, H8
1'	57.6	C				
2'	50.0	C				
3'	147.6	CH	5.80, d, 5.8	H4'	C1', C2', C5', C4'	H4', H9, H10
4'	124.8	CH	5.61, dd, 5.8, 1.9	H3', H5'	C1', C2', C5'	H3', H5'
5'	99.5	CH	5.27, d, 1.7	H4'	C1, C8, C3'	H4', H8, H10

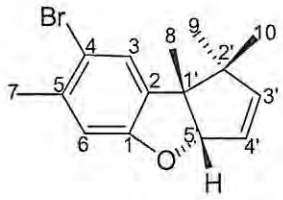

4.30

Acetylation of 4.29

To confirm the presence of hydroxyl groups, and in attempt to prevent intra-molecular cyclization, **4.29** was re-isolated and acetylated by reacting the compound with acetic anhydride in pyridine overnight to form **4.31**.

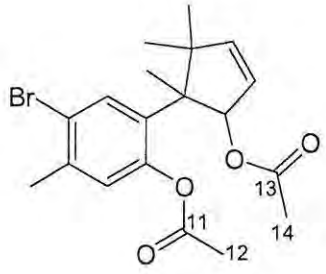

4.31

Table 4.7 ^{1}H and ^{13}C NMR, ^{1}H-^{1}H COSY and HMBC data for **4.31** ($CDCl_3$, 400 MHz, 100 MHz)

Carbon No.	d_C	DEPT	d_H, multi, *J* (Hz)	COSY	HMBC
1	147.2	C			
2	137.3	C			
3	132.8	CH	7.41, s		C1, C2, C4, C1'
4	121.6	C			
5	135.1	C			
6	126.0	CH	6.86, s		C1, C4, C5
7	22.4	CH_3	2.33, s		C2, C4, C5, C6, C11
8	25.9	CH_3	1.41, s		C1', C2', C3', C1
9	18.6	CH_3	1.13, s		C10, C1', C2', C5'
10	27.2	CH_3	0.66, s		C9, C1', C2', C5'
1'	55.6	C			
2'	46.6	C			
3'	147.2	CH	6.26, d, 5.9	H4'	C1', C2'
4'	125.1	CH	5.78, dd, 5.4, 2.1	H3', H5'	
5'	86.8	CH	5.30, d, 2.4	H4'	C1', C1 or C3', C13
11	169.4	C=O			
12	21.3	CH_3	2.06		
13	170.8	C=O			
14	21.6	CH_3	2.26		C13

Diacetylation of **4.29** confirms that two hydroxyl groups were present in the original compound prior to cyclization. **4.31** showed greater stability and failed to undergo any structural changes in $CDCl_3$, providing further evidence for the involvement of the free hydroxyl groups in the cyclization mechanism.

Compounds **4.29** and **4.30** are new members of the large class of cuparane derived sesquiterpenes. Acid catalyzed cyclization is a well documented phenomenon in these compounds and several highly similar structures have been published.

4.2.2.2 Structure determination of 4.32 and 4.33

The *n*-hexane-EtOAc (8:2) silica gel column fraction yielded the known compound (3*E*)-bromofucin (**4.33**) also isolated from *L. implicata* (Coll and Wright, 1989) and its geometric isomer (3*Z*)-bromofucin (**4.32**) previously isolated from the specialised digestive gland of the South African sea hare *Aplysia parvula* (M^{c}Phail and Davies-Coleman, 2005). The molecular formula for both compounds was established as $C_{15}H_{20}Br_2O_2$ by high resolution FABMS (389.9836 and 389.9830 respectively; calcd for $C_{15}H_{20}{}^{79}Br_2O_2$ 389.9830). The two isomers were isolated as brightly coloured yellow-orange oils which gave highly complex ^{1}H NMR spectra (Figure 4.9). The isomers are distinguished by the ^{1}H NMR chemical shifts attributed to H-3 and H-4 and their respective coupling constants (for 3-*E*- J = 16.0 Hz, for 3-*Z*- J = 10.9 Hz Table 4.8).

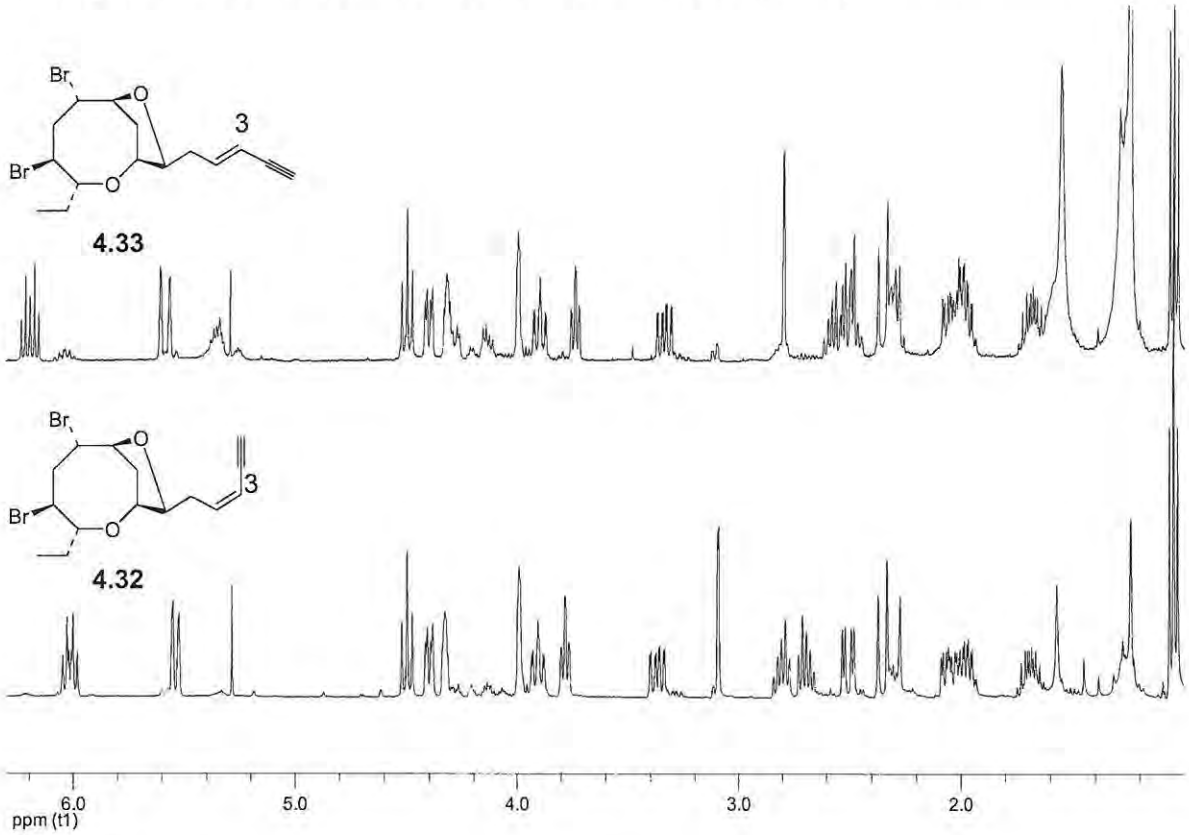

Figure 4.9 ^{1}H NMR spectra ($CDCl_3$, 400 MHz) of **4.32 and 4.33**

Fifteen resonances were observed in the ^{13}C NMR spectrum of **4.33**. Carbons resonating at d 141.8 (C-4) and 111.3 (C-3) revealed the presence of one olefin. A DEPT135 experiment indicated only one quaternary carbon, the terminal acetylene at d 82.1 (C-2). In determining the planar structure, an HMBC experiment on **4.33** established the two and three bond proton-carbon connectivity while a COSY experiment revealed important links between fragments (Table 4.8). The ^{1}H and ^{13}C NMR data obtained for both **4.33** and **4.32** is compatible with those reported by Coll and M^{c}Phail respectively

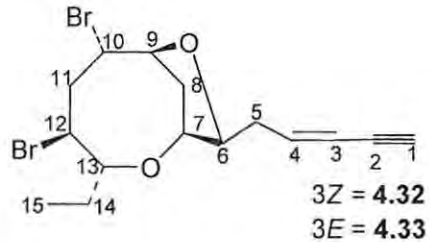

3*Z* = **4.32**
3*E* = **4.33**

Table 4.8 ^{1}H and ^{13}C NMR data for (3*Z*)-bromofucin (**4.32**) and ^{1}H and ^{13}C NMR, ^{1}H-^{1}H COSY and HMBC data for (3*E*)-bromofucin (**4.33**)

Carbon No.	**4.32**			**4.33**				
	δ_C		δ_H, multi, *J* (Hz)	δ_C		δ_H, multi, *J* (Hz)	^{1}H-^{1}H COSY	HMBC
1	82.0	CH	3.10, d, 2.1	76.4	CH	2.79, d, 2.2		
2	80.0	C		82.1	C			
3	110.4	CH	5.54, d, 10.9	111.3	CH	5.58, ddd, 1.6, 4.0, 16.0	H1, H4	
4	141.1	CH	6.02, dd, 7.5, 10.8	141.8	CH	6.19, ddd, 7.5, 8.1, 16.0	H3, H5	C2, C5
5	30.1	CH_2	2.70, m 2.81, m	32.5	CH_2	2.53, m	H4, H6	C3, C4, C6
6	84.3	CH	3.79, dt, 1.7 15.9	84.3	CH	3.73, dt, 1.8, 7.1	H5	
7	70.0	CH	3.99, br s	69.8	CH	4.00, br s		
8	33.6	CH_2	2.06, m 2.35, d, 15.6	33.5	CH_2	2.05, ddd, 3.3, 9.3, 15.8 2.36, d, 15.4	H7, H9	C6, C7, C10
9	79.6	CH	4. 40, dd, 3.4, 9.6	79.6	CH	4.40, dd, 3.6, 9.6	H8	
10	55.3	CH	4.33, m	55.2	CH	4.32, br s	H11	
11	38.5	CH_2	2.51, dd, 4.7, 15.8 3.37, ddd, 2.2, 8.9, 15.8	38.5	CH_2	2.53, m 3.34, ddd, 2.2, 8.9, 15.7	H10, H12	C9, C10, C12, C13
12	53.0	CH	4.50, t, 9.2	52.9	CH	4.49, t, 9.1	H11, H13	C10, C11, C13, C14
13	82.7	CH	3.90, dt, 2.6, 11.8	82.8	CH	3.89, dt, 2.5, 11.7	H12, H14	
14	23.0	CH_2	1.65, m 1.99, m	23.0	CH_2	1.68 m 1.98, ddq, 2.7, 7.6, 14.7	H13, H15	C15
15	11.8	CH_3	1.06, t, 7.4	11.8	CH_3	1.06, t, 7.2	H14	C13, C14

^{1}H NMR (400 MHz), ^{13}C NMR (100 MHz), $CDCl_3$

4.2.2.3 Structure Determination of 4.34

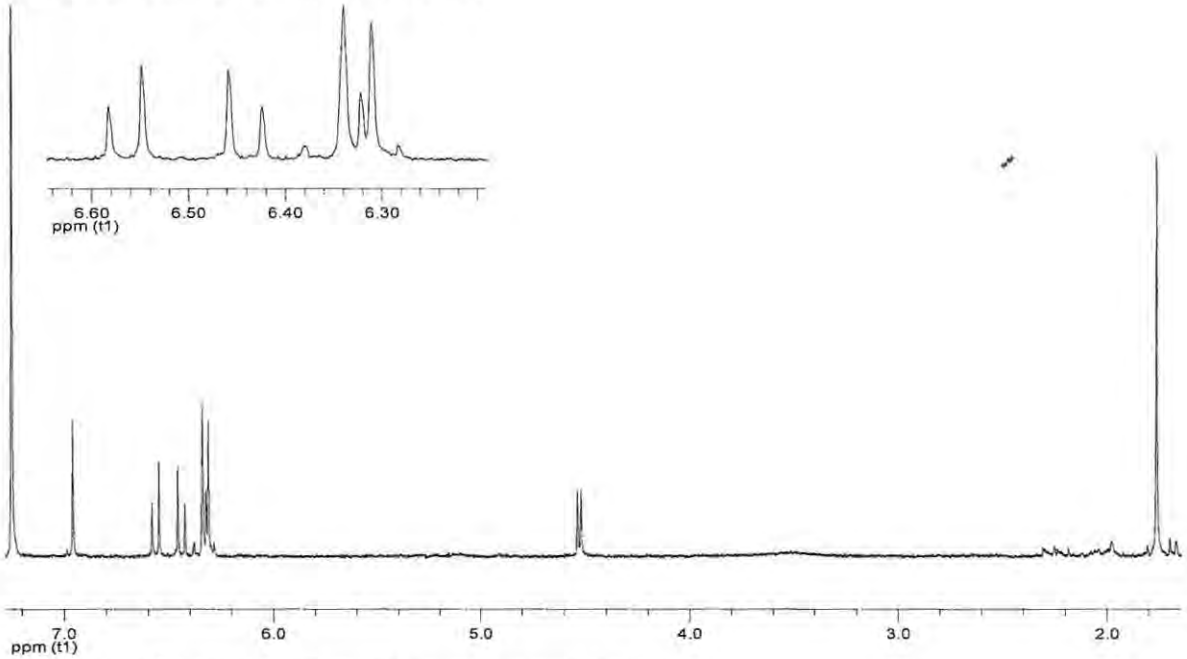

Figure 4.10 ^{1}H NMR spectra ($CDCl_3$, 400 MHz) of **4.34**

Compound **4.34** was isolated as an optically active transparent oil with a λ_{max} of 243.2 nm in the UV spectrum. High resolution FABMS indicated a molecular ion peak at *m/z* 383.8408 consistent with the molecular formula $C_{10}H_{10}BrCl_5$ (calcd for $C_{10}H_{10}{}^{79}Br^{35}Cl_5$ 383.8409). The ^{1}H NMR spectrum (Figure 4.10) showed a deshielded singlet at δ 6.96 consistent with a dichloromethyl substituent (Mynderse and Faulkner, 1975; Crews *et al.*, 1984). A mutually coupled pair of doublets resonating at δ 6.56 (d, *J* = 13.6 Hz) and 6.42 (d, *J* = 13.6 Hz) indicate a disubstituted double bond with trans geometry. What appears to be a multiplet from δ 6.34-6.30 is in fact a number of overlapping resonances including a singlet at δ 6.31 as well as a doublet at δ 6.34 (d, *J* = 15.6 Hz) coupled to a doublet of doublets at δ 6.31 (dd, *J* = 6.9, 15.6 Hz). The latter is also coupled to the resonance at δ 4.53 (d, *J* = 7.0). Also observed in the spectrum is a methyl singlet at δ 1.76.

Table 4.9 ^{1}H (400 MHz) and ^{13}C (100 MHz) NMR, ^{1}H-^{1}H COSY and HMBC data for **4.34** ($CDCl_3$)

Carbon No.	δ_C		δ_H, multi, *J* (Hz)	^{1}H-^{1}H COSY	HMBC	NOESY
1	110.2	CH	6.56, d, 13.6	H2	C2, C3	H2, H10
2	138.5	CH	6.42, d, 13.6	H1	C1, C3, C4, C10	H1
3	71.5	C				
4	68.2	CH	4.53, d, 7.0	H5	C2, C3, C5, C6, C10	H2, H10
5	129.6	CH	6.31, dd, 6.9, 15.6	H4, H6	C4, C8, C2	
6	127.4	CH	6.34, d, 15.6	H5	C4, C8, C9	
7	137.6	C				
8	119.6	CH	6.308, s			
9	65.5	CH	6.96, s		C8, C6, C7	
10	25.3	CH_3	1.76, s		C1, C2, C3, C4,	H1, H4

Ten resonances in the ^{13}C NMR spectrum confirmed the monoterpene hydrocarbon scaffold. Six sp^2 hybridized carbons resonated at δ 138.5 (C-2), 137.6 (C-7), 129.6 (C-5), 127.4 (C-6), 119.6 (C-8) and 110.2 (C-1) indicating three degrees of unsaturation. An aliphatic quaternary carbon was observed at δ 71.5. An absorbance at δ 68.2 (C-4) is consistent with a chloromethine, however a carbon with a ^{13}C NMR chemical shift of δ 65.5 coupled to a single proton at δ 6.96 may indicate a dichloromethyl functionality (Mynderse and Faulkner, 1975; Naylor *et al.*, 1983). The methyl carbon resonating at δ 25.3 is coupled to the protons resonating at δ 1.76, this data indicates that the relative (*) configuration around C-3 and C-4 is 3S* 4R* (Naylor *et al.*, 1983). The one-dimensional NMR data in association with data from HMBC and ^1H-^1H COSY experiments pointed towards the structure of **4.34** as illustrated below.

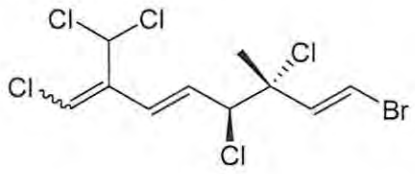

4.34

NOESY experimental data was ambiguous for the assignment of the geometry of the Δ^{7-8} double bond due to the overlap of ^1H NMR resonances for H-5, H-6 and H-8. The ^1H and ^{13}C NMR data was compared to that of known compounds reported to have the same or similar structures (Table 4.10). None of the reported NMR data was congruent with the experimental data obtained for **4.34**, although the ^1H NMR data published for 3*S**,4*R**-1-bromo-7-dichloromethyl-3-methyl-3,4,8-trichloro-1-*E*,5-*E*,7-*Z*-octatriene **4.36** (Mynderse and Faulkner, 1975) is the most compatible. The overlap of resonances attributed to H-5, H-6 and H-8 complicated the interpretation of the ^1H NMR spectrum, as a result Mynderse and Faulkner (1975) calculated the exact ^1H NMR shifts using an iterative NMR calculation program (Nicolet ITRCAL); the ^1H NMR shifts are not reported as relative to TMS or $CDCl_3$ as an internal standard. This could account for small differences in the ^1H NMR chemical shifts obtained for **4.34** and **4.36** (Table 4.10). No published ^{13}C NMR data for **4.36** was available for comparison. The possibility of **4.34** being the 7*E*- isomer was excluded by comparison of both ^1H and ^{13}C NMR data reported by Mynderse and Faulkner (1975) and Wessels *et al.* (2000) respectively (Table 4.10). Support for the structure was found in low resolution EIMS spectra of **4.34** which exhibited base peaks at 167/169/171. These peaks are attributed to the fragment [$C_4H_5BrCl^+$] and are characteristic of this group of compounds (Mynderse and Faulkner, 1975). It is likely, based on the evidence presented, that **4.34** is the known compound 3*S**,4*R**-1-bromo-7-dichloromethyl-3-methyl-3,4,8-trichloro-1*E*,5*E*,7*Z*-octatriene (**4.36**).

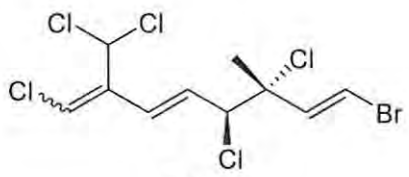

4.34

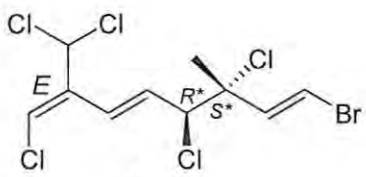

4.35

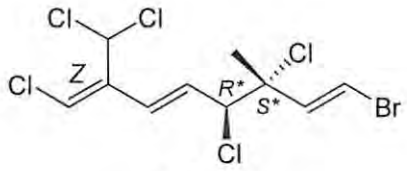

4.36

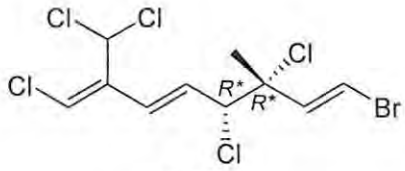

4.37

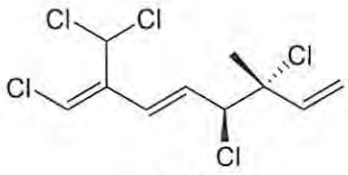

4.38

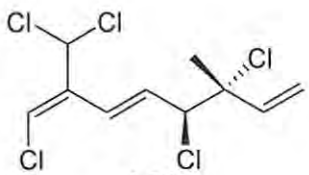

4.39

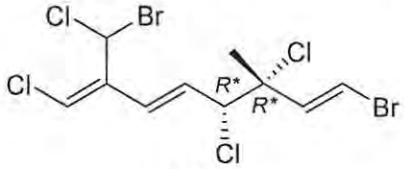

4.40

Table 4.10 A comparison of the ^{1}H and ^{13}C NMR chemical shifts of halogenated monoterpenes possessing similar structural characteristics to those of **4.34**

Carbon No.	**4.34**		**4.35**		**4.36**	**4.37**	**4.38**	**4.39**	**4.40**	
	δ_C	δ_H, multi, *J* (Hz)	δ_C	δ_H, multi, *J* (Hz)	δ_H, multi, *J* (Hz)	δ_H, multi, *J* (Hz)	δ_H, multi, *J* (Hz)	δ_H, multi, *J* (Hz)	δ_C	δ_H, multi, *J* (Hz)
1	110.2	6.56, d, 13.6	110.2	6.52, d, 13.5	6.52, d, 14.0	6.54, d, 13.5	5.37, d 17.0, 5.25, d, 10.5	5.38, d 17.0 5.24, d, 10.0	110.9	6.58, d, 13.5
2	138.5	6.42, d, 13.6	138.5	6.40, d, 13.5	6.38, d, 14.0	6.39, d, 13.5	6.04, dd, 10.5, 17.0	6.04, dd, 10.0, 17.0	131.5	6.45, d, 13.3
3	71.5		71.4						71.9	
4	68.2	4.53, d, 7.0	68.7	4.52, d, 8.0	4.49, d, 7.4	4.49, d, 7.5	4.51, d, 7.5	4.48, d, 7.5	69.2	4.55, dd, 0.7, 8.6
5	129.6	6.31, dd, 6.9, 15.6	131.3	6.43, dd, 8.0, 16.5	6.29, dd, 7.4, 15.6	6.22, dd, 7.5, 15.5	6.41, dd, 7.5, 16.0	6.32, dd, 7.5, 16.6	137.0	6.42, ddd, 0.7, 8.6, 16.2
6	127.4	6.34, d, 15.6	124.5	6.58, d, 16.5	6.32, d, 15.6	6.31, d, 15.5	6.56, d, 16.0	6.30, d, 16.6	124.4	6.60, d, 16.1
7	137.6		135.9						136.0	
8	119.6	6.308, s	124.4	6.38, s	6.28, s	6.27, s	6.33, s	6.27, s	124.6	6.75, d, 0.6
9	65.5	6.96, s	69.5	6.74, s	6.90, s	6.89, s	6.73, s	6.90, s	69.6	6.37, s
10	25.3	1.76, s	25.3	1.74, s	1.74, s	1.81, s	1.74, s	1.73, s	28.1	1.8, s

Mynderse and Faulkner (1975) ^{1}H NMR (CCl_4, 220 MHz) H-4, H-5, H-6 and H-8 were calculated using the Nicolet ITRCAL (iterative NMR calculation) program. The author does not specify to which standard the ^{1}H NMR chemical shifts are relative. Wessels *et al.* (2000) ^{13}C NMR ($CDCl_3$ 77.0, 100 MHz). Jongkolnee and Blackman (2000) ^{1}H NMR ($CDCl_3$, 400 MHz, TMS 0.0); ^{13}C NMR ($CDCl_3$, 100 MHz).

4.2.2.4 Summary and Conclusion

The objective of this part of the project was to isolate secondary metabolites that may have been responsible for the antimicrobial activity observed during screening (chapter 2). In total, four compounds were successfully isolated and their structures determined, they included two vinyl acetylene isomers, a halogenated monoterpene and a halogenated cuparene. The cuparene and its cyclized product were characterized. The uncyclized molecule was re-isolated and stabilized by acetylation of the hydroxyl groups which prevented dehydration and cyclization.

It was postulated that these compounds may have been responsible for the inhibition of microbial growth and were later employed in preliminary biofilm inhibition studies.

4.3 Experimental

4.3.1 General experimental

The following general procedures were followed unless otherwise stated. The ^{1}H (400 MHz), ^{13}C (100 MHz), DEPT-135, COSY, HSQC, HMBC and NOESY NMR spectra were recorded on a Bruker Avance 400 spectrometer using standard pulse sequences. Chemical shifts are reported in ppm and referenced to residual undeuterated solvent resonances ($CHCl_3$ δ_H 7.25, δ_C 77.0) and coupling constants are reported in Hz. Optical rotations were measured on a Perkin-Elmer 141 polarimeter. IR spectra were obtained as films on KBr disks using a Perkin-Elmer Spectrum 2000 FT-IR spectrometer. Low resolution electron impact mass spectra were recorded on a Finnigan MAT spectrometer at 70 eV. High performance liquid chromatographic separations were performed on a Spectra-Physics IsoChrom LC HPLC system which was equipped with a Rheodyne injector, a Waters R401 differential refractometer, or a Spectra SERIES UV100 detector and a Rikadenki chart recorder. In all cases, normal phase HPLC was performed using a Whatman Magnum 10 Partisil 9 column. All solvents were distilled before use or of HPLC grade (HiPerSolv^{TM}, Merck and Saarchem). High resolution FABMS data were acquired by Louis Fourie of the University of Potchefstroom on a Micromass VG70-70E Spectrometer.

4.3.2 Plant material

The alga was collected in April of 2006 from Kenton-On-Sea and Noordhoek, near Port Elizabeth on the Eastern Cape coast of South Africa. Voucher specimens of were identified by Prof. J Bolton at the Botany Department, University of Cape Town.

4.3.3 Biological material (extraction and isolation)

NDK06-6&11 (Noordhoek)

The frozen algae (24.7 g dry weight after extraction) was submerged in MeOH (400 ml) at 4 °C for 1 hour, the solvent decanted and the alga re-extracted with CH_2Cl_2-MeOH (2:1, 3 x 400 ml) at 30 °C for 30 minutes. The MeOH extract was separately extracted with CH_2Cl_2 with the addition of sufficient water for phase separation. The CH_2Cl_2-MeOH extract was combined with the CH_2Cl_2 extract, dried over anhydrous magnesium sulphate and concentrated *in vacuo* at 35 °C to give extract A (1.644 g). The remaining aqueous methanol extract was concentrated to an aqueous suspension and passed through an HP-20 column (2 x 10 cm) and eluted successively with methanol, CH_2Cl_2 and *n*-hexane to give an additional crude organic fraction (B, 0.312 g). A portion (500 mg) of the CH_2Cl_2-MeOH extract (A) was applied to a silica gel column (Kieselgel 0.04-0.063 nm, 10 g, 2.5 x 6 cm) and successively eluted with 50 ml portions of an *n*-hexane-EtOAc mixture in a ratio 1:0 (fr A1), 9:1 (fr A2), 8:2 (fr A3), 7:3 (fr A4), 6:4 (fr A5), 4:6 (fr A6), 2:8 (fr A7) 0:1 (fr A8) followed by a 1:1 EtOAc-MeOH mixture (fr A9). Normal phase HPLC (*n*-hexane-EtOAc 19:1) of

fraction A3 (*n*-hexane-EtOAc, 8:2) yielded **4.34**, **4.32** and **4.33**. The organic residue collected from the HP-20 column (B) was fractionated in an identical manner to that of the CH_2Cl_2-MeOH extract. Normal phase HPLC of the *n*-hexane-EtOAc (7:3) silica gel column fraction yielded **4.29**.

KOS06-6 (Kenton-On-Sea)

The frozen algae (15.0 g dry weight after extraction) was extracted in an identical manner to NDK06-6&11. The MeOH and CH_2Cl_2-MeOH extracts were separately extracted with CH_2Cl_2 (with the addition of sufficient water for phase separation) and the two organic extracts combined and concentrated. The CH_2Cl_2 extract was prefractionated by successive solvent partitioning between *n*-hexane-MeOH-H_2O (4:5:1), CH_2Cl_2-MeOH-H_2O (5:3:2) and EtOAc-H_2O (1:1) to give *n*-hexane (fr A, 0.242 g), CH_2Cl_2 (fr B, 0.229 g), EtOAc (fr C, 0.028 g) and an aqueous fraction. The aqueous fraction was passed through an HP-20 column (2 x 10 cm) and eluted successively with MeOH (20 ml) and CH_2Cl_2 (20 ml) to give an additional crude organic fraction (fr D, 0.123 g).

NDK06-6 (Noordhoek)

For antimicrobial screening, the frozen alga (33.3 g dry weight after extraction) was extracted as per the protocol outlined for KOS06-6.

4.3.4 Compounds

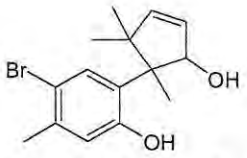

4.29 4-bromo-2-(5-hydroxy-1,2,2-trimethylcyclopent-3-enyl)-5-methylphenol: Clear oil; ^{1}H NMR ($CDCl_3$, 400 MHz) ^{13}C NMR ($CDCl_3$, 100 MHz) See **Table 4.5** HR-FABMS *m/z* 310.0567 (calcd for formula $C_{15}H_{19}{}^{79}BrO_2$ 310.0568).

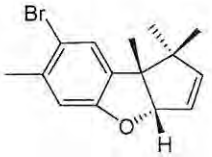

4.30 White crystals; $[\alpha]^{16}{}_{D}$ -25 °; UV λ_{max} (CH_2Cl_2) 232.0, 291.2 nm (c 4.1 x 10^{-8} M, $CHCl_3$); IR (dry film KBr)) v_{max} 3460, 2961, 1730, 1613, 1576, 1467, 1384, 1236 and 1017 cm^{-1}; ^{1}H NMR ($CDCl_3$, 400 MHz); ^{13}C NMR ($CDCl_3$, 100 MHz) see **Table 4.6**.

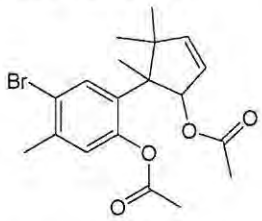

4.31 Acetylation of 4.29: (1 mg, 0.0032 mmol) was placed in a 20 ml round bottom flask with 10 drops pyridine and 2 drops acetic anhydride. The reaction mixture was allowed to stand overnight after which the solvents were removed *in vacuo* affording as a clear oil $[\alpha]^{16}{}_{D}$ -38.3 °; ^{1}H NMR ($CDCl_3$, 400 MHz); ^{13}C NMR ($CDCl_3$, 100 MHz) see **Table 4.7**.

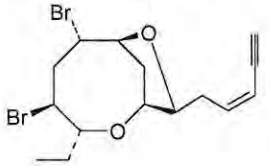

4.32 (3*Z*)-Bromofucin: Orange oil; ^{1}H NMR ($CDCl_3$, 400 MHz); ^{13}C NMR ($CDCl_3$, 100 MHz) see **Table 4.8**; HR-FABMS *m/z* 389.9830 (calcd for formula $C_{15}H_{20}{}^{79}Br_2O_2$ 389.9830).

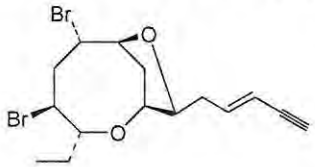

4.33 (3*E*)-Bromofucin: Yellow-orange oil; ^{1}H NMR ($CDCl_3$, 400 MHz); ^{13}C NMR ($CDCl_3$, 100 MHz) see **Table 4.8**; HR-FABMS *m/z* 389.9836 (calcd for formula $C_{15}H_{20}{}^{79}Br_2O_2$ 389.9830).

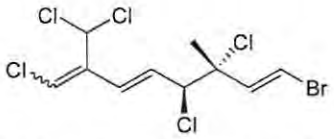

4.34 3,4-erythro-1-Bromo-3,4,8-trichloro-9-dichloromethyl-1-E,5-E,7-Z-octatriene: Colourless oil; $[\alpha]^{28}_{D}$ -0.45° (c 2.6 x 10^{-8} M, $CHCl_3$) UV (CH_2Cl_2) λ_{max} 243.2 nm; IR (dry film, KBr) ν_{max} 3439, 2924,1730, 1620 and 1460 cm^{-1}; ^1H NMR ($CDCl_3$, 400 MHz); ^{13}C NMR ($CDCl_3$, 100 MHz) see **Table 4.9**; HR-FABMS *m/z* 383.8408 (calcd for formula $C_{10}H_{10}{}^{79}Br^{35}Cl_5$ 383.8409).

4.4 References

Asakawa, Y.; Matsuda, R.; Schofield, W. B.; Gradstein, S. R. Cuparane and isocuparane-type sesquiterpenoids in liverworts of the genus *Herbertus*. *Phytochemistry* **1982**, *21*, (10), 2471-2473.

Blunt, J. W.; Copp, B. R.; Hu, W. P.; Munro, M. H. G.; Northcote, P. T.; Prinsep, M. R. Marine natural products. *Natural Product Reports* **2007**, *24*, 31-86.

Branch, G. M.; Griffiths C. L.; Branch, M. L.; Beckley, L. E. *Two oceans: A guide to the marine life of Southern Africa* Second Edition **2005**. ISBN 0-86486-672-0, **1994,** David Phillip Publishers, New Africa Books (Pty) Ltd. 99 Garfield Road, Claremont, Cape Town, South Africa.

Coll, J. C.; Wright, A. D. Tropical marine algae. IV. Novel metabolites from the red alga *Laurencia implicata* (Rhodophyta, Rhodophyceae, Ceramiales, Rhodomelaceae). *Australian Journal of Chemistry* **1989**, *42*, 1685-1693.

Crews, P.; Naylor, S.; Hanke, F. J.; Hogue, E. R.; Kho, E.; Braslau, R. Halogen Regiochemistry and Substituent Stereochemistry Determination in Marine Monoterpenes by ^{13}C NMR *Journal of Organic Chemistry* **1984**, *49*, 1371-1377.

Elsworth, J. F.; Thomson, R. H. A new chamigrane from *Laurencia glomerata*. *Journal of Natural Products* **1989**, *52*, (4), 893-895.

Fenical, W. Halogenation in the Rhodophyta A review. *Journal of Phycology* **1975**, *11*, 245-259.

Fusetani, N. Biofouling and antifouling. *Natural Product Reports* **2004**, *21*, 94-104.

Goldsmith, D. J.; Thottathill, J. K.; Kwong, C. D.; Painter, G. R. Preparation and rearrangement of trichothecane-like compounds. Synthesis of Aplysin and Filiformin. *Journal of Organic Chemistry* **1980**, *45*, 3989-3993.

Hay, M. E.; Fenical, W. Marine plant-herbivore interactions: The ecology of chemical defense. *Annual Review of Ecology and Systematics* **1988**, *19*, 111-145.

Ichiba, T.; Higa, T. New cuparene-derived sesquiterpenes with unprecedented oxygenation patterns from the sea hare *Aplysia dactylomela*. *Journal of Organic Chemistry* **1986**, *51*, 3364-3366.

Irie, T.; Suzuki, M.; Kurosawa, E.; Masamune, T. Laurinterol and Debromolaurinterol, constituents from *Laurencia intermedia*. *Tetrahedron Letters* **1966**, *17*, 1837-1840.

Jongkolnee, J.; Blackman, A. J. Polyhalogenated monoterpenes from a Tasmanian collection of the red seaweed *Plocamium cartilagineum*. *Journal of Natural Products* **2000**, *63*, 272-275.

König, G. M.; Wright, A. D. *Laurencia rigida*: Chemical investigation of its antifouling dichloromethane extract. *Journal of Natural Products* **1997**, *60*, 967-970.

Kladi, M.; Xenaki, H.; Vagias, C.; Papazafiri, P.; Roussis, V. New cytotoxic sesquiterpenes from the red algae *Laurencia obtusa* and *Laurencia microcladia*. *Tetrahedron* **2006**, *62*, 182-189.

Laronze, J. Y.; Boukili, R. E.; Patigny, D.; Dridi, S.; Cartier, D.; Lévy, J. The rearrangement of some cyclopentanone-aryloximes: Synthesis of (±)-Aplysin, (±)-Filiformin and of their debromo analogues. *Tetrahedron* **1991**, *47*, (48), 10003-10014.

M^{c}Phail, K. L.; Davies-Coleman, M. T. (3Z)-Bromofucin from a South African sea hare. *Natural Product Research* **2005**, *19*, (5), 449-452.

Mynderse, J. S.; Faulkner, D. J. Polyhalogenated monoterpenes from the red alga *Plocamium cartilagineum*. *Tetrahedron* **1975**, *31*, 1963-1967.

Naylor, S.; Hanke, F. J.; Manes, L. V.; Crews, P. Chemical and Biological Aspects of Marine Monoterpenes. *Progress in the Chemistry of Organic Natural Products* **1983**, *44*, 189-241 ISBN 3-211-81754-9 Springer-Verlag/Wien.

Rogers, C. N.; de Nys, R.; Steinberg, P. D. Ecology of the sea hare *Aplysia parvula* (Opisthobranchia) in New South Wales, Australia. *Molluscan Research* **2003**, *23*, 185-198.

Sims, J. J.; Donnell, M. S.; Leary, J. V.; Lacy, G. H. Antimicrobial agents from marine algae. *Antimicrobial Agents and Chemotherapy* **1975**, *7*, (3), 320-321.

Toyota, M.; Koyama, H.; Asakawa, Y. Sesquiterpenoids from the three Japanese Liverworts *Lejeunea aquatica, L. Flava* and *L. Japonica*. *Phytochemistry* **1997**, *46*, (1), 145-150.

Tholl, D.; Chen, F.; Petri, J.; Gershenzon, J.; Pichersky, E. Two sesquiterpene synthases are responsible for the complex mixture of sesquiterpenes emitted from *Arabidopsis* flowers. *The Plant Journal* **2005**, *42*, 757-771.

Vairappan, C. S.; Kawamoto, T.; Miwa, H.; Suzuki, M. Potent antibacterial activity of halogenated compounds against antibiotic resistant bacteria. *Planta Medica* **2004**, *70*, 1087-1090.

Wessels, M.; König, G. M.; Wright, A. D. New natural product isolation and comparison of the secondary metabolite content of three distinct samples of the sea hare *Aplysia dactylomela*. *Journal of Natural Products* **2000**, *63*, 920-928.

Yamada, K.; Yazawa, H.; Toda, M., Hirata, Y. The synthesis of (±)-Aplysin and (±)-Debromoaplysin. *Tetrahedron* **1969**, *25*, 3509-3520.

Yamamura, S.; Hirata, Y. Structures of Aplysin and Aplysinol, naturally occurring bromo-compounds. *Tetrahedron* **1963**, *19*, 1485-1496.

Chapter Five
The Origins of an Halogenated Monoterpene

5.1 Introduction

Halogenated monoterpenes are known to be produced mainly by red algae of the families Plocamiaceae and Rhizophyllidacae (Table 5.1, Naylor *et al.*, 1983); in addition they have been isolated from *Pantoneura plocamioides* (order Ceramiales, family Delesseriaceae) (Argandona *et al.*, 2002; Cueto *et al.*, 1998).

Table 5.1 Halogenated monoterpenes from marine algae

Order, Family	Genus and Species	Monoterpene type
Gigartinales, Rhizophyllidaceae	*Chondrococcus hornemanni*	Linear
	Chondrococcus japonicus	Cyclic
	Ochtodes crockery	Cyclic
	Ochtodes secundiramea	Cyclic
Gigartinales, Plocamiaceae	*Plocamium angustum*	Linear
	Plocamium cartilagineum	Linear, cyclic
	Plocamium coccineum	Linear [‡]
	Plocamium corallorhiza	Linear, cyclic [+]
	Plocamium cornutum	Linear [-]
	Plocamium costatum	Linear, cyclic
	Plocamium cruciferum	Linear
	Plocamium mertensii	Cyclic
	Plocamium oregonum	Linear
	Plocamium sandvicense	Linear
	Plocamium violaceum	Linear, cyclic
Ceramiales, Ceramiaceae	*Microcladia borealis*	Cyclic, cyclic
	Microcladia californica	Cyclic
	Microcladia coulteri	Linear

Adapted from Naylor *et al.*, 1983; Wessels *et al.*, 2000[1]; Imperato *et al.*, 1977[‡]; Afolayan, 2006[-] ; Knott, 2005, Mann *et al.*, 2007[+].

With more than 60 species of *Laurencia* having been studied, (Blunt *et al.*, 2007) the biosynthesis of halogenated monoterpenes in algae of this genus is unprecedented. Accordingly, the isolation of **4.34** from the non-polar extracts of *L. flexuosa*, raised questions as to its origins.

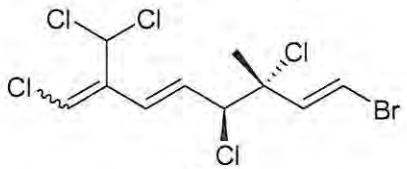

4.34

L. flexuosa is a small plant that grows on hard rocky surfaces as tufts in close association with other red algae including *Plocamium corallorhiza* and *P. suhrii*. *L. flexuosa* is therefore very difficult to collect.

Four scenarios could explain the presence of **4.34** in extracts of *L. flexuosa*.

a) The compound is produced by *L. flexuosa*.
b) The compound originated from a contaminating alga.
c) Surface transfer of the compound from one alga to another.
d) Transfer of the compound via root systems.

a) The compound is produced by *L. flexuosa*

Although this explanation cannot be ruled out at this stage, it is unlikely based on current knowledge of the chemistry of *Laurencia* species

b) The compound originated from a contaminating alga

The simplest explanation for this anomaly was the presence of a second genus in the sample extracted; it is not impossible that two morphologically similar algae could be confused (Fenical, 1975; Fenical and Norris, 1975; Yano *et al.*, 2005).

c) Surface transfer of the compound from one alga to another

An alternative theory is one of surface transfer. It has been established that certain algae such as *Delisea pulchra,* deposit secondary metabolites at their surface (de Nys *et al.*, 1998) as part of what is believed to be some form of chemical defense (Fenical, 1975; Wahl, 1989; de Nys and Steinberg, 2002). In theory, if sufficient compound was present in a lipophilic layer coating the thallus of one alga, and that surface came into contact with a second lipophilic layer, it is plausible that a suitably lipophilic metabolite could partition from an area of high concentration to an area of low concentration (Wollenweber *et al.*, 1999; Dearden, 1985), thus transferring the metabolite from one alga to another.

d) Transfer of the compound via root systems

On the other hand, it is not uncommon in terrestrial plants and marine algae for smaller, more delicate plants to grow epiphytically upon another more robust species (Branch *et al.*, 2005, Raven *et al.* 1999). The close association of the root and stem systems may offer a route for the transfer of the metabolite.

5.1.1 Chapter aims

The aim of this part of the project was to identify the source of the halogenated monoterpene **4.34** isolated from extracts of *L. flexuosa*. The following discussion will elaborate upon the investigation of the biological source of **4.34**, as well as the various hypotheses generated as to how the metabolite was transferred from one alga to another.

5.2 Results and Discussion

Prior to each study, gas chromatograms were obtained for the solvents used in the extraction and isolation process to exclude the possibility that the compound was being introduced by contaminating solvents. All solvents were found to be free of **4.34**.

5.2.1 Confirming the presence of 4.34 in *L. flexuosa*

Freshly collected *L. flexuosa* was sorted by hand, taking care to exclude all 'foreign' algal material. The species of algae present were noted (*P. corallorhiza*, *P. suhrii* and an unidentified alga) and these seaweeds were in turn sorted into separate portions making four in total. The four separate portions of algae were extracted with CH_2Cl_2-MeOH (2:1) overnight at ambient temperature. The solvent extract of each alga was decanted into an individual flask and concentrated *in vacuo*. The dried extracts were then dissolved in CH_2Cl_2 (2 ml). Gas chromatograms were obtained for the pure metabolite **4.34**, as well as the crude CH_2Cl_2-MeOH extracts of *L. flexuosa*, *P. corallorhiza*, *P. suhrii* and the unidentified alga (Figure 5.1). The GC method and conditions used for each sample were identical to allow comparison of metabolite retention times.

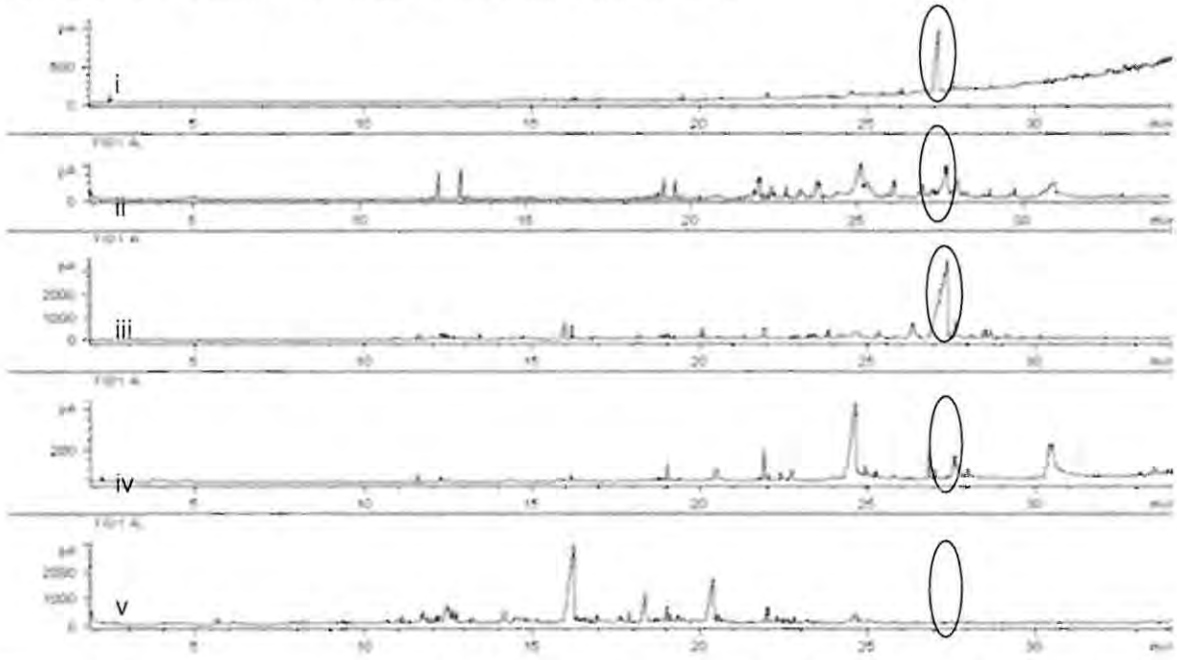

Figure 5.1 Gas chromatograms of i) **4.34**, ii) *L. flexuosa*, iii) *P. suhrii*, iv) *P. corallorhiza*, v) unidentified alga

The gas chromatograms of both *L. flexuosa* and *P. suhrii* exhibited prominent peaks at the same retention time as **4.34**. Tandem GC-EIMS was employed to investigate whether the peaks observed in the gas chromatograms obtained for *L. flexuosa* and *P. suhrii* were attributed to the monoterpene **4.34**. In each instance, the mass spectra for those peaks exhibited the base peaks of *m/z* 167/169/171 characteristic of the fragment $[C_4H_5BrCl^+]$ (Figure 5.2 and 5.3) and indicative of the monoterpene.

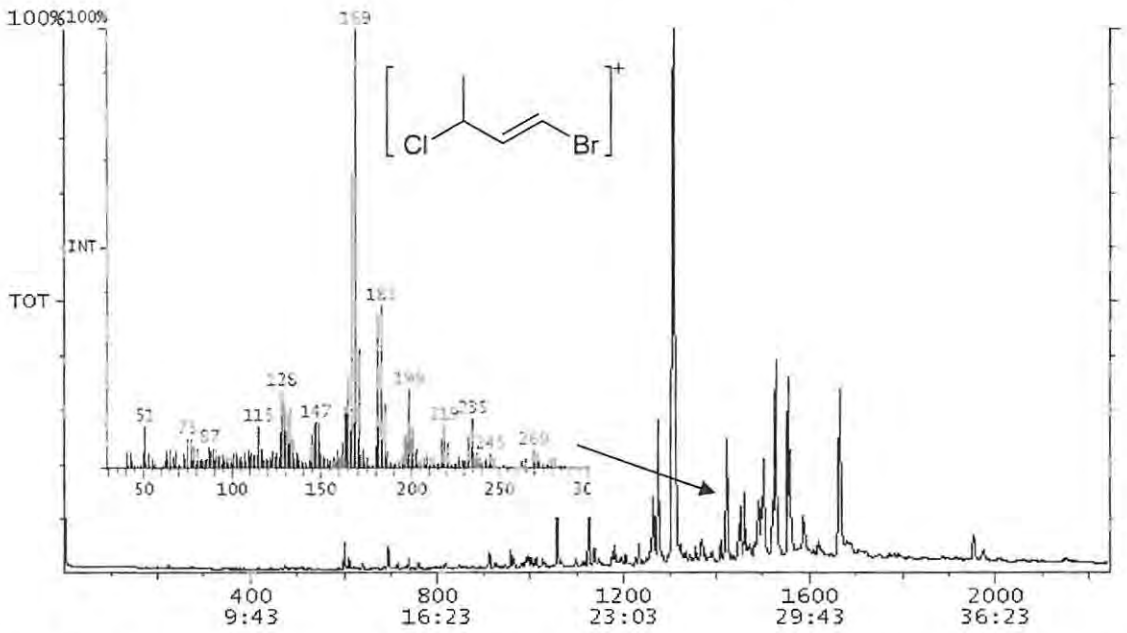

Figure 5.2 Gas chromatogram of CH_2Cl_2-MeOH extract of *L. flexuosa*; inset EIMS spectrum of the peak indicated

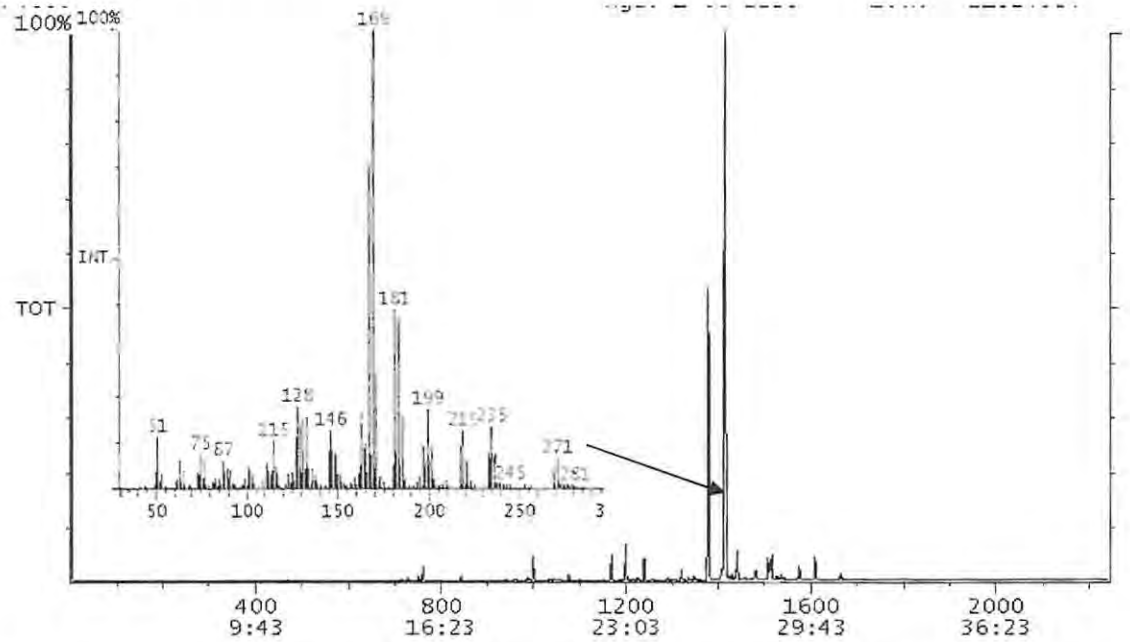

Figure 5.3 Gas chromatogram of CH_2Cl_2-MeOH extract of *P. suhrii*; inset EIMS spectrum of the peak indicated

The final piece of evidence in support of the presence of **4.34** in the two algae came from ^{1}H NMR spectroscopy of the crude CH_2Cl_2-MeOH extracts of *P. suhrii* and *L. flexuosa* which revealed that **4.34** was present in both algae (Figure 5.4). These results confirm the origins of **4.34**; nevertheless, the persistence of the monoterpene in extracts of *L. flexuosa* after re-extraction of meticulously sorted fronds, leaves the question of how **4.34** came to be in the extracts, unanswered.

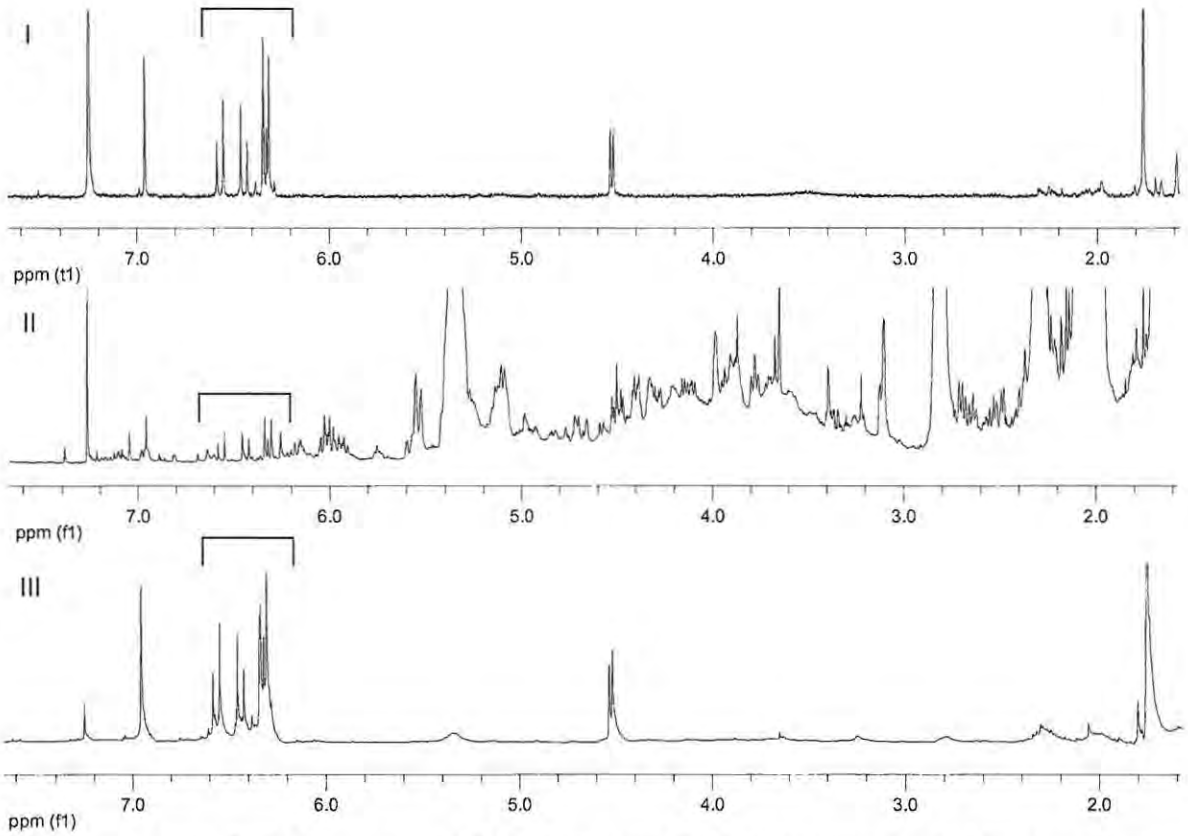

Figure 5.4 The ^{1}H NMR spectra of **4.34** (I), the CH_2Cl_2-MeOH (2:1) extract of *L. flexuosa* (II) and the crude CH_2Cl_2-MeOH (2:1) extract of *P. suhrii* (III) all exhibiting absorbances attributed to **4.34** ($CDCl_3$, 400 MHz).

5.2.2 Investigation into surface transfer

Little is known about the ecological role of toxic halogenated secondary metabolites produced by marine algae. It is suggested however, that surface mediated interactions require the compounds to be deposited to some extent on the exterior of the thallus (de Nys *et al.*, 1998; Fenical, 1975; Potin *et al.*, 2002). Results of experiments developed to quantify algal metabolites reveal that the ratio of mean surface concentration to whole plant levels differ significantly between algae and their metabolites (de Nys *et al.*, 1998, Sudatti *et al.*, 2006). The question raised concerning the mechanism of transfer of **4.34** from *P. suhrii* to *L. flexuosa* led to the following hypotheses:

H_0: that **4.34** is present on the surface of *P. suhrii* in such quantities* that on physical contact with *L. flexuosa*, (be it in the natural environment, or during transportation to the laboratory) a surface transfer could occur from one alga to the next.

H_1: that **4.34** is not present on the surface of *P. suhrii* in such quantities* that on physical contact with *L. flexuosa,* a surface transfer could occur from one alga to the next.

* Where "such quantities" is determined to be sufficient amounts of **4.34** that would reasonably justify the quantity of the metabolite isolated from *L. flexuosa*. Determinations were qualitative in nature and do not take into account long term exposure.

In order to determine whether or not H_o was valid, the following objectives were identified:

- Determine by GC-EIMS whether **4.34** could be detected at the surface of *P. suhrii*
- Determine whether a whole plant extraction with CH_2Cl_2 afforded a significantly greater amount of **4.34**
- Analyse the results and determine whether sufficient quantities are present on the surface of *P. suhrii* to reasonably justify the surface transfer hypothesis.

de Nys *et al.*, (1998) developed methodology that enabled the determination of surface concentrations of secondary metabolites in marine algae. It was reported that after extraction of algae with *n*-hexane for a period of not longer than 40 seconds no significant cell lysis occurred. In addition, the authors discovered no significant variations in concentrations of individual metabolites on the surface of cut plants and whole plants. Based upon the evidence published by de Nys *et al.*, (1998), surface extractions of *P. suhrii* using *n*-hexane were performed.

5.2.2.1 Collection and extraction

P. suhrii was collected from Noordhoek near Port Elizabeth. The alga was sorted on site and transported to the laboratory on ice. Fresh, whole plants as well as individual fronds of *P. suhrii* were blotted dry on adsorbent paper and extracted by immersion in *n*-hexane for 40 seconds. The alga was then extracted with CH_2Cl_2 (30 minute, 30 °C) and CH_2Cl_2-MeOH (2:1, 30 minute, 30 °C). The extractions were done in duplicate.

5.2.2.2 ^{1}H NMR Spectroscopy (Determination of optimum extraction solvent for total halogenated monoterpene extraction)

^{1}H NMR data for the CH_2Cl_2 extracts of *P. suhrii* revealed that after exposure to the solvent for thirty minutes at 30 °C, relatively small amounts of **4.34** had been extracted. In contrast to this, ^{1}H NMR data obtained for the CH_2Cl_2-MeOH extract (30 minutes 30 °C) showed that a significantly greater amount of the metabolite had been extracted (Figure 5.5). MeOH is known to cause substantial cell lysis, allowing access to whole plant metabolites (de Nys *et al.*, 1998). Although this data is not conclusive, it does appear to suggest that substantially greater quantities of the metabolite are present within the thalli, as opposed to on the surface. In light of this data, CH_2Cl_2-MeOH (2:1) was considered to be a better extraction solvent for total halogenated monoterpene content and was thus used in the GC-EIMS investigation.

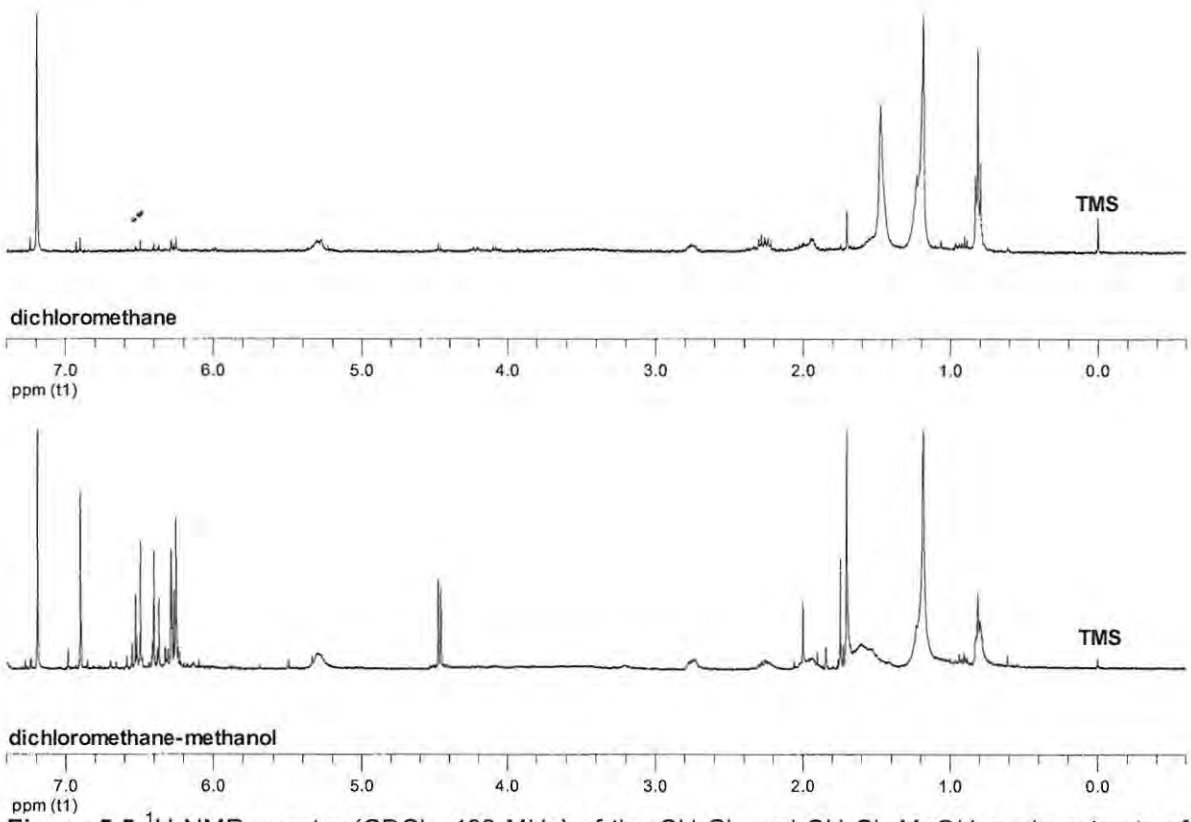

Figure 5.5 ^{1}H NMR spectra ($CDCl_3$, 400 MHz) of the CH_2Cl_2 and CH_2Cl_2-MeOH crude extracts of the same sample of *P. suhrii*

5.2.2.3 Tandem Gas Chromatography EIMS

The *n*-hexane and CH_2Cl_2-MeOH extracts of *P. suhrii* were dried and reconstituted in *n*-hexane for GC-MS analysis (Figures 5.6 through 5.9). The scale of the Y-axis used in each spectrum is unique and 100% is relative to the peak with the greatest count (in pico Amps), for example 100% = 20 000 pA or 100% = 1000000 pA.

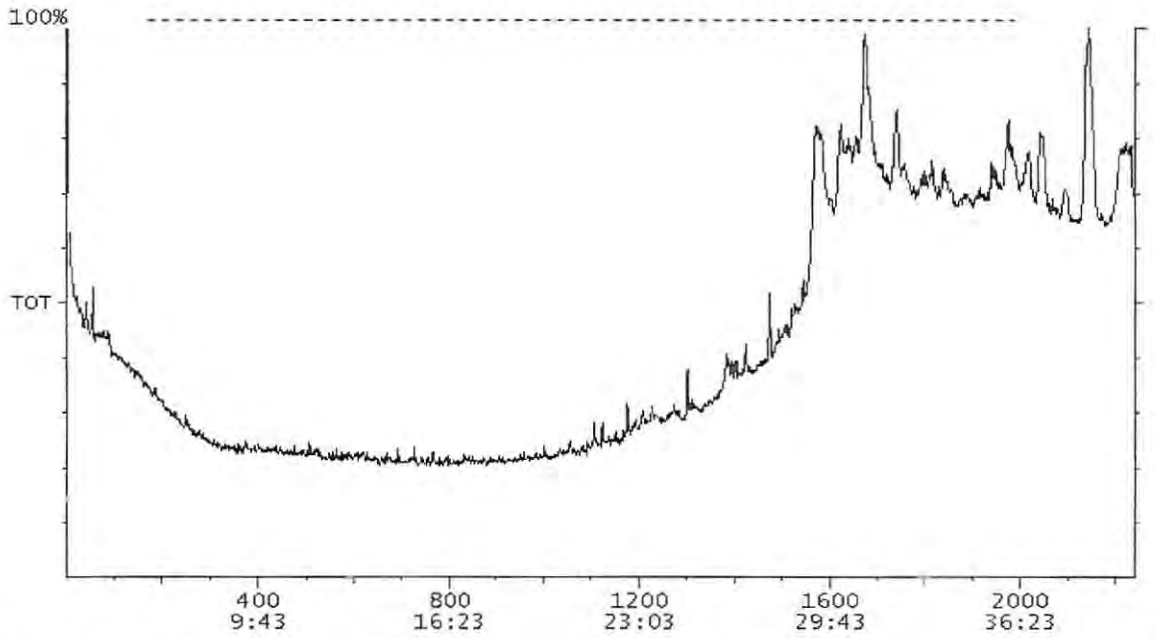

Figure 5.6 Gas chromatogram of *n*-hexane used to dissolve the extracts of *P. suhrii* for GCEIMS where 100% = **144142**

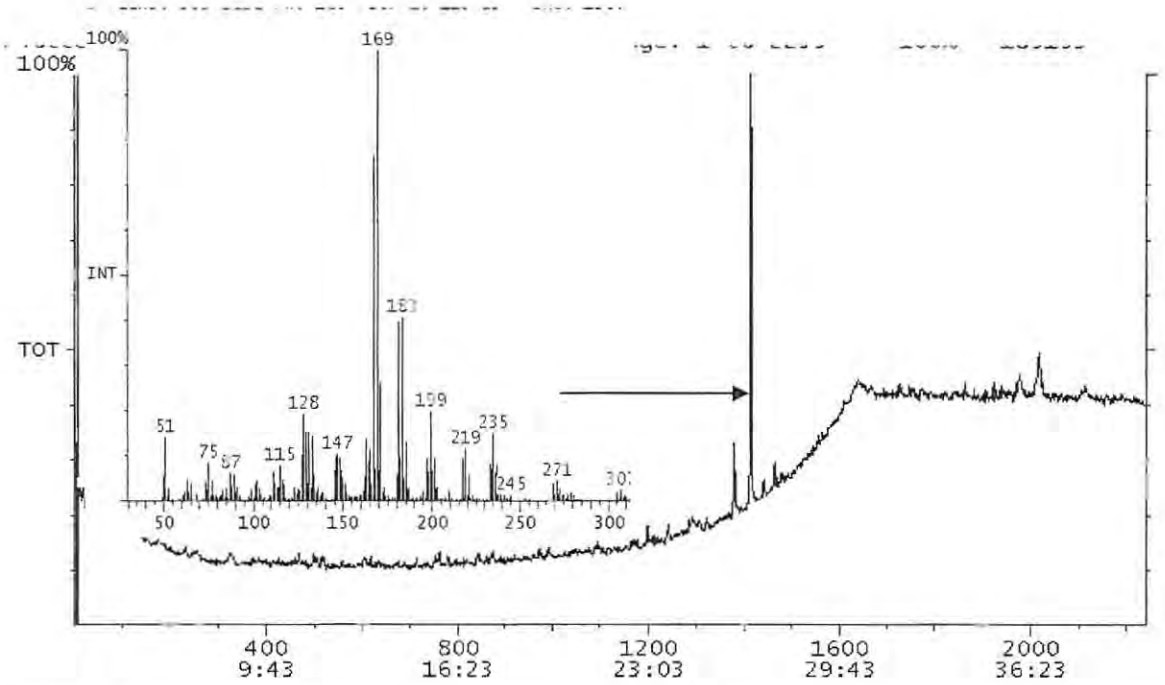

Figure 5.7 Gas chromatogram of the *n*-hexane extract of *P. suhrii* where 100% = **185153**; inset EIMS spectrum for the peak indicated

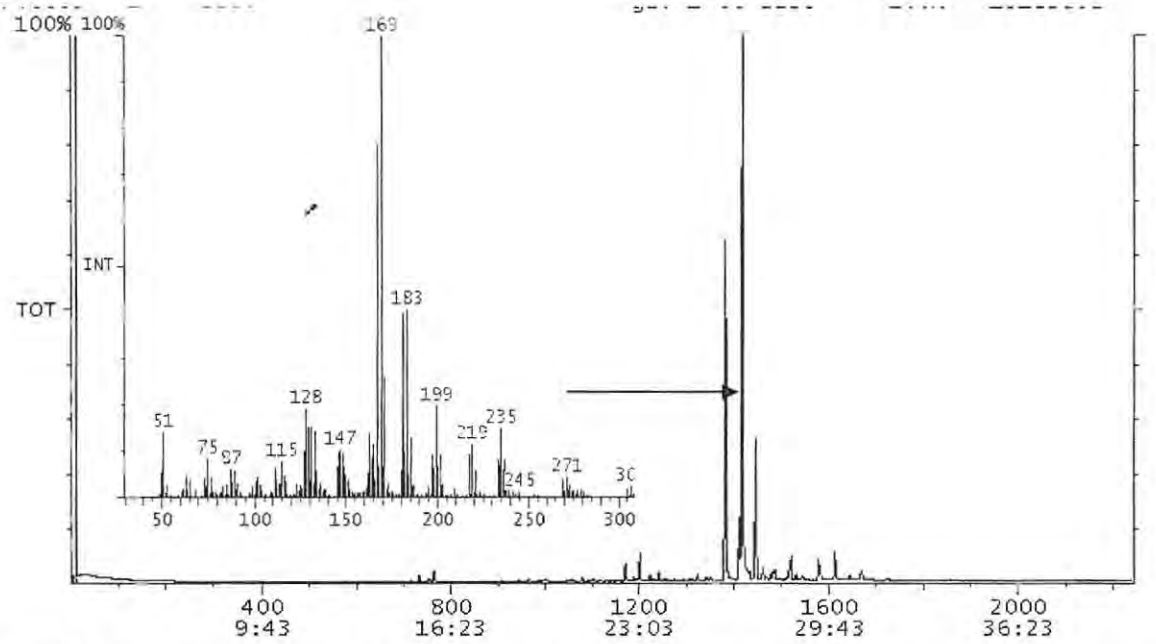

Figure 5.8 Gas chromatogram of the CH_2Cl_2-MeOH extract of *P. suhrii* where 100% = **19183852** inset EIMS spectrum for the peak indicated

For comparative purposes, the Y-axis scale for the gas chromatogram obtained for the *n*-hexane extract was adjusted to that of the CH_2Cl_2-MeOH extract where 100% = 19183852 (Figure 5.8) and the two peaks were integrated.

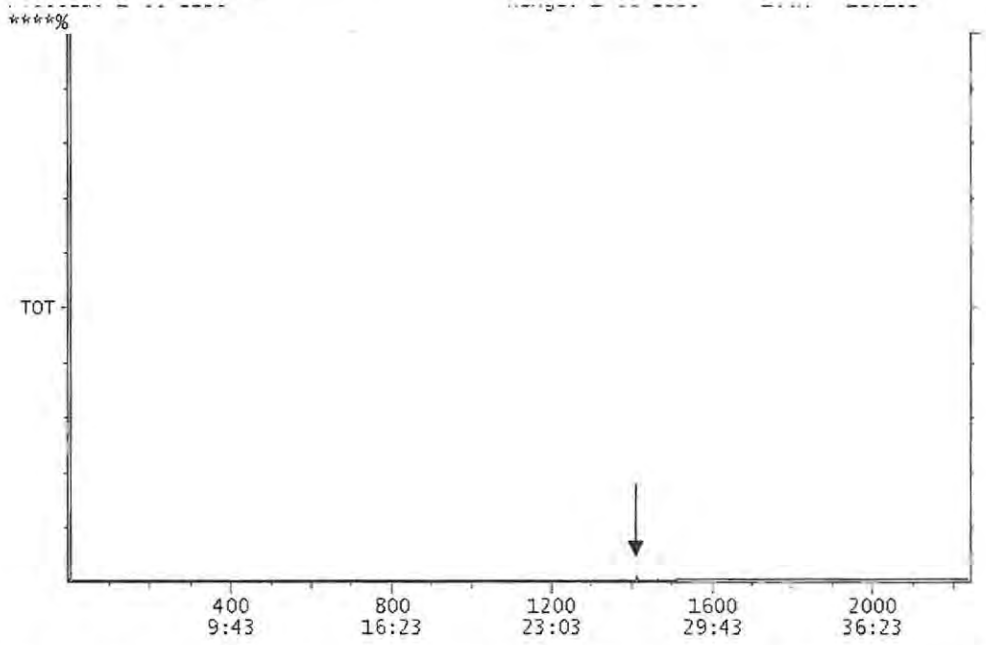

Figure 5.9 Gas chromatogram of the *n*-hexane extract of *P. suhrii* where 100% = **19183852**

The area under the curve of the peak obtained from the *n*-hexane extract is approximately 0.6% (470834 / 80068502 * 100%) of the area under the curve of the peak obtained from the CH_2Cl_2-MeOH extract.

The results indicate that **4.34** is detectable at the surface of *P. suhrii*, but that substantially greater amounts are present in the whole plant extracts than the surface extracts. Although it may yet be possible for **4.34** to be transferred by surface contact, this data suggests that it is unlikely to be the mechanism by which such a substantial amount of the metabolite was transferred to *L. flexuosa*. Based upon these findings, it is proposed that **4.34** is not present on the surface of *P. suhrii* in sufficient amounts to reasonably justify the transfer of the metabolite from one alga to another under the stated conditions, however bioaccumulation may still be a factor.

5.2.3 Bioaccumulation of 2,6-dimethyloctatrienes

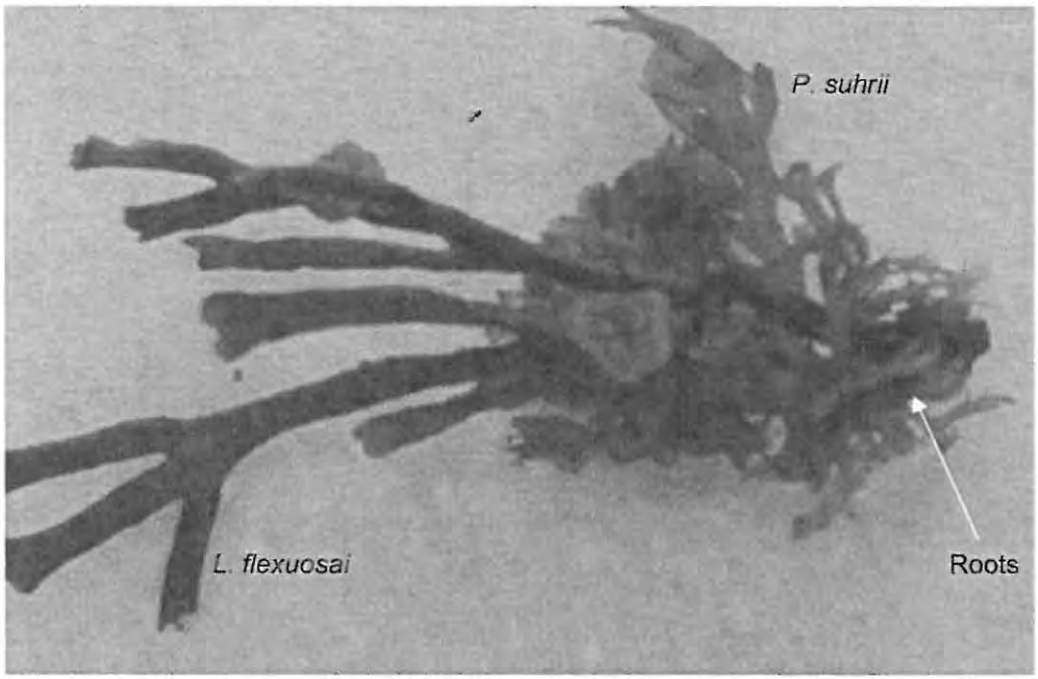

Figure 5.10 A photograph depicting a phenomenon often observed with *P. suhrii* and *L. flexuosa*

P. suhrii may be an example of an epibiont as defined by Wahl (1989). Figure 5.10 illustrates how the roots of *P. suhrii* can be seen anchored to the stem of *L. flexuosa*. The close association of the two plants represents an intriguing ecological relationship.

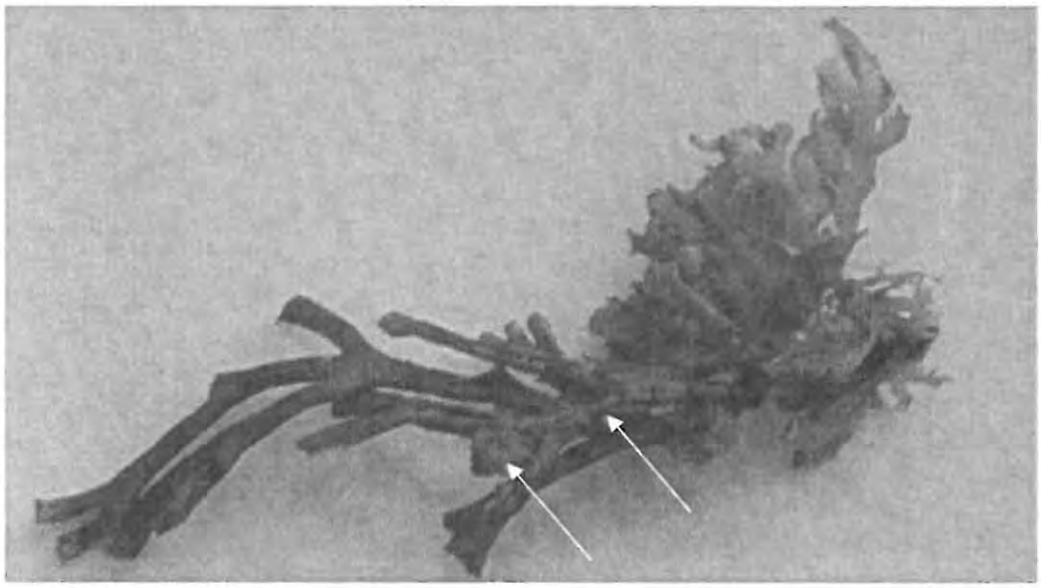

Figure 5.11 An example of fouling on the surface of *L. flexuosa* and lack thereof on *P. suhrii*

It remains to be established whether **4.34** has a beneficial or deleterious function in *L. flexuosa* but an interesting point to note when viewing Figure 5.11 is the unidentified biofouling apparent on the thallus of *L. flexuosa* yet the lack thereof on *P. suhrii*.

Is it possible that *P. suhrii* is a fouling organism, attaching itself to *L. flexuosa* introducing a toxin that gives it a competitive advantage over its host for space and nutrients? Or is it that *P. suhrii*, having a more powerful arsenal of antifouling compounds is symbiotically sharing them with *flexuosa*, the seemingly less powerfully defended alga?

There is a precedence of halogenated monoterpenes being sequestered by marine herbivores whose diet consists of red, brown and green algae. Examples include opisthobranch molluscs or sea hares of the genus *Aplysia* (Stallard and Faulkner, 1973; Naylor *et al.*, 1983; Ireland *et al.*, 1976; Pennings and Paul, 1993), cnidarians of the subclass hydroida (De Napoli *et al.*, 1984), a tunicate (Steffan, 1991) and a brittle star[1] (Lee *et al.*, 2007) (Table 5.2).

Table 5.2 Structurally similar monoterpenes that have been isolated from marine animals

No.	Monoterpene	Source	Biological activity	Reference
5.1	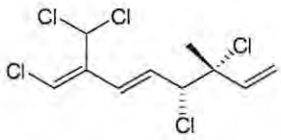	**Tunicates** *Clavelina lepadiformis* **Hydroids** *Aglaophenia pluma* *Halocordyle disticha* *Cudendrium glomeratum* *Sertulatella crassicaulis*		Steffan, 1991 De Napoli *et al.*, 1984
5.2	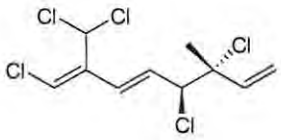	**Hydroids** *Aglaophenia pluma* *Halocordyle disticha* *Cudendrium glomeratum* *Sertulatella crassicaulis*		De Napoli *et al.*, 1984
5.3	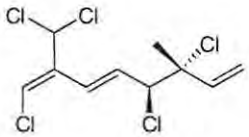	**Sea hare** *Aplysia californica* **Brittle star** *Ophiomastix mixta* **Hydroids** *Aglaophenia pluma* *Halocordyle disticha* *Cudendrium glomeratum* *Sertulatella crassicaulis*	Cancer cell line / ED_{50}* ‡ A549 / 1.15 SK-OV-3 / 11.70 SK-MEL-2 / 5.81 XF498 / 0.99 HCT15 / 4.56	Ireland *et al.*, 1976 Lee *et al.*, 2007 ‡ De Napoli *et al.*, 1984
5.4	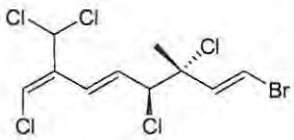	**Seahare** *Aplysia dactylomela*	Cancer cell line / IC_{50}** HMO 2 / 1.1 HEP G2 / 1.0 MCF 7 / 1.5	Wessels *et al.*, 2000
5.6	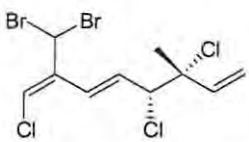	**Seahare** *Aplysia Limacina* **Hydroids** *Aglaophenia pluma* *Halocordyle disticha* *Cudendrium glomeratum* *Sertulatella crassicaulis*		Imperato *et al.*, 1977 De Napoli *et al.*, 1984

*ED_{50} = 50 % growth inhibition concentration (µg/ml); A549 human lung cancer, SK-OV-3 human ovarian cancer, SK-MEL-2 human skin cancer, XF498 human central nervous system cancer, HCT15 human colon cancer
**IC_{50} = 50% growth inhibition concentration (µg/ml); HMO2 gastric cancer, HEP G2 liver cancer, MCF 7 breast cancer

[1] Brittle stars are not exclusively herbivorous but may feed on organic debris, worms, crustaceans and bivalves; subsequently, both animal and vegetable matter is digested (Lee *et al.*, 2007).

The reasons for the sequestration of toxic metabolites such as halogenated monoterpenes are not fully comprehended. One school of thought is that these and other chemicals are utilized by the organisms for chemical defense (Paul and Puglisi, 2004). An alternate view is that; at least in the case of the sea hare; it is simply energetically more favourable to store the metabolites than to detoxify them (Pennings and Paul, 1993).

L. flexuosa is not an herbivorous animal, yet evidence has shown that some form of metabolite transfer has occurred. Coincidentally, the metabolite in question, **4.34** is structurally similar to the 2,6-dimethyloctatrienes sequestered by a diverse group of marine animals (Table 5.2).

The study has raised intriguing questions such as: How does this transfer occur? Why would *L. flexuosa* accumulate the metabolite? and Is *L. flexuosa* itself, producing the monoterpene?

It is apparent that further investigation is required to provide insight and answers to the many questions posed.

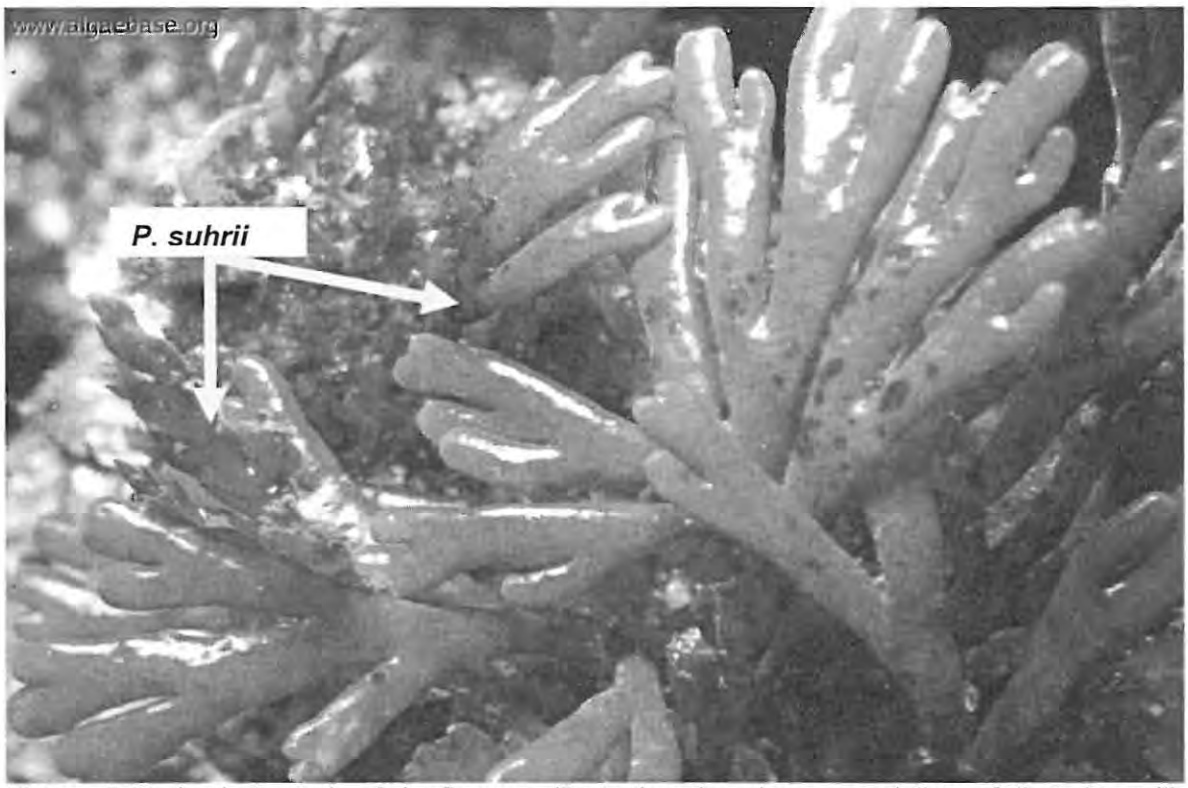

Figure 5.12 A photograph of *L. flexuosa* illustrating the close association of the alga with *Plocamium* species (Guiry and Guiry, 2008)

5.3 Experimental

5.3.1 General experimental

The following general procedures were followed unless otherwise stated. The ^{1}H NMR (400 MHz) spectra were recorded on a Bruker Avance 400 spectrometer using standard pulse sequences. Chemical shifts are reported in ppm and referenced to residual undeuterated solvent resonances ($CHCl_3$ d_H 7.25). All solvents were distilled before use or of HPLC grade (HiPerSolv^{TM}, Merck and Saarchem). Gas chromatography was performed using a Hewlett Packard HP 6890 Gas Chromatograph and an HP-5 phenyl methyl siloxane column (30 m length, 0.25 µm film thickness) or a FinniganMAT GCQ^{TM} and a J&W Scientific DB-1 column (30 m, 0.25 µm film thickness). Low resolution electron impact mass spectra were recorded on a Finnigan MAT spectrometer at 70 eV.

5.3.2 Plant material

The algae were all collected from Noordhoek, near Port Elizabeth, on the Eastern Cape coast of South Africa. NDK07-2a was collected in April 2007. Contained in this collection were *L. flexuosa*, *P. suhrii, P. corallorhiza* and an unidentified alga. NDK07-3 was collected in September 2007 and contained *L. flexuosa*, *P. suhrii* and *P. corallorhiza*.

5.3.3 Investigation into the biological origin of 4.34

5.3.3.1 Extraction

The alga was sorted using tweezers to separate individual plants and fronds. *L. flexuosa*, *P. corallorhiza* and *P. suhrii* were identified by comparison of morphological features with those of samples held in our repository. *P. corallorhiza* (2.0 g), *P. suhrii* (4.1 g) and an unidentified alga (1.8 g) were extracted individually with CH_2Cl_2-MeOH at ambient temperature overnight. The solvent extracts were decanted, dried over anhydrous magnesium sulphate and reduced *in vacuo* to yield an extract for each alga. *L. flexuosa* (12.1 g) was extracted with MeOH at 4 °C for 1 hour, the solvent decanted and the alga re-extracted with CH_2Cl_2-MeOH at ambient temperature overnight. The CH_2Cl_2-MeOH extract was dried over anhydrous magnesium sulphate and concentrated *in vacuo*.

5.3.3.2 Gas chromatography

Extracts and standard (**4.34**) for GC were dissolved in CH_2Cl_2. Whole plant extracts were made up in CH_2Cl_2 (2 ml). The standard used was **4.34** isolated from the CH_2Cl_2-MeOH extracts of *Laurencia flexuosa*, identified as described in chapter four. Gas chromatography was performed using a Hewlett Packard HP 6890 Gas Chromatograph and an HP-5 phenyl methyl siloxane

column (30 m length, 0.25 µm film thickness). All injections were performed in the split mode (Ratio 1:1) with an inlet pressure of 79 kPa. The injection port was held at 270 °C. For all samples the run was started at 75 °C and ramped at 5 °C min^{-1} to 250 °C (and held there for 20 min). Helium was used as the carrier gas.

Exclusion of contamination of solvents by monoterpene

Gas chromatograms were obtained for the volatile solvents employed in the isolation process. Conditions used were those used to assess **4.34** and the crude algal extracts.

5.3.3.3 Gas chromatography – electron impact mass spectrometry

Samples were made up in *n*-hexane (500 µl). Gas chromatography was performed using a FinniganMAT GCQ^{TM} and a J&W Scientific DB-1 column (30 m, 0.25 µm film thickness). All injections were performed using the splitless mode with a carrier gas velocity of 40 $cm.s^{-1}$. The injection port was held at 250 °C and the interface at 270 °C. For all samples the run was started at 75 °C and ramped at 5 °C min^{-1} to 225 °C and held there for 10 minutes. Helium was used as the carrier gas. The mass spectrometry was performed using a Finnigan MAT spectrometer at 70 eV. FullScan mode was employed and mass spectra of peaks at a specific retention time were obtained.

5.3.4 Investigation into surface transfer

5.3.4.1 Extraction of *P. suhrii*

P. suhrii was meticulously sorted at the laboratory using tweezers to separate individual fronds and plants. Two portions of similar mass (approx. 3 g) were sorted onto clean dry paper towels. The fronds were not excessively wet and thus no further attempts were made to dry the alga. The individual portions (including whole plants as well as individual fronds) were immersed in *n*-hexane for 40 seconds. These extracts were brought to dryness in air at ambient temperature then transferred using *n*-hexane to 2.5 ml vials. The alga was then extracted with 25 ml CH_2Cl_2 for 30 minutes at 30 °C and subsequently 25 ml CH_2Cl_2-MeOH for 30 minutes at 30 °C; these extracts were concentrated *in vacuo* and transferred using *n*-hexane to 2.5 ml vials. All extractions were done in duplicate.

5.3.4.2 ^{1}H NMR spectroscopy

All samples for NMR spectroscopy were dissolved in approximately 400 µl $CDCl_3$

5.3.4.3 Gas chromatography – electron impact mass spectrometry

Surface extracts as well as whole plant extracts were made up in *n*-hexane (500 µl). Gas chromatography was performed using a FinniganMAT GCQ^{TM} and a J&W Scientific DB-1 column (30 m, 0.25 µm film thickness). All injections were performed on the splitless mode with a carrier gas velocity of 40 cm.s^{-1}. The injection port was held at 250 °C and the interface at 270 °C. For all samples the GC was started at 75 °C and ramped at 5 °C min^{-1} to 225 °C and held there for 10 minutes. Helium was used as the carrier gas. The mass spectrometry was performed using a Finnigan MAT spectrometer at 70 eV. FullScan mode was employed and mass spectra of peaks at a specific retention time were obtained.

5.4 References

Afolayan, A. MSc Candidate, unpublished work, **2006**.

Argandona, V. H.; Rovirosa, J.; San-Martin, A.; Riquelme, A.; Diaz-Marrero, A. R.; Cueto, M.; Darias, J.; Santana, O.; Guadano, A.; Gonzalez-Coloma, A. Antifeedant effects of marine halogenated monoterpenes. *Journal of Agricultural and Food Chemistry* **2002**, *50*, 7029-7033.

Blunt, J. W.; Copp, B. R.; Hu, W. P.; Munro, M. H. G.; Northcote, P. T.; Prinsep, M. R. Marine natural products. *Natural Product Reports* **2007**, *24*, 31-86. And previous reviews in the series

Branch, G. M.; Griffiths C. L.; Branch, M. L.; Beckley, L. E. *Two oceans: A guide to the marine life of Southern Africa* Second Edition **2005**. ISBN 0-86486-672-0, **1994** David Phillip Publishers, New Africa Books (Pty) Ltd. 99 Garfield Road, Claremont, Cape Town, South Africa.

Cueto, M.; Darias, J.; Rovirosa, J.; San-Martin, A. Tetrahydropyran Monoterpenes from *Plocamium cartilagineum* and *Pantoneura plocamioides*. *Journal of Natural Products* **1998**, *61*, 1466-1468.

Dearden, J. C. Partitioning and lipophilicity in quantitative structure-activity relationships. *Environmental Health Perspectives* **1985**, *61*, 203-228.

De Napoli, L.; Fattorusso, E.; Magno, S.; Mayol, L. Acyclic polyhalogenated monoterpenes from four marine hydroids. *Biochemical Systematics and Ecology* **1984**, *12*, (3), 321-322.

de Nys, R.; Dworjanyn, S. A.; Steinberg, P. D. A new method for determining surface concentrations of marine natural products on seaweeds. *Marine Ecology Progress Series* **1998**, *162*, 79-87.

de Nys, R.; Steinberg, P. D. Linking marine biology and biotechnology. *Current opinions in Biotechnology* **2002**, *13*, 244-248.

Fenical, W. Halogenation in the Rhodophyta A Review. *Journal of Phycology* **1975** *11*, 245-259.

Fenical, W.; Norris, J. Chemotaxonomy in marine algae: chemical separation of some *Laurencia* species (Rhodophyta) from the Gulf of California. *Journal of Phycology* **1975**, *11*, 104-108.

Guiry, M. D.; Guiry, G. M. **2008**. AlgaeBase version 4.2. World-wide electronic publication, National University of Ireland, Galway. http://www.algaebase.org date accessed January 20, 2008.

Hay, M. E.; Fenical, W. Marine plant-herbivore interactions: the ecology of chemical defense. *Annual review of Ecology and Systematics* **1988**, *19*, 111-145.

Imperato, F.; Minale, L.; Riccio, R. Constituents of the digestive gland of molluscs of the genus Aplysia. II. Halogenated monoterpenes from *Aplysia limacine*. *Experientia* **1977**, *33*, (10), 1273-1274.

Ireland, C.; Stallard, M. O.; Faulkner, D. J. Some chemical constituents of the digestive gland of the sea hare *Aplysia californica*. *Journal of Organic chemistry* **1976**, *41*, (14), 2461-2465.

Knott, M.; Mkwananzi, H.; Arendse, C.; Hendricks, D. T.; Bolton, J. J.; Beukes, D. R. Plocoralides A-C, polyhalogenated monoterpenes from the marine alga *Plocamium corallorhiza*. *Phytochemistry* **2005**, *66*, 1108-1112.

Lee, J.; Wang, W.; Hong, J.; Lee, C.; Shin, S.; Kwang, S. I.; Jung, J. H. A new 2,3-Dimethyl Butenolide from the Brittle Star *Ophiomastix mixta*. *Chemical and Pharmaceutical Bulletin* **2007**, *55*, (3), 459-461.

Mann, M. G. A.; Mkwananzi, H. B.; Antunes, E. M.; Whibley, C. E.; Hendricks, D. T.; Bolton, J. J.; Beukes, D. R. Halogenated monoterpene aldehydes from the South African marine alga *Plocamium corallorhiza*. *Journal of Natural Products* **2007**, *70*, 596-599.

Naylor, S.; Hanke, F. J.; Manes, L. V.; Crews, P. Chemical and biological aspects of marine monoterpenes. *Progress in the Chemistry of Organic Natural Products* **1983**, *44*, 189-241. ISBN 3-211-81754-9 Springer-Verlag/Wien.

Paul, V. J.; Puglisi, M. P. Chemical mediation of interactions among marine organisms. *Natural Product Reports* **2004**, *21*, 189-209.

Pennings, S. C.; Paul, V. J. Sequestration of dietary secondary metabolites by three species of sea hares: location, specificity and dynamics. *Marine Biology* **1993**, *117*, 535-546.

Potin, P.; Bouarab, K.; Salaün, J. P.; Pohnert, G.; Kloareg, B. Biotic interactions of marine algae. *Current Opinion in Plant Biology* **2002**, *5*, 1-10.

Raven, P. H.; Evert, R. E.; Eichhorn, S. E. *Biology of Plants* Sixth Edition **1999**, W. H. Freeman and Company/Worth Publishers; ISBN 1-57259-041-6.

Stallard, M. O.; Faulkner, D. J. Chemical constituents of the digestive gland of the sea hare *Aplysia californica* – I. Importance of Diet. *Comparative Biochemistry and Physiology B* **1973**, *49*, 25-35.

Steffan, B. Lepadin A, A Decahydroquinoline alkaloid from the tunicate *Clavelina lepadiformis*. *Tetrahedron* **1991**, *47*, (41), 8729-8732.

Sudatti, D. B.; Rodrigues, S. V.; Pereira, R. C. Quantitative GC-ECD analysis of halogenated metabolites: Determination of surface and within-thallus elatol of *Laurencia obtusa*. *Journal of Chemical Ecology* **2006**, *32*, 835-843.

Wessels, M.; König, G. M.; Wright, A. D. New natural product isolation and comparison of the secondary metabolite content of three distinct samples of the sea hare *Aplysia dactylomela*. *Journal of Natural Products* **2000**, *63*, 920-928.

Wollenweber, E.; Doerr, M.; Siems, K.; Faure, R.; Bombarda, I.; Gaydou, E. M. Triterpenoids in lipophilic leaf and stem coatings. *Biochemical Systematics and Ecology* **1999**, 27, 103-105.

Yano, T.; Kamiya, M.; Murakami, A.; Sasaki, H.; Kawai, H. Biochemical phenotypes corresponding to molecular phylogeny of the red algae *Plocamium* (Plocamiales, Rhodophyta): Implications of incongruence with the conventional taxonomy. *Journal of Phycology* **2005**, *42*, (1) 155-169.

Chapter Six

A New Triphenoxybenzyloxy-a-alkyl Malate from *Martensia elegans*

6.1 Introduction

Martensia species have yet to be studied extensively with respect to their natural products chemistry; however, the first reported indole alkaloids isolated from marine algae were secondary metabolites of *Martensia fragilis* collected from Black Point, Mokuleia, Oahu. The indole alkaloid Martensine A (**6.1**) showed antibiotic activity against *Bacillus subtillis*, *Staphylococcus aureus* and *Mycobacterium smegmatis* (Kirkup and Moore, 1983).

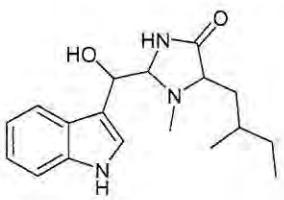

6.1

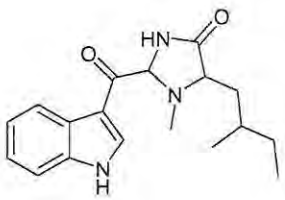

6.2

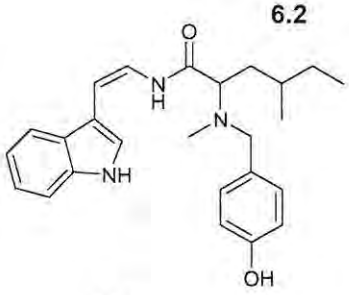

6.3

Recent studies on fragilamide (**6.3**) have shown the compound to be a potent anti-oxidant in solution-based anti-oxidant assays. More importantly in terms of possible anti-oxidant therapy is that fragilamide (**6.3**) can be taken up by living cells whilst maintaining anti-oxidant activity (Takamatsu *et al.*, 2003).

A study into the volatile compounds responsible for the odour of some marine algae revealed that one of the three components of the essential oil of *Martensia fragilis*, *p*-(methoxymethyl)phenol, was responsible for the alga's foul scent (Moore, 1977). *p*-(Methoxymethyl)phenol was also found to be a photooxidation product of fragilamide (**6.3**) by Kirkup and Moore (1983).

In our continuing search for new biologically active compounds from marine algae, we collected *Martensia elegans* (PE07-9) from Port Edward, Kwa-Zulu Natal. Although the extracts of this alga were not screened for antimicrobial activity prior to fractionation, the antibacterial compounds

previously reported from related species (Kirkup and Moore, 1983) prompted an investigation into the alga's secondary metabolite chemistry.

Martensia elegans is classified as an iridescent red alga and is described by taxonomists as having "beautiful mauve fans" of approximately 20 – 30 mm in diameter (Branch *et al.*, 2005). Taxonomy: Phylum Rhodophyta, Class Florideophyceae, Order Ceramiales, Family Delesseriaceae, Genus *Martensia* (Guiry and Guiry, 2007).

This genus is found on the East coast of South Africa and in several other locations around the world (Figure 6.1).

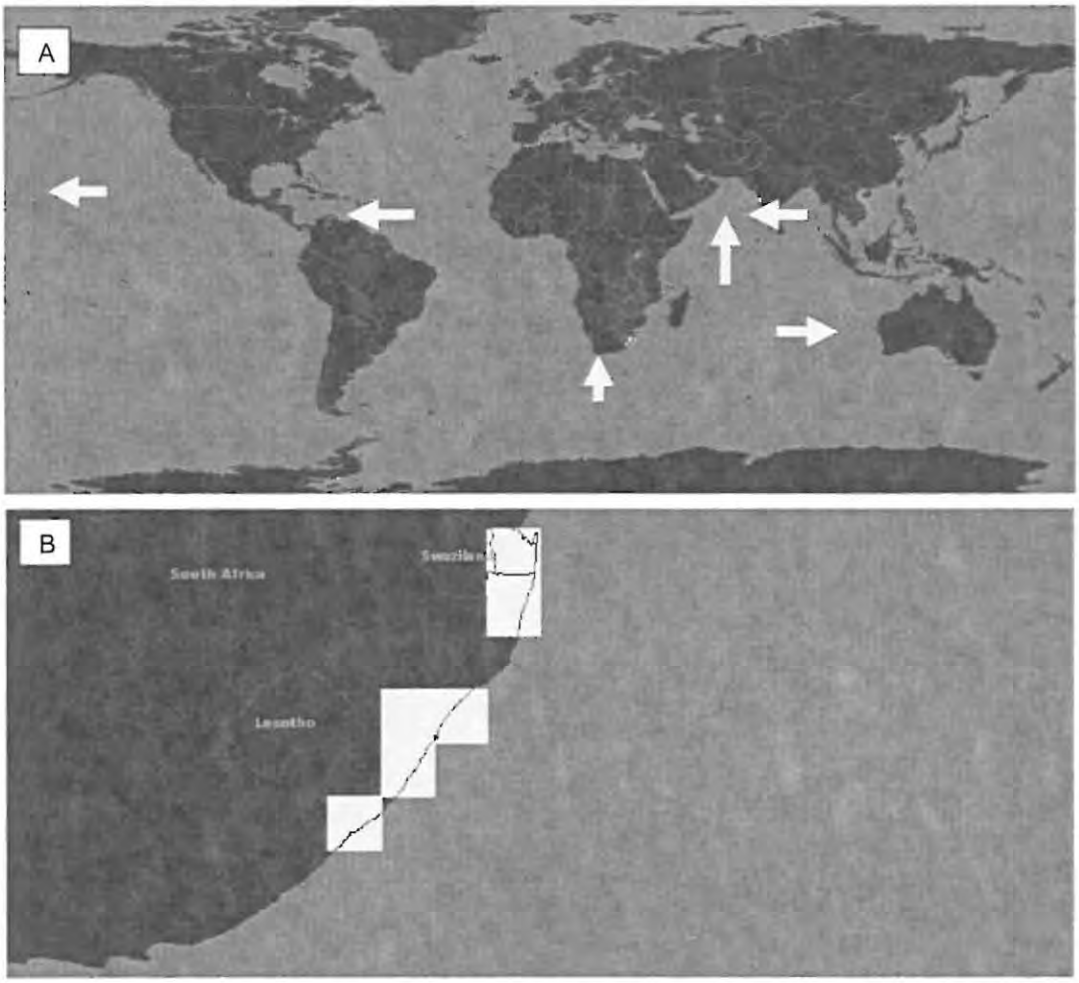

Figure 6.1 A) Global distribution of *Martensia species*, B) Distribution on *M. elegans* on the East coast of South Africa.

Biodiversity occurrence data provided by *Global Biodiversity Information Facility* Accessed through GBIF Data Portal, www.gbif.net, 2008-01-17

6.2 Results and Discussion

6.2.1 Collection and extraction of *Martensia elegans* (PE07-9 Port Edward)

The alga was collected in January 2007 from Port Edward, Kwa Zulu-Natal on the East coast of South Africa. Following protocol, the alga was stored over ice during transport and frozen at -4 °C. The frozen seaweed was extracted using MeOH and CH_2Cl_2-MeOH (2:1). Solvent partitioning of the combined solvent extracts afforded extract A (*n*-hexane soluble, 200 mg) and extract B (CH_2Cl_2 soluble, 123.5 mg). The remaining aqueous MeOH extract was reduced *in vacuo* and further partitioned between EtOAc-H_2O to afford an additional extract C (EtOAc soluble, 26.3 mg). Silica gel column chromatography performed on the *n*-hexane extract yielded seven fractions (A1-7, Scheme 6.1). The silica column fractions of the *n*-hexane partition contained chlorophylls. These primary metabolites were often observed in silica gel column chromatography fractions of the algae that our research group extracted. The CH_2Cl_2 and EtOAc partitions (B and C) were combined due to the similarities between their ^{1}H NMR spectra and their small mass (combined 149.8 mg). The possibility of very polar compounds in the EtOAc partition necessitated that the extract be passed through a small silica column prior to normal phase HPLC lest a polar substance become stuck on the HPLC column. The extract was passed through the silica gel column using *n*-hexane-EtOAc (7:3) as an eluent followed by MeOH. The fractions were collected separately and dried *in vacuo.* Normal phase HPLC using an *n*-hexane-EtOAc (7:3) mobile phase was performed on the non-polar fraction yielding the compound **6.4** (BC1b, Scheme 6.1). Reverse phase HPLC (MeOH) was employed to purify compounds from the polar fraction. No additional pure compounds were isolated, however, **6.4** (BC2e Scheme 6.1) was again isolated and two possible compounds (BC2d and BC2h Scheme 6.1) of very small quantity were noted but not investigated.

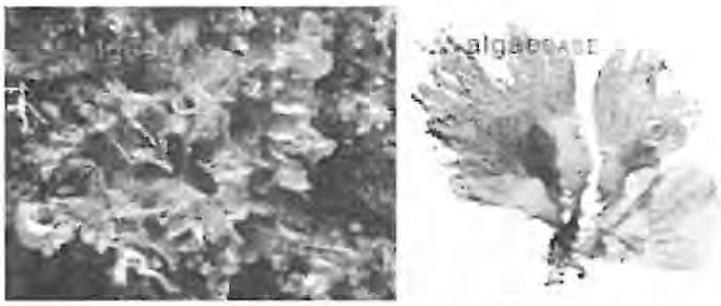

Figure 6.2 *Martensia elegans*, the elegant net fan (Guiry and Guiry, 2007)

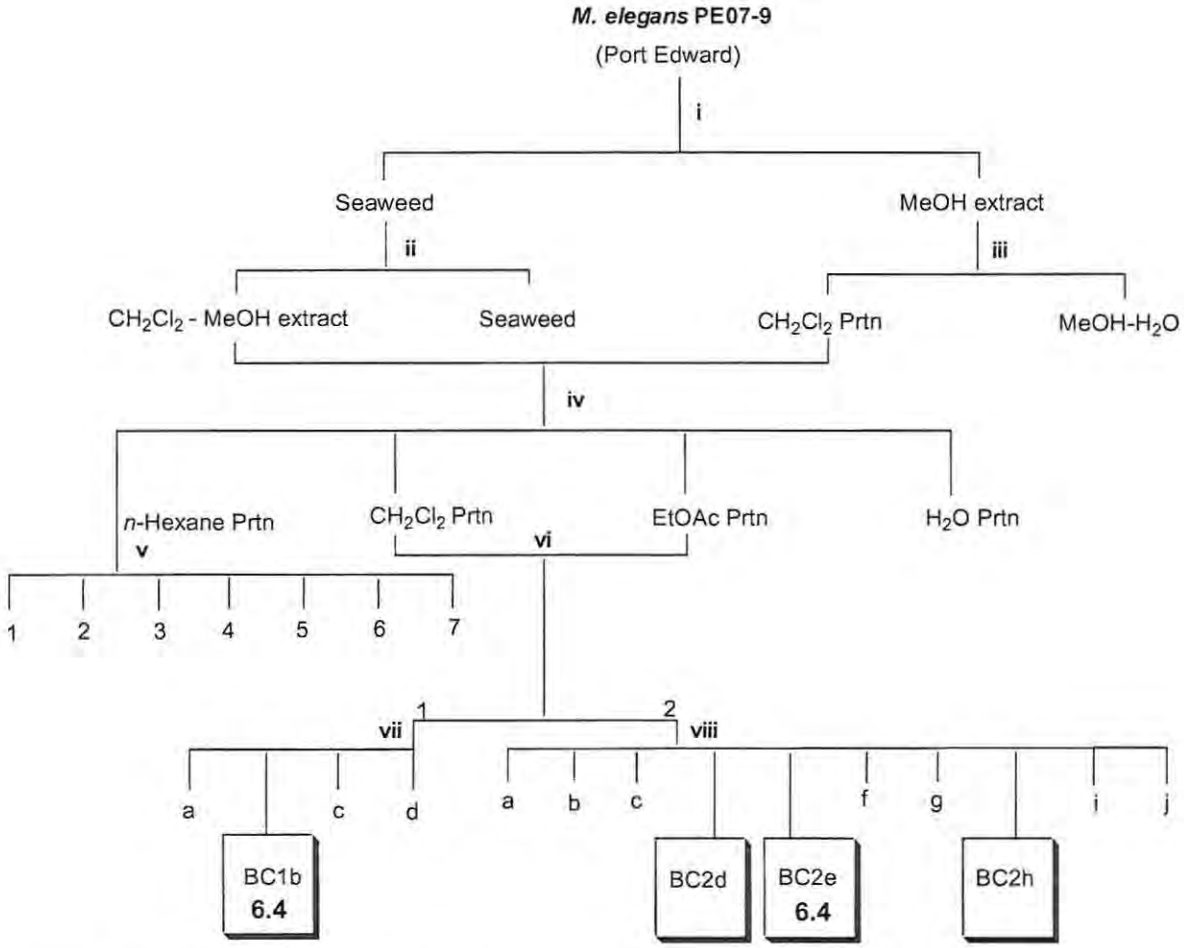

Scheme 6.1 Extraction and isolation of metabolites from *M. elegans* (Port Edward)

Conditions: i) MeOH 4 °C, 1 hour ii) CH_2Cl_2-MeOH (2:1) extraction iii) CH_2Cl_2 extraction iv) Solvent partitioning v) Silica gel column chromatography vi) silica gel column separation vii) normal phase HPLC (*n*-hexane 7:3) viii) reverse phase HPLC (MeOH)

Table 6.1 Mass and percentage yield* of **6.4** isolated from *M. elegans* (Port-Edward)

Isolation code[‡]	Compound #	Mass (mg)	% yield*
BC1b & BC2e	**6.4**	24.0 mg	0.3987

[‡]isolation code: Partition, silica gel column fr, HPLC fr e.g. * Percentage yields calculated relative to dry weight (dry weight after extraction 6.02 g)

6.2.2 Characterization of 6.4

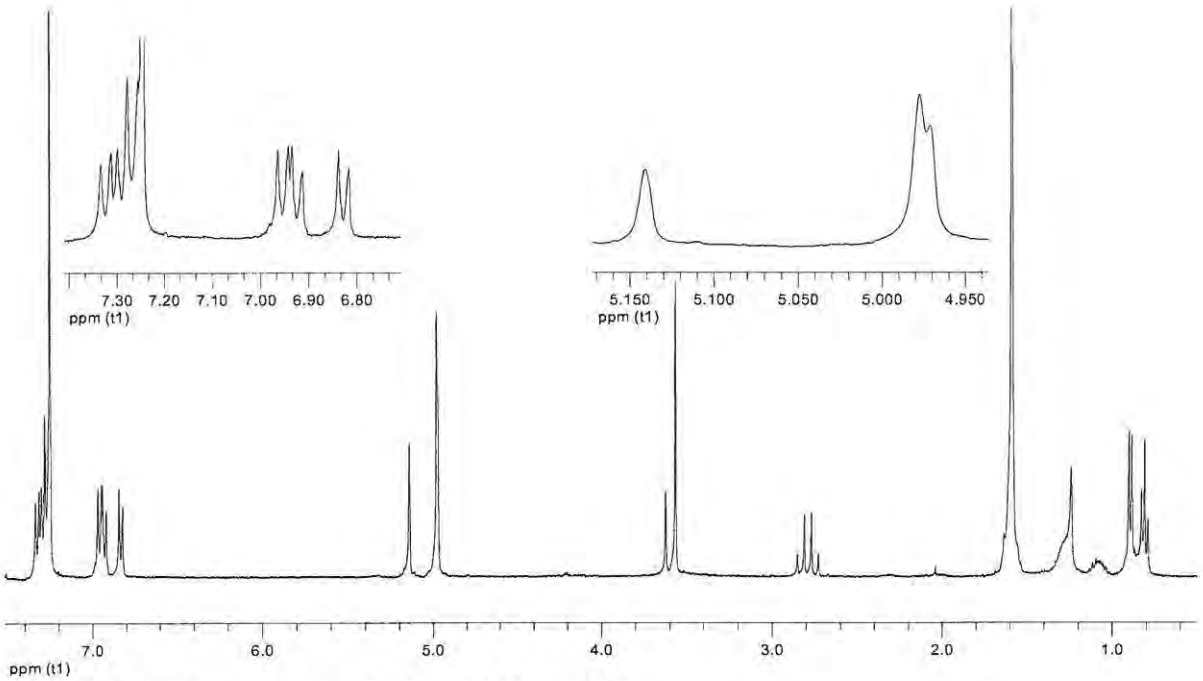

Figure 6.3 ^{1}H NMR spectrum ($CDCl_3$, 400 MHz) of **6.4**

Compound **6.4** was obtained as an off-white crystalline powder. High resolution ESIMS data indicated a molecular ion of *m/z* 545.2160 which is consistent with the molecular formula of $C_{30}H_{34}O_8$ + Na (Calcd for $C_{30}H_{34}NaO_8$ 545.2151). The infrared spectrum showed a broad absorption band indicative of hydroxyl groups (3438 cm^{-1}) and absorbances typical of carbonyl groups (1714 cm^{-1}) as well as aromatic rings (1513 and 1610 cm^{-1}).

Immediately apparent in the ^{1}H NMR spectrum (Figure 6.3) are the deshielded aromatic signals that include three pairs of mutually coupled doublets at d 6.83 (d, *J* = 8.3 Hz) and 7.27 (d, *J* = 8.3 Hz); d 6.93 (d, *J* = 8.7 Hz) and 7.29 (d, *J* = 8.0 Hz); d 6.96 (d, *J* = 8.7 Hz) and 7.33 (d, *J* = 8.7 Hz). Other signals include three deshielded singlets at d 4.97 (s), 4.98 (s) and 5.14 (s) indicating three benzylic methylene groups attached to electronegative atoms. The spectrum also shows three methyl resonances at d 3.57 (s), 0.90 (d, *J* = 6.8 Hz) and 0.80 (t, *J* = 7.4 Hz) as well as methylene absorbances at d 2.83 (d, *J* = 16.1 Hz) and 2.74 (d, *J* = 16.1 Hz). A rather indistinct absorbance at d 1.09-1.29 (m) was determined to be due to a methylene group by HSQC (^{13}C NMR shift d 23.7).

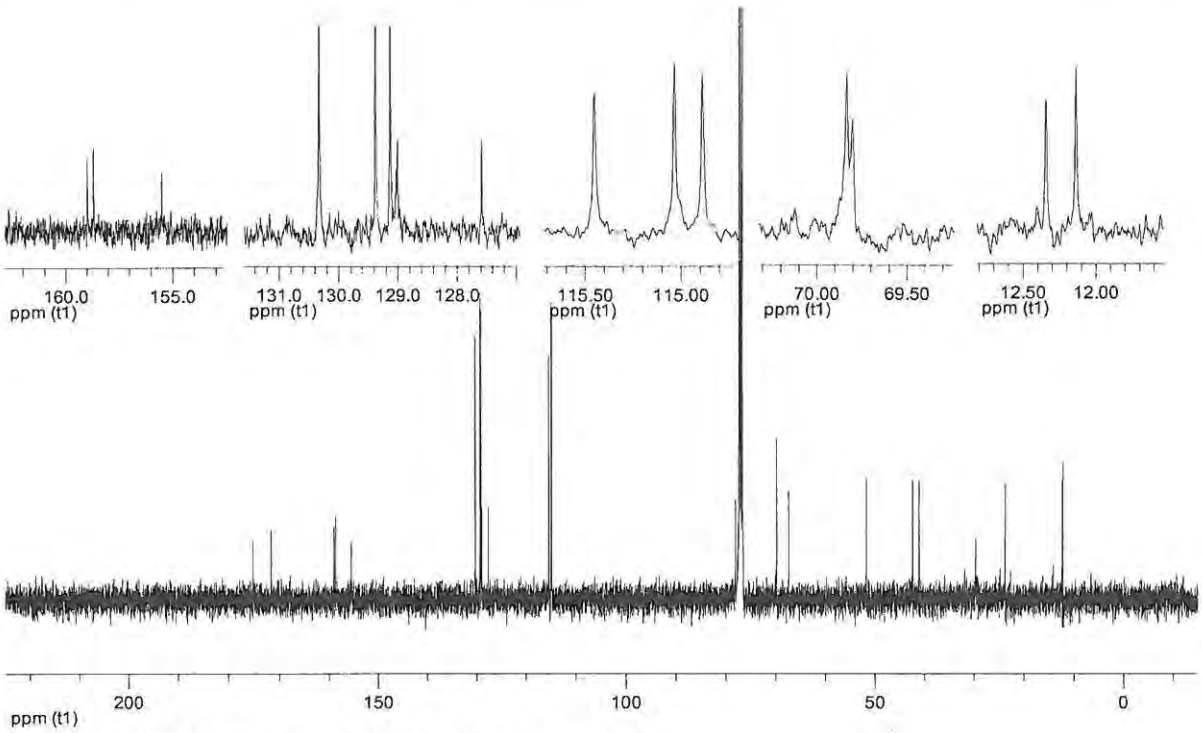

Figure 6.4 ^{13}C NMR spectrum ($CDCl_3$, 400 MHz) of **6.4**

The ^{13}C NMR spectrum of **6.4** (Figure 6.4) shows twenty four carbon resonances which, by way of a DEPT135 experiment were assigned as nine quaternary carbons (d 175.2, 172.7, 159.0, 158.9, 155.5, 129.02 129.00, 127.6 and 78.1), seven CH (methine) resonances, six of which consist of two carbons each (d 130.3, 129.4, 129.1, 115.5, 115.0, 114.9 all 2C, and 42.4, 1C), five CH_2 (methylene) absorbances (d 69.83, 69.80, 67.5, 41.1, and 23.7) and finally three methyl signals (d 51.8, 12.3 and 12.1).

Determination of the planar structure was performed using data obtained from the HMBC and ^1H-^1H COSY experiments. The molecule was divided into four distinct fragments designated A-D. The methyl protons at d 0.90 and 0.80 as well as the methylene protons at d 2.83 and d 2.74 showed important correlations that were instrumental in determining the fragment A (Figure 6.5). HMBC correlations between the methylene protons at d 5.14, 4.98 and 4.97 allowed for the distinction between fragments D to C, but also provided the key links between all four fragments.

^{13}C NMR chemical shifts of d 175.2 and 171.7 are typical of carbonyl carbons, while d 159.0, 158.7 and 155.5 are shifts indicative of carbon atoms in an aromatic ring which have oxygen substituents. The ^{13}C NMR chemical shift of d 51.8 for a methyl carbon indicates a methoxy group.

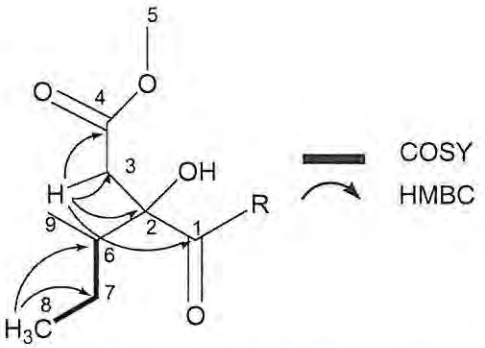

Figure 6.5 Key HMBC and ^{1}H-^{1}H COSY correlations in the determination of fragment A

Table 6.2 ^{1}H (400 MHz), ^{13}C (100 MHz) NMR, ^{1}H-^{1}H COSY and HMBC data for **6.4** in $CDCl_3$

Carbon No.	d_C		d_H, multi, *J* (Hz)	^{1}H-^{1}H COSY	HMBC
Fragment A					
1	175.2	C=O			
2	78.1	C			
3	41.1	CH_2	2.83, d, 16.1; 2.74, d, 16,1	H9, H7	C6, C2, C4,C1
4	171.7	C=O			
6	42.4	CH	1.58, m		C2
7	23.7	CH_2	1.09-1.29 m	H6, H8	
8	12.1	CH_3	0.81, t, 7.4	H7	C7, C6, C2
9	12.3	CH_3	0.90, d, 6.8	H6	C7, C6, C2
5	51.8	CH_3	3.57, s		C3
OH		OH			C1, C2, C6
Fragment B					
1'	127.6	C			
2'	130.3	CH	7.27, d, 8.3	H3'	C7', C4"
3'	115.5	CH	6.83, d, 8.5	H2'	C4', C1"
4'	155.5	C			
5'	115.5	CH	7.27, d, 8.3	H6'	C4', C1"
6'	130.3	CH	6.83, d, 8.5	H5'	C7', C4"
7'	67.5	CH_2	5.14, s		C1, C1', C2', C6'
Fragment C					
1"	129.00	C			
2"	129.1	CH	7.29, d, 8.0	H3"	C4'
3"	114.9	CH	6.93, d, 8.7	H2"	C1', C4"
4"	159.0	C			
5"	114.9	CH	6.93, d, 8.7	H6"	C1', C4"
6"	129.1	CH	7.29, d, 8.0	H5"	C4'
7"	69.83	CH_2	4.98, s	H2"	C2", C4"
Fragment D					
1"'	129.02	C			
2"'	129.4	CH	7.33, d, 8.7	H3"'	C7", C4"'
3"'	115.0	CH	6.96, d, 8.7	H2"'	C2"', C4"'
4"'	158.7	C			
5"'	115.0	CH	6.96, d, 8.7	H6"'	C2"', C4"'
6"'	129.4	CH	7.33, d, 8.7	H5"'	C7", C4"'
7"'	69.80	CH_2	4.97, s	H2"'	C4"', C2"'

HMBC data was ambiguous when it came to determining which protons correlate with which carbons. ^{1}H-^{1}H COSY data however, was very clear when in came to deducing which sets of protons were adjacent one another.

The methyl protons at d 0.81 (H-8) showed strong HMBC correlations to the carbons at d 23.7(C-7) and 42.4 (C-6) but very weak correlations to the carbon at d 78.1 (C-2). Strong ^{1}H-^{1}H COSY correlations between protons at d 0.81 and 1.09–1.29 indicate that the protons are coupled to adjacent carbon atoms. The methyl protons at d 0.90 (H-9) showed strong HMBC correlations to carbons at d 23.7(C-7), 42.4 (C-6) and d 78.1 (C-2) as well as ^{1}H-^{1}H COSY correlations to the multiplet at d 1.58 which is in turn coupled to C-6. The methylene protons at d 2.79 (H-3) showed HMBC correlations to carbons at d 175.2 (C-1), 171.7 (C-4), 78.1 (C-2) and 42.4 (C-6).

The protons at d 5.14 (H-7") showed HMBC correlations with the carbon at d 175 (C-1) which elucidated the link between fragment A and fragment B (Figure 6.6). These protons also showed HMBC correlations to the quaternary carbon at d 127.6 (C-1') and the aromatic carbons at d 130.3 (C-2' and C-6'). ^{1}H-^{1}H COSY correlations between protons at d 6.83 and 7.27 showed that these protons are attached to adjacent carbon atoms. Similarly in fragments C and D, the ^{1}H-^{1}H COSY correlations allowed the determination of the relative positions of the aromatic methines.

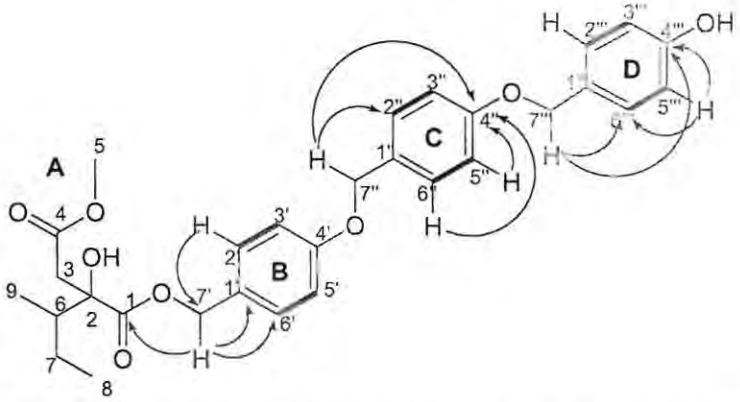

Figure 6.6 Key HMBC and ^{1}H-^{1}H COSY correlations in discerning the fragments of **6.4**

The protons at d 4.98 (H-7") showed HMBC correlations to the aromatic carbons at d 129.1 (C-2" and C-6") as well as the quaternary carbon at d 159.0 (C-4"). Likewise, the protons at d 4.97 (H-7"') showed HMBC correlations to the aromatic carbons at d 129.4 (C-2"' and C-6"') as well as the quaternary carbon at d 158.7 (C-4"') (Figure 6.6).

The ^{13}C NMR chemical shifts of the quaternary carbons C-4', C-4" and C-4"' of d 155.5, 158.7 and 159.0 respectively indicated oxygen atoms attached at these positions. This data in association with the absence of further groups attached to fragment D indicated that the para-substituent on fragment D is an hydroxyl group. ^{1}H-^{1}H COSY data indicating para substitution, the presence of oxygen substituents at the para-position on each ring and HMBC correlations from the methylene protons (H-7', H-7" and H-7"') to carbon atoms in the aromatic rings, provide evidence for the presence of three benzyloxy groups (fragments B, C and D) linked at the para position. As yet, no stereochemical

assignments have been made for the chiral centres in **6.4**. All spectroscopic data are consistent with the structure proposed for this compound.

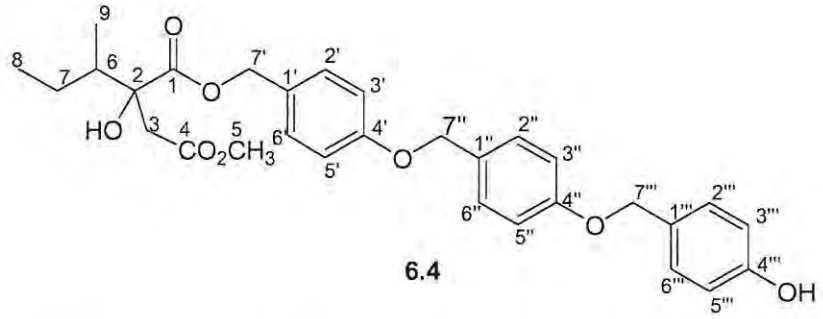

6.4

This compound, although not novel in structure, is an unusual metabolite. Moreover, such a combination of structural features is not common among known marine natural products. Metabolites possessing the a-alkyl malate side chain have, however, been isolated from terrestrial plants. These include the coelovirins, isolated from the terrestrial plant *Coeloglossum viride* (**6.5**) (Huang *et al.*, 2004) and alkaloids from *Cephalotaxus harringtonia* which include the antileukaemic compound harringtonine (**6.6**) (Delfel and Rothfus, 1977). Nevertheless, phenolic compounds are abundant in marine and terrestrial plant natural products, an example of which is the phenolic compound **6.7** which was isolated from *Gastrodia elata* rhizome extracts (Hayashi *et al.*, 2002).

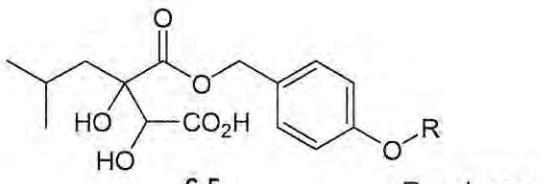

6.5 R = glucose

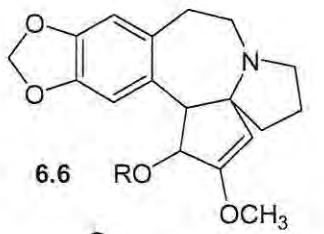

6.6

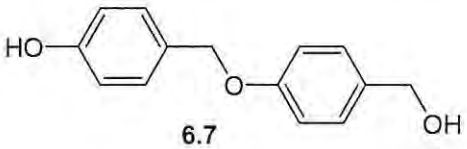

6.7

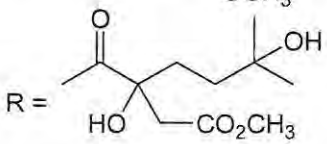

6.3 Experimental

6.3.1 General experimental

The following general procedures were followed unless otherwise stated. The ^{1}H (400 MHz), ^{13}C (100 MHz), DEPT-135, ^{1}H-^{1}H COSY, HSQC, HMBC and NOESY NMR spectra were recorded on a Bruker Avance 400 spectrometer using standard pulse sequences. Chemical shifts are reported in ppm and referenced to residual undeuterated solvent resonances ($CHCl_3$ d_H 7.25, d_C 77.0) and coupling constants are reported in Hz. Optical rotations were measured on a Perkin-Elmer 141 polarimeter. IR spectra were obtained as films on KBr disks using a Perkin-Elmer Spectrum 2000 FT-IR spectrometer. High performance liquid chromatographic separations were performed on a Spectra-Physics IsoChrom LC HPLC system which was equipped with a Rheodyne injector, a Waters R401 differential refractometer, or a Spectra SERIES UV100 detector and a Rikadenki chart recorder. In all cases, normal phase HPLC was performed using a Whatman Magnum 10 Partisil 9 column. Reverse phase HPLC was performed using a Phenomenex Luna 10u C18 column (250 x 10.00 mm). HR-ESIMS spectra were acquired on a Waters API-TOF Ultima mass spectrometer using positive ion electrospray ionization at the Mass Spectrometry Unit at Stellenbosch University, Stellenbosch, South Africa.

6.3.2 Biological material (collection, extraction and isolation)

PE07-9 (Port Edward)

Martensia elegans (K. Hering) was collected in January 2007 from Port Edward, (31°03' S, 30°13' E), Kwa Zulu-Natal on the East coast of South Africa. The frozen alga was stored over ice during transport and frozen at -4 °C. The frozen seaweed was steeped in MeOH at 4 °C for 1 hour. The MeOH extract was then reduced *in vacuo* to an aqueous suspension and extracted with CH_2Cl_2. The alga was immersed in CH_2Cl_2-MeOH (2:1) and heated at 30 °C for 30 minutes (x3). Resulting CH_2Cl_2-MeOH extracts were combined and separated into two layers by the addition of distilled water. The CH_2Cl_2 layer was run off and kept aside. The aqueous MeOH was reduced *in vacuo* to an aqueous mixture and extracted with CH_2Cl_2 (3 x 50 ml). All CH_2Cl_2 extracts were combined and dried over anhydrous magnesium sulphate after which the solvent was evaporated off to afford an oily green residue. Solvent partitioning of the residue between *n*-hexane-MeOH-H_2O (10:9:1) afforded extract A (*n*-hexane soluble 200 mg) and between CH_2Cl_2-MeOH-H_2O (10:9:1) and extract B (CH_2Cl_2 soluble 123.5 mg). The remaining aqueous methanol extract was reduced *in vacuo* and further partitioned between H_2O-EtOAc which afforded an additional extract C (26.3 mg). Silica gel column chromatography (2 g Kieselgel 0.040-0.063 nm) performed on the *n*-hexane extract employing an *n*-hexane-EtOAc step gradient of increasing polarity yielded seven fractions. The CH_2Cl_2 and EtOAc partitions were combined due to the similarities between their ^{1}H NMR spectra and their small mass

(combined 149.8 mg). The possibility of very polar compounds in the ethyl acetate partition necessitated that the extract be passed through a small silica column (500 mg Kieselgel 0.040-0.063 nm) prior to normal phase HPLC lest a polar substance become stuck on the HPLC column. The extract was passed through the silica column using *n*-hexane-EtOAc (7:3) as eluent and subsequently MeOH. The fractions were collected separately and dried *in vacuo.* Normal phase HPLC using a *n*-hexane-EtOAc (7:3) mobile phase was performed on the non-polar fraction yielding compound **6.4** (BC1b). Reverse phase HPLC (MeOH) was employed to purify compounds from the polar fraction; **6.4** (BC2e) was again isolated.

6.3.3 Compounds

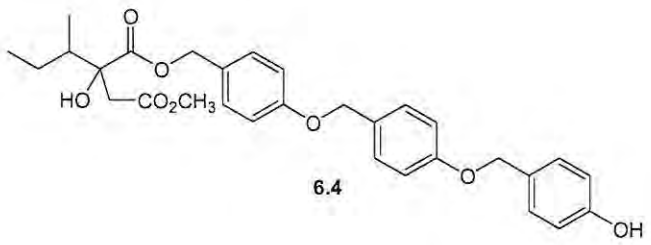

6.4

6.4 Martenzomalate: Off-white crystalline substance; $[a]^{16}_{D}$ 0°* ($CHCl_3$); UV (CH_2Cl_2) λ_{max} 240 nm, 274.4 nm (0.00012 mg/ml); IR (dry film) ν_{max} 3438.9, 2968.4, 2915.6, 2849.0, 2328.0, 2068.6, 1717.0, 1610.4, 1513.4, 1428.4, 1235.2, 1149.6, 1019.6, 1000.6, 901.8 cm^{-1} (KBr); ^1H NMR ($CDCl_3$, 400 MHz); ^{13}C NMR ($CDCl_3$, 100 MHz) see **Table 6.2** HMBC data: **C-3**/C-6, C-2, C-4, C-1; **C-5**/C-3; **C-6**/C-2; **C-8**/C-7, C-6, C2; **C-9**/C-7, C-6, C-2; **OH**/C-1, C-2, C-6; **C-2'**/C-7', C-4''; **C-3'**/C-4', C-1''; **C-5'**/C-4', C-1''; **C-6'**/C-7', C-4''; **C-7'**/C-1, C-1', C-2', C-6'; **C-2''**/C-4'; **C-3''**/C-1', C-4''; **C-5''**/C-1', C-4''; **C-6''**/C-4''; **C-7''**/C-2'', C-6'', C-4''; **C-2'''**/C-7''', C-4'''; **C-3'''**/C-2''', C-4'''; **C-5'''**/C-2''', C-4'''; **C-6'''**/C-7''', C-4'''; **C-7'''**/C 4''', C-2'''.

* OR was done to the best of the author's ability with the facilities available, however it is felt that this optical rotation is not reliable; re-isolation of the compound is required for further investigation.

6.4 References

Biodiversity occurrence data provided by *Global Biodiversity Information Facility* Accessed through GBIF Data Portal, www.gbif.net, **2008**-01-17

Branch, G. M.; Griffiths C. L.; Branch, M. L.; Beckley, L. E.; In *Two oceans: A guide to the marine life of Southern Africa*, Second Edition **2005**. ISBN 0-86486-672-0, **1994** David Phillip Publishers, New Africa Books (Pty) Ltd. Cape Town, South Africa.

Delfel, N. E.; Rothfus, J. A. Antitumour alkaloids in callus cultures of *Cephalotaxus harringtonia*. *Phytochemistry* **1977**, *16*, 1595-1598.

Guiry, M. D.; Guiry, G. M. 2008. AlgaeBase version 4.2. World-wide electronic publication, National University of Ireland, Galway. http://www.algaebase.org date accessed January 18, **2008**.

Hayashi, J.; Sekine, T.; Deguchi, S.; Lin, Q.; Horie, S.; Tsuchiya, S.; Yano, S.; Watanabe, K.; Ikegami, F. Phenolic compounds from *Gastrodia* rhizome and relaxant effects of related compounds on isolated smooth muscle preparation. *Phytochemistry* **2002**, *59*, 513-519.

Huang, S.; Li, G; Shi, J.; Mo, S.; Wang, S.; Yang, Y. Chemical constituents of the rhizomes of *Coeloglossum viride* var. *Bracteatum*. *Journal of Asian Natural Products Research* **2004**, *6*, (1), 49-61.

Kirkup, M. P.; Moore, R. E. Indole alkaloids from the marine red alga *Martensia Fragilis*. *Tetrahedron* **1983**, *24*, (20), 2087-2090.

Moore, R. E. Volatile compounds from marine algae. *Accounts of Chemical Research* **1977**, *10*, 40-47.

Takamatsu, S.; Hodges, T. W.; Rajbhandari, I.; Gerwick, W. H.; Hamann, M. T.; Nagle, D. G. Marine natural products as novel antioxidant prototypes. *Journal of Natural Products* **2003**, *66*, 605-608.

Chapter Seven

Antibacterial and biofilm inhibitory properties of selected algal metabolites

7.1 Introduction

7.1.1 Biofilm formation and quorum sensing

Biofilms are surface-attached sessile microbial communities encapsulated in a polymeric matrix that form at any suitable interface able to support microbial growth (O'Toole and Kolter, 1998). Formation of a biofilm is not merely the haphazard accumulation of cells, but a discriminate process involving a microbial community co-operating to form well-differentiated structures (Merritt *et al.*, 2003). These communities exhibit a primitive form of multicellular organisation which leads to co-ordinated behavioural patterns (Shapiro, 1998). Cells within the community employ cell-to-cell communication which is accomplished using small diffusible signals (Hentzer and Givskov, 2003). The concentration of signal molecules in a defined environment enables the cells to determine the population density and determine whether it is "quorate" meaning that there are sufficient cells to make group based decisions. This system allows the cells to perceive and respond to changing population density and is termed quorum sensing (Hentzer and Givskov, 2003). Achieving specific cell densities triggers the expression of phenotypic traits in the population. The signal concentration at receptor sites within the cell reaches a critical threshold, which activates the receptor. This activation switches on a specific gene responsible for the expression of a certain phenotype. It has been discovered that many of the phenotypes regulated by quorum sensing are involved in virulence of the pathogen (Rasmussen and Givskov, 2006; Hentzer *et al.*, 2003). Selected bacteria have evolved to exploit population control by quorum sensing. They are able to suppress the expression of phenotypes that elicit host immune responses until the population is sufficiently dense to overwhelm the host defense mechanisms and establish infection. This association between quorum sensing and virulence implies that inhibition of the quorum sensing system in virulent bacteria may render them non-pathogenic (Hentzer and Givskov, 2003).

Quorum sensing is a generic mechanism employed by Gram-positive and Gram-negative bacteria as well as fungi (Ren *et al.*, 2002; Hentzer and Givskov, 2003; Reading and Sperandio, 2006). In Gram-positive bacteria, quorum sensing systems rely on small peptides which are cleaved from oligopeptides within the cell. These peptides are often thiolactones and are specific for their cognate receptor (Reading and Sperandio, 2006).

Quorum sensing in Gram-negative bacteria has been well documented and is better understood than in Gram-positive bacteria. The LuxR-LuxI homologous system is widely used by Gram-negative bacteria. In this system, bacterial cells utilize small molecules called *N*-acyl-homoserine

lactones (AHLs) (Hentzer and Givskov, 2003, Rasmussen and Givskov, 2006). In fungi such as *Candida albicans*, farnesol (**7.1**) has been found to play a role in biofilm formation and quorum sensing (Ramage *et al.*, 2002).

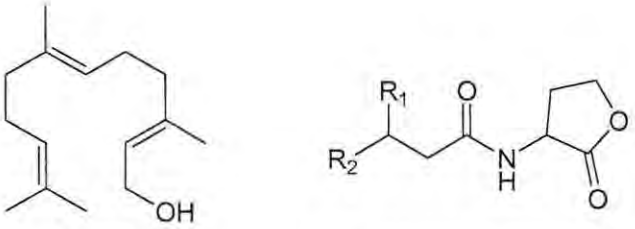

farnesol
7.1

AHL signal molecule
7.2

R_1 = H, OH or O, R_2 = C_1-C_{18}

Figure 7.1 Quorum sensing molecules farnesol (**7.1**) and and *N*-acyl-homoserine lactone.

7.1.2 Biofilm inhibition by eukaryotic interference

Returning to the theme of this project, i.e. the prevention of biofouling by inhibition of microbial growth, the question is raised as to how secondary metabolites isolated from marine algae may be employed in the prevention of biofilm formation.

Terrestrial and marine plants have been reported to inhibit biofilm formation by the production of small molecules that resemble the bacterial signal molecules. These secondary metabolites are thought to interfere with the microbial quorum sensing systems, hindering the co-ordination of bacterial populations (Teplitski *et al.*, 2000; Rasmussen and Givskov, 2006; Wright *et al.*, 2006).

The most well-known and scrutinized examples of the natural product quorum sensing inhibitors are the halogenated furanones (e.g. **7.3)** from the red marine macro-alga *Delisea pulchra*. This class of compounds is structurally similar to AHL's (**7.2**) produced by Gram-negative bacteria. Wright *et al.* (2006) demonstrated that the rigid conformation of the furan ring is an important structural feature and provided evidence that an hydroxyl or acetate group at C-6 and bulky electron-rich groups at C-6 are essential functionalities for furanone activity (Figure 7.2)

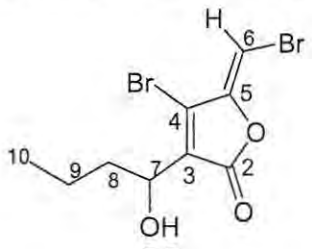

7.3

Figure 7.2 Compound **7.3**, an example for an Halogenated furanone from *Delisea pulcra*

They have been shown to inhibit a variety of quorum sensing regulated phenotypes in Gram-negative bacteria (Manfield *et al.*, 2000; Hentzer *et al*, 2002; Manefield *et al.*, 2002), but have also displayed activity against Gram-positive bacteria (Ren *et al.*, 2002).

Although quorum sensing is an attractive target for biofilm inhibition (Hentzer and Givskov, 2003; Rasmussen and Givskov, 2006), it is not the only mechanism employed in the natural environment. Natural products isolated from marine sources have been shown to be highly toxic to a variety of cells and should not be discounted as effective defense mechanisms against micro-organisms.

7.1.3 Chapter aims

The main aim of this research was to isolate algal secondary metabolites and explore their antimicrobial and antifouling potential. In this study, the Gram-negative biofilm forming bacterium *Pseudomonas aeruginosa* was used as a model system to evaluate the antibacterial and biofilm inhibitory properties of selected algal metabolites isolated during the course of this project.

7.2 Results and Discussion

7.2.1 Study design

Antibacterial and biofilm inhibitory activity was determined against *P. aeruginosa* using the combined 96-well microtitre plate methods of O Toole and Kolter (1998) and Hu *et al.* (2006). One of the objectives of this study was to determine whether the selected algal metabolites could inhibit biofilm formation without having bacteriostatic or bactericidal effects; this would indicate an alternative inhibitory mechanism such as the inhibition of quorum sensing. To this aim, the antibacterial activity of the algal metabolites was assessed in the same assay used to determine the inhibition of biofilm formation, prior to staining of the biofilms. In all cases, the algal metabolites and control substances were added prior to the formation of the biofilm. The objective of the assays was not to determine the effect of the metabolites on established biofilms, although this has been identified as an area for further study.

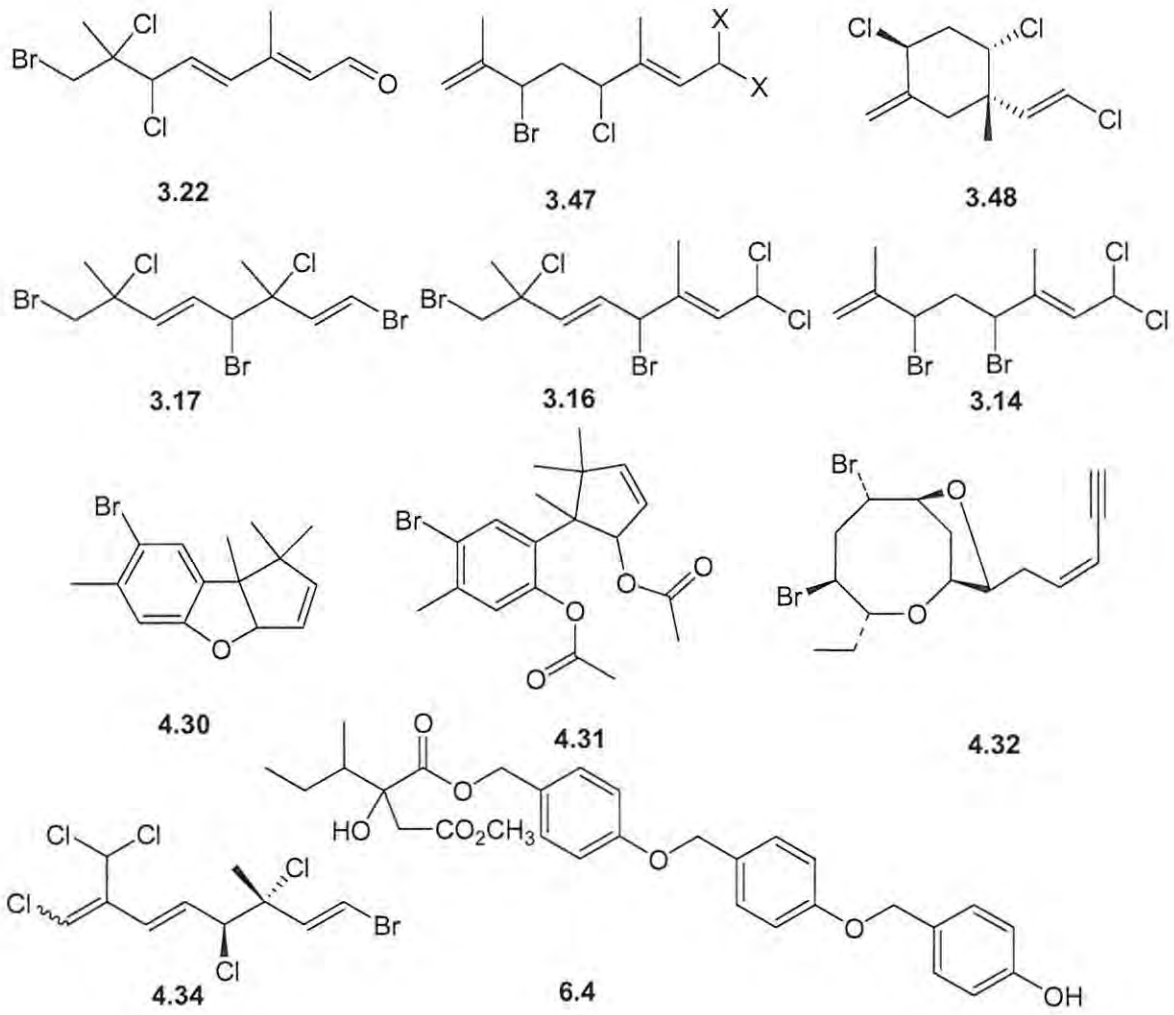

Figure 7.3 Selected algal metabolites tested for antibacterial and biofilm inhibitory activity

The samples tested in these assays included pure compounds from *P. corallorhiza*, *L. flexuosa*, *M. elegans* and *P. suhrii*.

7.2.2 Effect of co-solvents on antibacterial and biofilm formation

Ethanol (96%) and dimethylsulphoxide are commonly used solvents in biological assays and were employed in this to dissolve the algal metabolites and standard substances prior to the addition of the aqueous broth. The effects of these co-solvents were determined using the same method used to test the activity of the algal metabolites. The concentrations used for the co-solvents were 5%, 2.5% and 1.5%. The effect of ethanol 5% and 2.5% on microbial growth was statistically significant (Figure 7.4), thus a final ethanol concentration of 1.5% was considered acceptable for use in the assays. Biofilm formation was significantly inhibited only by ethanol at a concentration of 5%. The highest concentration of DMSO did not significantly affect microbial growth nor biofilm formation, however a final concentration of 1.5% DMSO was also used in this study. Only one compound (**4.32**) required dissolution in DMSO due to its insolubility in ethanol.

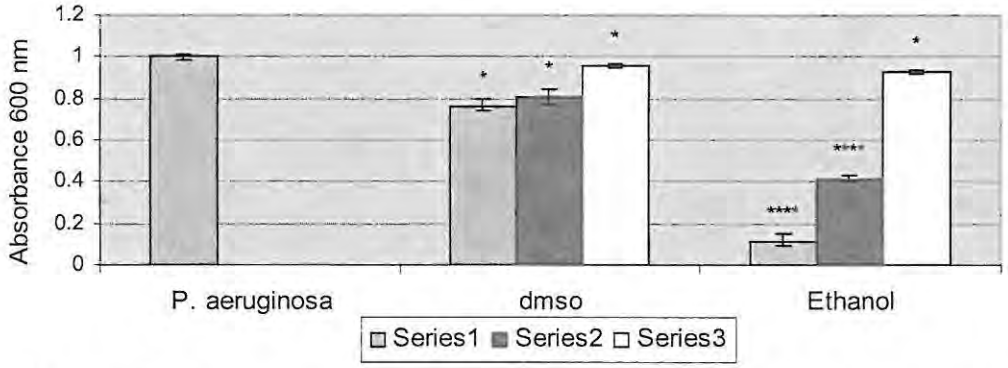

Figure 7.4 The effect of co-solvents on bacterial growth. If $P < 0.05$ difference in mean absorbance is significant. $P > 0.05$ *, $P < 0.05$ **, $P < 0.01$ ***, $P < 0.001$****
Series 1 5% ethanol; Series 2 2.5% ethanol; Series 3 1.5% ethanol.

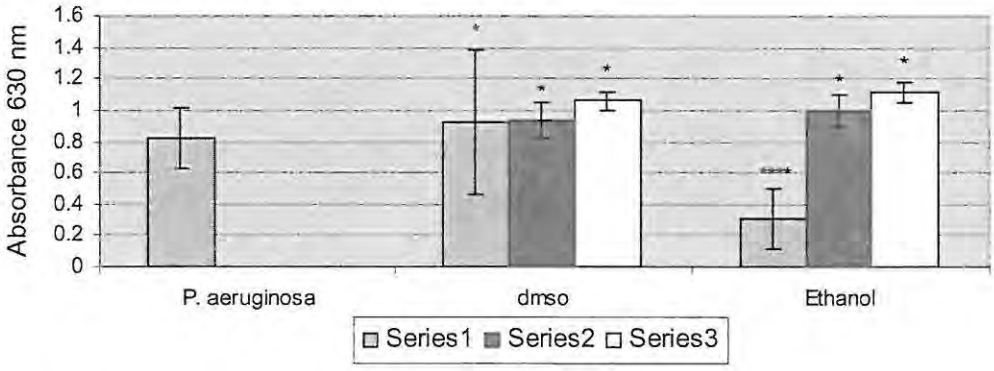

Figure 7.5 The effect of co-solvents on biofilm formation. If $P < 0.05$ difference in mean absorbance is significant. $P > 0.05$ *, $P < 0.05$ **, $P < 0.01$ ***, $P < 0.001$****
Series 1 5% ethanol; Series 2 2.5% ethanol; Series 3 1.5% ethanol.

The use of DMSO as a co-solvent appears to be preferable to ethanol due to a considerably lower influence on microbial growth. Ethanol is used as a disinfectant at higher concentrations, however it was surprising that such low concentrations had such a significant effect on bacterial growth.

7.2.3 Effect of algal metabolites in solution on bacterial growth and biofilm formation.

In this assay, an arbitrary metabolite concentration of 150 µg/ml was used to afford an indication of the activity of each metabolite. At this point in the project, the objective was not to obtain minimum inhibitory concentrations or IC_{50} values.

Antibacterial activity was determined by comparing the difference in mean absorbance of cultures in wells containing test compounds after incubation overnight, to the mean absorbance of control cultures in wells that contained no test substance. These readings were taken prior to staining of the bacteria with crystal violet dye. The effect of the metabolites on biofilm formation was measured by comparing the absorbance at λ 630 nm attributed to the concentration of crystal violet dye after staining the biofilms in treated and untreated wells. *Pseudomonas aeruginosa* forms biofilms at the interface between the nutrient medium and the air creating a ring of growth which may be stained by crystal violet dye (0.1%). The more dense the biofilm, the more crystal violet will be absorbed (O'Toole and Kolter, 1998; Musk *et al.*, 2005) and the greater the absorbance will be when measured using a plate reader. A wavelength of 630 nm was found to be appropriate for the reading of absorbance of crystal violet in the wells.

Salicylic acid (13.8 mg/ml) was used as the positive control for biofilm inhibition; the non-steroidal anti-inflammatory drug is reported to inhibit *P. aeruginosa* biofilm formation at 13.8 mg/ml (100 mM) (Bandara *et al.*, 2004). Gentamycin (150 µg/ml) was used as a positive control for antibacterial activity.

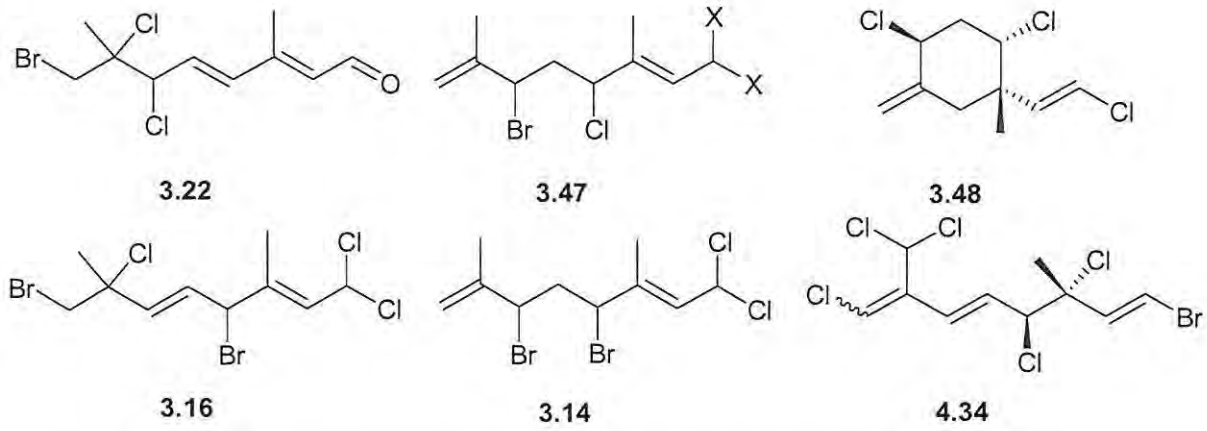

3.22 **3.47** **3.48**

3.16 **3.14** **4.34**

Figure 7.6 Halogenated monoterpenes that exhibited antibacterial activity against *P. aeruginosa*

Compounds **3.22, 3.47, 3.48**, **3.16**, **3.14** and **4.34** exhibited statistically significant antimicrobial activity (Figure 7.7). These metabolites were polyhalogenated monoterpenes isolated from the two *Plocamium* species (Figure 7.6). Of these compounds 67% contained a geminal dichloride functionality. The most potent compound (**4.34**) was also the only metabolite to have any significant effect on biofilm formation; it is probable that this is due to the toxic effects on the planktonic cells. Interestingly, this is the same metabolite found to have been transferred from *P. suhrii* to *L. flexuosa*, which only makes their relationship more intriguing.

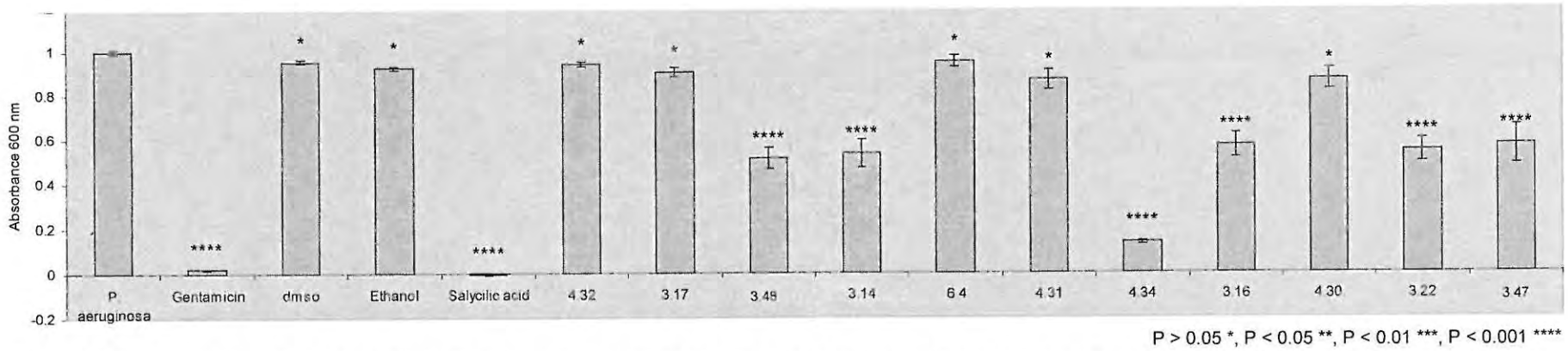

Figure 7.7 Antimicrobial activity of algal metabolites. Concentration of each metabolite 150 µg/ml. Salicylic acid 13.8 mg/ml

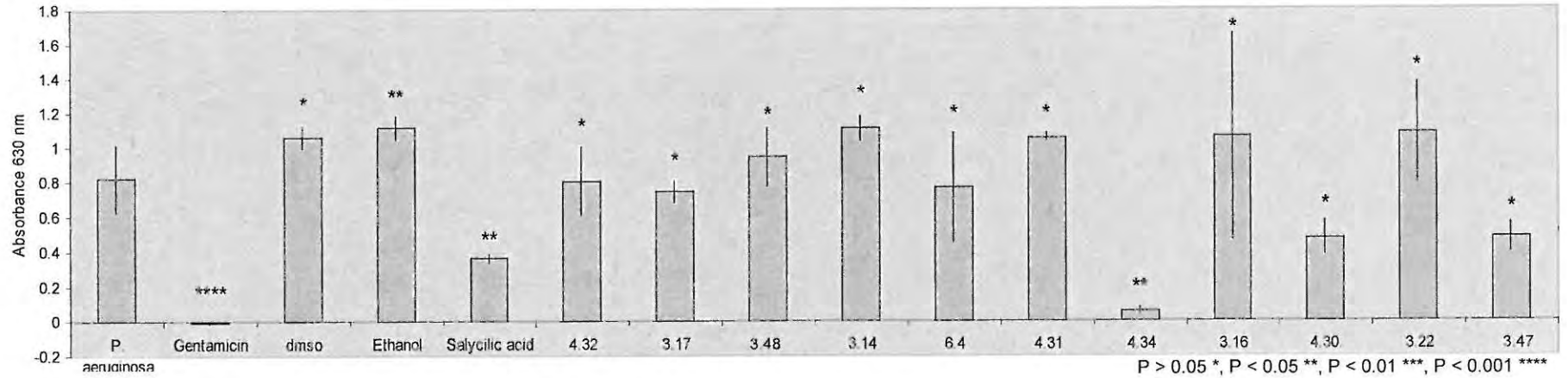

Figure 7.8 Effect of algal metabolites on biofilm formation. Concentration of each metabolite 150 µg/ml. Salicylic acid 13.8mg/ml

7.2.4 Effect of "dry films" on bacterial growth and biofilm formation.

The objective of this assay was to investigate the effect of coating the walls of the microtitre plate wells with the algal metabolites on biofilm formation. Compounds were dissolved in ethanol (96%) and measured into each well; the ethanol was then evaporated off leaving a dry film of the compound coating the well. Antimicrobial activity and inhibition of biofilm formation was measured using the same method as the previous assay. Halogenated monoterpenes from *P. corallorhiza* and *P. suhrii* and the control substance Gentamycin, were tested at 500, 250 and 150 µg/ml. Salicylic acid concentrations were much higher at 13.8, 6.9 and 4.1 mg/ml.

No algal metabolite tested in this assay exhibited statistically significant antimicrobial activity. The lack of activity in aqueous solution may be due to the low water solubility of the compounds. It may also be, that the volatile halogenated monoterpenes evaporated from the surface of the wells during the time it took to completely evaporate the ethanol.

The positive control, Gentamycin was effective at each concentration. Salicylic acid exhibited antimicrobial activity at 13.8 mg/ml.

The effects of the algal metabolites on biofilm formation were variable as evidenced by the large standard deviations about the means of several compounds (Figure 7.11). Compound **3.47** appeared to induce biofilm formation at higher concentrations. Compound **4.34**, found to be active in the previous assay, had no statistically significant effect on microbial growth nor biofilm formation. **3.14** inhibited biofilm formation at the two lower concentrations, 250 µg/ml and 150 µg/ml. **3.17** decreased biofilm formation at all three concentrations without having any effect on bacterial growth. These compounds may we worth exploring further with regard to their durability on a surface and their ability to inhibit biofilm formation for a prolonged period of time.

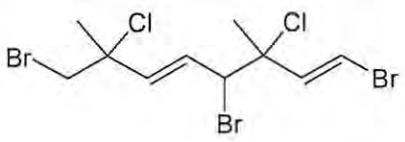

3.17

3.14

Figure 7.9 Halogenated monoterpenes that inhibited biofilm formation as a film coating the microtitre plate well

The positive control Gentamycin was effective at all three concentrations, while Salicylic acid inhibited biofilm formation at the two higher concentrations.

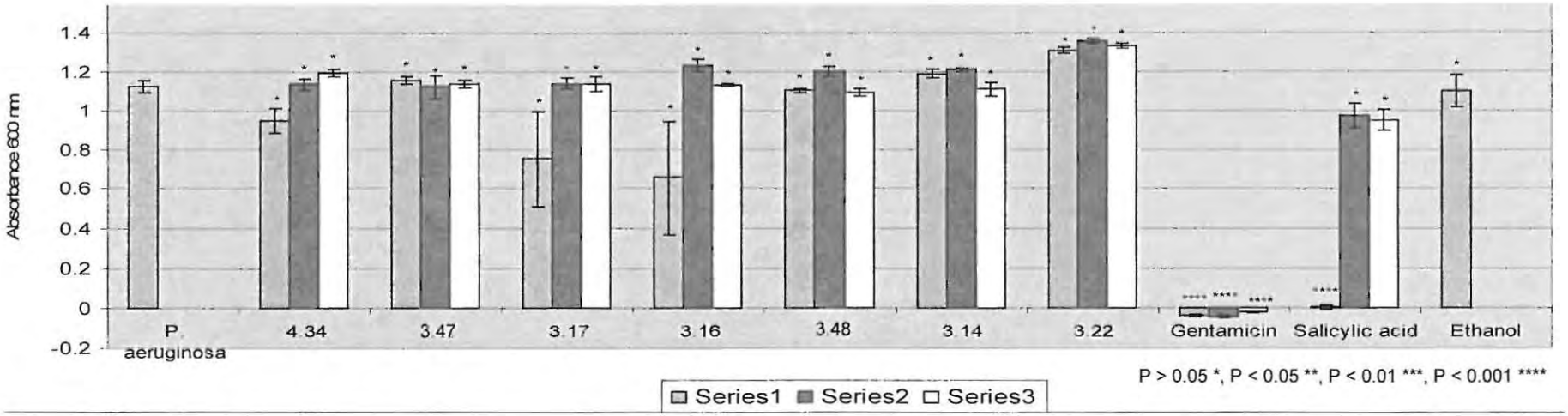

Figure 7.10 Antimicrobial activity, the mean difference in absorbance between wells prior to and post incubation. Series 1 500 µg/ml 5% ethanol; Series 2 250 µg/ml 2.5% ethanol; Series 3 150 µg/ml 1.5% ethanol.

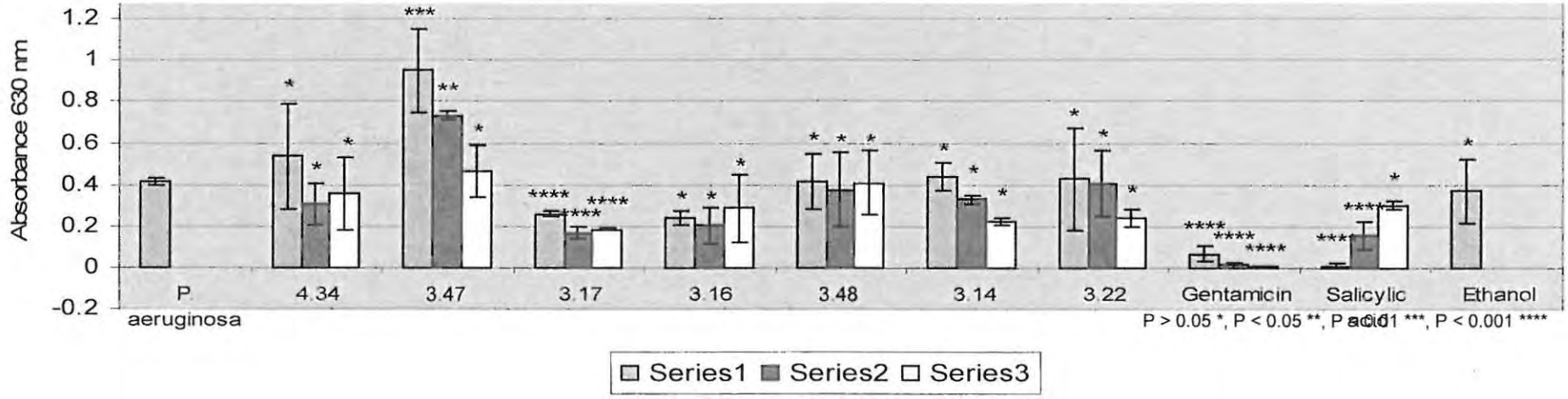

Figure 7.11 Effect of algal metabolites on biofilm formation. Series 1 500 µg/ml 5% ethanol; Series 2 250 µg/ml 2.5% ethanol; Series 3 150 µg/ml 1.5% ethanol.

7.2.5 Summary and conclusion

Although these assays were simple preliminary tests, some valuable insights were gained.

In developing the study design, it was found that ethanol (5% and 2.5%) significantly affected bacterial growth, based on these findings, DMSO should be used as the co-solvent in future assays. Coating the wells with the metabolites was shown to be a less sensitive indicator of antimicrobial activity, however it was demonstrated that selected non-polar compounds may be active at the surface, limiting biofilm formation. Flaws in the experimental procedure such as the extended time taken to evaporate the solvent requires investigation.

Pseudomonas aeruginosa is considered a valuable model bacterium for testing biofilm inhibitory activity. The number and type of micro-organisms tested, could however be increased and ecologically relevant strains may provide better insight for the development of antifouling agents for use in the maritime environment. The crude extracts demonstrated activity against the fungus *Candida albicans*, also known to form biofilms. Investigation into this activity is most certainly an area for further study. In retrospect, it is also thought that the use of crude extracts in this study may have afforded some interesting results, perhaps leading to the isolation of compounds that inhibit biofilm formation without bacteriostatic or bactericidal activity.

With regard to the general aim of this thesis, it has been demonstrated that metabolites from marine macro-algae do have the potential to inhibit bacterial growth. Whether this is their role in the algae and whether they would make useful antifouling agents requires further study, however preliminary findings are encouraging.

7.3 Experimental

7.3.1 Standards and marine algal metabolites

Gentamycin was obtained from Merck Spectramed, concentrations used were 500 µg/ml, 250 µg/ml and 150 µg/ml. Salicylic acid was obtained from Saarchem Holpro Analytic. Concentrations used were 13.8 mg/ml, 6.9 mg/ml and 4.1 mg/ml (Bandara *et al.*, 2004). Fourteen compounds were isolated from South African marine algae, concentrations used were 500 µg/ml, 250 µg/ml and 150 µg/ml.

7.3.2 Micro-organisms and culture conditions

The bacterial strain *P. aeruginosa* used in the study was grown overnight at 30 °C on nutrient agar (Biolab). *P. aeruginosa* was sub-cultured at 28 °C in 25 ml of Tryptone Soy Broth (TSB Biolab sterilised for 15 minutes at 121 °C in an autoclave). The cultures were grown to stationary phase with agitation (120 rpm) overnight; obtaining cells in the stationary phase will result in slower division upon dilution to allow more consistency in the number of cells per well (Sutton, 2006). Fresh, sterile TSB was inoculated with the sub-cultured broth and triturated to a optical density of approximately 0.4 at λ 600 nm. Unless otherwise stated, all microtitre plate readings were performed on a Power Wave X Plate reader (Bio-Tek instruments inc.)

7.3.3 Determination of number of cells/ml

P. aeruginosa was sub-cultured at 28 °C in 25 ml of TSB on a shaker water bath at 120 rpm overnight. The optical density was read and the sub-culture was diluted to a concentration (cells/ml) with an optical density of approximately 0.4 (OD_{600}) and a volume of 11.5 ml. 1.5 ml was pipetted into a cuvette for the optical density measurement. 10 ml was filtered under vacuum and the membrane filter was placed in an oven for 3 hours at 105 °C. Control membrane filters consisted of 3 clean membrane filters and 2 membrane filters that had filtered 10 ml of sterile TSB. These were also placed in the oven for 3 hours at 105 °C. After 3 hours, the membranes were removed from the oven and allowed to cool to room temperature in a dessicator. The mass of each membrane filter was measured and the average mass of the membrane and broth was subtracted from the mass of the test membrane filter which afforded a dry mass of cells in g/l. A conversion factor was obtained by dividing the optical density by the dry weight of cells. To calculate the number of cells per ml in the broth the absorbance of the sample with unknown bacterial concentration was divided by the conversion factor (0.28) to get the concentration of the sample in g dry weight/l, or mg dry weight/ml. This concentration was multiplied by the volume of the sample in ml to get the mass of bacterial biomass in the sample in mg. This mass in mg was then divided by 0.20 to get the wet weight of the entire bacterial population in the sample.

The mass of the bacterial population was by 0.000000002 (the approximate weight of a single *Pseudomonas* cell) to obtain the number of cells in the sample. The number of cells was divided by the total volume of the sample in ml. These calculations afforded the concentration of *P. aeruginosa* in cells/ml of sample broth.

7.3.4 Effect of metabolites in solution of bacterial growth and biofilm formation

Each metabolite (1 mg) was dissolved in 100 µl of 96% ethanol or dimethyl sulphoxide (DMSO) depending on solubility. 900 µl of sterile TSB was added to make a final volume of 1 ml. The solution (30 µl, 30 µg) was drawn up and placed in each well. 100 µl of TSB inoculated with *P. aeruginosa* (optical density of approx. OD_{600} 0.4) was placed in each well. A final volume of 200 µl in each well was made up by the addition of sterile TSB. The optical density was read at 600 nm prior to incubation. The plate was incubated at 30 °C for 14 hours. The optical density was again read at 600 nm prior to development with crystal violet 0.1% Control wells 1) dmso, 2) ethanol, 3) OD_{600} 0.4 inoculum 4) no cells, pure sterile TSB. All samples were assayed in triplicate on one occasion.

7.3.5 Effect of co-solvents on bacterial growth and biofilm formation

Each co-solvent (100 µl) was pipetted into a vial containing sterile TSB (900 µl) to make a final volume of 1 ml. 180 µl of solution was placed in the wells of row A, thereafter 80 µl was drawn up in an auto pipette and placed in each well of row B, similarly 30 µl was drawn from row B and placed in each well of row C. 100 µl inoculum was pipetted into each well after which wells in rows B and C were made up with sterile TSB to a final volume of 200 µl. The optical density was read at 600 nm and the plates were placed in the incubator at 30 °C for 14 hours. The optical density was again read at 600 nm prior to development with crystal violet 0.1%. Control wells 1) inoculum and TSB 2) sterile TSB. All samples were assayed in triplicate on one occasion.

7.3.6 Effect of "dry film" on bacterial growth and biofilm formation

Each metabolite (1 mg) was dissolved in 1 ml ethanol (96%). Gentamycin is fairly insoluble in ethanol (96%) and the standard required sonication prior to pipetting into the wells of the microtitre plate. 180 µl (180 µg) of compound in diluent was placed in the wells of row A, thereafter 80 µl (80 µg) was drawn up in an auto pipette and placed in each well of row B, similarly 30 µl (30 µg) was drawn from row B and placed in each well of row C. The wells were brought to dryness at ambient temperature in a sterile dessicator overnight. 100 µl sterile TSB was pipetted into each well after which 100 µl inoculum was pipetted into each well to make a final volume of 200 µl. The optical density was read at 600 nm and the plates were placed in the incubator at 30 °C for 14 hours. The optical density was again read at 600 nm prior to development with crystal violet 0.1% Control

wells 1) ethanol, 2) OD_{600} 0.4 inoculum 3) no cells, pure sterile TSB. All samples were assayed in triplicate on one occasion.

7.3.7 Development of plates

The broth and planktonic cells were aspirated from each well; the wells were then rinsed gently with phosphate buffered saline (PBS) three times. 200 µl 0.1% crystal violet dye was used to stain the biofilms that formed as rings at the air-medium interface. The plates were incubated for 10 - 15 minutes after which the excess dye was removed by exhaustive rinsing with sterile PBS. The plates were blotted on paper towels and left to dry. 250 µl 96% ethanol was used to solubilise the dye and the plate was read at 630 nm.

7.3.8 Measurement of biofilm density

Effect on biofilm formation was determined by measuring the absorbance of crystal violet at 630 nm. The more dense the biofilm, the greater the concentration of crystal violet. The absorbance of the concentration of crystal violet in each well treated with either standard compound or algal secondary metabolites was compared to the absorbance afforded by the concentration of crystal violet in untreated wells. The mean absorbance afforded by the concentration of crystal violet in blank wells previously containing only TSB was subtracted from each reading to negate the effect of the broth.

7.3.9 Statistical analysis

Data is presented as the mean ± standard deviation of experiments. Differences were considered significant at $p < 0.05$. One way ANOVA tests were performed using GraphPad Prism version 4.00 for Windows (GraphPad Software, San Diego, CA, www.graphpad.com).

A one way analysis of variance (ANOVA) test and the Tukey post test were used to analyse the data. Tests were performed at the 95% confidence interval. The P value yielded by the post test answers the following question: "If the populations all really have the same mean, what is the chance that random sampling would result in means as far apart as observed in the experiment?" If the P value for a post test wass small ($P < 0.05$) it was considered unlikely that the difference observed was due to random sampling. However, if the P values from a post test were greater than 0.05, it did not necessarily mean that the means were the same; there was merely insufficient evidence to say that they differ (Motulsky, 2003).

7.4 References

Bandara, B. M. K.; Sankaridurg, P. R.; Willcox, M. D. P. Non-steroidal anti inflammatory agents decrease bacterial colonisation of contact lenses and prevent adhesion to human corneal epithelial cells. *Current Eye Research* **2004**, *29*, (4–5), 245–251.

Hentzer, M.; Givskov, M. Pharmacological inhibition of quorum sensing for the treatment of chronic bacterial infections. *Journal of Clinical Investigation* **2003**, *112*, 1300-1307.

Hentzer, M.; Wu, H.; Andersen, J. B.; Riedel, K.; Rasmussen, T. B.; Bagge, N.; Kumar, N.; Schembri, M. A.; Song, Z.; Kristoffersen, P.; Manefield, M.; Costerton, J. W.; Molin, S.; Eberl, L.; Steinberg, P.; Kjelleberg, S.; Høiby, N.; Givskov, M. Attenuation of *Pseudomonas aeruginosa* virulence by quorum sensing. *The European Molecular Biology Organization Journal* **2003**, *22*, (15), 3803-3815.

Hentzer, M.; Riedel, K.; Rasmussen, T. B.; Heydorn, A.; Andersen, J. B.;Parsek, M. R.; Rice, S. A.; Eberl, L.; Molin, S.; Høiby, N.; Kjelleberg, S.; Givskov, M. Inhibition of quorum sensing in *Pseudomonas aeruginosa* biofilm bacteria by a halogenated furanone compound. *Microbiology* **2002**, *148*, 87-102.

Hu, J. F.; Garo, E.; Goering, M. G.; Pasmore, M.; Yoo, H.; Esser, T.; Sestrich, J.; Cremin, P. A.; Hough, G. W.; Perrone, P.; Lee, Y. L.; Le, N.; O'Neil-Johnson, M.; Costerton, J. W.; Eldridge, G. R. Bacterial biofilm inhibitors from *Diospyros dendo*. *Journal of Natural Products* **2006**, *69*, 118-120.

Manefield, M.; Harris, L.; Rice, S. A.; de Nys, R.; Kjelleberg, S. Inhibition of luminescence and virulence in the Black Tiger Prawn (*Penaeus monodon*) pathogen *Vibrio harveyi* by intercellular signal antagonists. *Applied and Environmental Microbiology* **2000**, *66*, (5), 2079-2084.

Manefield, M.; Rasmussen, T. B.; Hentzer, M.; Andersen, J. B.; Steinberg, P.; Kjelleberg, S.; Givskov, M. Halogenated furanones inhibit quorum sensing through accelerated LuxR turnover. *Microbiology* **2002**, *148*, 1119-1127.

Merritt, J.; Qi, F.; Goodman, S. D.; Anderson, M. H.; Shi, W. Mutation of *luxS* Affects biofilm formation in *Streptococcus mutans*. *Infection and Immunity* **2003**, *71*, (4), 1972-1979.

Motulsky, H.; Statistical analyses for laboratory and clinical researchers. *Statistics Guide* GraphPad Prism® Version 4.0 **2003.**

Musk, D. J.; Banko, D. A.; Hergenrother, P. J. Iron salts perturb biofilm formation and disrupt existing biofilms of *Pseudomonas aeruginosa*. *Chemistry and Biology* **2005**, *12*, (7), 789-796.

O'Toole, G. A.; Kolter, R. Initiation of biofilm formation in *Pseudomonas fluorescens* WCS365 proceeds via multiple, convergent signalling pathways: a genetic analysis. *Molecular Microbiology* **1998**, *28*, (3), 449-461.

Ramage, G.; Saville, S. P.; Wickes, B. L.; López-Ribot, J. L. Inhibition of *Candida albicans* biofilm formation by farnesol, a quorum sensing molecule. *Applied and Environmental Microbiology* **2002**, *68*, (11), 5459-5463.

Rasmussen, T. B.; Givskov, M. Quorum-sensing inhibitors as antipathogenic drugs. *International Journal of Medical Microbiology* **2006**, *296*, 149-161.

Reading, N. C.; Sperandio, V. Quorum sensing: the many languages of bacteria. *Federation of European Microbiological Studies Microbiology Letters* **2006**, 254, 1-11.

Ren, D.; Sims, J. J.; Wood, T. K. Inhibition of biofilm formation and swarming of *Bacillus subtilis* by (5*Z*)-4-bromo-5-(bromomethylene)-3-butyl-2(5*H*)-furanone. *Letters in Applied Microbiology* **2002**, *34*, 293-299.

Shapiro, J. A. Thinking about bacterial populations as multicellular organisms. *Annual Review of Microbiology* **1998**, *52*, 81-104.

Sutton, S.; Measurement of cell concentration in suspension by optical density, http://www.microbiol.org/white.papers/WP.OD.htm date accessed August 17, 2007.

Teplitski, M.; Robinson, J. B.; Bauer, W. D. Plants secrete substances that mimic bacterial N-acyl homoserine lactone signal activities and affect population density-dependent behaviors in associated bacteria. *Molecular Plant-Microbe Interactions* **2000**, *13*, (6), 637-648.

Wright, A. D.; de Nys, R.; Angerhofer, C. K.; Pezzuto, J. M.; Gurrath, M. Biological activities and 3D QSAR studies of a series of *Delisea pulchra* (cf. *fimbriata*) derived natural products. *Journal of Natural Products* **2006**, *69*, 1180-1187.

Chapter Eight

Summary and Conclusion

The extraction of fourteen Southern African marine algae was successfully completed, allowing for the screening of twenty four crude solvent extracts against the clinically relevant pathogens *Klebsiella pneumoniae*, *Staphylococcus aureus*, *Mycobacterium aurum* and *Candida albicans*. A number of extracts showed moderate antimicrobial activity and these results guided the fractionation of extracts from *Plocamium corallorhiza* and *Laurencia flexuosa*. A third alga, *Martensia elegans* was extracted and fractionated based on literature that reported antimicrobial compounds being isolated from related species.

Eight known metabolites were isolated from *P. corallorhiza* including members of the novel group of halogenated monoterpene aldehydes. A further two new halogenated monoterpenes were characterized. Challenges with respect to obtaining the aldehydic compounds' mass spectrometry data were overcome by the use of aldehyde trapping reagents CET-triphenylphosphorane and *O*-(2,3,4,5,6-pentafluorobenzyl)hydroxylamine hydrochloride.

The fractionation of solvent extracts from *L. flexuosa* afforded two acetogenins previously isolated from a related algal species and an opisthobranch mollusc. A new cuparane derived sesquiterpene was isolated and characterized. The metabolite experienced intramolecular cyclization in $CDCl_3$ which was found to be prevented by the acetylation of hydroxyl groups present in the molecule. Curiously, a halogenated monoterpene was isolated from the same extracts; the compound was immediately suspected as a contaminant and investigation into the source of the compound ensued. It was found that the metabolite was produced by a second red alga *Plocamium suhrii* that grows in close proximity to *L. flexuosa*.

M. elegans was found to produce an unusual a-alkyl malate derivative which bears resemblance to metabolites isolated from terrestrial plants of the family Orchidaceae.

Metabolites isolated in sufficient quantities were tested in preliminary antibacterial and biofilm formation inhibition assays employing the Gram-negative biofilm forming bacterium *P. aeruginosa*. The halogenated monoterpene isolated from extracts of *L. flexuosa* and *P. suhrii* was the only compound to have a significant effect on bacterial growth and inhibited both reproduction and biofilm formation at a concentration of 150 µg/ml. Two halogenated monoterpenes inhibited biofilm formation without negatively influencing bacterial growth when present as a surface film.

The study of the natural product chemistry of marine algae continues to provide useful leads in the search for natural product antifouling agents. The project has offered some insight into the chemistry of South African marine flora, but has also raised many intriguing questions that present areas for new research.